

Synthese und Untersuchung verschiedener BN-substituierter polyzyklischer Aromaten

Dissertation

der Mathematisch-Naturwissenschaftlichen Fakultät

der EBERHARD KARLS UNIVERSITÄT TÜBINGEN

zur Erlangung des Grades eines

Doktors der Naturwissenschaften

(Dr. rer. nat.)

vorgelegt von

Michael Fingerle

aus Reutlingen

Tübingen

2021

Gedruckt mit Genehmigung der Mathematisch-Naturwissenschaftlichen Fakultät der Eberhard Karls Universität Tübingen.

Tag der mündlichen Qualifikation: 20.05.2021

Dekan: Prof. Dr. Thilo Stehle

1. Berichterstatter: Prof. Dr. Holger F. Bettinger

2. Berichterstatter: Jun.-Prof. Dr. Ivana Fleischer

Danksagung

Mein größter Dank gilt meinem Doktorvater Prof. Dr. Holger F. Bettinger für die Bereitstellung der interessanten Themen, die Möglichkeit eigene Ideen mit einzubringen, sowie die viele Zeit, die er für fachliche Diskussionen und Hilfestellungen geopfert hat.

Ich bedanke mich bei allen ehemaligen und aktuellen Mitgliedern des Arbeitskreises für die gemeinsame Zeit. Besonders bei Dr. Ralf Einholz für das Korrekturlesen dieser Arbeit und Mario Rapp, der im letzten Jahr mein Laborkollege auf Ebene 12 war. Mein Dank gilt auch Dr. Christina Tönshoff für die Messung der Absorptionsspektren mittels Matrix Experimenten. Ebenfalls möchte ich mich bei meinen Praktikanten Simon Stocker, Christian Mahlenbrey, Juliane Dingerkus und Roman Kimmich für die Unterstützung bei Synthesen bedanken.

Bedanken möchte ich mich auch bei den Mitarbeitern in der NMR-Abteilung, Dr. Markus Kramer, Paul Schuler, Dominik Brzecki, Priska Kolb und Dr. Norbert Grzegorzek für die Durchführung sehr vieler Sondermessungen und die Wartung der Routinemessgeräte.

Mindestens genauso viele Messungen durfte ich in der Analytikabteilung für Molekülmassenbestimmung abgeben, für die ich mich herzlich bei Dr. Dorothee Wistuba, Dr. Peter Haiss und Claudia Krause bedanken möchte.

Ich danke Dr. Thorsten Hummel für die Durchführung der Sublimationsexperimente, sowie Dr. Markus Ströbele, Dr. Hartmut Schubert und Dr. Cäcilia Maichle-Mössmer für die Durchführung von Röntgenbeugungsexperimenten und das Lösen der Strukturen.

Für Cyclovoltammetrie Messungen an verschiedenen Molekülen möchte ich mich bei Prof. Dr. Bernd Speiser und Simon Schundelmeier bedanken, ebenso bei Prof. Dr. Marcus Scheele und Kai Wurst.

Ein großer Dank gilt meinen Eltern, die mir das Studium ermöglicht haben und die mich zu jeder Zeit in so vielerlei Weise unterstützen.

Zuletzt bin ich sehr dankbar für meine Frau, die immer hinter mir steht und mich besonders in angespannten Lagen der Arbeit unterstützt bzw. mir den nötigen Freiraum gegeben hat.

Inhaltsverzeichnis

Zusammenfassung	13
Abstract	14
Publikationsliste und Eigenanteile	15
1 Einleitung	17
1.1 Polyzyklische aromatische Kohlenwasserstoffe und ihre Eigenschaften	17
1.2 Der isoelektronische Austausch	17
1.3 Fortschritte in der Synthese von BN-dotierten PAKs	19
1.3.1 Synthesestrategien für BN-dotierte PAKs	19
1.3.2 Darstellungen des BN-HBCs	21
1.3.3 Das (BN) ₂ -Dibenzoperylen als BN-HBC-Ausschnitt	23
1.3.4 Benzo-tetracene	25
2 Zielsetzung	27
2.1 Synthese eines BNB-Benzo-tetracens	27
2.2 Entwicklung einer neuen Syntheseroute für ein (BN) ₂ -Dibenzoperylen zur Untersuchung der Reaktivität	27
2.3 Cycloadditionen von PAKs in der Buchtregion unter Beteiligung von Heteroatomen	28
2.4 Darstellung eines Nanographenmoleküls mit einem B ₃ N ₂ O-Kern	28
3 Ergebnisse und Diskussion	29
3.1 Das erste stabile BNB-Benzo-tetracene	29
3.2 Neue Syntheseroute (BN) ₂ -Dibenzoperylen	34

3.3	Cycloadditionsreaktionen des (BN) ₂ -Dibenzoperylens	38
3.3.1	Die Wahl des Dienophils	38
3.3.2	Cycloadditionen des (BN) ₂ -Dibenzoperylens mit Benzaldehyd	39
3.3.3	Untersuchungen zum Reaktionsmechanismus	43
3.3.4	Hydridabstraktion	45
3.3.5	Cycloadditionen des (BN) ₂ -Dibenzoperylens mit anderen Dienophilen .	47
3.4	Gezielte Synthese eines Nanographenmoleküls mit B ₃ N ₂ O-Kern	49
Literaturverzeichnis		53

Abbildungsverzeichnis

1.1	Isoelektronischer Austausch von einer CC-Doppelbindung durch eine BN-Einheit.	18
1.2	Ausschnitte aus Graphen (1) und hexagonalem Bornitrid (2).	18
1.3	Elektrophile Borylierung am 2-Aminobiphenyl (3) mittels Ausbildung einer B-N- und B-C-Bindung.	19
1.4	Aufbau eines im Inneren dotierten Polyzyklus mittels C-C-Ringschluss.	20
1.5	N-C-Bindungsknüpfung als Möglichkeit zum Aufbau von BN-dotierten PAKs.	21
1.6	Erste Synthese des BN-HBCs 13	21
1.7	Erste BN-HBC Synthese von Bonifazi et al.	22
1.8	Optimierte BN-HBC Synthese von Bonifazi et al.	23
1.9	Syntheseroute des BN-Dibenzoperylen 20	23
1.10	Reaktion von Maleinsäureanhydrid (22) mit Dibenzoperylen 21 in der Buchtregion.	24
1.11	Heteroatom-beteiligte Cycloaddition von Diazadiboretidine 24	25
1.12	Auswahl verschiedener NBN-Benzotetracene.	25
1.13	Darstellung des BNB-Benzotetracens 28 als reaktive Zwischenstufe.	26
1.14	Synthese eines BNB-dotierten Benzotetracens nach Scholz et al.	26
3.1	Syntheseroute für das erste stabile BNB-Benzotetracen.	30
3.2	(a) Molekülstrukturen von 37 ; (b) Molekülpackung.	31
3.3	Absorptions- und Fluoreszenzspektrum von 37	32
3.4	Berechnete Molekülorbitale von BNB-Benzotetracen 38 , BNB-Benzotetracen mit zwei Wasserstoffatome 39 und dem PAK-Kation 40	33

3.5	Berechnete NICS(0)-Werte des BNB-Benzotetracene 38 mit Clars Sextetstruktur; im Vergleich das BNB-Benzotetracene Grundgerüst 39 und Zahardiks PAK-Kation 40	34
3.6	Neue Syntheseroute für das (BN) ₂ -Dibenzoperylen.	35
3.7	Absorptions- und Fluoreszenzspektrum von 48	37
3.8	Quantenchemisch berechnete NICS(0)- und NICS(1)-Werte von den PAKs Perylen 49 und Dibenzoperylen 50 , sowie dem (BN) ₂ -Dibenzoperylen 20	38
3.9	Berechnungen von ΔG für die Cycloaddition von 20 mit verschiedenen Dienophilen.	39
3.10	Säurekatalysierte Cycloaddition von 48 mit Benzaldehyd 51	40
3.11	Molekülstruktur von 52a im Kristall und Packung von 52a	40
3.12	Absorptions- und Fluoreszenzspektren der erhaltenen Cycloadditionsprodukte in Dichlormethan im Vergleich zu 48 . Bildausschnitt: Fluoreszenzspektrum von 52c	42
3.13	Übersicht zweier möglicher Mechanismen der säurekatalysierten Cycloaddition.	44
3.14	Hydridabstraktion am Heteroatomring in 52a	45
3.15	Oxidation der Verbindung 52a	46
3.16	Getestete Dienophile in Reaktionen und berechnete Energiebilanz ausgewählter Beispiele auf dem M062X/6-311+G** Theorieniveau	48
3.17	Gezielte Syntheseroute für den B ₃ N ₂ O-PAK.	49
3.18	Kristallstruktur von 69 und Molekülpackung.	50
3.19	Absorptions- und Fluoreszenzspektrum von 69 ; im Vergleich das Absorptionsspektrum unter Matrixisolationstechnik bei 10 K.	51
3.20	NICS(1)-Werte von 70 , Strukturformel nach Clar und grafische Darstellung „anisotropy of current-induced density“ mittels quantenchemischer Rechnung.	52

Abkürzungsverzeichnis

Å	Ångström
ACID	Anisotropy Of The Current Induced Density
APCI	Atmospheric Pressure Chemical Ionization
Äq.	Äquivalent
B	Bor
cm	Zentimeter
eV	Elektronenvolt
h	Stunden
h-	hexagonal
HOMO	Highest Occupied Molecular Orbital
LDI	Laser-Desorption-Ionisation
LUMO	Lowest Unoccupied Molecular Orbital
M	Molar
<i>m</i>	meta
max	maximal
m/z	Masse-zu-Ladung-Verhältnis
N	Stickstoff
NICS	Nucleus-Independent-Chemical-Shift
nm	Nanometer
NMR	Nuclear Magnetic Resonance
NTO	Natural Transition Orbitals
oFET	Organischer Feldeffekttransistor

oLED	Organische Leuchtdiode
oSC	Organische Solarzelle
PAK	Polyzyklischer aromatischer Kohlenwasserstoff
pm	Pikometer
ppm	Chemische Verschiebung im NMR-Experiment
rt	Raumtemperatur
<i>tert</i>	tertiär
UV	Ultravioletter Teil des elektromagnetischen Spektrums
Vis	Sichtbarer Teil des elektromagnetischen Spektrums

Zusammenfassung

Bor-Stickstoff-dotierte polyzyklische aromatische Kohlenwasserstoffe (PAKs) finden aufgrund ihrer Halbleitereigenschaften bereits Anwendung in organischen Leuchtdioden (oLEDs), Feldeffekttransistoren (oFETs) und organischen Solarzellen (oSZs). In dieser Arbeit wurden neue BN-substituierte PAKs synthetisiert und ihre Eigenschaften untersucht.

Für das erste Projekt wurde das erste stabile BNB-Benzo[*fg*]tetracen dargestellt. Mesitylsubstituenten bewirken eine kinetische Stabilisierung der Borzentren. Die Verbindung konnte über vier Synthesestufen mit insgesamt 44 % Ausbeute erhalten werden. Quantenchemische Rechnungen beschreiben das Molekül als *m*-Terphenyl mit einer BNB-Verbrückung.

Für das bekannte (BN)₂-Dibenzoperylen konnte eine neue sechsstufige Syntheseroute mit einer Gesamtausbeute von 12 % entwickelt werden. Diese Route ist zwar länger als die vorher im Arbeitskreis entdeckte, hat aber die Vorzüge, dass Alkylgruppen zur Erhöhung der Löslichkeit eingeführt werden können. Außerdem sind größere Substanzmengen, wie sie für weitergehende Untersuchungen benötigt werden, leichter zugänglich. Dieser PAK besitzt eine chemisch interessante heteroatom-dotierte Buchtregion.

PAKs mit einer Buchtregion können Cycloadditionsreaktionen eingehen. Im folgenden Projekt konnte die erste säurekatalysierte Cycloaddition eines PAK mit BN-Dotierung in der Buchtregion untersucht werden. Als Dienophile wurden insbesondere Benzaldehyde eingesetzt. Diese Reaktionsart erweitert die Möglichkeiten zum Aufbau von PAKs.

Das letzte Projekt beschäftigte sich mit der ersten gezielten Synthese und Charakterisierung eines PAK mit Boroxazinring. Dieser konnte über vier Stufen und mit einer Gesamtausbeute von 34 % dargestellt werden. Quantenchemische Rechnungen erweiterten die Charakterisierung und beschreiben das Molekül als *m*-Quinquephenyl mit innen liegendem B₃N₂O-Kern. Alle Verbindungen wurden hinsichtlich ihrer optischen Eigenschaften untersucht und weisen meist hohe Fluoreszenzquantenausbeuten auf.

Abstract

Boron-nitrogen doped polycyclic aromatic hydrocarbons (PAHs) are used in organic light-emitting diodes (oLEDs), organic field-effect transistors (oFET), and organic solar cells (oSC) due to their semiconducting properties. In this thesis, new BN-substituted PAHs were synthesized and their properties were investigated.

For the first project, the first stabilized BNB-benzo[*fg*]tetracene was established. Mesityl substituents cause a kinetic stabilization of the boron atoms. The molecule can be synthesized in four steps with an overall yield of 44 %. Computations describe the molecule as *m*-terphenyl with an BNB zigzag edge.

For the known (BN)₂-dibenzoperylene, a new synthesis route with six steps and an overall yield of 12 % could be developed. Although, this route is longer than the previous one of the workgroup, it has the advantage of introducing alkyl groups for increasing the solubility. Moreover, larger amounts of substance, which are needed for further investigations, are accessible. This PAH possesses an interesting chemical heteroatom-doped bay-region.

PAHs with a bay-region can undergo cycloaddition reactions. In the following project, the first acid catalyzed cycloaddition reaction of a PAH with BN doping in the bay-region was investigated. As dienophiles, especially benzaldehydes were used. This type of reaction increases the obtained to create BN-PAHs.

The last project employed the first directed synthesis and characterization of a PAH with a boroxazin ring. This can be obtained in four steps with an overall yield of 34 %. Computations extended the characterization and describe the molecule as a *m*-quinquephenyl with an inner B₃N₂O core.

The optical properties of all compounds were investigated and the most compounds feature high fluorescence quantum yields.

Publikationsliste und Eigenanteile

- [1] Fingerle, M.; Maichle-Mössmer, C.; Schundelmeier, S.; Speiser, B.; Bettinger, H. F., *Org. Lett.* **2017**, *19*, 4428-4431.

Synthese und Charakterisierung aller in der Publikation enthaltenen Verbindungen, sowie vollständige, zur Publikation geeignete spektroskopische Charakterisierung der BNB-dotierten Zielverbindung, mittels NMR- und UV/Vis-Spektroskopie, sowie Massenspektrometrie. Züchtung eines Einkristalls der Verbindung zur Aufklärung der Kristallstruktur erfolgten. Quantenchemische Rechnungen am Zielsystem, sowie an zwei Vergleichsmoleküle erweiterten die Charakterisierung.

Röntgenbeugungsexperimente führte Dr. Cäcilia Maichle-Mössmer durch und löste die Struktur.

Simon Schundelmeier sowie Prof. Dr. Bernd Speiser brachten Cyclovoltammetrieexperimente ein und die Analyse der daraus erhaltenen Daten.

Die gesamte Projektidee und Betreuung gehen auf Prof. Dr. Holger F. Bettinger zurück.

- [2] Fingerle, M.; Stocker, S.; Bettinger, H. F., *Synthesis* **2019**, *51*, 4147-4152.

Synthese der bekannten Verbindung auf neuer Route sowie vollständige, zur Publikation geeignete spektroskopische Charakterisierung aller Verbindungen, mithilfe von NMR- und UV/Vis-Spektroskopie, sowie Massenspektrometrie. Weitere Charakterisierung erfolgt mittels quantenchemischen Rechnungen.

Von Prof. Dr. Holger Bettinger stammt die Projektidee. Simon Stocker half unter meiner Anleitung bei den Synthesen und Charakterisierungen.

- [3] Fingerle, M.; Bettinger, H. F., *Chem. Commun.* **2020**, *56*, 3847-3850.

Synthese aller in der Publikation enthaltenen Verbindungen, sowie vollständige, zur Publikation geeignete spektroskopische Charakterisierung mit Massenspektrometrie, sowie

NMR- und UV/Vis-Spektroskopie. Die Züchtung von Einkristallen zur Aufklärung der Struktur erfolgte. Quantenchemische Rechnungen erweitern die Charakterisierungen. Die Projektidee stammt von Prof. Dr. Holger F. Bettinger, der auch quantenchemische Rechnungen (NTOs und ACID) beisteuerte.

Dr. Hartmut Schubert stand für das Röntgenbeugungsexperiment, sowie zur Lösung der Struktur bereit und Dr. Christina Tönshoff lieferte UV/Vis-Experimente mittels Matrixisolationstechnik.

- [4] Fingerle, M.; Dingerkus, J., Schubert, H., Wurst, K., Scheele, M., Bettinger, H. F., *Angew. Chem. Int. Ed.* **2021**, *60*, 15798-15802.

Synthese aller in der Publikation enthaltenen Verbindungen, sowie vollständige, zur Publikation geeignete Charakterisierung mittels NMR- und UV/Vis-Spektroskopie, sowie der Massenspektrometrie. Die Züchtung eines Einkristalls erfolgte und konnte zur Aufklärung einer Struktur beitragen. Quantenchemische Rechnungen ergaben ein Vorschlag zum Mechanismus der neuen heteroatom-beteiligten Cycloaddition.

Juliane Dingerkus unterstützte bei den Synthesen und bei der Züchtung von Einkristallen. Dr. Hartmut Schubert stand für das Röntgenbeugungsexperiment zur Verfügung und löste die Struktur. Kai Wurst und Prof. Dr. Marcus Scheele brachten Cyclovoltammetrieexperimente ein und die Analyse der daraus erhaltenen Daten.

Die Projektidee und Betreuung gehen auf Prof. Dr. Holger F. Bettinger zurück.

Alle Publikationen sind im Anhang hinterlegt und deren Ergebnisse werden in der vorliegenden Dissertation diskutiert. Für die Reproduktion und Vervielfältigung wurde die Zustimmung der jeweiligen Verlage eingeholt. Verwendete Abbildungen aus den Publikationen wurden hinsichtlich ihrer Größe und Verbindungsnummer in die vorliegende Dissertation eingebunden, sowie deren Beschriftung ins Deutsche übersetzt.

1 Einleitung

1.1 Polyzyklische aromatische Kohlenwasserstoffe und ihre Eigenschaften

Polyzyklische aromatische Kohlenwasserstoffe (PAKs) oder auch „polycyclic aromatic hydrocarbons“ (engl. PAHs) erlangten in den vergangenen Jahren eine zunehmende Bedeutung in der Forschung. Begründet liegt dies in ihren interessanten photophysikalischen und elektrochemischen Eigenschaften.¹⁻⁵ Ein dabei wichtiger Zusammenhang ist die Größe der Moleküle und der daraus resultierende Abstand zwischen den Grenzorbitalen HOMO (engl. „Highest Occupied Molecular Orbital“) und LUMO (engl. „Lowest Unoccupied Molecular Orbital“). Kleine organische π -Systeme besitzen im Allgemeinen ein großen HOMO-LUMO-Abstand, was sie zu elektrischen Isolatoren macht. Im 2D-unendlich ausgedehnten Graphen verschwindet der HOMO-LUMO-Abstand und es handelt sich um einen elektrischen Leiter.⁶ Wird genau an dieser Stellschraube für die Größe des π -Systems feiner gedreht, können Moleküle mit Halbleitereigenschaften synthetisiert werden, die ihren Einsatz in elektrischen Bauteilen, wie organische Leuchtdioden (oLEDs),⁷⁻¹⁰ organischen Feldeffekttransistoren (oFETs)^{11,12} oder auch organischen Solarzellen finden.^{6,12} Moleküle, die große Ausschnitte aus Graphen darstellen werden auch als Nanographenmoleküle bezeichnet.^{13,14}

1.2 Der isoelektronische Austausch

Ein isoelektronischer Austausch ist ein Austausch auf atomarer Ebene, ohne die Anzahl der Valenzelektronen zu verändern. Zwei Kohlenstoffatome (je 4 Valenzelektronen) bringen zusammen 8 Valenzelektronen ein und für Bor (3 Valenzelektronen) und Stickstoff (5 Valenzelektronen) erhält man ebenfalls 8 Valenzelektronen. Trotz dieser isoelektronischen Bezie-

lung wirken sich solche Änderungen auf die Moleküleigenschaften aus.^{15,16} Bor und Stickstoff besitzen unterschiedliche Elektronegativitäten (B 2.01 und N 3.07 nach Allred-Rochow¹⁷), was sich in der Entstehung eines Dipolmoments zeigt und den HOMO-LUMO-Abstand beeinflusst.^{18,19}

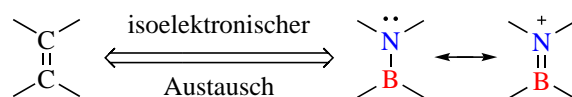


Abbildung 1.1: Isoelektronischer Austausch von einer CC-Doppelbindung durch eine BN-Einheit.

Gleichzeitig wird dieser BN-Austausch als isosterisch bezeichnet, da sowohl die Bindungslängen als auch die Kovalenzradien der BN- und CC-Einheit sehr ähnlich sind (Graphen: C-C-Bindung = 142 pm, h-Bornitrid: B-N-Bindung = 144 pm).^{20,21}

Das anorganische Analogon zu Graphen ist das hexagonale Bornitrid (h-BN), das durch vollständigen isoelektronischen Austausch von je zwei Kohlenstoff-Atomen (CC-Einheit) durch Bor- und Stickstoffatome (BN-Einheit) entsteht.^{22–24}

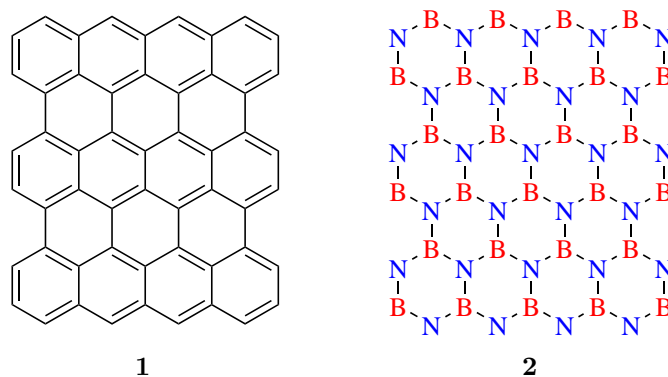


Abbildung 1.2: Ausschnitte aus Graphen (**1**) und hexagonalem Bornitrid (**2**).

Das hexagonale Bornitrid **2** besitzt eine Bandlücke von 6 eV und ist somit als Isolator zu betrachten.²⁵ Folglich verändert das Austauschen von CC-Paaren durch isoelektronische und isosterische BN-Paare den HOMO-LUMO-Abstand in Abhängigkeit der Position und der Substitutionskonzentration.^{26,27} Ist man in der Lage diesen Austausch gezielt auszuführen

erhält man eine weitere Stellschraube, um Moleküle mit Halbleitereigenschaften zu entwickeln und zu synthetisieren.

1.3 Fortschritte in der Synthese von BN-dotierten PAKs

1.3.1 Synthesestrategien für BN-dotierte PAKs

Die Synthese von BN-dotierten PAKs erfordert den Aufbau von Bindungen zwischen unterschiedlichen Atomen. Dazu zählen die B-N- und B-C-Bindungen, sowie die C-C- und N-C-Bindungen. Für alle vier Bindungsknüpfungen im Zuge des Aufbaus von BN-PAKs soll je ein Beispiel gezeigt werden.

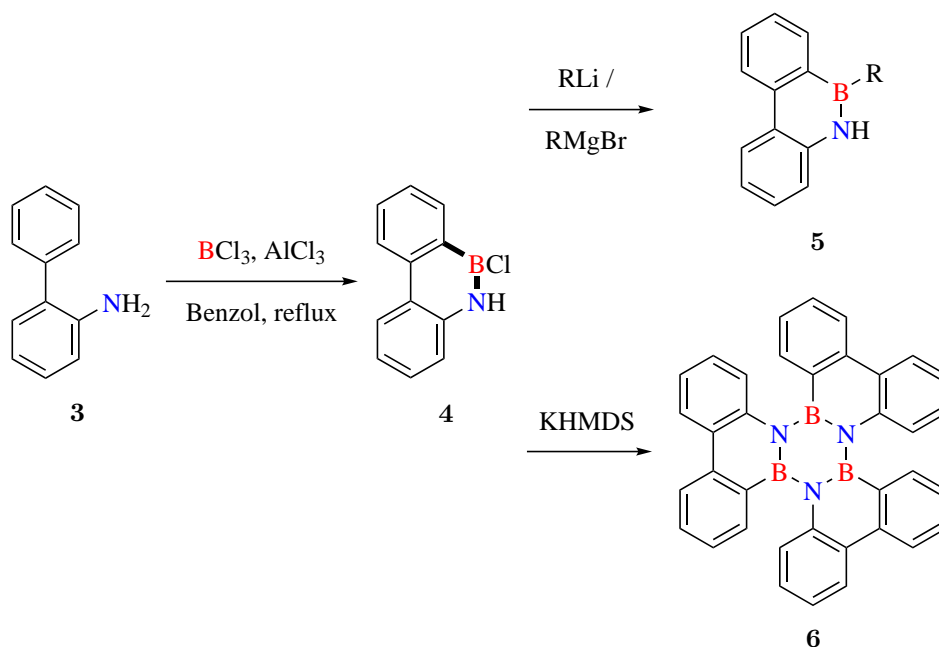


Abbildung 1.3: Elektrophile Borylierung am 2-Aminobiphenyl (**3**) mittels Ausbildung einer B-N- und B-C-Bindung.

Die Anfänge der BN-Substitution von PAKs gehen auf Dewar et al. zurück.²⁸ Die Arbeitsgruppe untersuchte die Synthese und Eigenschaften des 10-Chlor-10,9-borazarophenanthrens (**4**). Dabei wurde das 2-Aminobiphenyl (**3**) in einer elektrophilen Borylierung umgesetzt (s. Abb. 1.3). Es wird zunächst ein Lewis-Säure-Base-Komplex aus dem 2-Aminobiphenyl (**3**)

und Bortrichlorid (BCl_3) gebildet. In der Reaktionshitze erfolgt die Abspaltung von Salzsäure (HCl). Mittels katalytischen Mengen von Aluminiumtrichlorid (AlCl_3) kann jetzt zusätzlich eine B-C-Zyklisierung ablaufen, was vergleichbar ist mit einer Friedel-Crafts-Reaktion. Derartige elektrophile Borylierungen liefern folglich BN-dotierte PAKs mittels B-N-, sowie B-C-Bindungsknüpfung.

Verbindung **4** weist zudem BN-Substitution an der äußeren Peripherie des Moleküls auf, welche eine gewisse Reaktivität mit sich bringt. So kann beispielsweise eine Substitution am Boratom zu Derivaten von **5** erfolgen^{28,29} oder unter basischen Bedingungen eine Trimerisierung unter Ausbildung des Borazinkerns in **6**.³⁰

Ein CC-Ringschluss nach der BN-Bindungsbildung wurde von Bosdet et al. für das BN-Pyren **9** beschrieben.³¹ Ausgehend von einem Boracyclohexadien **7** und einem bis(*ortho*-ethinyl)-substituierten Pyridin **8** wird zuerst eine BN-Bindung ausgebildet. Dieses Borabenzol-Pyridinderivat geht rasch eine C-C-Knüpfung zum BN-Phenanthren ein, bevor die zweite C-C-Knüpfung in einer palladiumkatalysierten Cycloisomerisierung zum BN-Pyren **9** erfolgt.

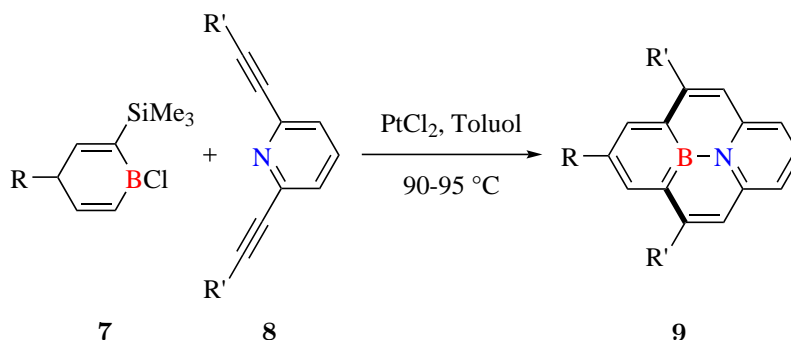


Abbildung 1.4: Aufbau eines im Inneren dotierten Polyzyklus mittels C-C-Ringschluss.

Damit konnte der erste PAK mit BN-Substitution erhalten werden, welche vollständig von einem Kohlenstoffgerüst umgeben ist. Die Reaktivität der BN-Einheit in **9** wird im Vergleich zu Dewars BN-Phenanthren **4** stark reduziert.

Die letzte Synthesestrategie besteht aus einem abschließenden N-C-Ringschluss und wurde

von Kähler et al. 2019 beschrieben (s. Abb. 1.5).³² In einer goldkatalysierten Addition der NH-Funktionen an die Alkynylgruppen bildet sich das zweifach BN-dotierte Perylen **11** aus.

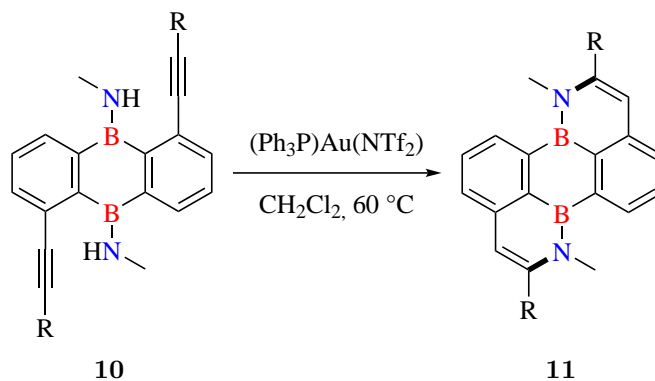


Abbildung 1.5: N-C-Bindungsknüpfung als Möglichkeit zum Aufbau von BN-dotierten PAKs.

Seit Beginn der BN-Substitution von Dewar et al. entstand eine Vielzahl von 1,2-Dihydro-1,2-azaborinverbindungen,^{16,33–35} ebenso wie 1,4-Azaborine.^{35–47} Diese und weitere BN-dotierte PAKs wurden hinsichtlich ihres möglichen Einsatzes in oLEDs^{32,48–57} oder im weiten Feld der Halbleitertechnik hin entwickelt.^{15,31,58–74}

Weitere BN-dotierte PAKs dienen dieser Arbeit als Grundlage und sollen hier vorgestellt werden. Sie sind Abwandlungen und Ausschnitte des dreifach BN-dotierten Hexa-*peri*-benzocoronon (BN-HBC) **13**, dessen Synthesen ebenfalls genauer beleuchtet werden sollen.

1.3.2 Darstellungen des BN-HBCs

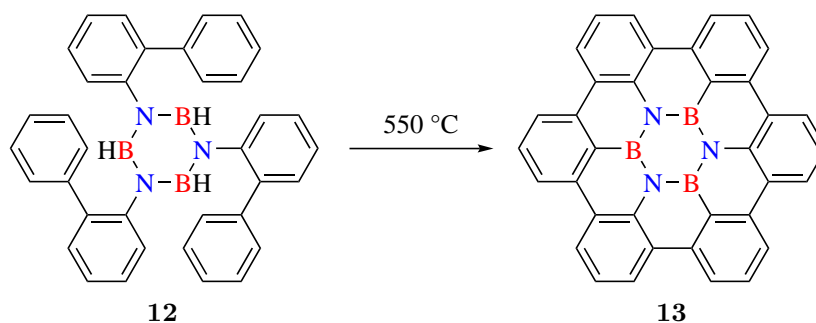


Abbildung 1.6: Erste Synthese des BN-HBCs **13**.

Das Nanographenmolekül **13** konnte 2015 erstmals von Krieg et al. in einer Festkörperreaktion bei 550 °C aus dem Borazin **12** synthetisiert werden.⁶⁹ Während der Reaktion werden drei B-C-, sowie drei C-C-Bindungen unter Abspaltung von sechs Äquivalenten Wasserstoff ausgebildet. Um den Wasserstoff aus der Reaktion zu entfernen, wird ein Stickstoffstrom über die Reaktionsmischung geleitet. Das BN-HBC **13** stellt ein planares Hexabenzocoronon dar, mit einem innen liegenden und völlig eingebauten Borazinring. Das Borazin selbst ist seit 1926 durch A. Stock und E. Pohland als Benzolanalogon bekannt.⁷⁵ Weitere Synthesen eines BN-HBC-Derivats erfolgten von der Gruppe um Bonifazi.^{76,77}

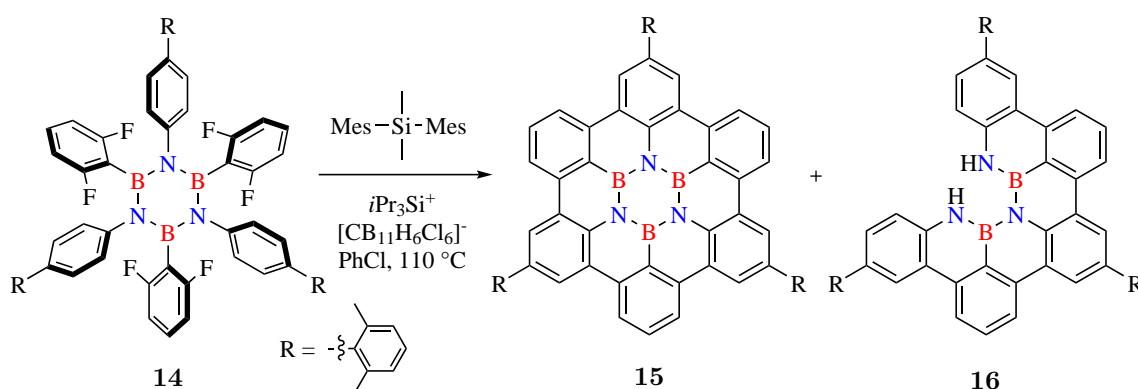


Abbildung 1.7: Erste BN-HBC Synthese von Bonifazi et al.

Das Hexaphenylborazinmolekül **14** wurde in einer Friedel-Crafts-artigen Reaktion umgesetzt. Mittels dieser durch Silylkationen katalysierten Reaktion nach Allemann et al.,⁷⁸ konnten sechs C-C-Bindungen geschlossen werden.⁷⁶ Die Reaktion liefert das BN-HBC **15** mit einer Ausbeute von 5 %. Das Nebenprodukt **16** konnte ebenfalls erhalten werden, was auf eine teilweise Hydrolyse während der Reaktion hindeutet.

Um diese Reaktion zu optimieren, wurde ein anderes Ausgangsprodukt gewählt, indem sich nun mono-fluorierte Phenylreste um den Borazinkern anordnen (s. Abb. 1.7).⁷⁷ Die Ausbeute von **15** konnte hierbei auf 15 % gesteigert werden. Gleichzeitig wurde ein anderes Nebenprodukt **18** erhalten, das nun einen Boroxazinring ($\text{B}_3\text{N}_2\text{O}$) trägt. Verbindung **18** kann als Abwandlung des BN-HBCs **15** angesehen werden, indem eine Anilineinheit entfernt wird und ein Sauerstoffatom die beiden Boratome verbrückt. Boroxazine sind bislang nur als kleine

Moleküle bekannt,^{79–84} während gezielte Synthesen und Charakterisierungen von Boroxaziningen in PAKs trotz ihrer möglichen oLED-Anwendung noch nicht erforscht sind.⁸⁵

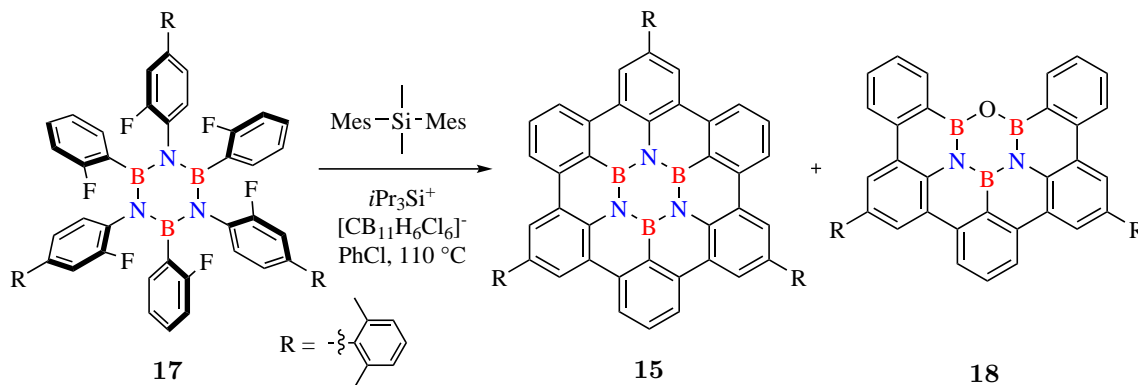


Abbildung 1.8: Optimierte BN-HBC Synthese von Bonifazi et al.

1.3.3 Das (BN)₂-Dibenzoperylen als BN-HBC-Ausschnitt

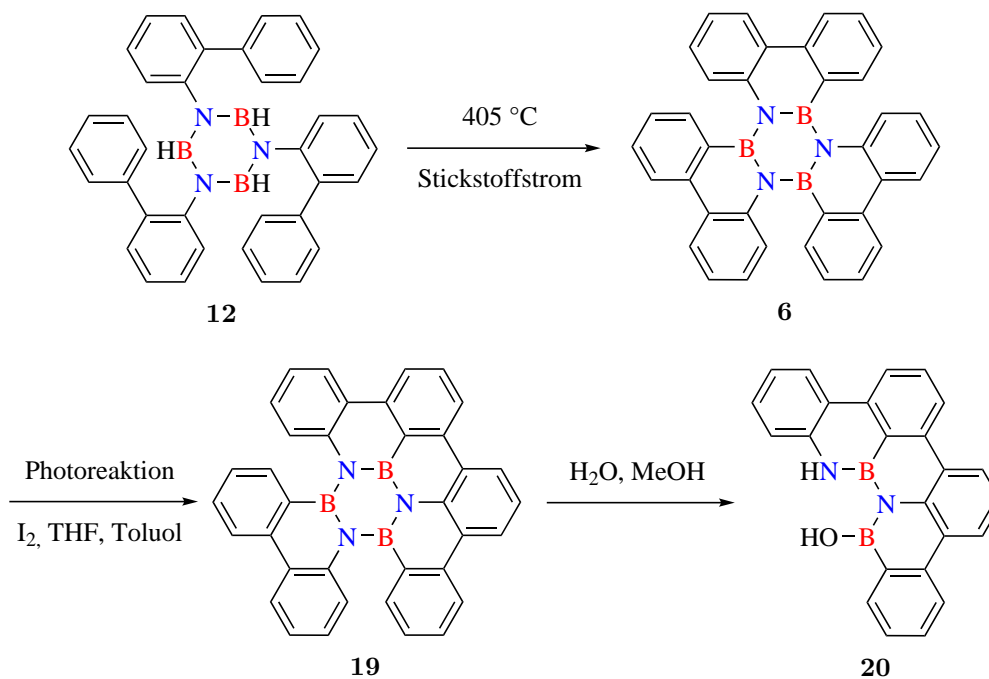


Abbildung 1.9: Syntheseroute des BN-Dibenzoperylen 20.

Entfernt man aus dem BN-HBC **13** eine BN-substituierte Phenanthreneinheit, wird ein NBNB-dotiertes Dibenzoperylen **20** erhalten. Die Synthese der Verbindung **20** ist von Müller et al. bekannt (s. Abb. 1.9).⁸⁶ In einem ersten Schritt wird die Borazinverbindung **12** nach Köster et al. auf 405 °C erhitzt.^{87,88} Hierbei bilden sich drei B-C-Bindungen aus und es entstehen zueinander verdrehte Phenanthreneinheiten um den Borazinring in **6**. Anschließend erfolgt in einer Belichtungsreaktion eine oxidative CC-Knüpfung zu **19**, welche unter Hydrolyse in das (BN)₂-Dibenzoperylen **20** zerfällt.⁸⁶ Verbindung **20** bringt eine interessante Buchtregion-Dotierung mit sich, da solche bisher wenig bekannt sind (als Beispiel sei hier die in Abb. 1.7 gezeigte NBNBN-Dotierung in **16** genannt⁷⁶) und Kohlenstoffsysteme genau an diesen Stellen Cycloadditionsreaktionen eingehen.^{89–94}

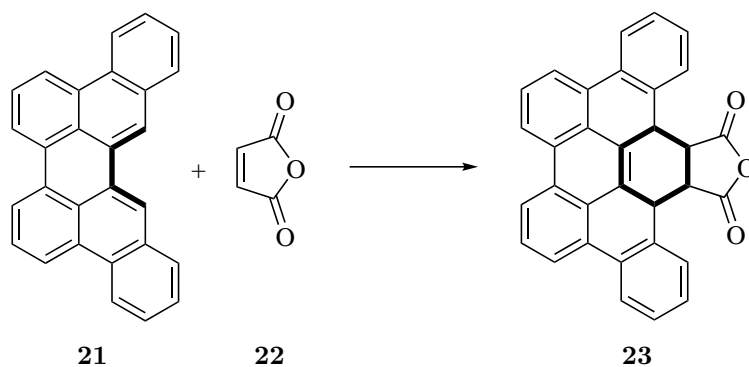


Abbildung 1.10: Reaktion von Maleinsäureanhydrid (**22**) mit Dibenzoperylen (**21**) in der Buchtregion (markiert).

Diese wurden besonders am Perylen und Dibenzoperylen untersucht (s. Abb. 1.10).⁸⁹ Mit geeigneten Dienophilen konnten so die bisher erhaltenen PAKs erweitert und auch deren Eigenschaften verändert werden. Außerdem wurde postuliert, dass mittels Cycloadditionsreaktionen, Kohlenstoffnanoröhren vergrößert werden könnten.^{95,96}

Bislang sind keine analogen Cycloadditionen von buchtregion-dotierten PAKs bekannt. Lediglich Paetzold beobachtete Hetero-Diels-Alder Reaktionen von Diazadiboretidinen **24** unter Ringerweiterung mit verschiedenen Aldehyden (s. Abb. 1.11) und Iminoboranen, sowie dem Dimethylacetylendicarboxylat (DMAD).^{97–99}

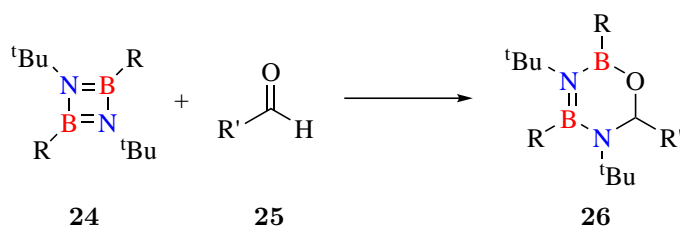


Abbildung 1.11: Heteroatom-beteiligte Cycloaddition von Diazadiboretidine **24**.

1.3.4 Benzotetracene

Teilt man das BN-HBC **13** in zwei Hälften, erhält man je ein Terphenyl, das mit einer NBN- sowie einer BNB-Einheit verbrückt ist. Diese Moleküle könnte man auch als NBN- respektive BNB-Benzo[*fg*]tetracene bezeichnen. Das NBN-Benzotetracene erlangte einige Aufmerksamkeit, sowohl als Grundgerüst für weitere Synthesen, als auch in der Materialwissenschaft (s. Abb. 1.12).^{71,100–103}

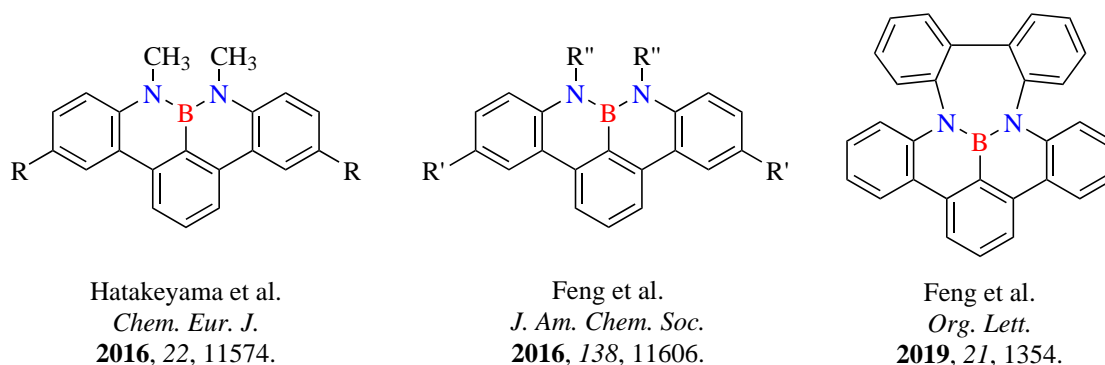


Abbildung 1.12: Auswahl verschiedener NBN-Benzotetracene.

Dagegen konnte das Pendant, das BNB-Benzotetracene, bis 2017 nur als Zwischenstufe **28** postuliert, aber nicht isoliert werden.¹⁰⁴ Die Gruppe um Shibasaki und Kumagai wiesen **28** mit den zwei Hydroxygruppen eine hohe Reaktivität zu, da das Molekül instantan mit Boronsäuren zu **29** reagiert.

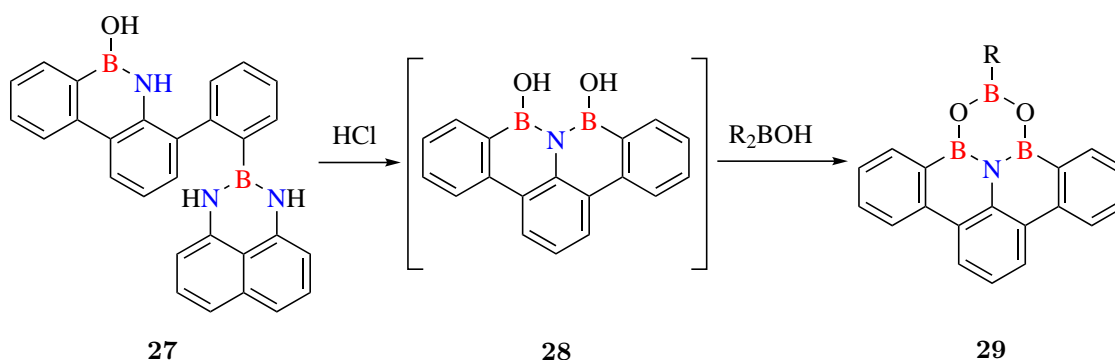


Abbildung 1.13: Darstellung des BNB-Benzotetracens **28** als reaktive Zwischenstufe.

Scholz et al. beschrieben 2020 die Synthese und Untersuchung eines BNB-dotierten Benzotetracens hinsichtlich der optoelektronischen Eigenschaften, das dank einer Naphtylverbrückung der beiden Boratome hohe Stabilität aufweist.⁷⁴ In einem ersten Schritt reagierten dabei das Aminoterphenyl **30** mit dem Diboran des Naphthalins unter Abspaltung von molekularem Wasserstoff. Mittels Magnesiumspänen konnte die Zielverbindung **32** in einer nukleophilen B-C-Kupplung dargestellt werden.

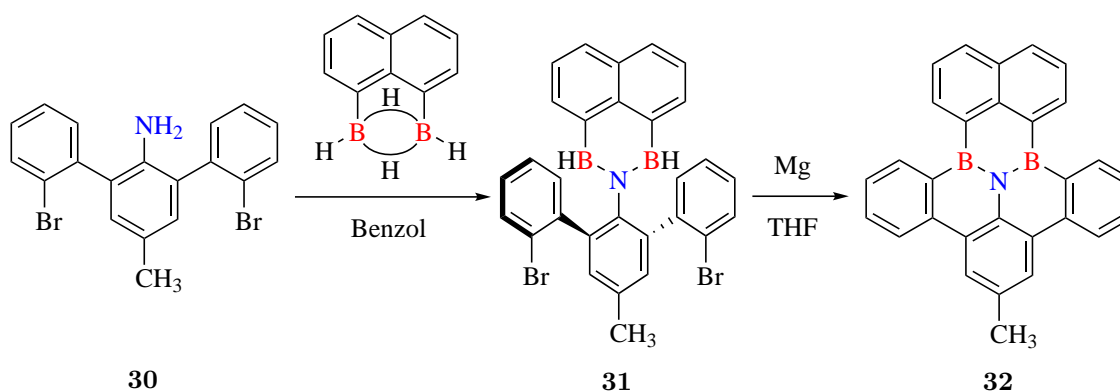


Abbildung 1.14: Synthese eines BNB-dotierten Benzotetracens nach Scholz et al.

2 Zielsetzung

2.1 Synthese eines BNB-Benzotetracens

Ausgehend von kleinen kommerziellen Molekülen wie dem Anilin sollte das Ziel dieses Projektes die Synthese eines stabilisierten BNB-Benzotetracens sein. Shibasaki und Kumagai postulierten für solch ein Dotierungsmuster lediglich eine Zwischenstufe und verfolgten mit ihren Synthesen auch andere Ziele, nämlich neue Katalysatoren für die Carbonsäureamidbildung zu untersuchen.¹⁰⁴

Für die Darstellung sollte das Augenmerk besonders auf der Einführung des zweiten Boratoms liegen, denn die erste Borylierung konnte bereits erfolgreich in meiner Masterarbeit durchgeführt werden.¹⁰⁵ Nach Erhalt der Zielverbindung sollte das Molekül mittels Kristallstrukturanalyse nachgewiesen und mit allen gängigen Methoden die physiko-chemischen Eigenschaften erforscht werden. Dazu wurden auch quantenchemische Rechnungen angestellt.

2.2 Entwicklung einer neuen Syntheseroute für ein

(BN)₂-Dibenzoperylen zur Untersuchung der Reaktivität

Um die Reaktivität des bereits bekannten (BN)₂-Dibenzoperylens besser untersuchen zu können, soll im Rahmen dieses Projektes eine neue Syntheseroute entwickelt werden, die zum einen im Grammmaßstab durchführbar ist und gleichzeitig die Einführung von *n*-Butylresten zur Verbesserung der Löslichkeit mit sich bringt. Die Route von Müller et al. wäre hierfür nicht gut geeignet, da die Photoreaktion nur in sehr verdünnten Lösungen stattfinden kann und so ein Hochskalieren der Syntheseroute einen erheblichen Aufwand bedeuten würde.⁸⁶

2.3 Cycloadditionen von PAKs in der Buchtregion unter Beteiligung von Heteroatomen

Vor dem Hintergrund der Cycloadditionen von PAKs soll im folgenden untersucht werden, ob diese Reaktionen an heteroatom-dotierten Buchtregionen ebenfalls möglich sind. Das dafür infrage kommende Perylen und Dibenzoperylen wurde bereits in Abb. 1.5 und Abb. 1.9 beschrieben.^{32,86} In Kap. 3.2 wird ebenfalls die Syntheseroute eines (BN)₂-Dibenzoperylens **48** vorgestellt, die speziell für diese weitere Untersuchung entwickelt wurde.

Für **48** sollen zuerst mittels quantenchemischen Rechnungen geeignete Dienophile gesucht und diese dann zur Reaktion gebracht werden. Alle so erhaltenen Cycloadditionsprodukte sollen charakterisiert und ein möglicher Mechanismus der Cycloaddition postuliert werden.

2.4 Darstellung eines Nanographenmoleküls mit einem B₃N₂O-Kern

Grundlage und Ideengabe für dieses Projekt war die Synthese des (BN)₂-Dibenzoperylen. Dort konnte bereits das zweifach bromierte NBN-Benzotetracen als Nebenprodukt isoliert werden.¹⁰⁶ Ausgehend von diesem Molekül soll die erste gezielte Synthese eines Nanographenmoleküls mit Boroxazinring etabliert werden. Nach erfolgreicher Synthese soll der neuartige PAK mittels physiko-chemischen Methoden, sowie quantenchemischen Rechnungen untersucht und charakterisiert werden.

3 Ergebnisse und Diskussion

3.1 Das erste stabile BNB-Benzotetracen

Mit der in Abb. 3.1 gezeigten Syntheseroute konnte ausgehend von **33**, einem bekannten Aminoterphenylmolekül,¹⁰⁷ das erste stabile BNB-Benzotetracen dargestellt werden. Erste Versuche, **33** in einer doppelten Borylierungsreaktion mit BCl_3 und Aluminiumtrichlorid zu erhalten, scheiterten. Auch elektrophilere Reagenzien wie BBr_3 und BI_3 führten lediglich zu einem 1,2-Dihydro-1,2-azaborin Derivat von **34**. Daraus lässt sich schließen, dass nach einem ersten Angriff die Nukleophilie des Stickstoffatoms stark herabgesetzt wird und die Boratome schrittweise eingeführt werden müssen. Für die erste Borylierung konnte auf die Anleitung von Dewar et al. zurückgegriffen werden.²⁸ Aufgrund der hohen Empfindlichkeit gegenüber Wasser, wurde **34** nicht aufgereinigt, sondern direkt mit einer Mesitylgruppe behandelt. Damit konnte eine stabile Verbindung erhalten werden, die säulenchromatographischer Aufreinigung stand hält. Die Synthese konnte allerdings erst erfolgreich ablaufen, als vom gekauften Mesitylmagnesiumbromid in Diethylether das Lösungsmittel entfernt und der verbleibende Feststoff für die Reaktion eingesetzt wurde. Andernfalls führen etherische Lösemittel zu Nebenreaktionen und erheblichen Mengen an Nebenprodukten.

Für eine zweite Borylierung musste die Nukleophilie des Stickstoffatoms in **35** gesteigert werden. Dies gelang durch Deprotonierung mit Kaliumhexamethyldisilazid (KHMDs), einer nicht nukleophilen Base. Durch die wiederholte Umsetzung mit BCl_3 und AlCl_3 konnte das zweite Boratom erfolgreich eingeführt werden. Jedoch wurde in der Massenspektrometrie das Produkt **36** mit $m/z = 389$ gefunden, was für eine Abspaltung der Mesitylgruppe während der zweiten Borinsertion spricht. Aufgrund des erneut hohen Hydrolysepotentials von **36** und der Tatsache, dass hier ein stabiles BNB-Benzotetracenderivat synthetisiert werden soll, wurde auch **36** mit Mesitylmagnesiumbromid (als Feststoff) behandelt. Verbindung **37** kann-

te mittels Säulenchromatographie aufgereinigt und in einer Gesamtausbeute von 44 % über vier Stufen erhalten werden. Die Charakterisierung von **37** erfolgte über NMR-Spektroskopie und Massenspektrometrie, sowie Elementar- und Kristallstrukturanalyse.

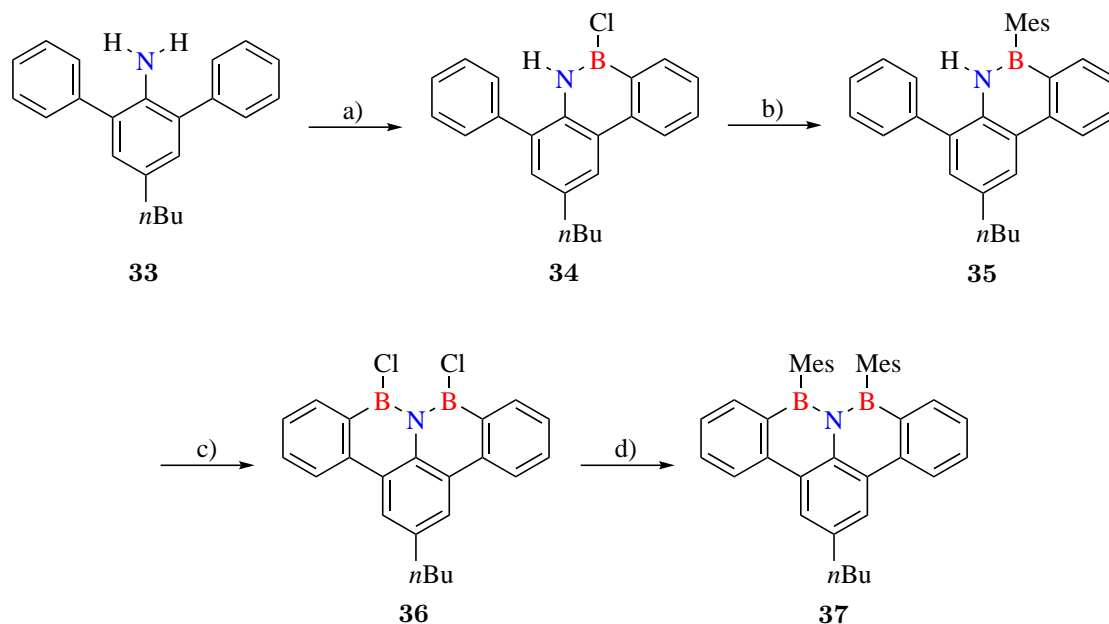


Abbildung 3.1: Syntheseroute für das erste stabile BNB-Benzotetracen **37**; a) 1.0 Äq. **33**, 1.8 Äq. BCl_3 , Toluol, 6 h reflux, 0.2 Äq. AlCl_3 , 18 h reflux, Rohprodukt wird nicht aufgereinigt; b) 1 Äq. **34**, 3 Massen-Äq. MesMgBr (als Feststoff), Benzol, 1 h, rt, 67 % über zwei Stufen; c) (i) 1.0 Äq. **35**, 1.0 Äq. KHMDs , Toluol, $-10\text{ }^\circ\text{C}$, (ii) 3.0 Äq. BCl_3 , 0.2 Äq. AlCl_3 , 18 h reflux, Rohprodukt wird nicht aufgereinigt; (d) 1 Äq. **36**, 6 Massen-Äq. MesMgBr (als Feststoff), Benzol, 1 h, rt, 65 % über zwei Stufen.

Einkristalle zur Strukturaufklärung konnten aus *n*-Hexan gewonnen werden. Dabei kristallisiert **37** in der monoklinen Raumgruppe $P2_1$ mit zwei Enantiomeren und zeigt C_2 -Symmetrie (s. Abb. 3.2). Aufgrund der großen Mesitylreste und den dafür benötigten Raum, ist die Tetraceneinheit um 32° verdreht, gemessen an den äußeren Kohlenstoffatomen C1-C4. Die Mesitylreste orientieren sich nahezu senkrecht zu ihren jeweils geknüpften Ringen im Tetracengerüst. Aufgrund dieser Molekülstruktur und der dadurch nicht ausprägbarer π -Stapelpackung zeigen die vier Moleküle in der Zelle eine helikale Anordnung. Die BN-Bindungsängen betragen im Mittel 1.46 \AA und sind vergleichbar mit typischen BN-Bindungen in PAKs ($1.45 - 1.47\text{ \AA}$).^{15,31}

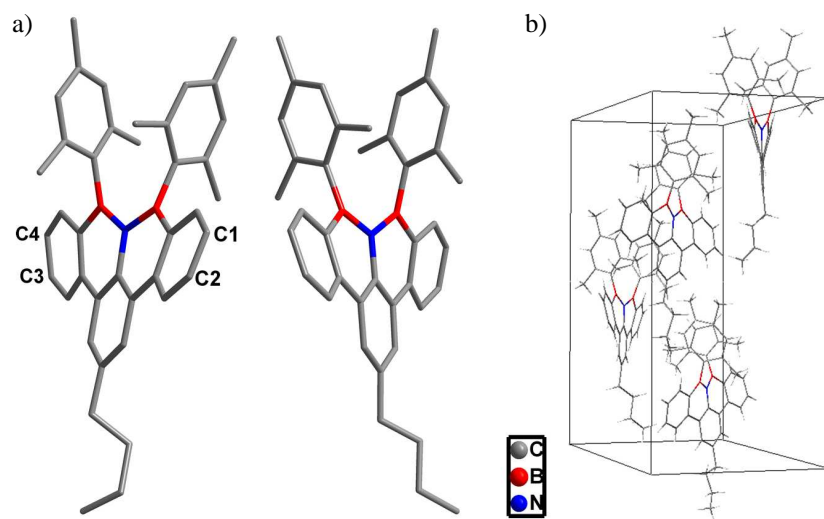


Abbildung 3.2: (a) Molekülstrukturen von **37** (ohne Wasserstoffatome); (b) Molekülpackung.

Mittels quantenchemischer Rechnungen (B3LYP/6-311+G**) sollte die Racemisierungsbarriere der beiden Enantiomere untersucht werden. Um Rechenkapazität zu sparen, wurde hierfür Molekül **38** ohne *n*-Butylgruppe betrachtet. Der Übergangszustand, der die beiden Enantiomere verknüpft weist C_S -Symmetrie auf und ist gerade einmal 4.2 kcal/mol höher in Energie als die einzelnen Enantiomere. Eine sehr kleine Barriere lässt sich auch aus den NMR-Experimenten ablesen, da dort die ortho-CH₃ Gruppen der Mesityleinheiten lediglich ein gemeinsames Signal zeigen. Aufgrund dieser Erkenntnisse sollte keine Trennung des Enantiomerengemischs möglich sein.

Um diese neue Verbindung weiter zu charakterisieren, wurde ein Absorptionsspektrum von **37** in Dichlormethan aufgenommen (s. Abb. 3.3), welches zwei Hauptabsorptionsbanden in der Region von 280 - 300 nm sowie 325 - 375 nm zeigt. Das Fluoreszenzspektrum von **37**, gemessen bei einer Anregungswellenlänge von 366 nm, zeigt eine breite Bande bei 413 nm ohne Feinstruktur und ohne Spiegelbild zum Absorptionsspektrum. Ein Spiegelbildverhältnis der Spektren tritt gewöhnlich bei Tetracen Verbindungen auf.^{108,109} Ungleichheit zwischen Absorption und Emission impliziert eine Veränderung der Molekülgeometrie im angeregten Zustand S_1 . Dadurch ändern sich die Energieabstände der Vibrationszustände und können

nicht mehr mit denen im Grundzustand verglichen werden.¹¹⁰ Quantenchemische Berechnungen des angeregten Zustandes S_1 zeigen eindeutig einen Rückgang der Verdrehung im Tetracengerüst auf 21° (vgl. Abb. 3.2). Mit diesem veränderten Twist lässt sich auch die große Stokesverschiebung von 3109 cm^{-1} erklären. Quantenchemischen Rechnungen zeigen weiter, dass hierbei zusätzlich ein Charge-Transfer Effekt auftritt (s. Abb. 3.4). Das HOMO von **38** ist auf den Mesitylresten lokalisiert, während das LUMO sich auf dem Benzotetracengerüst verteilt. Vergleichssysteme wie das 5,12-Bis(triisopropylsilylethynyl)tetracene oder NBN-Benzo[*fg*]tetracene weisen Stokesverschiebungen von $241 - 411\text{ cm}^{-1}$,^{108,109,111} bzw. $800 - 1500\text{ cm}^{-1}$ auf.^{100,101}

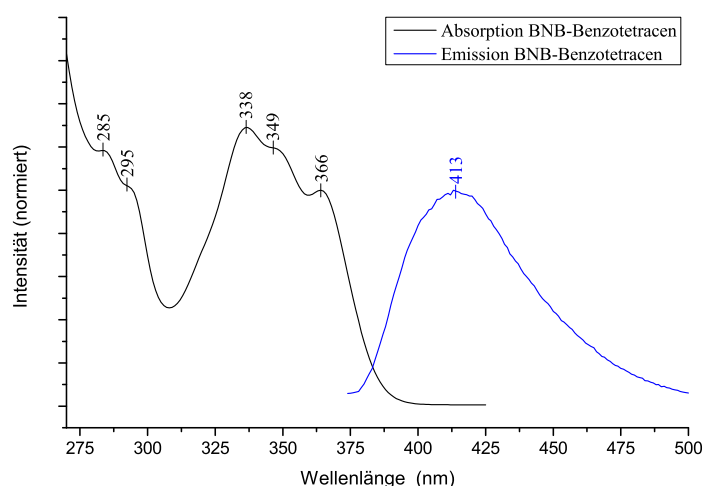


Abbildung 3.3: Absorptions- (schwarz) und Fluoreszenzspektrum (blau, $\lambda_{\text{ex}} = 366\text{ nm}$) von **37** (10^{-5} M in CH_2Cl_2).

Zusätzlich zu den UV/Vis- und Fluoreszenzmessungen konnte die Fluoreszenzquantenausbeute von **37** in Dichlormethan mit $\phi_{\text{Fl}} = 0.21$ ermittelt werden. Vergleichssysteme wie NBN-Benzo[*fg*]tetracene weisen mit $\phi_{\text{Fl}} = 0.21 - 0.24$ sehr ähnliche Messwerte auf.¹⁰⁰ Als Referenz konnte auf Anthracen in Ethanol zurück gegriffen werden ($\phi_{\text{Fl}} = 0.27$).^{112,113} Das isoelektronische Pendant zum synthetisierten BNB-Benzo[*fg*]tetracene **37** ist das bislang unbekannte Kohlenwasserstoffkation **40**. Zahradnik et al. postulieren aufgrund einer Extrapolation, dass die größte Absorption des Moleküls im Bereich von 575 nm zu liegen

kommt.¹¹⁴ Quantenchemische Rechnungen (TD-B3LYP/6-311+G**) unterstützen diese Behauptung mit einer Absorption von 545 nm. Obwohl das planare BNB-Benzotetracen **39** (mit Wasserstoffsubstitution an den Boratomen) und **40** den Berechnungen nach sehr ähnliche Molekülorbitale aufweisen, unterscheiden sich die Orbitalenergien der beiden aufgrund der BNB-Substitution bzw. der positiven Ladung (s. Abb. 3.4). Dies verursacht eine bathochrome Verschiebung um 1.5 eV.

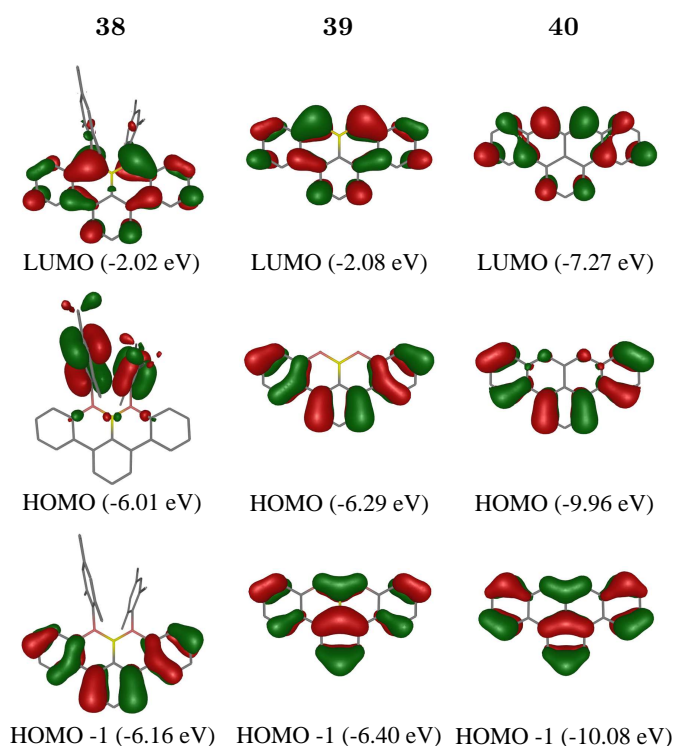


Abbildung 3.4: Berechnete Molekülorbitale (B3LYP/6-311+G**) von BNB-Benzotetracen **38** (ohne *n*-Butylgruppe), BNB-Benzotetracen mit zwei Wasserstoffatome **39** und dem PAK-Kation **40**.

Abb. 3.5 zeigt quantenchemische Untersuchungen (B3LYP/6-311+G**) der Aromatizität von Verbindung **38**. Die kernunabhängige chemische Verschiebung (engl. „nucleus-independent chemical shift“, NICS), in diesem Fall der NICS(0)-Wert, kann ein Maß für die Aromatizität individueller Ringe in PAKs sein.^{115–117} Die drei äußeren Ringe von **38** zeigen mit Werten von -6.5 und -7.2 aromatischen Charakter. Die beiden anderen Ringe mit BN-Substitution haben mit positiven Werten von 2.4 nicht-aromatische Eigenschaften. Das ver-

wandte NBN-Benzotetracen **39** besitzt mit C_{2v} zwar eine höhere Symmetrie als **38**, jedoch ähnliche NICS(0)-Werte. Diese Ergebnisse stehen in Einklang mit Clars Theorie des aromatischen Sextetts, die ebenfalls den drei äußeren Ringen Aromatizität zuordnen würde.^{118,119}

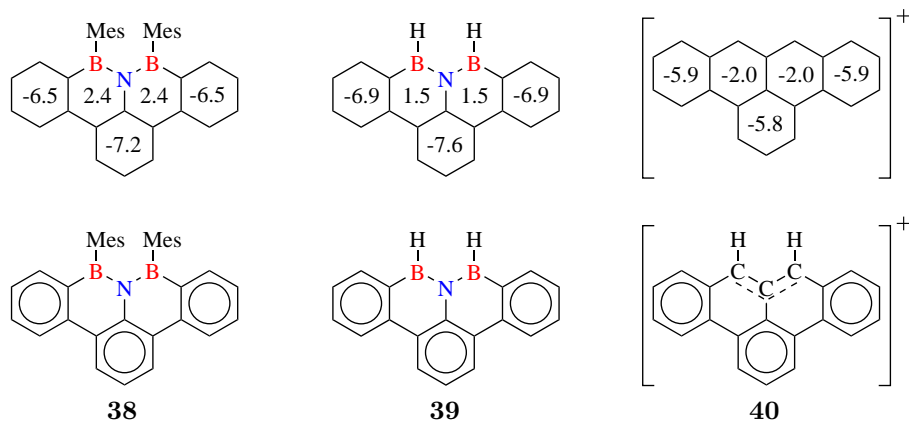


Abbildung 3.5: Berechnete NICS(0)-Werte (B3LYP/6-311+G**) des BNB-Benzo[*fg*]tetracene **38** (links oben) mit Clars Sextetstruktur (links unten); im Vergleich das BNB-Benzo[*fg*]tetracene Grundgerüst **39** und Zahardiks PAK-Kation **40**; NICS(0) von Benzol beträgt -8.1.

NICS-Berechnungen zum Kation **40** geben ebenfalls ein ähnliches Bild ab. Daraus lässt sich schließen, dass **40** als ein *m*-Terphenyl betrachtet werden kann, dass durch eine Allylgruppe verknüpft wird. Die BNB-Gruppe in **38** und **39** kann als isoelektronischer und isosterischer Vergleich zur Allylgruppe betrachtet werden und verknüpft ebenfalls die *m*-Terphenyle.

3.2 Neue Syntheseroute (BN)₂-Dibenzoperylen

Ausgehend von dem bekannten 2-Bromo-4-*n*-butylanilin (**41**), das durch eine Bromierung von 4-*n*-Butylanilin mit *N*-Bromsuccinimid (NBS) erhalten wird,¹²⁰ konnte in einer Suzuki-Kupplung das Terphenylmotiv **42** dargestellt werden. Für die folgende Borylierung, wurde auf eine Vorschrift von Hatakeyama et al. zurückgegriffen, in der Bortribromid als Borylierungsreagenz und Tetraphenylborat als nicht koordinierende Base verwendet werden.¹⁰¹ Lediglich das Lösemittel *o*-Dichlorbenzol wurde mit Toluol getauscht, da Toluol nach der Reaktion leichter entfernbar ist und die Ausbeute nicht beeinträchtigt wird. Wird das so erhaltene NBN-Benzo[*fg*]tetracene **43** mit einem Äquivalent NBS umgesetzt, erhält man das

einfach bromierte Benzotetracen **44** als Hauptprodukt. Als Nebenprodukt kann ein zweifach bromiertes NBN-Benzotetracen isoliert werden, welches für ein weiteres Projekt in Kap. 3.4 zum Einsatz kommt.

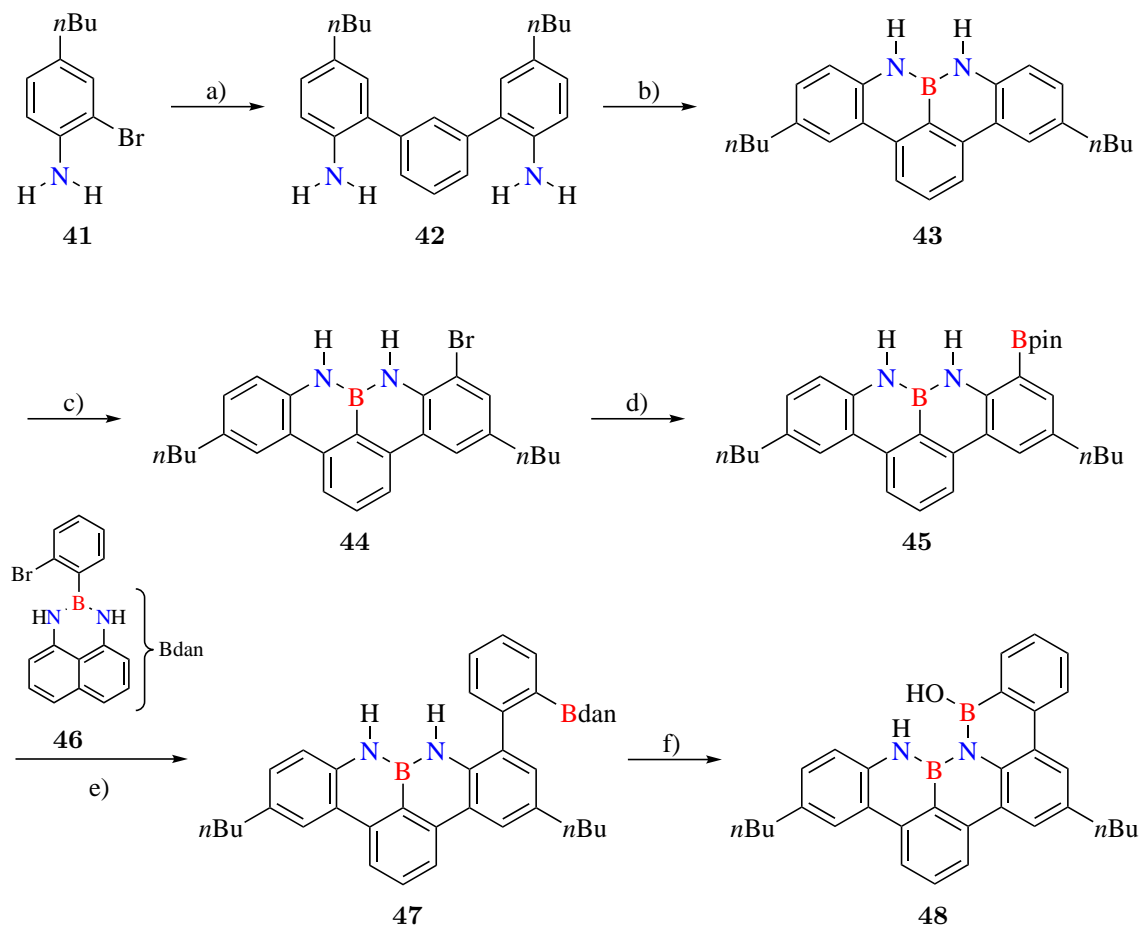


Abbildung 3.6: Neue Syntheseroute für das (BN)₂-Dibenzoperylen; a) 2.4 Äq. **41**, 1.0 Äq. 1,3-Phenyldiboronsäure-bis(pinacolat)ester, 6.5 Äq. K₂CO₃, 5 mol% Pd(PPh₃)₄, Toluol/Ethanol/Wasser Gemisch, reflux, 18 h, 92 %; b) 1.0 Äq. **42**, 1.0 Äq. BBr₃, 1.5 Äq. NaBPh₄, Toluol, reflux, 18 h, 65 %; c) 1 Äq. **43**, 1 Äq. NBS, Chloroform/Dichlormethan/Acetonitril Gemisch, rt, 12 h, 48 %; d) 1.0 Äq. **44**, 2.5 Äq. B₂pin₂, 6.0 Äq. KOAc, 10 mol% Pd(dppf)Cl₂, 1,4-Dioxan, 90 °C, 18 h, 61 %; e) 1 Äq. **45**, 1 Äq. **46**, 4 Äq. K₂CO₃, 10 mol% Pd(PPh₃)₄, reflux, 12 h, 73 %; f) 1 Äq. **47**, 24 Äq. H₂SO₄ (2 M in Wasser), THF, 50 °C, 5 Tage, 92 %.

Aufgrund des Nebenproduktes erfolgt keine vollständige Umsetzung des Edukts **43**. Für eine mögliche Optimierung der Reaktion wurden 1.2 Äquivalente NBS verwendet. Dies verschlechtert aber das Produkt-Nebenprodukt-Verhältnis in Richtung der Mehrfachbromierung, wes-

halb die Optimierung verworfen wurde.

Verbindung **44** hat sich während dieses Projektes als schlechtes Kupplungsreagenz gezeigt. Durch den Austausch des Bromatoms gegen eine Bpin-Gruppe in **45**, konnte mittels der Umpolungsreaktion eine höhere Reaktivität für die anschließende Suzukikupplung erreicht werden. Dies erlaubt nun die Einführung eines Phenylrestes, welcher das zweite, dansylgeschützte Boratom mitbringt.¹⁰⁴

Diese dansylgeschützte Einführung ist essentiell notwendig, da eine zweite elektrophile Borylierung, wie schon in Kapitel 3.1 beschrieben, nicht zum Erfolg führt. Im letzten Schritt der Syntheseroute wird die Dansylgruppe unter sauren Bedingungen abgespalten. Dabei bildet sich eine stark elektrophile Borspezies, die mit dem sehr schwach nukleophilen Stickstoff reagiert und das (BN)₂-Dibenzoperylen **48** bildet. Erste Versuche unter Verwendung von Salzsäure nach Noda et al. führten unter oxidativen Bedingungen zur Abspaltung der gesamten Bdan-Gruppe und zur Bildung eines Phenolderivats.¹⁰⁴ Erstmals konnte das gewünschte Produkt **48** mit *p*TSA unter inerten Bedingungen erhalten werden, jedoch nur in Ausbeuten von 20 %. Auch hier wurde das Oxidationsprodukt in großen Mengen gefunden. Schließlich konnte unter Verwendung von 2 M Schwefelsäure und striktem Ausschluss von Sauerstoff, sowohl bei der Reaktion als auch bei der wässrigen Aufarbeitung, die Ausbeute auf 92 % gesteigert werden.¹²¹ Somit gelang die neue Syntheseroute in sechs Stufen mit einer Gesamtausbeute von 12 %.

Alle Produkte konnten mittels NMR (¹H-, ¹³C-, ¹¹B- und 2D-Spektren) sowie der hochauflösten Massenspektrometrie charakterisiert werden. Dabei fällt auf, dass für **48** nur ein breites ¹¹B Signal auftritt. Dies kann mit quantenchemischen Rechnungen (M062X/6-31G*) erklärt werden, denn die berechneten Verschiebungen unterscheiden sich nur um 1 ppm und kommen somit übereinander zu liegen.

Das Absorptionsspektrum von **48** zeigt zwei Hauptabsorptionsbanden bei 250 - 320 nm sowie 325 - 390 nm, welche sehr ähnlich zum bereits bekannten, unsubstituierten (BN)₂-Dibenzoperylen **20** sind.⁸⁶ Die Butylgruppen zeigen nur eine marginal bathochrome Verschie-

bung. Gleichzeitig wurde ein Fluoreszenzspektrum von **48** mit einer Anregungswellenlänge von 377 nm aufgenommen, das ebenfalls sehr ähnliche Banden zu **20** zeigt, mit teilweise aufgelöster Schwingungsfineinstruktur und einer schwachen Rotverschiebung.

Die Stokesverschiebung für **48** beträgt 1209 cm^{-1} und ist vergleichbar mit der des Grundgerüsts **20** (1194 cm^{-1}).⁸⁶ Für **48** wird eine hohe Fluoreszenzquantenausbeute von $\phi_{\text{F1}} = 0.84$ erhalten, gemessen gegen 9,10-Diphenylantracen in Ethanol als Referenz ($\phi_{\text{F1}} = 0.95$).^{112,113}

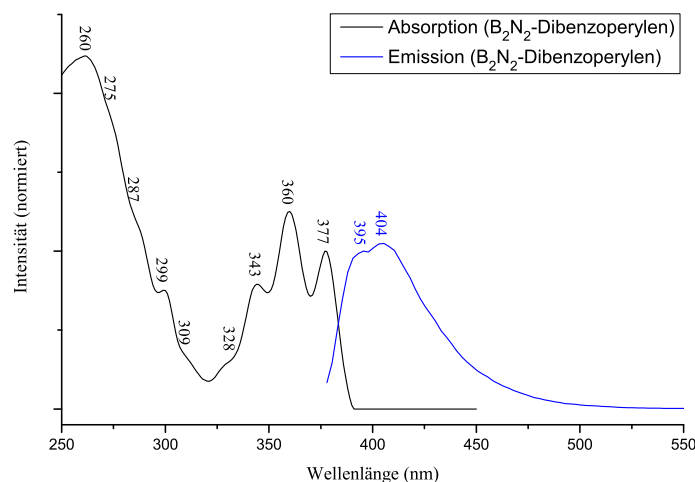


Abbildung 3.7: Absorptions- (schwarz) und Fluoreszenzspektrum (blau, $\lambda_{\text{ex}} = 377\text{ nm}$) von **48** ($4 \cdot 10^{-5}\text{ M}$ in CH_2Cl_2).

Für weitere Untersuchungen wurden die NICS(0)- und NICS(1)-Werte von **20**, sowie von den beiden Vergleichssystemen Perylen **49** und Dibenzoperylen **50** quantenchemisch (M062X/6-31G*) bestimmt.^{115–117} Wie schon in Kap. 3.1 erwähnt, wird auch hier mit dem Stammsystem **20** ohne *n*-Butylgruppen gerechnet, um Rechenkapazität zu sparen. Perylen **49** weist dabei zwei aromatische Naphtalineinheiten auf, die mit einem inneren, nicht aromatischen Ring verbunden sind. In Dibenzoperylen **50** erkennt man zwei Phenanthreneinheiten, die ebenfalls über einen nicht aromatischen Ring verknüpft sind. Dabei zeigt jeweils der mittlere Ring der Phenanthreneinheiten wie erwartet weniger Aromatizität.^{115,117} Im Gegensatz dazu enthält **20** ein Quaterphenyl, das mit einer BNB-Brücke alle vier aromatischen Ringe verknüpft.

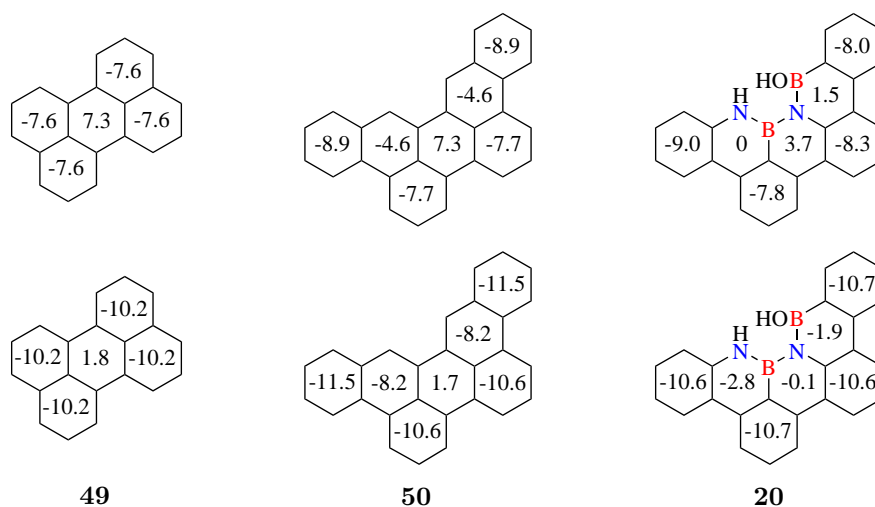


Abbildung 3.8: Quantenchemisch berechnete NICS(0)- (oben) und NICS(1)-Werte (unten, M062X/6-31G*) von den PAKs Perylen **49** und Dibenzoperylen **50**, sowie dem (BN)₂-Dibenzoperylen **20**; NICS(0) von Benzol ist -9.2 und NICS(1) -11.6.

3.3 Cycloadditionsreaktionen des (BN)₂-Dibenzoperylens

3.3.1 Die Wahl des Dienophils

Um geeignete Dienophile zu finden, wurden quantenchemische Rechnungen durchgeführt (M062X/6-311+G**). Das (BN)₂-Dibenzoperylen **20** ohne Butylgruppen ersetzt hierbei das eigentlich verwendete (BN)₂-Dibenzoperylen **48**, um Rechenkapazität zu sparen. Abb. 3.9 zeigt die Ergebnisse der Berechnungen, indem die Energiesumme der Edukte (**20** und Dienophil) auf 0 kcal/mol gesetzt werden. Alle berechneten Energiewerte der Cycloadditionszwischenprodukte **A** sowie der Produkte **B** (Cycloadditionsprodukt und Wasser) sind ins Verhältnis zu den Ausgangsprodukten gesetzt.

Typische elektronenreiche (Methylvinylether) und elektronenarme Dienophile (TCNE, TME, s. Abb. 3.9) zeigen für die Cycloadditionszwischenprodukte **A** zu große Energiedifferenzen gegenüber den Ausgangsverbindungen und verlaufen insgesamt, selbst nach der Dehydratisierung, endergon. Einzig Benzaldehyd, mit einer polaren Carbonylgruppe, zeigt mit 25.9 kcal/mol einen erreichbaren Wert in siedenden Lösungsmitteln und einen leicht exergo-

nen Gesamtverlauf. Damit fiel die Wahl für ein Dienophil auf Benzaldehyd.

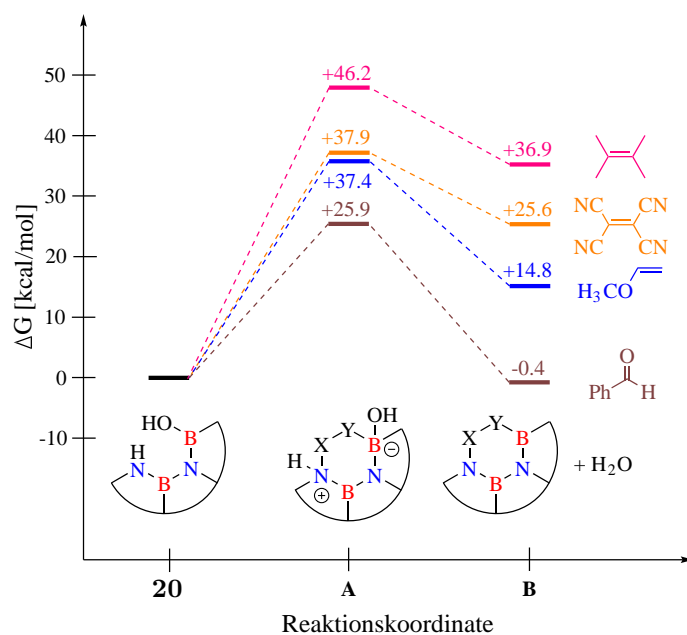


Abbildung 3.9: Berechnungen von ΔG für die Cycloaddition von **20** mit verschiedenen Dienophilen (M062X/6-311+G**); Verbindung **20** (ohne Butylgruppen) wird zur Verbesserung der Übersichtlichkeit hier abgekürzt.

3.3.2 Cycloadditionen des (BN)₂-Dibenzoperylens mit Benzaldehyd

Erste Versuche **48** mit Benzaldehyd zur Reaktion zu bringen blieben erfolglos. Es wurde angenommen, dass die Dehydratisierung der Grund für die nicht ablaufende Reaktion ist. Dies wurde durch Zugabe von *para*-Toluolsulfonsäure (*p*TSA) im Überschuss untersucht. Durch die nun säurekatalysierte Dehydratisierung konnte das erste Cycloadditionsprodukt **52a** dargestellt werden (s. Abb. 3.10). Um das entstehende Wasser aus der Reaktion zu entfernen und so das Reaktionsgleichgewicht zu beeinflussen, wurde ein Soxhletextraktor mit Molekularsieb verwendet. Die Reaktionszeit ergab 5 Tage und das erste Cycloadditionsprodukt konnte mit einer Ausbeute von 67 % erhalten werden.

Verbindung **52a** zeigt große Stabilität gegenüber Sauerstoff und Wasser und kann säulenchromatographisch aufgereinigt werden. Charakterisierungen mittels NMR-Spektroskopie (¹H- und ¹³C-, sowie ¹¹B- und 2D-Spektren) und Massenspektrometrie erfolgten, wobei das Proton

am B_2N_2CO -Ring eine auffallende Tieffeldverschiebung von 7.02 ppm im 1H -NMR-Spektrum zeigt.

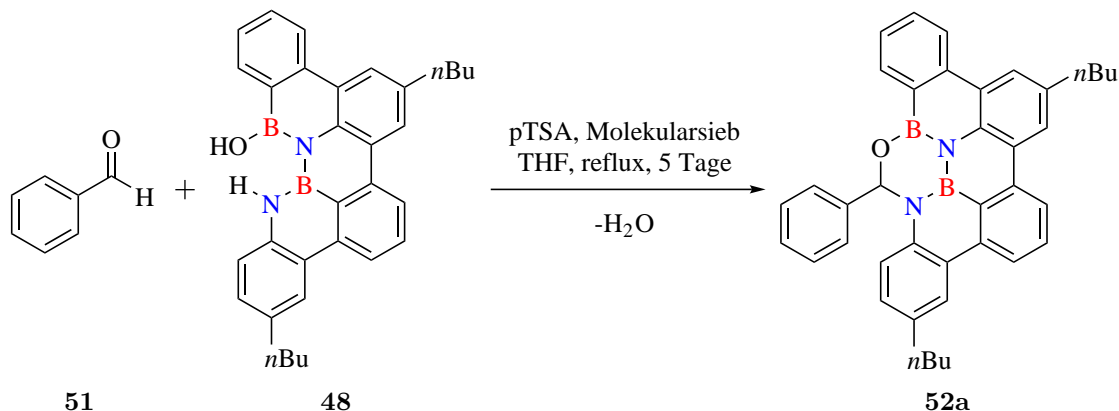


Abbildung 3.10: Säurekatalysierte Cycloaddition von 48 mit Benzaldehyd 51.

Einkristalle von Verbindung 52a konnten aus THF erhalten werden (s. Abb. 3.11). Das Cycloadditionsprodukt 52a kristallisiert in der triklinen Raumgruppe P-1 mit zwei Enantiomeren aufgrund des asymmetrischen sp^3 -Kohlenstoffs im B_2N_2CO -Ring.

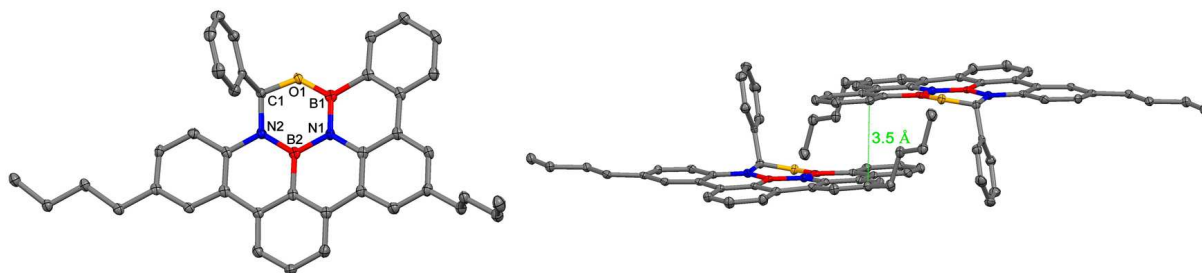
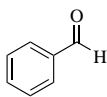
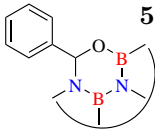
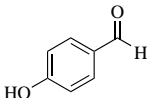
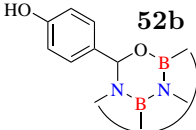
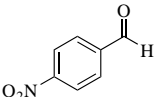
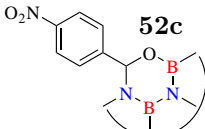
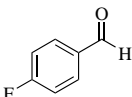
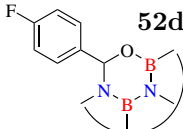
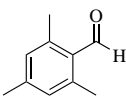
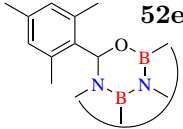
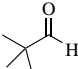
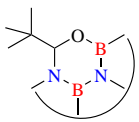
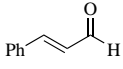
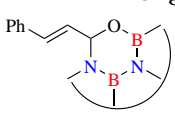


Abbildung 3.11: Molekülstruktur von 52a im Kristall (links), Schwingungsellipsoide sind mit 50 % Wahrscheinlichkeit angegeben; ausgewählte Bindungslängen von 52a in Å: O1-B1 1.376, B1-N1 1.420, N1-B2 1.444, B2-N2 1.422, N2-C1 1.468, C1-O1 1.430; Packung von 52a (rechts); Wasserstoffatome werden zur besseren Übersichtlichkeit nicht dargestellt.

Das Dibenzopyrrolengerüst führt zu π - π -Wechselwirkungen zwischen den Molekülen mit einem Abstand von 3.5 Å. Eine der Butylgruppen zeigt in die Molekülebene, während die andere Butylgruppe sowie der Phenylrest in Richtung der nächsten Molekülebene gerichtet sind. Die BN-Bindungslängen liegen im Mittel bei 1.43 Å und sind etwas kürzer als in ver-

gleichbaren BN-dotierten PAKs (1.45-1.47 Å).^{15,64} Die CO-, BO- und NC-Bindungslängen sind sehr ähnlich zu bekannten Verbindungen.¹²²

Tabelle 3.1: Eingesetzte Aldehyd und deren Cycloadditionsprodukte.

#	Dienophil	Produkt	Ausbeute
1		 52a	67 %
2		 52b	74 %
3		 52c	73 %
4		 52d	80 %
5		 52e	40 %
6		 52f	15 %
7		 52g	77 %

Um die neuartige Reaktion weiter zu untersuchen, wurden Benzaldehyde (BA-X) mit verschiedenen Substituenten in *para*-Position eingesetzt (s. Tab. 3.1). Mit diesen Dienophilen läuft die Cycloaddition ebenfalls ab. Die Substituenten zeigen keinen Einfluss auf die Re-

aktionsgeschwindigkeit. Das Cycloadditionsprodukt **52e** kann aufgrund seines sterisch anspruchsvollen Dienophils nur mit einer Ausbeute von 40 % erhalten werden. Pivalaldehyd, ein nicht aromatischer Aldehyd, zeigt ebenfalls geringere Ausbeute und das Reaktionsprodukt **52f** enthält noch Verunreinigungen, die mittels Säulenchromatographie nicht abgetrennt werden konnten. Ob für die geringe Ausbeute in dieser Reaktion die *tert*-Butylgruppe als sterisch anspruchsvoller Rest verantwortlich gemacht werden kann ist unklar. Denkbar wäre auch, dass in den anderen Cycloadditionen die Phenylgruppe des Dienophils die Reaktion auf Grund von π - π -Wechselwirkungen mit dem Dien **48** begünstigt. Diese Phenylgruppe ist in Zimtaldehyd wieder vorhanden und die Reaktion zu **52g** verläuft in guten Ausbeuten. Zimtaldehyd unterscheidet sich jedoch durch die CC-Doppelbindung zwischen der Phenylgruppe und der Aldehydfunktion. Dies scheint im Vergleich zu den Benzaldehyden weder einen Einfluss auf die Reaktionszeit noch auf die Produktausbeute zu haben. Allerdings wird nur das Produkt **52g** erhalten, wohingegen ein mögliches Cycloadditionsprodukt mit der unpolaren CC-Doppelbindung nicht beobachtet wurde.

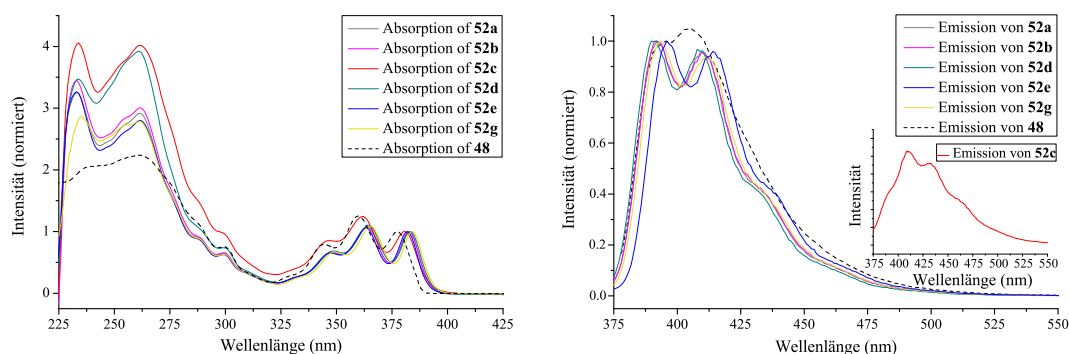


Abbildung 3.12: Absorptions- (normiert auf das langwelligste Maximum, links) und Fluoreszenzspektren (normiert auf das kurzwelligste Maximum, rechts) der erhaltenen Cycloadditionsprodukte in Dichlormethan im Vergleich zu **48** (gestrichelte Linie). Bildausschnitt: Fluoreszenzspektrum von **52c** ($\Phi_{Fl} = 0.07$).

Von allen Cycloadditionsprodukten wurden Absorptions- und Fluoreszenzspektren in Dichlormethan aufgenommen, die starke Ähnlichkeit zeigen. Die Substituenteneffekte wirken sich lediglich durch Verschiebung der Maxima um 1-2 nm aus. Außerdem sind die aufgenommenen Spektren sehr ähnlich zur Ausgangsverbindung **48**. Die Stokesverschiebungen

variieren je nach Substituenten zwischen 600 - 755 cm^{-1} . Ebenso sind die Fluoreszenzquantenausbeuten zwischen 78 % und 84 % sehr ähnlich. Eine Ausnahme stellt das nitrosubstituierte Produkt **52c** dar, welches mit einer Quantenausbeute von nur 7 % Fluoreszenzlösung aufweist. Dass PAKs mit Nitrogruppen diesen Effekt zeigen können, ist hinreichend bekannt.¹²³⁻¹²⁶

3.3.3 Untersuchungen zum Reaktionsmechanismus

Wie bereits erwähnt, erfolgt die Cycloadditionsreaktion in diesem Fall nicht ohne die Säure. Um den Mechanismus aufklären zu können, soll deshalb zuerst der Einfluss der Säure untersucht werden.

Dazu werden in einem NMR-Experiment jeweils das $(\text{BN})_2$ -Dibenzoperylen **48**, sowie Benzaldehyd (BA-H) einzeln mit *p*TSA gelöst in THF- d_8 vermessen. Dabei zeigt sich, dass nur die OH-Gruppe von **48** Wechselwirkungen, in Form eines schnellen Protonenaustausches, mit der Säure zeigt. Die Signale des Benzaldehyds bleiben unverändert. Dies steht in Einklang mit den $\text{p}K_{\text{S}}$ -Werten der Säure (-2.8)¹²⁷ sowie des BA-H (-7.1).¹²⁸

Aus diesen Erkenntnissen können die Reaktionsmechanismen auf drei Möglichkeiten eingegrenzt werden. Als erstes wäre denkbar, dass sich unter säurekatalytischer Dehydratisierung ein Diazadiboretidinring im Dibenzoperylen **53** ausbildet (s. Abb. 3.13).⁹⁷⁻⁹⁹ Quantenchemische Rechnungen (M062X/6-311+G** in THF, T = 339 K) widersprechen dieser Theorie, da die Bildung von **53** und Wasser mit 81.1 kcal/mol zu viel Energie benötigt.

Die zweite Möglichkeit wird ebenfalls in Abb. 3.13 beschrieben. Im ersten Schritt erfolgt hier die konzertierte Cycloaddition von BA-H mit **20** zu **A**. Mittels quantenchemischen Rechnungen wird ein Übergangszustand (engl. „transition state“, TS) von 30.1 kcal/mol ermittelt, der gerade einmal 1.1 kcal/mol höher in Energie liegt, als das Zwischenprodukt **A**. Im zweiten Schritt erfolgt nun die Dehydratisierung unter Verwendung der Säure zu **C**. Zuletzt erfolgt die Rückgewinnung der Säure unter Produktbildung von **B**. Alle berechneten Energiewerte für die in *para*-Position substituierten Benzaldehyde (BA-OH, BA-NO₂ und BA-F) sind in Tab. 3.2 abgebildet und zeigen nur wenig Abweichung vom Stammsystem BA-H.

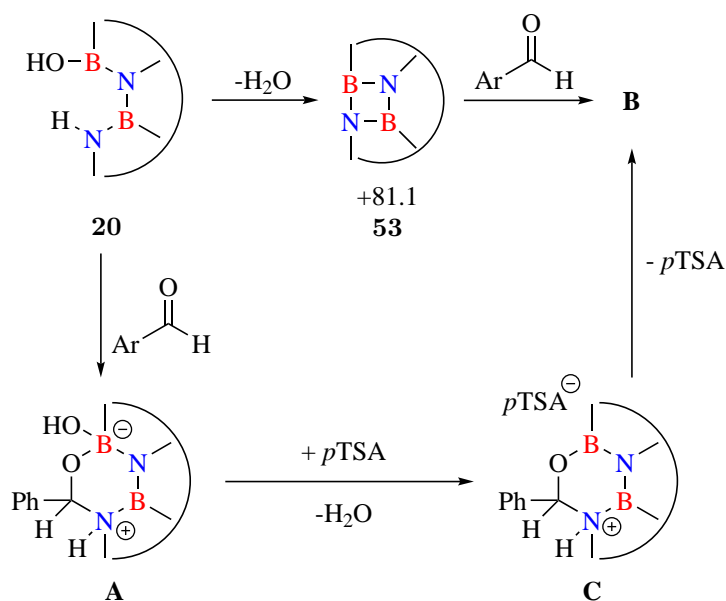


Abbildung 3.13: Übersicht zweier möglicher Mechanismen der säurekatalysierten Cycloaddition.

Damit bildet in dieser Reaktion die säurekatalysierte Dehydratisierung den geschwindigkeitsbestimmenden Schritt. Dies steht im Einklang mit Versuchsreihen unter Verwendung unterschiedlicher Säurekonzentrationen. Konzentrationsänderungen des Benzaldehyds wirken sich nicht auf die Reaktionsgeschwindigkeit aus, ebenso wenig wie die Substituenten, weshalb eine konzertierte Cycloaddition postuliert wird.

Tabelle 3.2: Berechnete Energiedifferenzen (M062X/6-311+G** in THF, T = 339 K) in kcal/mol zur Aufklärung des Mechanismus.

Dienophil	TS	A _{BA}	C _{BA}
BA-H	+30.1	+29.0	+36.0
BA-OH	+30.5	+29.4	+36.4
BA-NO ₂	+29.5	+26.4	+36.6
BA-F	+29.9	+28.4	+36.6

Die dritte und letzte Möglichkeit für den Mechanismus wäre eine vorangehende Protonierung des Perylens **20** mittels *pTSA* und anschließender Cycloaddition.

3.3.4 Hydridabstraktion

Mit dieser Cycloaddition von **48** mit Benzaldehyden wird ein B_2N_2CO -Ring im Polyzyklus erhalten, wie er bereits von Paetzold bekannt ist.^{97,98} Dieser Ring enthält ein sp^3 -hybridisierten Kohlenstoff, dessen Reste aus einem Phenylring und einem Wasserstoffatom bestehen. Um eine Planarität bzw. eine Aromatizität in dem Heteroatomring zu erzielen, müsste die Hybridisierung des Kohlenstoffs von sp^3 zu sp^2 mittels Hydridabstraktion umgewandelt werden. Für solche Reaktionen sind Hydridabstraktoren wie das Triphenylmethylkation bekannt, das im Vergleich zu anderen Hydridabstraktoren als der Stärkste gilt.^{129,130}

Erste Versuche **52a** mit dem Triphenylmethylkation in Benzol bei Raumtemperatur zur Reaktion zu bringen blieben erfolglos. Erst die Erhöhung der Reaktionstemperatur und die Verlängerung der Reaktionszeit auf 24 Stunden zeigte im 1H -NMR die Entstehung des Triphenylmethans und damit einen Reaktionsumsatz an. Da nicht sicher ist, welche Stabilität das Kation **54** aufweist, wurde die Reaktionsmischung mit Caesiumfluorid behandelt. Massenspektrometrische Analysen (APCI) zeigen zwar ein kleines Signal für die fluorierte Spezies, jedoch konnte nach säulenchromatographischer Aufreinigung das Edukt **52a** nahezu vollständig zurückgewonnen werden. Das führt zu dem Schluss, dass die Reaktion langsam abläuft und weiter optimiert werden muss.

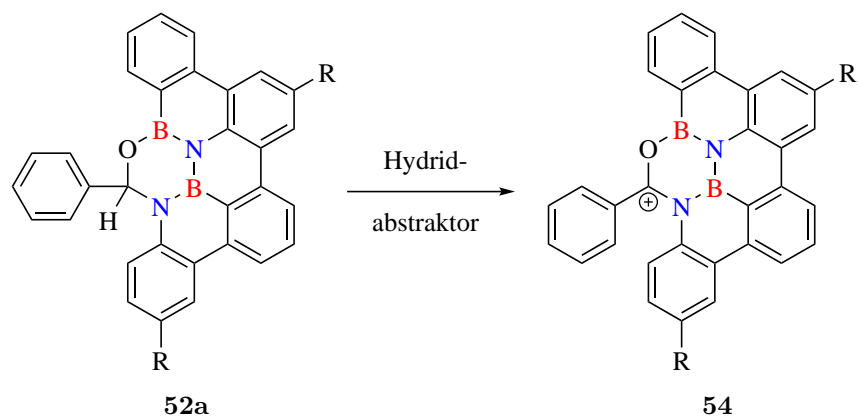


Abbildung 3.14: Hydridabstraktion am Heteroatomring in **52a**.

Das Ziel der Hydridabstraktion könnte auch in einer anderen Form von statten gehen, in-

dem das Wasserstoffatom als Proton entfernt wird und der Kohlenstoff oxidiert wird. Unter Verwendung von 2,3-Dichlor-5,6-dicyano-1,4-benzochinon (DDQ) könnte auch zusätzlich eine oxidative CC-Bindungsknüpfung zu **55** ablaufen (s. Abb. 3.15), bzw. zuerst die CC-Bindungsknüpfung und aufgrund der daraus resultierenden Verzerrung des Moleküls die Oxidation des sp^3 -Kohlenstoffs.

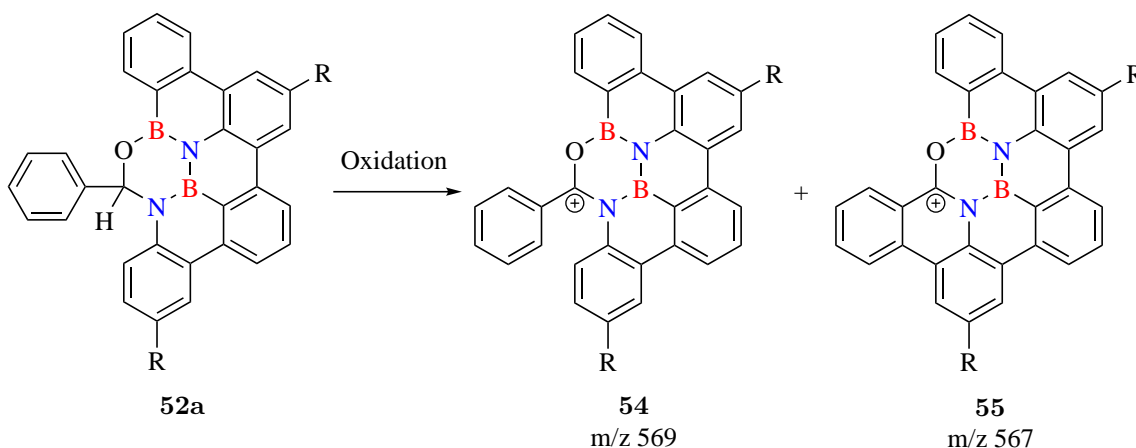


Abbildung 3.15: Oxidation der Verbindung **52a**.

Bei Verwendung von je einem Äquivalent DDQ und **52a** in Benzol zeigt sich bei einer Reaktionstemperatur von 60 °C eine schnelle Reaktion. Mittels NMR-Spektroskopie können aber aufgrund vieler überlagernder Aromatensignale keine Aussagen über den Reaktionsverlauf gemacht werden. Massenspektrometrische Analysen (LDI) liefern ein Masse-zu-Ladungs-Verhältnis m/z von 568. Dieser Wert liegt genau zwischen den beiden erwarteten m/z Werten (s. Abb. 3.15) und könnte aus einer Überlagerung entstehen. Um das Produktverhältnis in Richtung **55** zu drücken, wurden mehrere Versuche mit bis zu 5 Äquivalenten DDQ unternommen. Es konnten aber keine Produktsignale mittels Massenspektrometrie gefunden werden, was auf eine vollständige Zersetzung unter den stark oxidativen Bedingungen hindeutet. Simulationen der Isotopenmuster im Massenspektrum zeigten nun auch, dass der Peak mit einem m/z -Verhältnis von 568 keine Überlagerung aus den beiden erwarteten Produkten darstellen kann und damit ist DDQ als Oxidationsmittel für solch eine Reaktion ungeeignet.

Ein alternative Scholl-Reaktion mit Eisen(III)chlorid und Nitromethan in DCM konnte ebenfalls durchgeführt werden. Massenspektrometrische Analysen (LDI) zeigen das Molekül mit m/z 567, allerdings auch eine Vielzahl an Nebenprodukten, die sich nur durch Zersetzung erklären lassen. Eine Isolierung des Produktes **55** mittels Löslichkeitsversuchen und Sublimationen erwiesen sich bislang als erfolglos. Grund hierbei sind nicht nur die vielen Nebenprodukte, sondern vor allem der große Anteil an Eisenverbindungen in der Reaktion. Auch ist bislang nicht geklärt, welches Gegenion zu **55** gehört. Möglicherweise würden Untersuchungen und ein Anionenaustausch diesbezüglich eine Lösung für die Aufreinigung liefern.

Eine letzte Möglichkeit bestünde, wenn analog zu Paetzold et al. Ketene als Dienophil in die Cycloaddition eingesetzt werden würden.⁹⁸ Diese besitzen eine CO-Gruppe, die sich in Cycloadditionen mit Heteroatomen bewährt haben und eine CC-Doppelbindung, die nach der Reaktion den benötigten sp^2 -Kohlenstoff direkt mit bringen.

3.3.5 Cycloadditionen des $(BN)_2$ -Dibenzoperylens mit anderen Dienophilen

Es bleibt die Frage zu beantworten, ob andere Dienophile eine Cycloaddition mit **48** eingehen. Dies konnte bisher noch nicht bestätigt werden. Abb. 3.16 zeigt getestete Dienophile mit unterschiedlichen Eigenschaften.

Zuerst wäre das Nitrosobenzol zu nennen, das als Analogon zum Benzaldehyd in Betracht gezogen wurde. Mit Aceton und Essigsäure wurde enolisierbare Dienophile untersucht. Benzophenon, Benzophenonimin und Benzylidenanilin decken zwei Gruppen ab, sowohl sterisch anspruchsvollere Dienophile, sowie die Stoffklasse der Imine. Ein typisches Dienophil wie Maleinsäureanhydrid, was auch aus der Reaktion mit Perylen (**49**) bekannt ist,⁸⁹ zeigte nicht das gewünschte Produkt. Ebenfalls beim Versuch blieb es, CO_2 mit **48** in einem Druckreaktor zur Reaktion zu bringen. Dass diese Reaktion von ihrer Energiebilanz nur schwer zu erzielen ist, konnte später in quantenchemischen Untersuchungen gezeigt werden (s. Energiediagramm in Abb. 3.16). Ein in situ erzeugtes Arin geht, nach bisherigen Erkenntnissen, eine Reaktion mit der OH-Gruppe des Perylens **48** ein, spaltet sich aber nach wässriger

Aufarbeitung als Phenol wieder ab. DMAD und Tolan gehören zur Gruppe der Alkine. Da DMAD in Cycloadditionen mit den von Paetzold beschriebenen Diazadiboretidine reagiert hat,⁹⁸ konnte eine Reaktion mit der B₂N₂-Gruppe des Perylens **48** erwartet, jedoch nicht beobachtet werden.

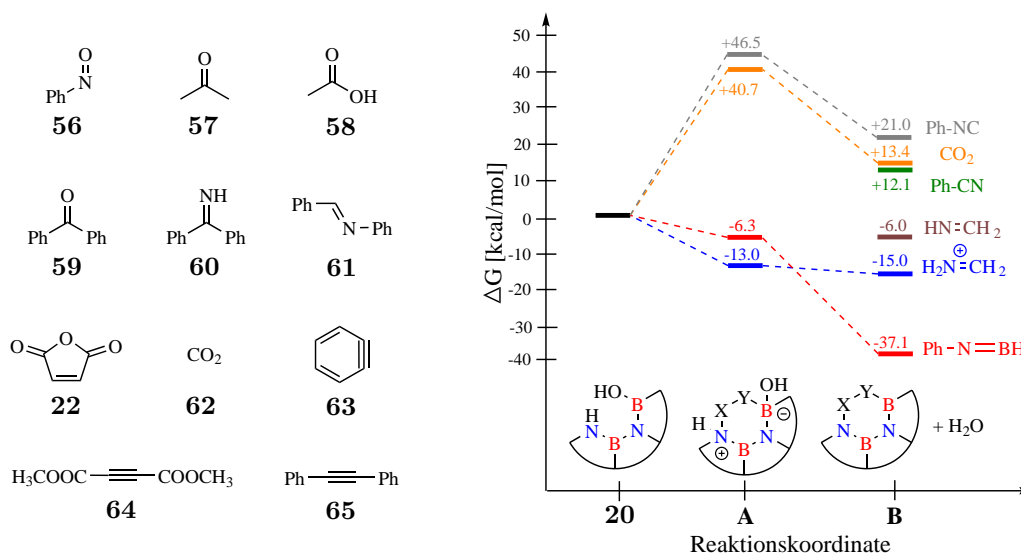


Abbildung 3.16: Getestete Dienophile in Reaktionen (links) und berechnete Energiebilanz ausgewählter Beispiele (rechts) auf dem M062X/6-311+G** Theorieniveau.

Aufgrund des großen Bedarfs an **48** für die vielen Reaktionen und dessen Syntheseaufwands sollten vorerst abschließend die Energiebilanzen einiger Dienophile quantenchemisch untersucht werden (M062X/6-311+G**). Benzonitril und ebenso das Isonitrilderivat zeigen einen insgesamt endergonischen Reaktionsverlauf, wobei das Zwischenprodukt **A** mit Isonitril und 46.5 kcal/mol, einen, in siedendem Lösungsmittel nicht erreichbaren Energiewert aufweist. Das Zwischenprodukt **A** im Falle des Benzonitrils zeigt sich als nicht stabil und öffnet den gebildeten Heteroatom-Ring wieder. Lediglich kleine Imine und Iminiumionen, sowie das Iminoboran weisen einen exergonischen Verlauf für die gewünschten Cycloaddition auf und könnten untersucht werden. Da bei der Reaktion aber Wasser entsteht und die sehr reaktiven Dienophile damit hydrolysieren würden, müssten diese entweder im großen Überschuss eingesetzt werden, oder die OH-Funktion des Perylens **48** gegen geeignete Gruppen wie Chlorid oder Hydrid getauscht werden.

3.4 Gezielte Synthese eines Nanographenmoleküls mit B_3N_2O -Kern

In Kap. 3.2 konnte bereits die zweifache Bromierung des NBN-Benzotetracens **43** beschrieben werden. Dies wurde im folgenden Projekt für die Synthese eines Nanographenmoleküls mit B_3N_2O -Kern verwendet.

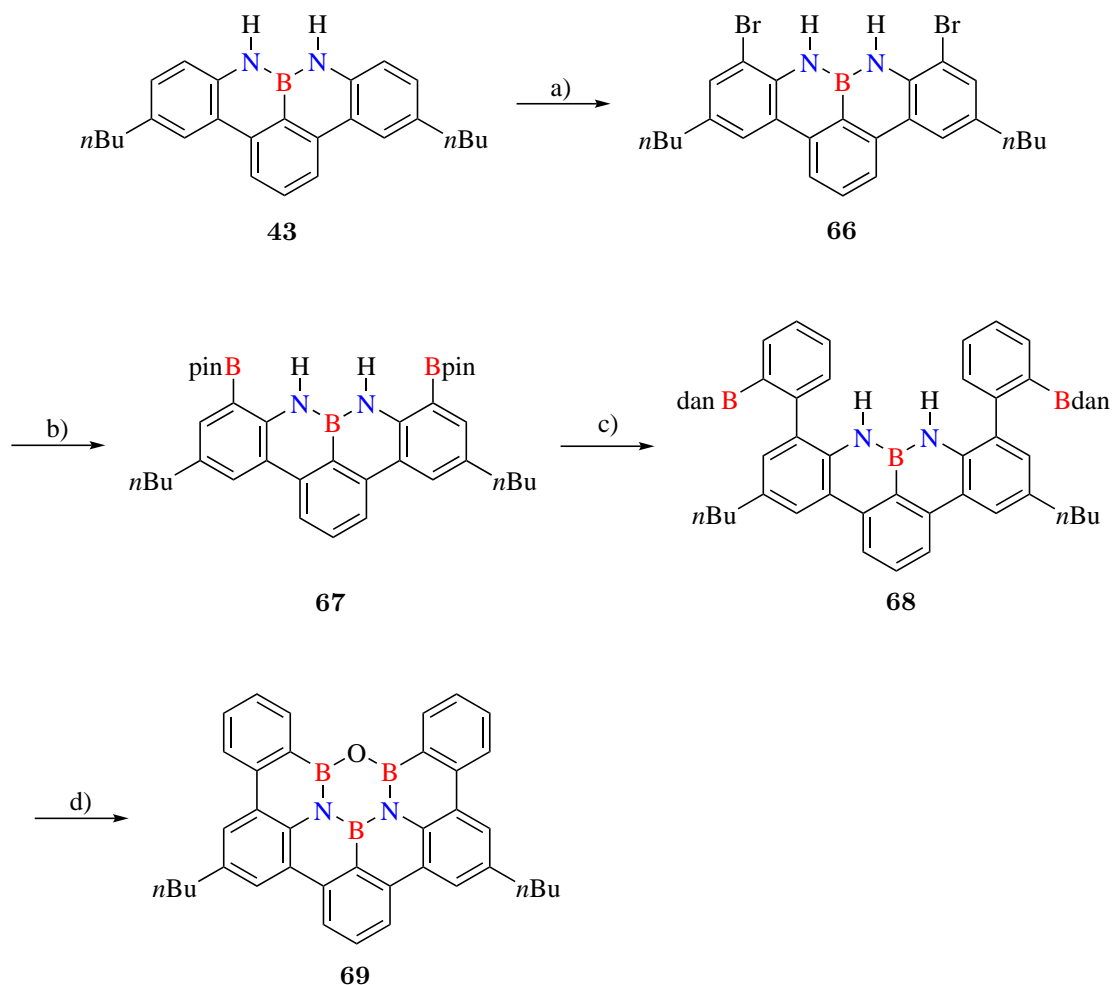


Abbildung 3.17: Gezielte Syntheseroute für den B_3N_2O -PAK; a) 1 Äq. **43**, 2 Äq. NBS, Chloroform/Dichlormethan/Acetonitril Gemisch, rt, 12 h, 80 %; b) 1 Äq. **66**, 5 Äq. B_2pin_2 , 12 Äq. KOAc, 10 mol% Pd(dppf)Cl₂, 1,4-Dioxan, 90 °C, 18 h, 68 %; c) 1.0 Äq. **67**, 2.5 Äq. **46**, 12 Äq. K_2CO_3 , 10 mol% Pd(PPh₃)₄, reflux, 12 h, 70 %; d) 1 Äq. **68**, 48 Äq. H_2SO_4 (2 M in Wasser), THF, 50 °C, 5 Tage, 90 %.

Reagiert nicht nur ein Äquivalent NBS mit **43**, sondern zwei, kann eine gezielte doppelte Bro-

mierung zu **66** erfolgen. Aufgrund der ebenfalls in Kap. 3.2 beschriebenen wenig kupplungs-freudigen Verbindung **44** und der starken Ähnlichkeit zu **66**, wird auch hier eine Umpolung mit Bpin-Gruppen vollzogen. Mittels Suzuki-Kupplung können zwei Phenylreste eingeführt werden, die jeweils eine dansylgeschützte Borspezies in ortho-Position tragen. Im letzten Schritt werden nach Hattori et al. diese Schutzgruppen unter sauren und insbesondere sauerstofffreien Bedingungen abgespalten.¹²¹ Dabei reagieren die nun elektrophilen Borspezies mit je einem schwach nukleophilen Stickstoffatom und bilden eine B-O-B-Brücke zum Boroxazinring. Aufgrund der schlechten Löslichkeit von **69** kann es erst durch Waschen mit THF und Wasser, sowie Aceton und Dichlormethan aufgereinigt werden, bevor das Produkt **69** sowohl in Reinstform als auch in Einkristallen durch Vakuumsublimation (10^{-3} mbar und $300\text{ }^{\circ}\text{C}$) erhalten wird. NMR-Daten und die daraus resultierende Charakterisierung können in 1,4-Dioxan- d_8 bei $80\text{ }^{\circ}\text{C}$ aufgenommen werden. Alle Zwischenstufen sind ebenfalls durch NMR-Spektroskopie (^1H -, ^{13}C -, ^{11}B - und 2D-Spektren) sowie mittels hochauflöster Massenspektrometrie nachweisbar.

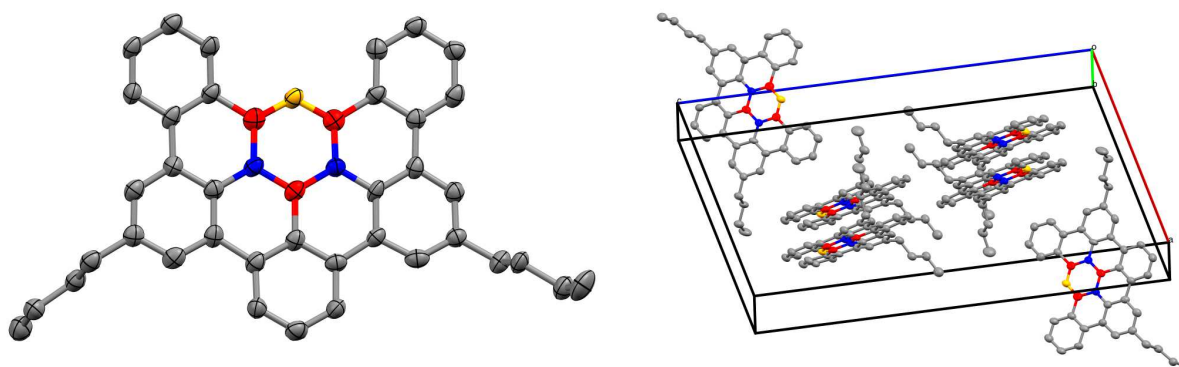


Abbildung 3.18: Kristallstruktur von **69** (ohne Wasserstoffatome, links) und Molekülpackung (rechts).

Die aus der Aufreinigung erhaltenen Einkristalle konnten für eine Kristallstrukturanalyse verwendet werden. Jedoch zeigte die Messung nur eine Auflösung bis zu $1\text{ }^{\circ}\text{Å}$, wodurch Konnektivitäten im Molekül bestätigt, aber keine Bindungslängen diskutiert werden können. Die Zellgröße ($a = 18.67\text{ }^{\circ}\text{Å}$, $b = 4.93\text{ }^{\circ}\text{Å}$, $c = 31.56\text{ }^{\circ}\text{Å}$) deutet darauf hin, dass **69** in einem

β -Motiv¹³¹ mit einer intermolekularen π - π -Stapelpackung von 3.3 Å kristallisiert. Bessere Kristalle konnten weder durch Sublimationen noch durch Kristallisation aus Lösungen erhalten werden.

Für die Charakterisierung von **69** wurde das Absorptionsspektrum in 1,4-Dioxan aufgenommen (Abb. 3.19). Dieses zeigt zwischen 330 nm und 370 nm drei breite Maxima und besitzt bei 367 nm die langwelligste Absorption.

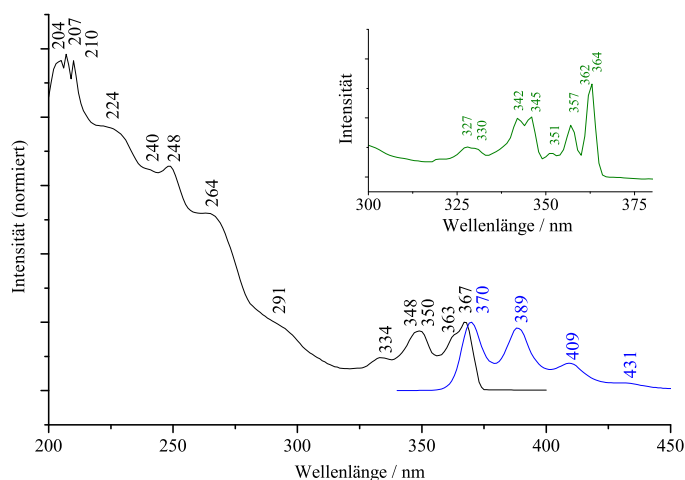


Abbildung 3.19: Absorptions- (schwarz) und Fluoreszenzspektrum (blau) von **69** ($1.1 \cdot 10^{-6}$ M in 1,4-Dioxan); im Vergleich das Absorptionsspektrum (grün) unter Matrixisolationstechnik bei 10 K.

Der isoelektronische Kohlenwasserstoff Dibenzo[*fg,ij*]phenanthro[9,10,1,2,3-*pqrst*]pentaphen dagegen weist bei 430 nm (α -Bande) die Absorption mit geringster Energie auf.^{132,133} Daraus lässt sich schließen, dass die Einführung des Boroxazinrings die Bandlücke signifikant vergrößert. Das Absorptionsspektrum des Kohlenwasserstoffs zeigt erstens andere charakteristische Banden und zweitens wird die Schwingungsfeinstruktur, wie sie bei **69** zwischen 330 - 370 nm auftritt, vermisst.^{132,133} Diese Feinstruktur wird mittels Matrixisolationstechnik bei 10 K sogar noch verschärft und spaltet die Banden deutlicher auf. Somit kann zunächst Aggregation bei Messungen mit einer Konzentration von $1.1 \cdot 10^{-6}$ M ausgeschlossen werden, die aber bei Erhöhung der Konzentration auf $8 \cdot 10^{-6}$ M in Form einer weiteren Absorptionsbande bei 379 nm auftritt.

Abb. 3.19 zeigt außerdem das Fluoreszenzspektrum von **69** mit einer Stokesverschiebung von 221 cm^{-1} , was für eine Steifigkeit des Nanographenmoleküls im angeregten Zustand spricht. Da die Schwingungsfeinstruktur im Fluoreszenzspektrum, mit jeweils einem gemittelten Abstand von 1270 cm^{-1} , kein Spiegelbild des Absorptionsspektrum darstellt, muss davon ausgegangen werden, dass ein zweiter angeregter Zustand involviert ist. Quantenchemische Rechnungen (TD-B3LYP/6-311+G*) am Stammsystem **70** (ohne *n*-Butylgruppen) bestätigen ein Energieniveau, das nur 0.05 eV höher liegt und eine ähnliche Oszillatorstärke aufweist ($f(S_1 = 0.17)$, $f(S_2 = 0.14)$).

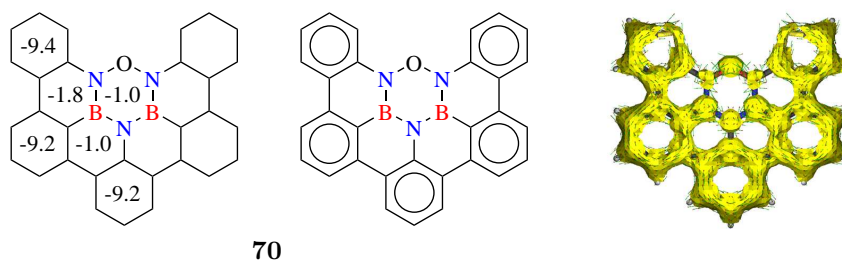


Abbildung 3.20: NICS(1)-Werte (links) von **70**, NICS(1) von Benzol beträgt im Vergleich -10.2 , Strukturformel nach Clar (Mitte) und grafische Darstellung „anisotropy of current-induced density“ (ACID, rechts) mittels quantenchemischer Rechnung (B3LYP/6-311+G**).

Um die Eigenschaften des Nanographenmoleküls weiter interpretieren zu können, wurden sowohl NICS(1)-Werte als auch ein „anisotropy of current-induced density“-Plot (ACID) quantenchemisch berechnet (B3LYP/6-311+G**). Der Boroxazinring zeigt mit einem NICS(1)-Wert von -1.0 keine Aromatizität, während die NICS(1)-Werte der fünf äußeren Ringe dem Benzol ähneln und damit aromatischen Charakter besitzen. Das entspricht auch dem Clar-Sextett und wird durch den ACID-Plot bestätigt. Dieser Plot soll die delokalisierte Elektronendichte und damit die Aromatizität veranschaulichen.^{134,135} Auch hier zeigen die fünf äußeren Ringe eine delokalisierte Elektronendichte, also ein planares *m*-Quinquephenyl, das durch den Boroxazinring verbunden ist. Dieser Heteroatomring ist nicht Teil der delokalisierten Elektronendichte, was sich auch auf vier Ringe, die anteilig Heteroatom-Substitution haben, auswirkt. Dass jedoch **69** respektive **70** neuartige und interessante Moleküle sind

und nicht auf ein *m*-Quinquephenyl Derivat reduziert werden können, lässt sich anhand der Absorptionsspektren ($\lambda_{max} = 367$ nm von **69** in 1,4-Dioxan, $\lambda_{max} = 249$ nm von *m*-Quinquephenyl in Cyclohexan¹³⁶) ableiten.

Literaturverzeichnis

- [1] Bendikov, M.; Wudl, F.; Perepichka, D. F. *Chem. Rev.* **2004**, *104*, 4891–4946.
- [2] Wu, J.; Müllen, K. *Carbon Rich Compounds*; John Wiley & Sons, Ltd, 2006; pp 90–139.
- [3] Wu, J.; Pisula, W.; Müllen, K. *Chem. Rev.* **2007**, *107*, 718–747.
- [4] Ortmann, F.; Radke, K. S.; Günther, A.; Kasemann, D.; Leo, K.; Cuniberti, G. *Adv. Funct. Mater.* **2015**, *25*, 1933–1954.
- [5] Sun, S.-S.; Dalton, L. R. *Introduction to Organic Electronic and Optoelectronic Materials and Devices*, 2nd ed.; CRC Press, 2016; pp 129–172.
- [6] Adil, S. F.; Khan, M.; Kalpana, D. In *Multifunctional Photocatalytic Materials for Energy*; Lin, Z., Ye, M., Wang, M., Eds.; Woodhead Publishing in Materials; Woodhead Publishing, 2018; pp 127 – 152.
- [7] Mitschke, U.; Bäuerle, P. *J. Mater. Chem.* **2000**, *10*, 1471–1507.
- [8] Hung, L.; Chen, C. *Mater. Sci. Eng. R Rep.* **2002**, *39*, 143–222.
- [9] Bin, J.-K.; Hong, J.-I. *Org. Electron.* **2011**, *12*, 802–808.
- [10] Zhang, D.; Duan, L. *J. Phys. Chem. Lett.* **2019**, *10*, 2528–2537.
- [11] Zhang, W.; Yu, G. In *Organic Optoelectronic Materials*; Li, Y., Ed.; Springer International Publishing: Cham, 2015; pp 51–164.
- [12] Zhang, L.; Cao, Y.; Colella, N. S.; Liang, Y.; Brédas, J.-L.; Houk, K. N.; Briseno, A. L. *Acc. Chem. Res.* **2015**, *48*, 500–509.
- [13] Zhi, L.; Müllen, K. *J. Mater. Chem.* **2008**, *18*, 1472–1484.

- [14] Müllen, K.; Rabe, J. P. *Acc. Chem. Res.* **2008**, *41*, 511–520.
- [15] Liu, Z.; Marder, T. *Angew. Chem. Int. Ed.* **2008**, *47*, 242–244.
- [16] Campbell, P. G.; Marwitz, A. J. V.; Liu, S.-Y. *Angew. Chem. Int. Ed.* **2012**, *51*, 6074–6092.
- [17] Allred, A.; Rochow, E. *J. Inorg. Nucl. Chem.* **1958**, *5*, 264 – 268.
- [18] Pritchard, R. H.; Kern, C. W. *J. Am. Chem. Soc.* **1969**, *91*, 1631–1635.
- [19] Sugie, M.; Takeo, H.; Matsumura, C. *Chem. Phys. Lett.* **1979**, *64*, 573–575.
- [20] Cooper, D. R.; D’Anjou, B.; Ghattamaneni, N.; Harack, B.; Hilke, M.; Horth, A.; Majlis, N.; Massicotte, M.; Vandsburger, L.; Whiteway, E.; Yu, V. *Condens. Matter Phys.* **2012**, *2012*, 1–56.
- [21] Li, L. H.; Chen, Y.; Behan, G.; Zhang, H.; Petracic, M.; Glushenkov, A. M. *J. Mater. Chem.* **2011**, *21*, 11862–11866.
- [22] Hassel, O. *Nor. Geol. Tidsskr.* **1927**, *9*, 266–270.
- [23] Goldschmidt, V. M. *Nor. Geol. Tidsskr.* **1927**, *9*, 258–265.
- [24] Breger, A. K. *Zh. Fiz. Khim.* **1938**, *11*, 1938.
- [25] Tarrío, C.; Schnatterly, S. E. *Phys. Rev. B* **1989**, *40*, 7852–7859.
- [26] Narita, A.; Wang, X.-Y.; Feng, X.; Müllen, K. *Chem. Soc. Rev.* **2015**, *44*, 6616–6643.
- [27] Wang, X.-Y.; Yao, X.; Narita, A.; Müllen, K. *Acc. Chem. Res.* **2019**, *52*, 2491–2505.
- [28] Dewar, M. J. S.; Kubba, V. P.; Pettit, R. *J. Chem. Soc.* **1958**, 3073–3076.
- [29] Dewar, M. J. S.; Dewar, R. B. K.; Gaibel, Z. L. F. *Org. Synth.* **1966**, *46*, 65.
- [30] Biswas, S.; Müller, M.; Tönshoff, C.; Eichele, K.; Maichle-Mössmer, C.; Ruff, A.; Speiser, B.; Bettinger, H. F. *Eur. J. Org. Chem.* **2012**, 4634–4639.

- [31] Bosdet, M. D.; Piers, W.; Sorensen, T.; Parvez, M. *Angew. Chem. Int. Ed.* **2007**, *46*, 4940–4943.
- [32] Kaehler, T.; Bolte, M.; Lerner, H.-W.; Wagner, M. *Angew. Chem. Int. Ed.* **2019**, *58*, 11379–11384.
- [33] Bonifazi, D.; Fasano, F.; Lorenzo-Garcia, M. M.; Marinelli, D.; Oubaha, H.; Tasseroul, J. *Chem. Commun.* **2015**, *51*, 15222–15236.
- [34] Brown, A. N.; Li, B.; Liu, S.-Y. *J. Am. Chem. Soc.* **2015**, *137*, 8932–8935.
- [35] Giustra, Z. X.; Liu, S.-Y. *J. Am. Chem. Soc.* **2018**, *140*, 1184–1194.
- [36] Escande, A.; Ingleson, M. J. *Chem. Comm.* **2015**, *51*, 6257–6274.
- [37] Agou, T.; Kobayashi, J.; Kawashima, T. *Chem. Eur. J.* **2007**, *13*, 8051–8060.
- [38] Hatakeyama, T.; Shiren, K.; Nakajima, K.; Nomura, S.; Nakatsuka, S.; Kinoshita, K.; Ni, J.; Ono, Y.; Ikuta, T. *Adv. Mater.* **2016**, *28*, 2777–2781.
- [39] Nakanotani, H.; Furukawa, T.; Hosokai, T.; Hatakeyama, T.; Adachi, C. *Adv. Opt. Mater.* **2017**, *5*, 1700051.
- [40] Nakatsuka, S.; Gotoh, H.; Kinoshita, K.; Yasuda, N.; Hatakeyama, T. *Angew. Chem. Int. Ed.* **2017**, *56*, 5087–5090.
- [41] Oda, S.; Kawakami, B.; Kawasumi, R.; Okita, R.; Hatakeyama, T. *Org. Lett.* **2019**, *21*, 9311–9314.
- [42] Wu, J.; Kan, Y.; Xue, Z.; Huang, J.; Chen, P.; Yu, X.; Guo, Z.; Su, Z. *J. Mater. Chem. C* **2017**, *5*, 9088–9097.
- [43] Park, I. S.; Matsuo, K.; Aizawa, N.; Yasuda, T. *Adv. Funct. Mater.* **2018**, *28*, 1802031.
- [44] Liang, X.; Yan, Z.-P.; Han, H.-B.; Wu, Z.-G.; Zheng, Y.-X.; Meng, H.; Zuo, J.-L.; Huang, W. *Angew. Chem. Int. Ed.* **2018**, *57*, 11316–11320.

- [45] Knöllner, J. A.; Meng, G.; Wang, X.; Hall, D.; Pershin, A.; Beljonne, D.; Olivier, Y.; Laschat, S.; Zysman-Colman, E.; Wang, S. *Angew. Chem. Int. Ed.* **2020**, *59*, 3156–3160.
- [46] Han, S. H.; Jeong, J. H.; Yoo, J. W.; Lee, J. Y. *J. Mater. Chem. C* **2019**, *7*, 3082–3089.
- [47] Ando, M.; Sakai, M.; Ando, N.; Hirai, M.; Yamaguchi, S. *Org. Biomol. Chem.* **2019**, *17*, 5500–5504.
- [48] Nakatsuka, S.; Yasuda, N.; Hatakeyama, T. *J. Am. Chem. Soc.* **2018**, *140*, 13562–13565.
- [49] Fukagawa, H.; Oono, T.; Iwasaki, Y.; Hatakeyama, T.; Shimizu, T. *Mater. Chem. Front.* **2018**, *2*, 704–709.
- [50] Saint-Louis, C. J.; Shavnore, R. N.; McClinton, C. D. C.; Wilson, J. A.; Magill, L. L.; Brown, B. M.; Lamb, R. W.; Webster, C. E.; Schrock, A. K.; Huggins, M. T. *Org. Biomol. Chem.* **2017**, *15*, 10172–10183.
- [51] Zhang, W.; Zhang, F.; Tang, R.; Fu, Y.; Wang, X.; Zhuang, X.; He, G.; Feng, X. *Org. Lett.* **2016**, *18*, 3618–3621.
- [52] Wang, S.; Yang, D.-T.; Lu, J.; Shimogawa, H.; Gong, S.; Wang, X.; Møllerup, S. K.; Wakamiya, A.; Chang, Y.-L.; Yang, C.; Lu, Z.-H. *Angew. Chem. Int. Ed.* **2015**, *54*, 15074–15078.
- [53] Li, G.; Zhao, Y.; Li, J.; Cao, J.; Zhu, J.; Sun, X. W.; Zhang, Q. *J. Org. Chem.* **2015**, *80*, 196–203.
- [54] Hashimoto, S.; Ikuta, T.; Shiren, K.; Nakatsuka, S.; Ni, J.; Nakamura, M.; Hatakeyama, T. *Chem. Mater.* **2014**, *26*, 6265–6271.
- [55] Chang, Y.-L.; Rao, Y.-L.; Gong, S.; Ingram, G. L.; Wang, S.; Lu, Z.-H. *Adv. Mater.* **2014**, *26*, 6729–6733.

- [56] Wang, X.; Zhang, F.; Liu, J.; Tang, R.; Fu, Y.; Wu, D.; Xu, Q.; Zhuang, X.; He, G.; Feng, X. *Org. Lett.* **2013**, *15*, 5714–5717.
- [57] Ishida, N.; Narumi, M.; Murakami, M. *Helv. Chim. Acta* **2012**, *95*, 2474–2480.
- [58] Bosdet, M. J. D.; Piers, W. E. *Can. J. Chem.* **2009**, *87*, 8–29.
- [59] Wang, X.-Y.; Wang, J.-Y.; Pei, J. *Chem. Eur. J.* **2015**, *21*, 3528–3539.
- [60] Helten, H. *Chem. Eur. J.* **2016**, *22*, 12972–12982.
- [61] Morgan, M. M.; Piers, W. E. *Dalton Trans.* **2016**, *45*, 5920–5924.
- [62] Stępień, M.; Gońka, E.; Żyła, M.; Sprutta, N. *Chem. Rev.* **2017**, *117*, 3479–3716.
- [63] Iqbal, S. A.; Pahl, J.; Yuan, K.; Ingleson, M. J. *Chem. Soc. Rev.* **2020**, *49*, 4564–4591.
- [64] Bosdet, M. J. D.; Jaska, C. A.; Piers, W. E.; Sorensen, T. S.; Parvez, M. *Org. Lett.* **2007**, *9*, 1395–1398.
- [65] Hatakeyama, T.; Hashimoto, S.; Seki, S.; Nakamura, M. *J. Am. Chem. Soc.* **2011**, *133*, 18614–18617.
- [66] Müller, M.; Maichle-Mössmer, C.; Sirsch, P.; Bettinger, H. F. *ChemPlusChem* **2013**, *78*, 988–994.
- [67] Wang, X.-Y.; Zhuang, F.-D.; Wang, R.-B.; Wang, X.-C.; Cao, X.-Y.; Wang, J.-Y.; Pei, J. *J. Am. Chem. Soc.* **2014**, *136*, 3764–3767.
- [68] Bonifazi, D.; Fasano, F.; Lorenzo-Garcia, M. M.; Marinelli, D.; Oubaha, H.; Tasseroul, J. *Chem. Comm.* **2015**, *51*, 15222–15236.
- [69] Krieg, M.; Reichert, F.; Haiss, P.; Ströbele, M.; Eichele, K.; Treanor, M.-J.; Schaub, R.; Bettinger, H. F. *Angew. Chem. Int. Ed.* **2015**, *54*, 8284–8286.
- [70] Otero, N.; El-kelany, K. E.; Pouchan, C.; Rérat, M.; Karamanis, P. *Phys. Chem. Chem. Phys.* **2016**, *18*, 25315–25328.

- [71] Fu, Y.; Zhang, K.; Dmitrieva, E.; Liu, F.; Ma, J.; Weigand, J. J.; Popov, A. A.; Berger, R.; Pisula, W.; Liu, J.; Feng, X. *Org. Lett.* **2019**, *21*, 1354–1358.
- [72] Møllerup, S. K.; Wang, S. *Trends Chem.* **2019**, *1*, 77 – 89.
- [73] Pati, P. B.; Jin, E.; Kim, Y.; Kim, Y.; Mun, J.; Kim, S. J.; Kang, S. J.; Choe, W.; Lee, G.; Shin, H.-J.; Park, Y. S. *Angew. Chem. Int. Ed.* **2020**, *59*, 14891–14895.
- [74] Scholz, A. S.; Massoth, J. G.; Bursch, M.; Mewes, J.-M.; Hetzke, T.; Wolf, B.; Bolte, M.; Lerner, H.-W.; Grimme, S.; Wagner, M. *J. Am. Chem. Soc.* **2020**, *142*, 11072–11083.
- [75] Stock, A.; Pohland, E. *Ber. Dtsch Chem. Ges.* **1926**, *59*, 2215–2223.
- [76] Dosso, J.; Tasseroul, J.; Fasano, F.; Marinelli, D.; Biot, N.; Fermi, A.; Bonifazi, D. *Angew. Chem. Int. Ed.* **2017**, *56*, 4483–4487.
- [77] Dosso, J.; Battisti, T.; Ward, B. D.; Demitri, N.; Hughes, C. E.; Williams, P. A.; Harris, K. D. M.; Bonifazi, D. *Chem. Eur. J.* **2020**, *26*, 6608–6621.
- [78] Allemann, O.; Duttwyler, S.; Romanato, P.; Baldrige, K. K.; Siegel, J. S. *Science* **2011**, *332*, 574–577.
- [79] Hoffmann, K. F.; Engelhardt, U. *Z. Naturforsch.* **1970**, *25b*, 317–318.
- [80] Møller, A.; Habben, C. *Monatsh. Chem.* **1982**, *113*, 139–153.
- [81] Møller, A.; Habben, C.; Noltemeyer, M.; Sheldrick, G. M. *Z. Naturforsch.* **1982**, *37b*, 1504–1506.
- [82] Oesterle, R.; Maringele, W.; Møller, A. *J. Organomet. Chem.* **1985**, *284*, 281–289.
- [83] Kawashima, Y.; Takeo, H.; Matsumura, C. *Inorg. Chem.* **1989**, *28*, 666–669.
- [84] Komorowska, M.; Niedenzu, K.; Weber, W. *Inorg. Chem.* **1990**, *29*, 289–294.
- [85] Fitzgerald, G.; Lin, C.; Dyatkin, A. B.; Lahti, P. M. Organic electroluminescent materials and devices. US 20180226580A1, 2018.

- [86] Müller, M.; Behnle, S.; Maichle-Mössmer, C.; Bettinger, H. F. *Chem. Comm.* **2014**, *50*, 7821–7823.
- [87] Köster, R.; Hattori, S.; Morita, Y. *Angew. Chem.* **1965**, *77*, 719–720.
- [88] Köster, R.; Iwasaki, K.; Hattori, S.; Morita, Y. *Liebigs Ann. Chem.* **1968**, *720*, 23–31.
- [89] Clar, E.; Zander, M. *J. Chem. Soc.* **1957**, 4616–4619.
- [90] Tokita, S.; Hiruta, K.; Kitahara, K.; Nishi, H. *Synthesis* **1982**, *3*, 229–231.
- [91] Tokita, S.; Hiruta, K.; Ishikawa, S.; Kitahara, K.; Nishi, H. *Synthesis* **1982**, *10*, 854–855.
- [92] Fort, E. H.; Jeffreys, M. S.; Scott, L. T. *Chem. Commun.* **2012**, *48*, 8102–8104.
- [93] Głodek, M.; Makal, A.; Plažuk, D. *J. Org. Chem.* **2018**, *83*, 14165–14174.
- [94] Kurpanik, A.; Matussek, M.; Szafraniec-Gorol, G.; Filapek, M.; Lodowski, P.; Marcol-Szumilas, B.; Ignasiak, W.; Małecki, J. G.; Machura, B.; Małecka, M.; Danikiewicz, W.; Pawlus, S.; Krompiec, S. *Chem. Eur. J.* **2020**, *26*, 12150–12157.
- [95] Fort, E. H.; Donovan, P. M.; Scott, L. T. *J. Am. Chem. Soc.* **2009**, *131*, 16006–16007.
- [96] Fort, E. H.; Scott, L. T. *J. Mater. Chem.* **2011**, *21*, 1373–1381.
- [97] Paetzold, P.; Richter, A.; Thijssen, T.; Würtenberg, S. *Chem. Ber.* **1979**, *112*, 3811–3827.
- [98] Schreyer, P.; Paetzold, P.; Boese, R. *Chem. Ber.* **1988**, *121*, 195–205.
- [99] Paetzold, P.; Kiesgen, J.; Krahé, K.; Meier, H.-U.; Boese, R. *Z. Naturforsch. B* **1991**, *46*, 853–860.
- [100] Wang, X.; Zhang, F.; Schellhammer, K. S.; Machata, P.; Ortmann, F.; Cuniberti, G.; Fu, Y.; Hunger, J.; Tang, R.; Popov, A. A.; Berger, R.; Müllen, K.; Feng, X. *J. Am. Chem. Soc.* **2016**, *138*, 11606–11615.

- [101] Numano, M.; Nagami, N.; Nakatsuka, S.; Katayama, T.; Nakajima, K.; Tatsumi, S.; Yasuda, N.; Hatakeyama, T. *Chem. Eur. J.* **2016**, *22*, 11574–11577.
- [102] Yang, D.-T.; Nakamura, T.; He, Z.; Wang, X.; Wakamiya, A.; Peng, T.; Wang, S. *Org. Lett.* **2018**, *20*, 6741–6745.
- [103] Sun, Z.; Yi, C.; Liang, Q.; Bingi, C.; Zhu, W.; Qiang, P.; Wu, D.; Zhang, F. *Org. Lett.* **2020**, *22*, 209–213.
- [104] Noda, H.; Furutachi, M.; Asada, Y.; Shibasaki, M.; Kumagai, N. *Nat. Chem.* **2017**, *9*, 571.
- [105] Fingerle, M. *Beiträge zur Synthese von BN-substituierter polyzyklischer Aromaten*; Masterarbeit, 2016.
- [106] Fingerle, M.; Stocker, S.; Bettinger, H. F. *Synthesis* **2019**, *51*, 4147–4152.
- [107] Wang, F.; Tanaka, R.; Cai, Z.; Nakayama, Y.; Shiono, T. *Appl. Organomet. Chem.* **2015**, *29*, 771–776.
- [108] Odom, S. A.; Parkin, S. R.; Anthony, J. E. *Org. Lett.* **2003**, *5*, 4245–4248.
- [109] Bettinger, H. F.; Einholz, R.; Göttler, A.; Junge, M.; Sättele, M.-S.; Schnepf, A.; Schrenk, C.; Schundelmeier, S.; Speiser, B. *Org. Chem. Front.* **2017**, *4*, 853–860.
- [110] Lakowicz, J. R. *Principles of Fluorescence Spectroscopy* **2006**, Springer Verlag Berlin, 3rd Edition.
- [111] Ponce Ortiz, R.; Malavé Osuna, R.; Ruiz Delgado, M. C.; Casado, J.; Hernández, V.; López Navarrete, J. T.; Sakamoto, Y.; Suzuki, T. *Proc. of SPIE* **2006**, *6192*, 61922V–1.
- [112] Melhuish, W. H. *J. Phys. Chem.* **1961**, *65*, 229–235.
- [113] Brouwer, A. M. *Pure Appl. Chem.* **2011**, *83*, 2213–2228.

- [114] Zahradnik, R.; Tichy, M.; Hochmann, P.; Reid, D. H. *J. Phys. Chem.* **1967**, *71*, 3040–3046.
- [115] Schleyer, P. v. R.; Maerker, C.; Dransfeld, A.; Jiao, H.; van Eikema Hommes, N. J. R. *J. Am. Chem. Soc.* **1996**, *118*, 6317–6318.
- [116] Schleyer, P. v. R.; Jiao, H.; Hommes, N. J. R. v. E.; Malkin, V. G.; Malkina, O. L. *J. Am. Chem. Soc.* **1997**, *119*, 12669–12670.
- [117] Chen, Z.; Wannere, C. S.; Corminboeuf, C.; Puchta, R.; Schleyer, P. v. R. *Chem. Rev.* **2005**, *105*, 3842–3888.
- [118] Clar, E. *The aromatic sextet.*; Wiley-Interscience: London, 1972.
- [119] Solà, M. *Front. Chem.* **2013**, *1*, 22.
- [120] Lee, C.-I.; Zhou, J.; Ozerov, O. V. *J. Am. Chem. Soc.* **2013**, *135*, 3560–3566.
- [121] Hattori, Y.; Ogaki, T.; Ishimura, M.; Ohta, Y.; Kirihata, M. *Tetrahedron Lett.* **2008**, *49*, 4977–4980.
- [122] Allen, F. H.; Watson, D. G.; Brammer, L.; Orpen, A. G.; Taylor, R. *International Tables for Crystallography*; American Cancer Society, 2006; Chapter 9.5, pp 790–811.
- [123] Catalfo, A.; Serrentino, M. E.; Librando, V.; Perrini, G.; Guidi, G. D. *Appl. Spectrosc.* **2008**, *62*, 1233–1237.
- [124] Mohammed, O. F.; Vauthey, E. *J. Phys. Chem. A* **2008**, *112*, 3823–3830.
- [125] Reichardt, C.; Vogt, R. A.; Crespo-Hernández, C. E. *J. Chem. Phys.* **2009**, *131*, 224518.
- [126] Vogt, R. A.; Reichardt, C.; Crespo-Hernández, C. E. *J. Phys. Chem. A* **2013**, *117*, 6580–6588.
- [127] Guthrie, J. P. *Can. J. Chem.* **2014**, *1*, 2342–2354.
- [128] de Lijser, H. J. P.; Rangel, N. A. *J. Org. Chem.* **2004**, *69*, 8315–8322.

- [129] Clark, E. R.; Ingleson, M. J. *Angew. Chem. Int. Ed.* **2014**, *53*, 11306–11309.
- [130] Bagheri, S.; Zarei, M.; Zolfigol, M. A.; Mallakpour, S.; Behranvand, V. *J. Iran. Chem. Soc.* **2020**, *17*, 2737–2843.
- [131] Desiraju, G. R.; Gavezzotti, A. *Acta Crystallogr. B* **1989**, *45*, 473–482.
- [132] Clar, E.; Ironside, C. T.; Zander, M. *J. Chem. Soc.* **1959**, 142–147.
- [133] Kübel, C.; Eckhardt, K.; Enkelmann, V.; Wegner, G.; Müllen, K. *J. Mater. Chem.* **2000**, *10*, 879–886.
- [134] Herges, R.; Geuenich, D. *J. Phys. Chem. A* **2001**, *105*, 3214–3220.
- [135] Geuenich, D.; Hess, K.; Köhler, F.; Herges, R. *Chem. Rev.* **2005**, *105*, 3758–3772.
- [136] Ozasa, S.; Fujioka, Y.; Fujiwara, M.; Ibuki, E. *Chem. Pharm. Bull* **1980**, *28*, 3210–3222.

Anhang

Fingerle, M.; Maichle-Mössmer, C.; Schundelmeier, S.; Speiser, B.; Bettinger, H. F., *Org. Lett.* **2017**, *19*, 4428-4431.

Fingerle, M.; Stocker, S.; Bettinger, H. F., *Synthesis* **2019**, *51*, 4147-4152.

Fingerle, M.; Bettinger, H. F., *Chem. Commun.* **2020**, *56*, 3847-3850.

Fingerle, M.; Dingerkus, J., Schubert, H., Wurst, K., Scheele, M., Bettinger, H. F., *Angew. Chem. Int. Ed.* **2021**, *60*, 15798-15802.

Synthesis and Characterization of a Boron–Nitrogen–Boron Zigzag-Edged Benzo[fg]tetracene Motif

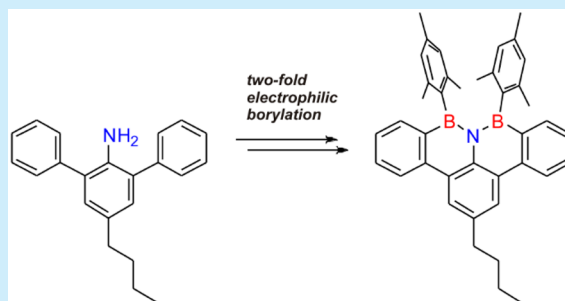
Michael Fingerle,[†] Cécilia Maichle-Mössmer,[‡] Simon Schundelmeier,[†] Bernd Speiser,[†] and Holger F. Bettinger^{*,†}

[†]Institut für Organische Chemie, Universität Tübingen, Auf der Morgenstelle 18, 72076 Tübingen, Germany

[‡]Institut für Anorganische Chemie, Universität Tübingen, Auf der Morgenstelle 18, 72076 Tübingen, Germany

S Supporting Information

ABSTRACT: The boron–nitrogen–boron (BNB) zigzag edged benzo[fg]tetracene is accessible from 4-butyl-2,6-diphenylaniline in four steps in good yields. The two mesityl groups stabilize the boron centers toward nucleophilic attack and result in two enantiomeric forms in the solid state. The title compound has a large optical gap, shows blue fluorescence, and is quite resistant toward oxidation and reduction.



Current research is attempting to introduce heteroatoms into organic structural motifs for modifying electronic properties of potential organic semiconductors.^{1–6} A quite popular strategy is to incorporate the boron–nitrogen (B=N) unit that is isoelectronic and isosteric to a pair of doubly bonded carbon atoms (C=C), and this has led to the burgeoning field of 1,2-dihydro-1,2-azaborine chemistry.^{7–14} The incorporation of an adjacent nitrogen atom has made available nitrogen–boron–nitrogen (NBN) zigzag edged polycyclic aromatic hydrocarbons (PAH) recently (A),^{15,16} while the incorporation of a NBNB unit into the bay region of a perylene derivative (B) was reported by us earlier (Figure 1).¹⁷

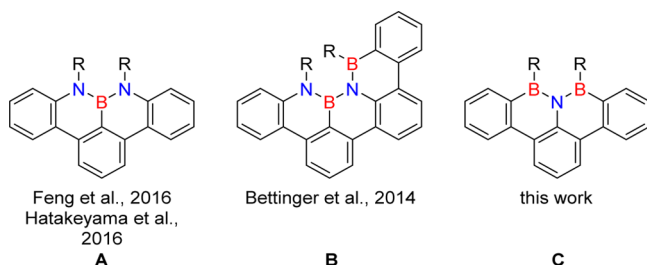
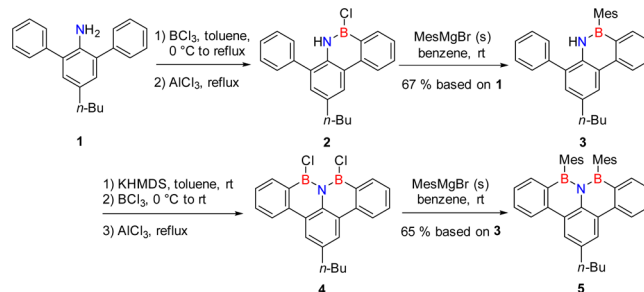


Figure 1. NBN-type, NBNB-type, and BNB-type edges of polycyclic aromatic hydrocarbons.

The boron–nitrogen–boron (BNB) type edge (C) was only obtained as a reactive intermediate that was trapped with a boronic acid to yield a central B₃NO₂ ring.¹⁸ The structural and spectroscopic properties of molecules of type C are unknown currently. Here we describe the synthesis and full characterization of a derivative of C that is stabilized by mesityl groups (R = Mes).

We started the synthesis from the known 4-*n*-butyl-2,6-diphenylaniline (1).¹⁹ Preliminary experiments showed that the 2-fold addition of boron atoms to the aniline with BCl₃ or BBr₃ is not successful. Presumably bonding of the first boron atom reduces the nucleophilicity of the nitrogen atom to such an extent that a second reaction with a boron species is not possible. We hence had to build up the system in a stepwise fashion (Scheme 1). Following Dewar et al.,^{20,21} the electro-

Scheme 1. First Borylation of 4-*n*-Butyl-2,6-diphenylaniline



philic borylation of one phenyl group was achieved using boron trichloride and aluminum trichloride. The resulting 1,2-dihydro-1,2-azaborine derivative 2 was not isolated due to its facile hydrolysis, but was transformed into the mesityl derivative 3. This was achieved using the commercially available mesityl Grignard reagent MesMgBr in diethyl ether. After removal of the diethyl ether, 3 mass equiv of the resulting solid were reacted with 2 to give 3 in an overall yield of 67%

Received: June 20, 2017

Published: August 16, 2017

on **1**. The progress of the reaction can be followed by ^{11}B NMR as the chemical shift of **2** is around 34 ppm while that of compound **3** is in the region of 40 ppm. The mesityl group significantly increases the stability of compound **3** toward hydrolysis so that purification by column chromatography and characterization by NMR spectroscopy, ESI/TOF mass spectrometry, and elemental analysis is possible.

The key to successful second borylation is the utilization of a sterically hindered base, such as KHMDS.^{22–24} After deprotonation of the nitrogen center, borylation of the phenyl ring proceeds upon addition of boron trichloride and aluminum trichloride. Analysis of the crude reaction product by MS ($m/z = 389$) and NMR ($\delta^{11}\text{B} = 44$ ppm) revealed that the mesityl group was substituted by a chlorine atom resulting in **4**. Due to the expected facile hydrolysis, no attempts were made to purify **4**. Instead, the crude reaction product was transformed into the dimesityl compound **5** by treatment with 6 mass equiv of MesMgBr. In this way, target compound **5** was obtained in 65% yield based on **3**. The target compound **5** could be isolated as colorless needles by column chromatography followed by crystallization from *n*-hexane. BNB-Benzo[*fg*]tetracene **5** was characterized by multinuclear (^1H , ^{13}C , ^{11}B) and correlated (H–H–COSY, HMBC, HSQC) NMR spectroscopy as well as by high resolution ESI/TOF mass spectrometry and elemental analysis.

Single crystals suitable for X-ray crystallography were obtained by recrystallization from *n*-hexane. The BNB-benzo[*fg*]tetracene **5** crystallizes in the monoclinic space group $P2_1$ with two pairs of enantiomeric molecules of approximate C_2 symmetry in the unit cell. The tetracene unit is strongly twisted causing the approximate C_2 symmetric structure of the molecule. The twist angle measured based on the four external carbon atoms C1–C4 (see Figure 2a) is 32° . The B–N bond

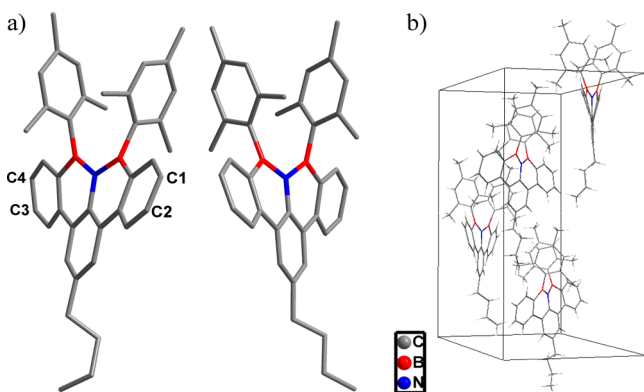


Figure 2. (a) Molecular structures of **5** (hydrogen atoms omitted for clarity); (b) packing of molecules of **5**.

lengths are on average 1.46 Å in the molecular structures, similar to the analogous bonds in typical BN-embedded PAHs (1.45–1.47 Å).^{7,25} The mesityl groups are oriented almost perpendicularly with respect to the rings to which they are attached. This arrangement of the mesityl groups is responsible for the lack of π -stacking between the molecules. Instead, the four molecules in the unit cell show a helical arrangement with large intermolecular distances (see Figure 2b).

Computations at the B3LYP/6-311+G** level of theory were performed to shed light on the barrier for racemization of the two enantiomeric forms of **5**. To facilitate the computations, the model system **5*** without the *n*-butyl

group was employed throughout this study. We located a transition state of C_s symmetry that interconnects the two enantiomers of **5*** with a barrier of only 4.2 kcal/mol. A low barrier for racemization is in agreement with the observation of only one signal for the ortho- CH_3 groups of the mesityl substituents in NMR experiments. Hence, no attempts were made to separate the two enantiomeric forms experimentally. Furthermore, computations reveal that the steric interaction of the two *peri*-positioned mesityl groups is responsible for the twisting of the molecular structure of **5***. If these are omitted, compound **C** ($R = \text{H}$) is a minimum of C_{2v} symmetry.

In the absorption spectrum (Figure 3) of **5**, there are two main absorption features in the wavelength regions of 280–300

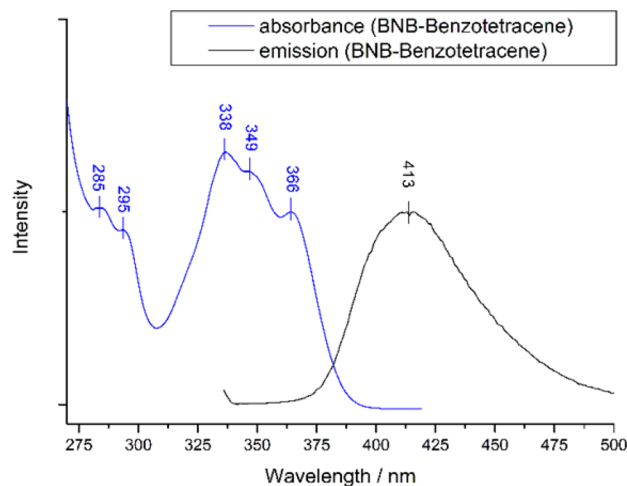


Figure 3. Normalized absorption (blue) and fluorescence (black, $\lambda_{\text{ex}} = 338$ nm) spectrum of **5** (10^{-5} M in CH_2Cl_2).

nm and 325–375 nm. An excited state computation (TD-B3LYP/6-311+G**) places the S_1 state at 371 nm and shows that it involves primarily an excitation from the HOMO that is centered on the mesityl groups to the LUMO that is delocalized over the BNB-benzo[*fg*]tetracene unit (Figure 4).

The BNB-benzo[*fg*]tetracene is isolectronic to the unknown parent all-carbon cation **D** (see Figure 5) that was investigated by Zahradnik et al. in the context of phenalenyl derivatives.²⁶ These authors estimated the lowest wavelength absorption of **D** to be at around 575 nm based on extrapolation.²⁶ Computations (TD-B3LYP/6-311+G**) confirm this estimate ($E(S_1) = 545$ nm). Although the shape of the frontier orbitals is similar (see Figure 4), the orbital energies of **D** and **C** differ as a consequence of BNB-substitution and the positive charge. This causes a considerable bathochromic shift of 1.5 eV.

The fluorescence spectrum of compound **5** was recorded with an excitation wavelength of 338 nm, but it is independent of the excitation energy indicative of Kasha-rule emission behavior (Figure 3). The fluorescence spectrum is broad, featureless, and not a mirror image of the absorption spectrum, as usually observed for tetracene derivatives. If the electronic excitation alters the nuclear geometry of the S_1 state, the spacing of the vibrational energy level of the excited states will not be similar to that of the ground state, and hence the vibrational structures between the absorption and the emission spectra are not similar.²⁷ The Stokes shift of 3109 cm^{-1} is quite large compared to tetracene or disubstituted 5,12-bis(triisopropylsilyl ethynyl)tetracene for which Stokes shifts of only 242 and 411 cm^{-1} , respectively, were measured.^{28–30} Increased

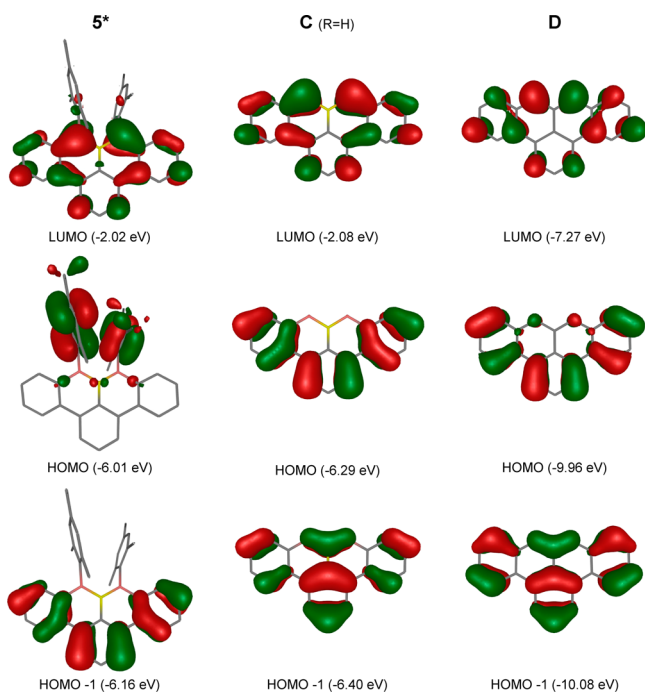


Figure 4. Molecular orbitals of **5*** (the *n*-butyl group is omitted), and compounds **C** and **D** as computed at the B3LYP/6-311+G** level of theory.

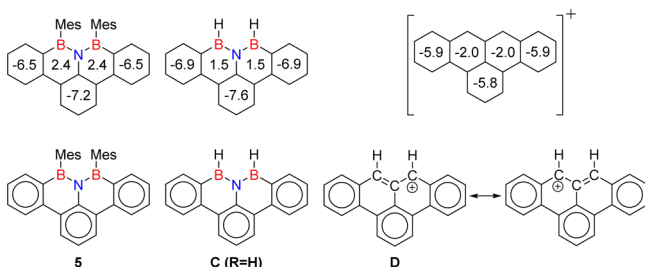


Figure 5. NICS(0) values of the BNB-benzo[*fg*]tetracene motif **5*** computed at the B3LYP/6-311+G** level of theory (top left) and Clar's sextet (bottom left); BNB-benzo[*fg*]tetracene scaffold **C** and carbocation **D** for comparison. The NICS(0) of benzene is -8.1 .

Stokes shifts of 800 cm^{-1} up to 1500 cm^{-1} were detected for various NBN-benzo[*fg*]tetracene derivatives.^{15,16} The large Stokes shift of compound **5** indicates significant structural reorganization in the lowest energy excited state of **5**, which is possibly associated with the twisting of the molecule in the ground state. Indeed, the twist of the molecular structure is significantly smaller in the S_1 state (21° ; see Figure S4 in Supporting Information (SI)) according to geometry optimization at the TD-B3LYP/6-311+G** level of theory. The fluorescence quantum yield of **5** in CH_2Cl_2 , measured with reference to anthracene in ethanol ($\phi_{\text{Fl}} = 0.27$), is sizable, $\phi_{\text{Fl}} = 0.21$.^{27,31} The known NBN-benzo[*fg*]tetracene analogues have similar fluorescence quantum yields ($\phi_{\text{Fl}} = 0.21\text{--}0.24$).¹⁵

Cyclic voltammograms of **5** in a $\text{CH}_2\text{Cl}_2/0.1\text{ M NBu}_4\text{PF}_6$ electrolyte at a Pt electrode (see SI, Figure S3) indicate redox processes at fairly positive potentials ($E^0 = +1.012\text{ V vs Fc/Fc}^+$) for oxidation and strongly negative potentials ($E_p = -2.705\text{ V vs Fc/Fc}^+$) for reduction. While the oxidation product shows some stability at a scan rate of $\nu = 0.2\text{ V s}^{-1}$ (reverse peak), the reduction is chemically totally irreversible at this time scale. Further mechanistic interpretations are precluded by the fact

that the reduction of **5** is superimposed on the solvent decomposition and that irreversible variations of the electrode properties occur upon passing through the oxidation signal. Nevertheless, the large gap of $\sim 3.7\text{ V}$ between electrochemical oxidation and reduction of **5** is consistent with the large HOMO–LUMO gap indicated by the DFT calculations and the UV/vis results.

We calculated the nucleus-independent chemical shift (NICS(0) values; for NICS(1) values see SI, Figure S5) at the B3LYP/6-311+G** level to investigate the influence of BNB substitution on the aromaticity of the benzo[*fg*]tetracene motif.³² The three rings on the periphery of the molecule **5*** have relatively negative NICS(0) values of -6.5 and -7.2 and can be identified as aromatic rings (Figure 5).³² The rings with BN substitution show positive NICS(0) values ($+2.4$), indicating that they are nonaromatic. The parent NBN-benzotetracene **C** is of C_{2v} symmetry and has qualitatively similar NICS(0) values (see Figure 5). The picture obtained from the NICS computations is in agreement with the expectations based on Clar's^{33,34} theory of the aromatic sextet that would ascribe aromatic sextets to the three peripheral rings.

Our NICS computations for carbocation **D** (see Figure 5) give a qualitatively similar picture of the aromatic nature of individual rings as obtained for **C** ($R = \text{H}$). In this sense, **D** can be rationalized as a *m*-terphenyl that is interconnected by an allyl cation unit. Likewise, the BNB linkage, isosteric and isoelectronic to the allyl cation, interconnects the *m*-terphenyl unit in structure **C**.

In summary, we have shown that the novel BNB-type zigzag-edged benzo[*fg*]tetracene structural motif is accessible synthetically in four steps from a *m*-terphenyl. Employing bulky mesityl groups for steric protection of the boron centers toward nucleophilic attack provides stability under atmospheric conditions for target compound **5**. This allows application of standard purification techniques and full characterization including single-crystal X-ray crystallography. Incorporation of the BNB moiety at the zigzag periphery of the benzo[*fg*]tetracene results in significant bathochromic shifts of the absorption spectrum and reasonably strong fluorescence ($\phi_{\text{Fl}} = 0.21$) with a large Stokes shift (3100 cm^{-1}). The BNB-benzo[*fg*]tetracene unit present in **5** is best considered to be comprised of a *m*-terphenyl moiety with a BNB interconnect. The new compound class serves as an example for the experimental realization of heteroatom functionalized PAHs that are unknown in their all-carbon form. The introduction of other groups than mesityl at the BNB-zigzag edges is expected to be straightforward to allow tuning of the (optical) properties as well as to provide opportunities for using the BNB building block in syntheses of larger boron–nitrogen substituted PAH molecules.

■ ASSOCIATED CONTENT

Supporting Information

The Supporting Information is available free of charge on the ACS Publications website at DOI: 10.1021/acs.orglett.7b01873.

Experimental procedures, spectra, cyclic voltammogram, and computed Cartesian coordinates (PDF)

Single-crystal X-ray data for **5** (CIF)

AUTHOR INFORMATION

Corresponding Author

*E-mail: Holger.Bettinger@uni-tuebingen.de.

ORCID

Bernd Speiser: 0000-0001-5111-8314

Holger F. Bettinger: 0000-0001-5223-662X

Notes

The authors declare no competing financial interest.

ACKNOWLEDGMENTS

This work was supported in part by the Deutsche Forschungsgemeinschaft. S.S. thanks the Karl und Anna Buck Stiftung for a fellowship. We acknowledge support by the state of Baden-Württemberg through bwHPC and the German Research Foundation (DFG) through grant no INST 40/467-1 FUGG.

REFERENCES

- (1) Wu, J.; Pisula, W.; Müllen, K. *Chem. Rev.* **2007**, *107*, 718.
- (2) Otero, N.; El-kelany, K. E.; Pouchan, C.; Rerat, M.; Karamanis, P. *Phys. Chem. Chem. Phys.* **2016**, *18*, 25315.
- (3) Morgan, M. M.; Piers, W. E. *Dalton Trans.* **2016**, *45*, 5920.
- (4) Escande, A.; Ingleson, M. J. *Chem. Commun.* **2015**, *51*, 6257.
- (5) Stępień, M.; Gońka, E.; Żyła, M.; Sprutta, N. *Chem. Rev.* **2017**, *117*, 3479.
- (6) Jiang, W.; Li, Y.; Wang, Z. *Chem. Soc. Rev.* **2013**, *42*, 6113.
- (7) Liu, Z.; Marder, T. B. *Angew. Chem., Int. Ed.* **2008**, *47*, 242.
- (8) Campbell, P. G.; Marwitz, A. J. V.; Liu, S.-Y. *Angew. Chem., Int. Ed.* **2012**, *51*, 6074.
- (9) Wang, X.-Y.; Wang, J.-Y.; Pei, J. *Chem. - Eur. J.* **2015**, *21*, 3528.
- (10) Bonifazi, D.; Fasano, F.; Lorenzo-Garcia, M. M.; Marinelli, D.; Oubaha, H.; Tasseroul, J. *Chem. Commun.* **2015**, *51*, 15222.
- (11) Helten, H. *Chem. - Eur. J.* **2016**, *22*, 12972.
- (12) Brown, A. N.; Li, B.; Liu, S.-Y. *J. Am. Chem. Soc.* **2015**, *137*, 8932.
- (13) Bosdet, M. J. D.; Piers, W. E. *Can. J. Chem.* **2009**, *87*, 8.
- (14) Bosdet, M. J. D.; Jaska, C. A.; Piers, W. E.; Sorensen, T. S.; Parvez, M. *Org. Lett.* **2007**, *9*, 1395.
- (15) Numan, M.; Nagami, N.; Nakatsuka, S.; Katayama, T.; Nakajima, K.; Tatsumi, S.; Yasuda, N.; Hatakeyama, T. *Chem. - Eur. J.* **2016**, *22*, 11574.
- (16) Wang, X.; Zhang, F.; Schellhammer, K. S.; Machata, P.; Ortmann, F.; Cuniberti, G.; Fu, Y.; Hunger, J.; Tang, R.; Popov, A. A.; Berger, R.; Müllen, K.; Feng, X. *J. Am. Chem. Soc.* **2016**, *138*, 11606.
- (17) Müller, M.; Behnle, S.; Maichle-Mössmer, C.; Bettinger, H. F. *Chem. Commun.* **2014**, *50*, 7821.
- (18) Noda, H.; Furutachi, M.; Asada, Y.; Shibasaki, M.; Kumagai, N. *Nat. Chem.* **2017**, *9*, 571.
- (19) Wang, F.; Tanaka, R.; Cai, Z.; Nakayama, Y.; Shiono, T. *Appl. Organomet. Chem.* **2015**, *29*, 771.
- (20) Dewar, M. J. S.; Kubba, V. P.; Pettit, R. *J. Chem. Soc.* **1958**, 3073.
- (21) Harris, K. D. M.; Kariuki, B. M.; Lambropoulos, C.; Philp, D.; Robinson, J. M. *Tetrahedron* **1997**, *53*, 8599.
- (22) Ishibashi, J. S. A.; Dargelos, A.; Darrigan, C.; Chrostowska, A.; Liu, S.-Y. *Organometallics* **2017**, *36*, ASAP DOI: [10.1021/acs.organo- met.7b00296](https://doi.org/10.1021/acs.organo- met.7b00296).
- (23) Hatakeyama, T.; Hashimoto, S.; Seki, S.; Nakamura, M. *J. Am. Chem. Soc.* **2011**, *133*, 18614.
- (24) Wang, X.-Y.; Zhuang, F.-D.; Wang, R.-B.; Wang, X.-C.; Cao, X.-Y.; Wang, J.-Y.; Pei, J. *J. Am. Chem. Soc.* **2014**, *136*, 3764.
- (25) Bosdet, M. J. D.; Piers, W. E.; Sorensen, T. S.; Parvez, M. *Angew. Chem., Int. Ed.* **2007**, *46*, 4940.
- (26) Zahradnik, R.; Tichy, M.; Hochmann, P.; Reid, D. H. *J. Phys. Chem.* **1967**, *71*, 3040.
- (27) Lakowicz, J. R. *Principles of Fluorescence Spectroscopy*, 3rd ed.; Springer: Berlin, 2006; pp 5–8.
- (28) Bettinger, H. F.; Einholz, R.; Göttler, A.; Junge, M.; Sättele, M.-S.; Schnepf, A.; Schrenk, C.; Schundelmeier, S.; Speiser, B. *Org. Chem. Front.* **2017**, *4*, 853.
- (29) Ponce Ortiz, R.; Malavé Osuna, R.; Ruiz Delgado, M. C.; Casado, J.; Hernández, V.; López Navarrete, J. T.; Sakamoto, Y.; Suzuki, T. *Proc. SPIE* **2006**, *6192*, 61922V–1.
- (30) Odom, S. A.; Parkin, S. R.; Anthony, J. E. *Org. Lett.* **2003**, *5*, 4245.
- (31) Melhuish, W. H. *J. Phys. Chem.* **1961**, *65*, 229.
- (32) Schleyer, P. v. R.; Maerker, C.; Dransfeld, A.; Jiao, H.; Hommes, N. J. R. v. E. *J. Am. Chem. Soc.* **1996**, *118*, 6317.
- (33) Clar, E. *The Aromatic Sextet*; Wiley-Interscience: London, 1972.
- (34) Solà, M. *Front. Chem.* **2013**, *1*, 22.

Supporting Information (SI)

Synthesis and Characterization of a Boron–Nitrogen–Boron Zigzag–Edged Benzo[fg]tetracene Motif

Michael Fingerle,^a Cécilia Maichle-Mössmer,^b Simon Schundelmeier,^a Bernd Speiser,^a

Holger F. Bettinger^{a,*}

^a Institut für Organische Chemie, Auf der Morgenstelle 18, 72076 Tübingen, Germany;

^b Institut für Anorganische Chemie, Auf der Morgenstelle 18, 72076 Tübingen, Germany

E-Mail: Holger.Bettinger@uni-tuebingen.de

CONTENTS:

1. General	S2
2. Synthetic procedures	S4
3. Cyclic voltammetry	S7
4. X-Ray Crystallographic data	S7
5. Cartesian coordinates of stationary points in Ångström	S8
6. Computed structures of 5*	S13
7. Computed NICS(1) values	S14
8. Spectra	S14

1. GENERAL

All reactions were done under dry and inert conditions by flaming all glassware with a heat gun under vacuum and purging with argon. Chemicals and solvents were purchased in anhydrous form from commercial suppliers. Deuterated dichloromethane was dried over 4 Å molecular sieve and degassed by three freeze-pump-thaw cycles. For working under inert conditions, a MBraun UNILab Glovebox was used. Column chromatography was done with a medium pressure liquid chromatography (MPLC) system (PuriFlash 430 evo, Interchim) using Si-HP 20 µm columns. Thin layer chromatography (TLC) was conducted on pre-coated polyester sheets (40 x 80 mm) from Machery-Nagel (POLYGRAM® SIL G/UV254) with 0.2 mm silica gel 60 with fluorescent indicator. For visualization, a UV light source (254 nm and 366 nm) was used. Nuclear magnetic resonance spectroscopy (NMR) was measured on a Bruker Avance III HD 400 or on a Bruker Avance III HDX 600 both equipped with a dual (¹H/¹³C) probe head. Chemical shifts (δ) are given in ppm, coupling constants *J* in Hertz (Hz) and the multiplicities of the signals are designated as follows: s = singlet, bs = broad singlet, d = doublet, t = triplet, and m = multiplet. Reference for ¹H and ¹³C is tetramethylsilane (TMS) and for ¹¹B BF₃·OEt₂ in CDCl₃. The solvent signal of CD₂Cl₂ was calibrated on 5.32 ppm for ¹H-NMR and 53.84 ppm for ¹³C spectra. High resolution electron spray ionization time of flight mass spectrometry (ESI-TOF-MS) was measured on a maXis 4G Bruker system. Low resolution electron impact mass spectrometry was measured on a MSD 5977 (Agilent Technology) with a DIP (direct inlet probe, SIM) system (EI-MS, 70 eV). Elemental analyses were determined using the Euro EA 3000 system (HEKAtech GmbH).

1.1 UV/VIS ABSORPTION AND FLUORESCENCE SPECTROSCOPY

Optical spectra were recorded on a PerkinElmer Lambda 1050 spectrometer with a PerkinElmer 3D WB Det Module. Emission and excitation spectra were measured on a Cary Varian SPVF spectrometer using Hellma Analytics quartz cuvettes. All spectra were recorded in spectroscopic grade solvents.

The fluorescence quantum yield of **5** in dichloromethane was also recorded with an excitation wavelength $\lambda_{\text{ex}} = 373$ nm. The reference was anthracene in ethanol ($\phi_{\text{Fl}} = 0.27$).¹

1.2 CRYSTAL STRUCTURE DETERMINATION

Compound **5** was crystallized from *n*-hexane as colorless needles. A serviceable crystal was selected under an optical microscope and mounted on a Bruker SMART APEX II instrument equipped with a fine focus sealed tube and curved graphite monochromator using MoK_α radiation ($\lambda = 0.71073$ Å). The crystal was kept at *T* = 100 K during data collection. The data collection strategy was determined using COSMO² employing ω and ϕ scans. Raw data were processed using APEX³ and SAINT,⁴ corrections for absorption effects were applied using SADABS.⁵

The structure was solved by direct methods and refined against all data by full-matrix least-squares methods on F^2 using SHELXTL⁶ and Shelxle.⁷ The data were refined with the following twin law (Twin 0 0 1 0 -1 0 1 0 0) and additionally as an inversion twin. The CCDC reference number is 1557246.

1.3 COMPUTATIONAL METHODS

Geometry optimizations on the S_0 and S_1 potential energy surfaces were performed using the hybrid density functional B3LYP^{8,9} as implemented in Gaussian 09¹⁰ in conjunction with the 6-311+G** basis set.¹¹ The time-dependent version of DFT was employed for computing vertical excitation energies and for geometry optimization on the S_1 PES.¹² Computation of second derivatives either analytically (S_0) or by finite differences (S_1) confirmed that minima and transition states have no or only one imaginary vibrational frequency. The harmonic vibrational frequencies were employed in the standard approximation for obtaining Gibbs free energies at 298.15 K.

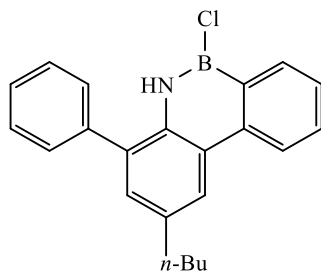
1.4 CYCLIC VOLTAMMETRY

Solvents used for electrochemical experiments were purified by distillation under an argon atmosphere. Amylene free dichloromethane was distilled over P_2O_5 and K_2CO_3 and stored over dried basic Al_2O_3 . It was used within the next 5 days without deterioration of quality. Acetonitrile was distilled successively over P_2O_5 , CaH_2 , and P_2O_5 again. NBu_4PF_6 was recrystallized four times from ethanol/water 3:1 and dried at ≈ 2 mbar and 120 °C for three days.

Electroanalytical experiments were performed at 17 °C under an argon atmosphere with an ECO-Autolab PGSTAT100 (Metrohm) with GPES-Software 4.9.007. As the working electrode, a Pt disk electrode tip (Metrohm part No. 6.1204.310; nominal diameter 3 mm) was used. The electrode was polished with alumina (0.3 μm ; Buehler Micropolish) prior to experiments. The counter electrode consisted of a Pt wire with 1 mm diameter. A Haber-Luggin double reference electrode with a potential determining Ag/Ag^+ redox system (0.01 M $AgClO_4$ in 0.1 M NBu_4PF_6/CH_3CN)¹³ was used as the potential standard. iR drop was compensated by positive feedback under control of the GPES software. Cyclic voltammetric experiments were performed at a scan rate of 0.2 V s^{-1} . The potentials are referenced to an external ferrocene standard ($E^0(Fc/Fc^+)$ vs. $Ag/Ag^+ = +209$ mV).

2. SYNTHETIC PROCEDURES

SYNTHESIS OF 2-BUTYL-6-CHLORO-5,6-DIHYDRO-4-PHENYLDIBENZO[C,E][1,2]AZABORININE (2)

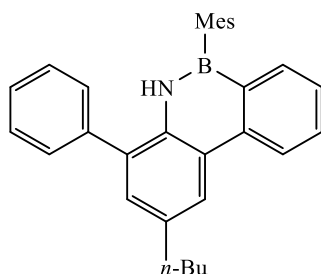


To an ice cooled solution of 1.0 g (3.3 mmol, 1 eq) 4-*n*-butyl-2,6-diphenylbenzenamine in 40 mL dry toluene was added dropwise 5.9 mL (1 M in *n*-hexane, 5.9 mmol, 1.8 eq) BCl₃. After stirring for ½ h, the solution was warmed to room temperature and stirred for 1 h. The resulting mixture was stirred for 6 h under reflux. After being cooled to room temperature, 88 mg (0.7 mmol, 0.2 eq) AlCl₃ was added and the suspension was stirred for 18 h under reflux. After the reaction was finished, all solvents were removed under vacuum to obtain the crude product of **2** (1.5 g) as a grey solid.

¹H NMR (400 MHz, CD₂Cl₂, δ): 8.51-8.55 (m, 1H), 8.24-8.29 (m, 2H), 7.99 (bs, 1H), 7.80-7.86 (m, 1H), 7.44-7.67 (m, 6H), 7.27 (s, 1H), 2.77-2.83 (m, 2H), 1.67-1.77 (m, 2H), 1.39-1.50 (m, 2H), 0.93-1.02 (m, 3H).

¹¹B NMR (128 MHz, CD₂Cl₂, δ): 34.4.

SYNTHESIS OF 2-BUTYL-5,6-DIHYDRO-6-MESITYL-4-PHENYLDIBENZO[C,E][1,2]AZABORININE (3)



To a solution of 1.5 g **2** (crude product) in 50 mL dry benzene was added 4.5 g MesMgBr. Solid MesMgBr was obtained by removing the solvent from 20 mL of a 1 M solution in diethyl ether. After transferal into a glovebox, the appropriate amount was taken from the solid. The resulting suspension was stirred for 1 h at room temperature. All solid materials were filtered and washed with 2 x 15 mL *n*-hexane and 3 x 10 mL dichloromethane. The combined organic layers were washed with 3 x 30 mL water and dried over MgSO₄. All solvents were removed in vacuum and the obtained yellow oil was purified by column chromatography (silica gel, *n*-hexane/DCM 19:1, R_f = 0.4) yielding 949 mg (2.21 mmol, 67 % over 2 steps) **3** as colorless solid.

^1H NMR (400 MHz, CD_2Cl_2 , δ): 8.57-8.62 (m, 1H), 8.33-8.36 (m, 1H), 7.94 (bs, 1H), 7.75-7.80 (m, 1H), 7.66-7.69 (m, 1H), 7.48-7.55 (m, 4H), 7.39-7.45 (m, 2H), 7.26-7.28 (m, 1H), 6.87 (s, 2H), 2.84 (t, $J = 7.7$ Hz, 2H), 2.31 (s, 3H), 2.09 (s, 6H), 1.71-1.81 (m, 2H), 1.43-1.52 (m, 2H), 1.00 (t, $J = 7.3$ Hz, 3H).

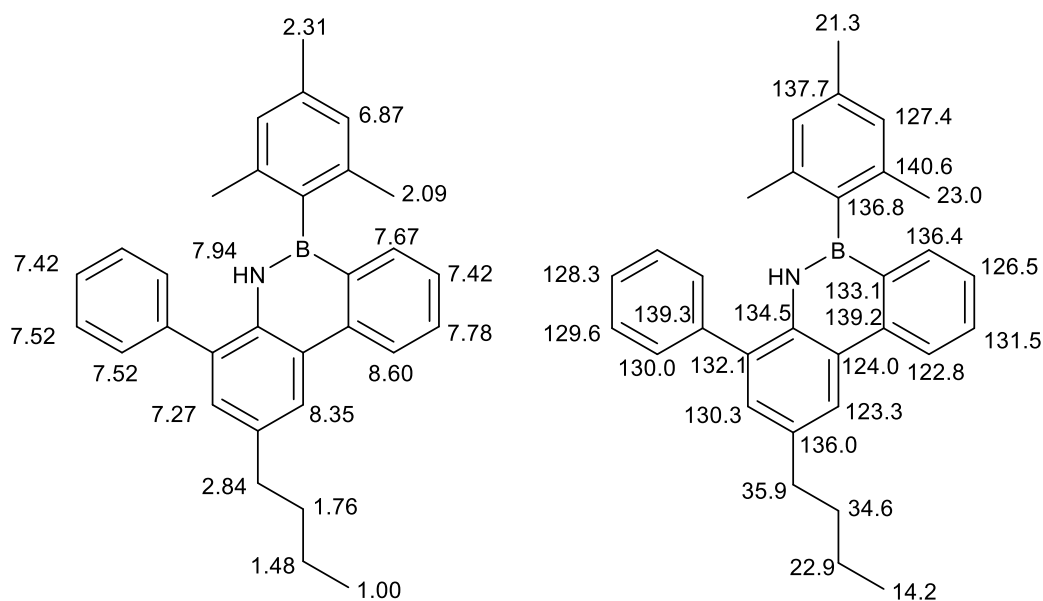


Figure S1: Assignments to **3** of ^1H (left) and ^{13}C signals (right).

^{13}C NMR (151 MHz, CD_2Cl_2 , δ): 140.6, 139.3, 139.2, 137.7, 136.8, 136.4, 136.0, 134.5, 133.1, 132.1, 131.5, 130.3, 130.0, 129.6, 128.3, 127.4, 126.5, 124.0, 123.3, 122.8, 35.9, 34.6, 23.0, 22.9, 21.3, 14.2.

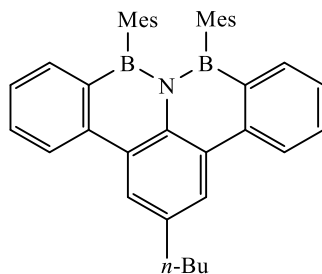
^{11}B NMR (128 MHz, CD_2Cl_2 , δ): 39.0.

EA: calcd. for $\text{C}_{31}\text{H}_{32}\text{BN}$: C 86.71 %, H 7.51 %, N 3.26 %; found: C 86.75 %, H 7.56 %, N 3.13 %.

HRMS (ESI): m/z calcd. for $[\text{C}_{31}\text{H}_{32}\text{BKN}, \text{M}+\text{K}]^+$: 468.2259; found: 468.2266.

Melting point: 115 $^\circ\text{C}$.

SYNTHESIS OF 2-BUTYL-8,9-DIMESITYL-8H,9H-8A-AZA-8,9-DIBORABENZO[FG]TETRA-CENE (5)



To a solution of 180 mg (0.42 mmol, 1 eq) **3** in 5 mL dry toluene was added 0.84 mL (0.5 M in toluene, 0.42 mmol, 1 eq) KHMDS dropwise. After stirring for $\frac{1}{2}$ h, all volatile compounds were removed in vacuum at 50 $^\circ\text{C}$. The resulting solid was suspended in 15 mL dry toluene. To the suspension was added dropwise 1.26 mL (1 M in *n*-hexane, 1.26 mmol, 3 eq) BCl_3 at -10 $^\circ\text{C}$ and the reaction mixture was stirred for 1 h at room temperature. After

adding 11 mg (84 μmol , 0.2 eq) AlCl_3 , the suspension was stirred for 18 h under reflux. After being cooled to room temperature, all volatile compounds were removed in vacuum. The resulting solid was suspended in 10 mL dry benzene, to the suspension was added 1.2 g MesMgBr as a solid. Solid MesMgBr was obtained by removing the solvent from 20 mL of a 1 M solution in diethyl ether. After transferal into a glovebox, the appropriate amount was taken from the solid. and the reaction mixture was stirred for 1 h at room temperature. All solid materials removed by filtration with a frit (P3) and washed with 4 x 10 mL dichloromethane. The combined organic layers were washed with 3 x 15 mL water and dried over MgSO_4 . All solvents were removed in vacuum and the obtained yellow oil was purified by column chromatography (silica gel, *n*-hexane/DCM 19:1, $R_f = 0.4$). The amorphous solid can be crystallized in *n*-hexane yielding 152 mg (0.27 mmol, 65 %) **5** as colorless crystals.

^1H NMR (400 MHz, CD_2Cl_2 , δ): 8.49-8.56 (m, 4H), 7.74-7.80 (m, 2H), 7.51-7.54 (m, 2H), 7.33-7.39 (m, 2H), 6.52 (s, 4H), 2.99 (t, $J = 7.8$ Hz, 2H), 2.25 (s, 3H), 1.84-1.93 (m, 2H), 1.72 (s, 12H), 1.50-1.61 (m, 2H), 1.06 (t, $J = 7.3$ Hz, 3H).

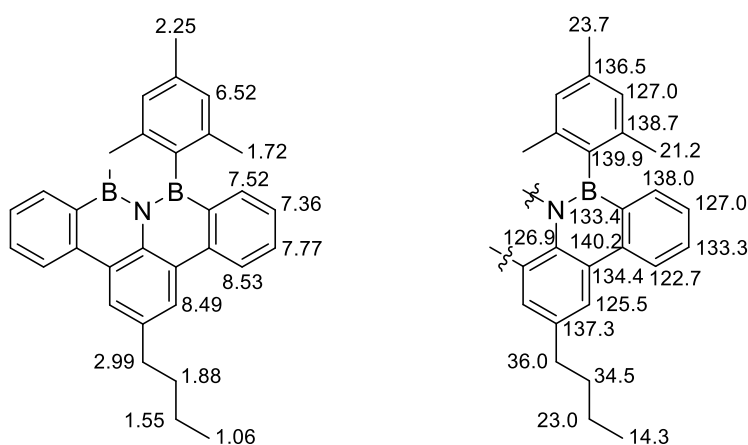


Figure S2: Assignments to **5** of ^1H (left) and ^{13}C signals (right).

^{13}C NMR (151 MHz, CD_2Cl_2 , δ): 140.2, 139.9, 138.7, 138.0, 137.3, 136.5, 134.4, 133.4, 133.3, 127.0, 127.0, 126.9, 125.5, 122.7, 36.0, 34.5, 23.7, 23.0, 21.2, 14.3.

^{11}B NMR (128 MHz, CD_2Cl_2 , δ): 51.1.

EA: calcd. for $\text{C}_{40}\text{H}_{41}\text{B}_2\text{N}$: C 86.19 %, H 7.41 %, N 2.51 %; found: C 86.10 %, H 7.45 %, N 2.47 %.

HRMS (ESI): m/z calcd. for $[\text{C}_{40}\text{H}_{41}\text{B}_2\text{NNa}, \text{M}+\text{Na}]^+$: 580.3317; found: 580.3333.

Melting point: 229 $^\circ\text{C}$.

Fluorescence quantum yield: $\phi_{\text{Fl}} = 0.21$.

UV/Vis (CH_2Cl_2 , $c \approx 10^{-5}$ M) $\lambda_{\text{max}}/\text{nm}$ (ϵ): 285 (10620), 295 (9300), 338 (13570), 349 (12490), 366 (10240).

3. CYCLIC VOLTAMMETRY

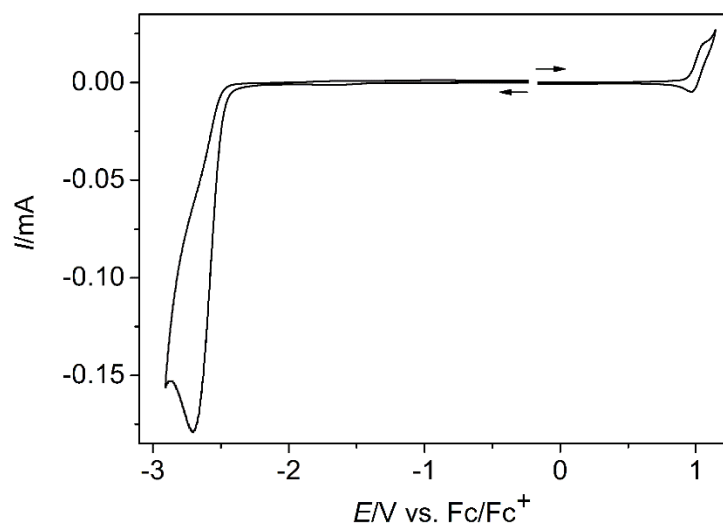


Figure S3: Cyclic voltammograms of **5** in $\text{CH}_2\text{Cl}_2/0.1 \text{ M NBu}_4\text{PF}_6$, scan rate $\nu = 0.2 \text{ Vs}^{-1}$, bulk concentration $c = 0.66 \text{ mM}$; recorded separately for oxidation and reduction.

4. X-RAY CRYSTALLOGRAPHIC DATA

Empirical formula	C ₄₀ H ₄₁ B ₂ N
Formula weight	557.36
Temperature	100(2) K
Wavelength	0.71073 Å
Crystal system	Monoclinic
Space group	P 21
Unit cell dimensions	$a = 11.8877(2) \text{ Å}$ $\alpha = 90^\circ$. $b = 24.3685(4) \text{ Å}$ $\beta = 115.5680(10)^\circ$. $c = 11.9282(2) \text{ Å}$ $\gamma = 90^\circ$.
Volume	$3117.05(9) \text{ Å}^3$
Z	4
Density (calculated)	1.188 Mg/m^3
Absorption coefficient	0.067 mm^{-1}
F(000)	1192
Crystal size	$0.438 \times 0.176 \times 0.142 \text{ mm}^3$
Theta range for data collection	1.671 to 29.238° .
Index ranges	$-16 \leq h \leq 16$, $-33 \leq k \leq 33$, $-16 \leq l \leq 16$
Reflections collected	61660
Independent reflections	16724 [R(int) = 0.0356]
Completeness to theta = 25.242°	99.9 %
Absorption correction	Semi-empirical from equivalents
Max. and min. transmission	0.7458 and 0.7096
Refinement method	Full-matrix least-squares on F^2

Data / restraints / parameters	16724 / 1 / 792
Goodness-of-fit on F ²	1.020
Final R indices [I>2sigma(I)]	R1 = 0.0428, wR2 = 0.0995
R indices (all data)	R1 = 0.0521, wR2 = 0.1046
Absolute structure parameter	?
Extinction coefficient	n/a
Largest diff. peak and hole	0.358 and -0.250 e.Å ⁻³

5. CARTESIAN COORDINATES OF STATIONARY POINTS IN ÅNGSTRÖM

5.1 S₀ POTENTIAL ENERGY SURFACE, B3LYP/6-311+G**

a) Compound **5*** (C₁), S₀

72
scf done: -1496.6921586

6	-0.457441	3.778154	-0.614592
6	-1.131170	4.858781	-1.159836
6	-1.095082	2.537088	-0.412926
6	-2.474936	4.713417	-1.520586
6	-2.469053	2.419453	-0.717048
6	-3.136226	3.515567	-1.298705
5	-0.315555	1.283788	0.047112
7	-1.019414	-0.000037	0.000016
6	-2.443651	-0.000135	-0.000015
6	-3.165305	1.173017	-0.362966
1	0.586336	3.881031	-0.342995
1	-0.622540	5.803640	-1.314739
1	-3.008659	5.542615	-1.972605
1	-4.174640	3.438407	-1.593090
6	-3.165153	-1.173390	0.362904
6	-4.566562	1.142878	-0.343545
6	-5.267441	-0.000362	-0.000147
6	-4.566412	-1.143485	0.343340
1	-5.119990	2.038843	-0.587970
1	-6.351101	-0.000451	-0.000211
1	-5.119714	-2.039542	0.587713
6	-2.468735	-2.419698	0.717108
6	-1.094737	-2.537158	0.413041
6	-3.135767	-3.515854	1.298845
6	-0.456926	-3.778117	0.614819
6	-2.474311	-4.713591	1.520844
6	-1.130517	-4.858795	1.160135
1	-4.174197	-3.438806	1.593207
1	0.586873	-3.880867	0.343260
1	-3.007924	-5.542825	1.972927
1	-0.621756	-5.803568	1.315131
5	-0.315380	-1.283774	-0.047051
6	1.122550	-1.472615	-0.679038
6	2.280220	-1.787753	0.057982
6	1.190817	-1.529970	-2.094761
6	3.466960	-2.117349	-0.607971
6	2.386672	-1.875996	-2.723902
6	3.544624	-2.166577	-1.997244
1	4.349854	-2.352629	-0.019406
6	1.122381	1.472791	0.679040

6	1.190720	1.530127	2.094749
6	2.279992	1.788037	-0.058046
6	2.386588	1.876248	2.723833
6	3.466733	2.117718	0.607841
6	3.544473	2.166920	1.997121
1	2.413867	1.928015	3.809070
6	2.299647	-1.761241	1.569828
1	1.298490	-1.827091	1.999322
1	2.889030	-2.592154	1.968169
1	2.748122	-0.832726	1.932801
6	4.834823	-2.511921	-2.701449
1	5.542718	-2.992724	-2.022629
1	4.660756	-3.186978	-3.543975
1	5.319244	-1.613987	-3.100893
6	-0.027916	1.251783	2.951324
1	-0.350893	0.209196	2.875526
1	0.180973	1.457553	4.003044
1	-0.880761	1.872313	2.657120
6	4.834762	2.512154	2.701210
1	4.660501	3.184872	3.545551
1	5.320630	1.613819	3.098000
1	5.541551	2.995522	2.023049
1	4.349574	2.353089	0.019229
6	2.299332	1.761549	-1.569896
1	2.888542	2.592575	-1.968258
1	2.747955	0.833120	-1.932907
1	1.298139	1.827228	-1.999330
1	2.413898	-1.927763	-3.809141
6	-0.027892	-1.251752	-2.951273
1	0.180950	-1.457550	-4.002997
1	-0.880672	-1.872335	-2.656994
1	-0.350944	-0.209188	-2.875499

b) Compound **5*** (C_s), S₀

72

scf done: -1496.6854168

6	0.342545	-2.760668	-4.945303
6	0.057132	-2.655050	-2.531685
6	0.205503	-3.396507	-3.722965
5	0.026466	-0.417859	-1.291012
7	0.005202	-1.128533	0.000000
6	-0.073919	-2.563602	0.000000
6	-0.125329	-3.299565	-1.223705
1	0.228316	0.454281	-3.905876
1	0.436680	-0.866566	-5.979229
1	0.458151	-3.354254	-5.845904
1	0.234060	-4.477208	-3.706969
6	-0.125329	-3.299565	1.223705
6	-0.366580	-4.680795	-1.187726
6	-0.509288	-5.371319	0.000000
6	-0.366580	-4.680795	1.187726
1	-0.468422	-5.223673	-2.115833
1	-0.723930	-6.433420	0.000000
1	-0.468422	-5.223673	2.115833
6	0.057132	-2.655050	2.531685
6	0.092612	-1.249524	2.593851
6	0.205503	-3.396507	3.722965
6	0.219490	-0.627440	3.855191

6	0.342545	-2.760668	4.945303
6	0.337669	-1.363925	5.020924
1	0.234060	-4.477208	3.706969
1	0.228316	0.454281	3.905876
1	0.458151	-3.354254	5.845904
1	0.436680	-0.866566	5.979229
5	0.026466	-0.417859	1.291012
6	-0.008705	1.152122	-1.509825
6	-1.240008	1.799524	-1.745036
6	1.178610	1.879131	-1.734874
6	-1.267220	3.153880	-2.083691
6	1.118093	3.233426	-2.072828
6	-0.097059	3.898340	-2.232945
1	-2.228061	3.637241	-2.241687
1	2.045854	3.780099	-2.221687
6	-0.008705	1.152122	1.509825
6	-1.240008	1.799524	1.745036
6	1.178610	1.879131	1.734874
6	-1.267220	3.153880	2.083691
6	1.118093	3.233426	2.072828
6	-0.097059	3.898340	2.232945
1	-2.228061	3.637241	2.241687
1	2.045854	3.780099	2.221687
6	-0.145661	5.374164	2.546362
1	0.747947	5.697872	3.085787
1	-0.206084	5.967812	1.627185
1	-1.018808	5.625503	3.153962
6	-0.145661	5.374164	-2.546362
1	0.747947	5.697872	-3.085787
1	-1.018808	5.625503	-3.153962
1	-0.206084	5.967812	-1.627185
6	2.535883	1.207607	-1.715024
1	2.543800	0.286496	-1.130587
1	2.843431	0.940398	-2.732437
1	3.303671	1.869738	-1.307713
6	-2.548599	1.037083	-1.733965
1	-3.366423	1.651825	-1.350085
1	-2.819815	0.731442	-2.750950
1	-2.503512	0.128799	-1.131281
6	2.535883	1.207607	1.715024
1	2.543800	0.286496	1.130587
1	3.303671	1.869738	1.307713
1	2.843431	0.940398	2.732437
6	-2.548599	1.037083	1.733965
1	-3.366423	1.651825	1.350085
1	-2.503512	0.128799	1.131281
1	-2.819815	0.731442	2.750950

c) Compound C (R = H; C_{2v}), S_0

34

scf done: -795.5191236

6	0.000000	-2.536310	-0.255246
6	0.000000	-2.558574	1.159076
6	0.000000	-3.790840	1.841176
6	0.000000	-4.992360	1.153686
6	0.000000	-4.969619	-0.246047
6	0.000000	-3.768829	-0.939587
1	0.000000	-3.784696	2.926294

1	0.000000	-5.937187	1.685126
1	0.000000	-5.901979	-0.800525
1	0.000000	-3.808131	-2.020332
6	0.000000	1.197096	-2.359532
6	0.000000	0.000000	-3.055591
6	0.000000	-1.197096	-2.359532
6	0.000000	-1.237093	-0.958465
6	0.000000	0.000000	-0.247011
6	0.000000	1.237093	-0.958465
1	0.000000	2.119158	-2.923031
1	0.000000	0.000000	-4.139282
1	0.000000	-2.119158	-2.923031
6	0.000000	4.992360	1.153686
6	0.000000	3.790840	1.841176
6	0.000000	2.558574	1.159076
6	0.000000	2.536310	-0.255246
6	0.000000	3.768829	-0.939587
6	0.000000	4.969619	-0.246047
1	0.000000	5.937187	1.685126
1	0.000000	3.784696	2.926294
1	0.000000	3.808131	-2.020332
1	0.000000	5.901979	-0.800525
7	0.000000	0.000000	1.166084
5	0.000000	-1.234987	1.912044
5	0.000000	1.234987	1.912044
1	0.000000	-1.174221	3.098030
1	0.000000	1.174221	3.098030

d) Compound **D** (C_{2v}), S_0

34

scf done: -808.0658955

6	0.282936	3.538378	0.935748
6	0.919499	4.713069	1.246467
6	1.035190	2.369628	0.626648
6	2.328510	4.750761	1.256493
6	2.472311	2.406005	0.636334
6	3.084535	3.629380	0.959931
6	0.380746	1.173373	0.310199
6	1.081225	-0.000026	-0.000080
6	2.519306	-0.000136	-0.000030
6	3.218913	1.195862	0.316313
1	-0.799587	3.481809	0.920736
1	0.351384	5.604141	1.482124
1	2.833739	5.677851	1.501720
1	4.161861	3.716141	0.982925
6	3.218750	-1.196242	-0.316323
6	4.623770	1.165419	0.308345
6	5.312020	-0.000352	0.000068
6	4.623612	-1.166017	-0.308257
1	5.193128	2.054130	0.543424
1	6.395018	-0.000436	0.000106
1	5.192849	-2.054816	-0.543295
6	2.471984	-2.406271	-0.636395
6	1.034868	-2.369672	-0.626809
6	3.084042	-3.629741	-0.959949
6	0.282456	-3.538307	-0.935959
6	2.327865	-4.751005	-1.256561
6	0.918859	-4.713096	-1.246632

1	4.161356	-3.716668	-0.982868
1	-0.800060	-3.481571	-0.921022
1	2.832968	-5.678174	-1.501752
1	0.350623	-5.604082	-1.482327
6	0.380586	-1.173315	-0.310408
1	-0.704951	-1.153458	-0.305218
1	-0.704794	1.153681	0.304939

5.2 S₁ POTENTIAL ENERGY SURFACE, B3LYP/6-311+G**

a) Compound 5* (C₁), S₁

72

scf done: -1496.5723232

6	-0.576010	3.848995	-0.098962
6	-1.282604	5.007685	-0.326202
6	-1.200518	2.568583	-0.091953
6	-2.667474	4.934905	-0.572870
6	-2.617933	2.513508	-0.264404
6	-3.311635	3.711900	-0.536871
5	-0.443565	1.273597	0.051964
7	-1.155326	-0.000065	0.000023
6	-2.583097	-0.000211	0.000107
6	-3.303705	1.229945	-0.128294
1	0.492510	3.916006	0.076922
1	-0.778496	5.968369	-0.327940
1	-3.231591	5.835666	-0.787756
1	-4.374936	3.692415	-0.736559
6	-3.303475	-1.230494	0.128599
6	-4.713328	1.190757	-0.097523
6	-5.406454	-0.000405	0.000630
6	-4.713124	-1.191472	0.098440
1	-5.271540	2.114538	-0.140142
1	-6.491118	-0.000478	0.000910
1	-5.271228	-2.115299	0.141369
6	-2.617452	-2.513984	0.264229
6	-1.200026	-2.568719	0.091816
6	-3.310910	-3.712644	0.536182
6	-0.575205	-3.848970	0.098608
6	-2.666468	-4.935505	0.571888
6	-1.281542	-5.007894	0.325456
1	-4.374255	-3.693529	0.735645
1	0.493355	-3.915673	-0.077144
1	-3.230426	-5.836466	0.786351
1	-0.777201	-5.968455	0.327034
5	-0.443325	-1.273548	-0.051965
6	1.123091	-1.331552	-0.373672
6	2.112771	-1.686290	0.598955
6	1.536181	-1.282487	-1.755914
6	3.442228	-1.817971	0.220187
6	2.867003	-1.438633	-2.091868
6	3.849188	-1.681825	-1.113930
1	4.186395	-2.063827	0.971411
6	1.122828	1.331877	0.373749
6	1.535871	1.282857	1.756008
6	2.112509	1.686743	-0.598845
6	2.866663	1.439125	2.092010
6	3.441942	1.818519	-0.220031

6	3.848867	1.682367	1.114100
1	3.163471	1.393535	3.135535
6	1.735498	-2.003166	2.023067
1	0.797455	-1.537757	2.316468
1	1.594067	-3.083438	2.133728
1	2.520963	-1.698820	2.718533
6	5.289011	-1.844548	-1.510607
1	5.930507	-2.022502	-0.646513
1	5.407885	-2.685324	-2.202229
1	5.653953	-0.954005	-2.032513
6	0.501687	1.155159	2.844055
1	-0.242067	0.389349	2.621719
1	0.963173	0.933104	3.808127
1	-0.048383	2.097445	2.937758
6	5.288708	1.844887	1.510791
1	5.407389	2.683953	2.204495
1	5.654203	0.953185	2.030361
1	5.929890	2.025203	0.646956
1	4.186116	2.064467	-0.971215
6	1.735244	2.003670	-2.022943
1	1.593332	3.083895	-2.133443
1	2.520916	1.699786	-2.718375
1	0.797429	1.537901	-2.316509
1	3.163849	-1.392973	-3.135380
6	0.502046	-1.154867	-2.844020
1	0.963549	-0.932511	-3.808014
1	-0.047738	-2.097300	-2.937951
1	-0.241948	-0.389314	-2.621608

6. COMPUTED STRUCTURES OF 5*

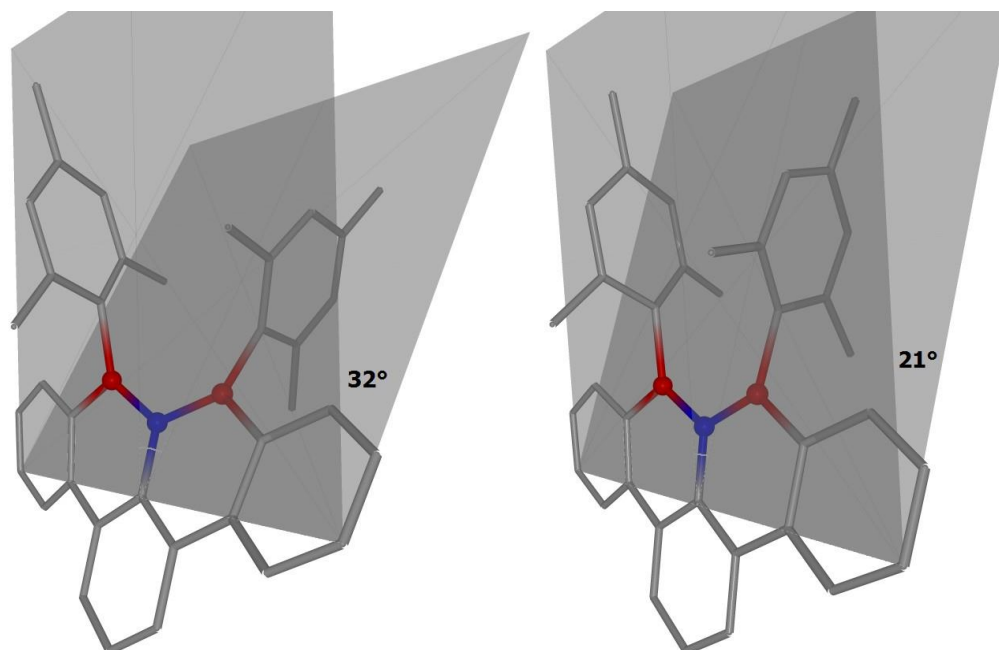


Figure S4: Optimized structure of **5*** (S_0 , hydrogens are omitted for clarity) with measured torsion angle at the B3LYP/6-311+G** level of theory (left) and the optimized S_1 state structure (right) at the TD-B3LYP/6-311+G** level of theory.

7. COMPUTED NICS(1) VALUES

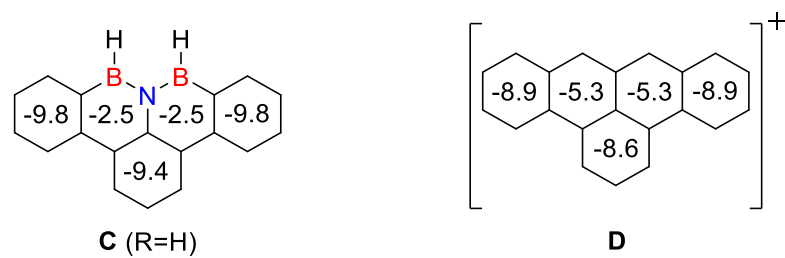


Figure S5: NICS(1) values of **C** (R = H) and **D** computed on the B3LYP/6-311+G** level of theory. NICS(1) of benzene is -10.2.

8. SPECTRA

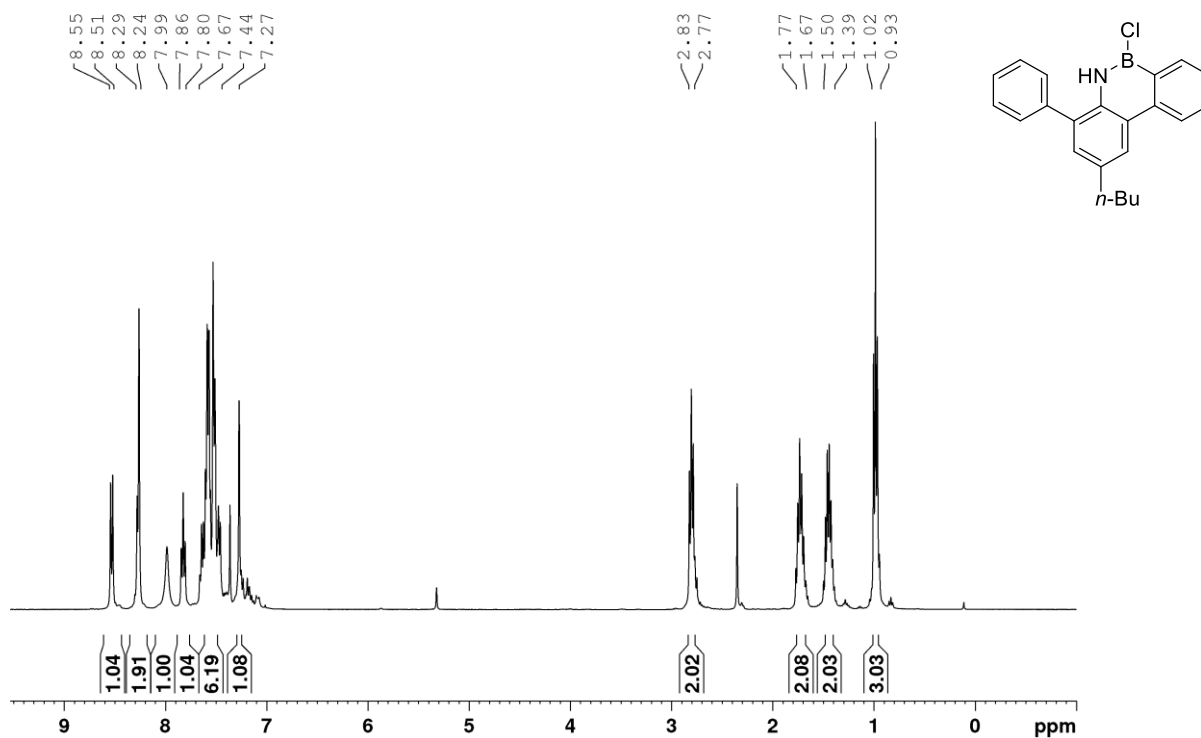


Figure S6: ¹H-NMR of **2** in CD₂Cl₂

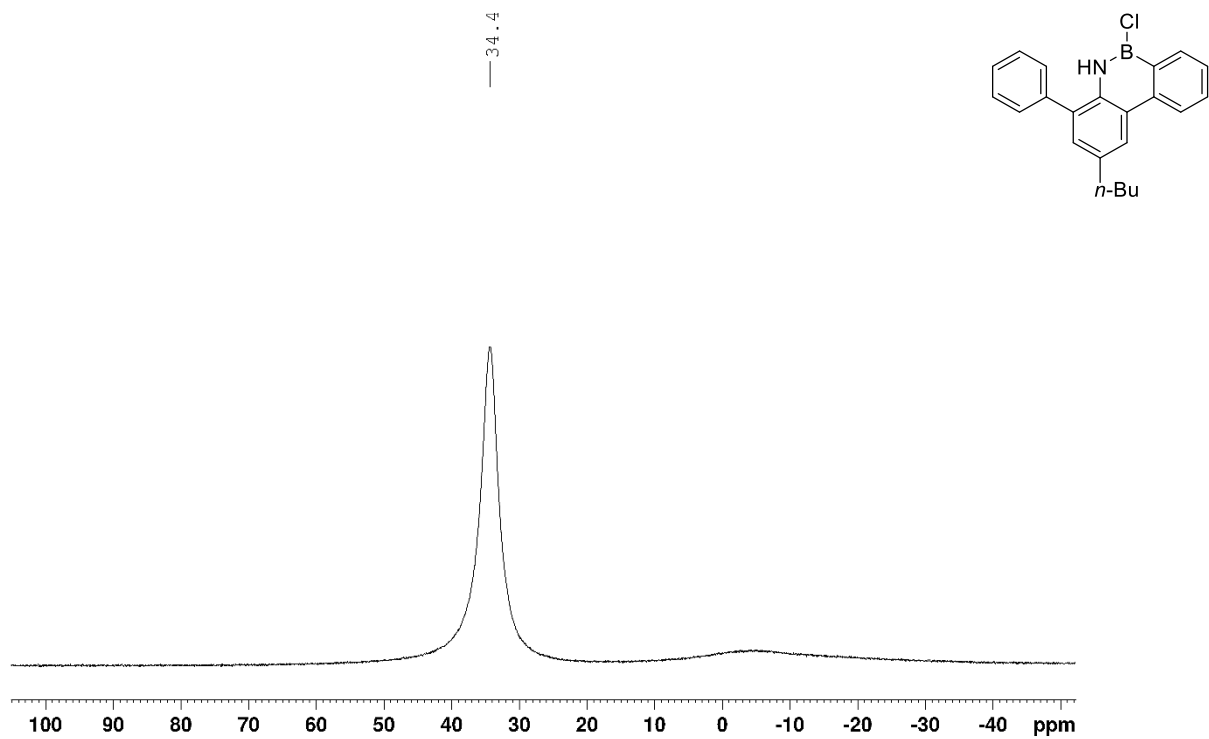


Figure S7: ^{11}B -NMR of 2 in CD_2Cl_2

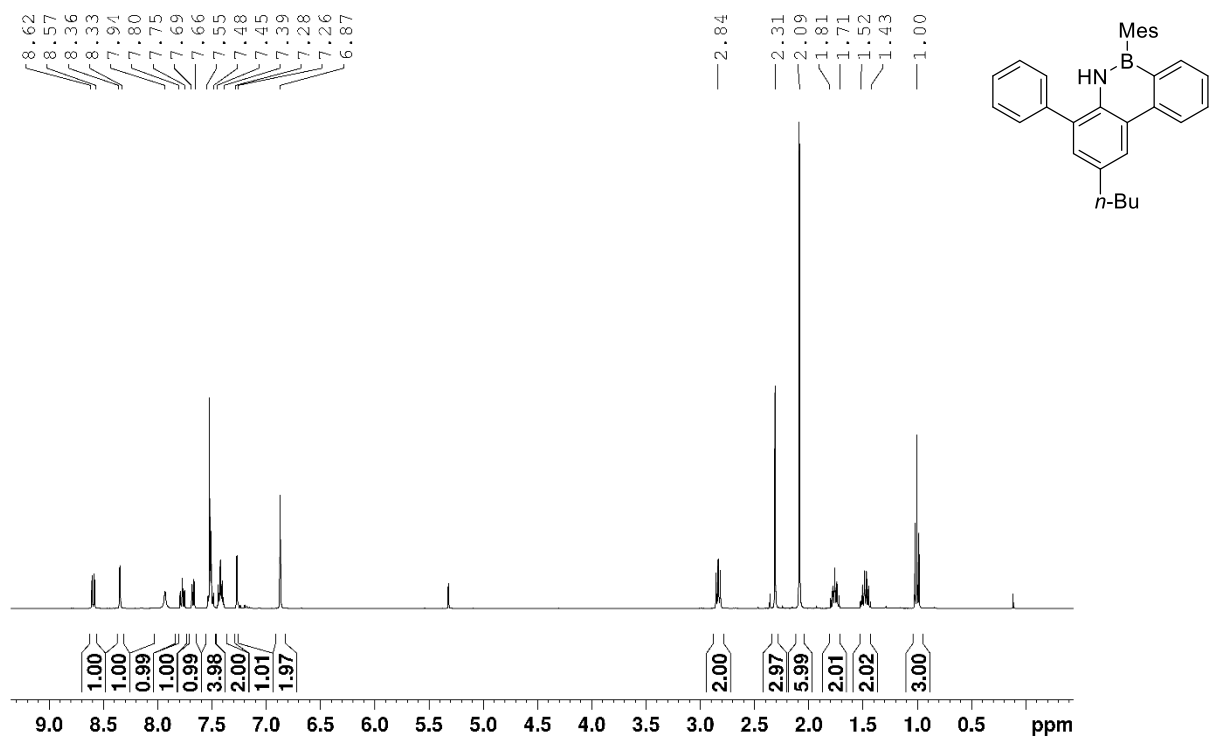


Figure S8: ^1H -NMR of 3 in CD_2Cl_2

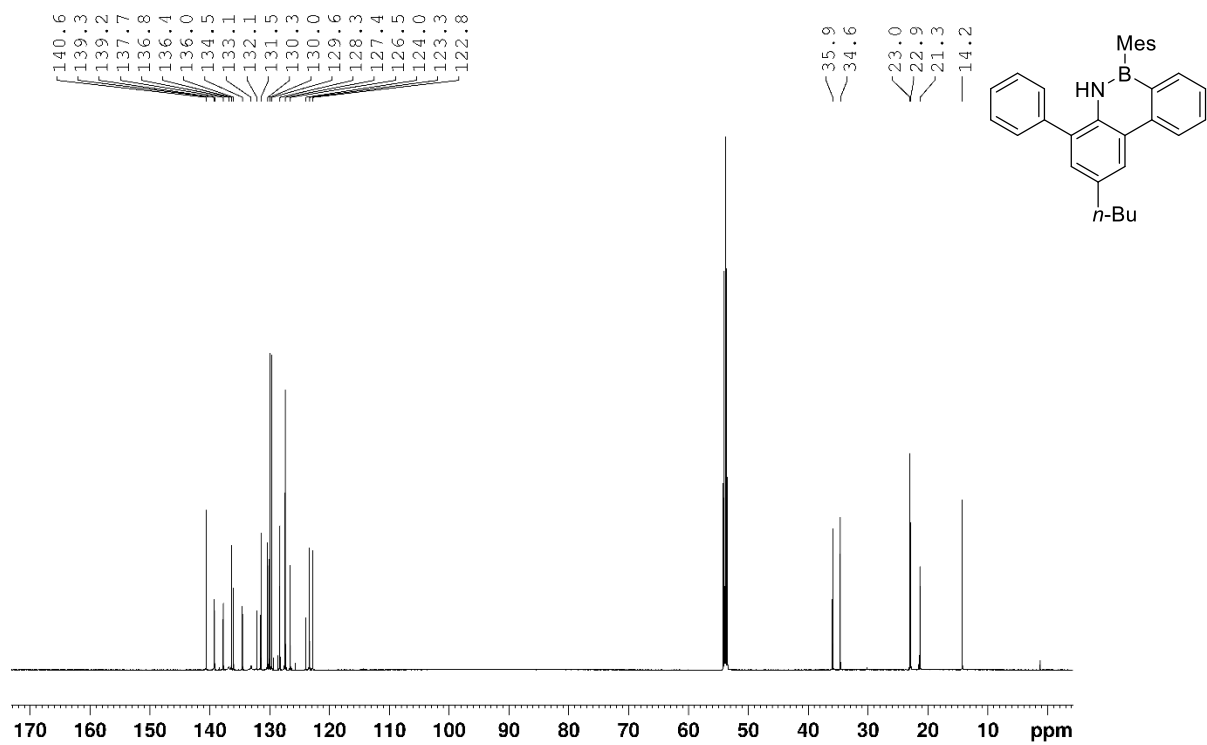


Figure S9: ^{13}C -NMR of **3** in CD_2Cl_2

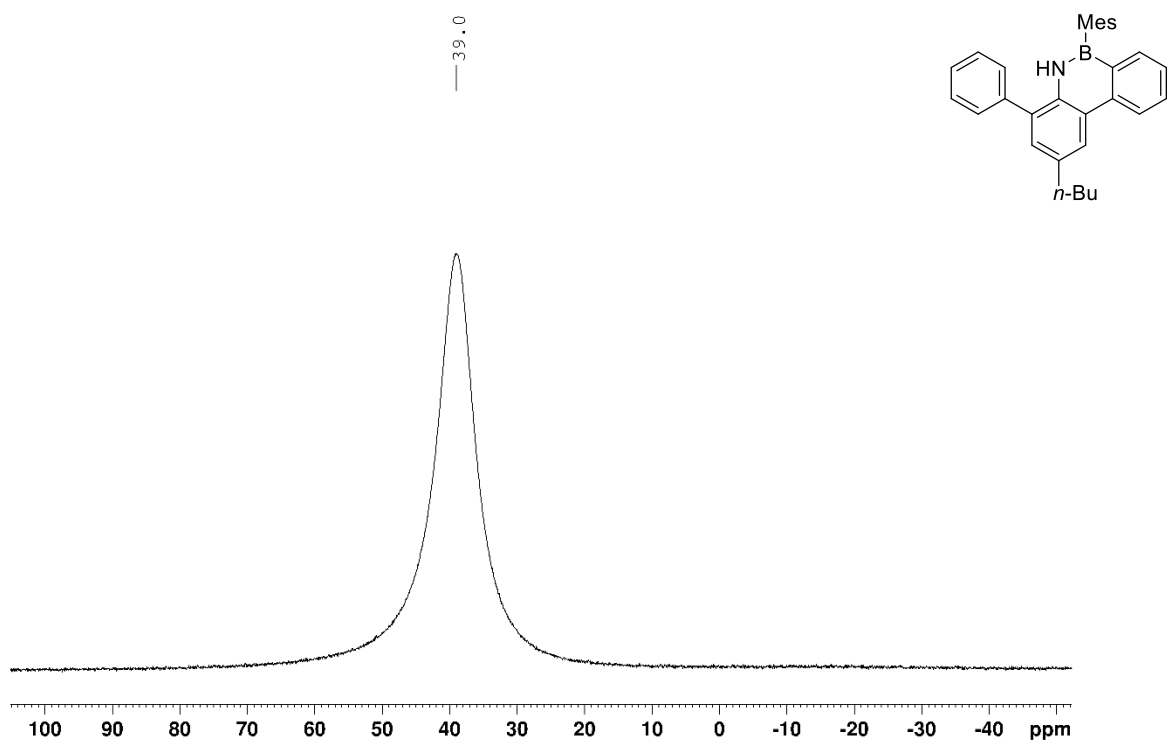


Figure S10: ^{11}B -NMR of **3** in CD_2Cl_2

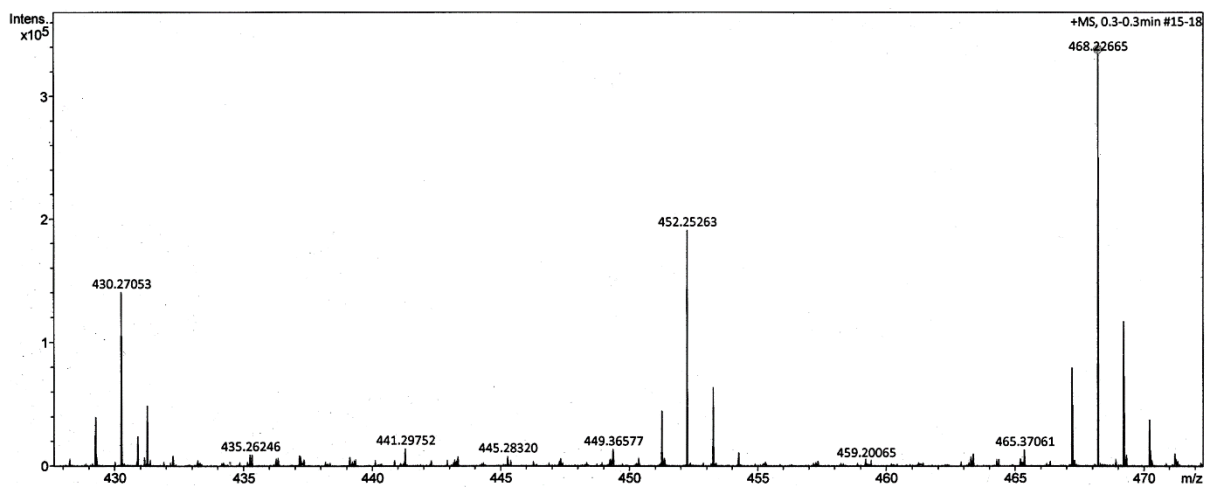


Figure S11: HR-ESI of **3** in acetonitrile

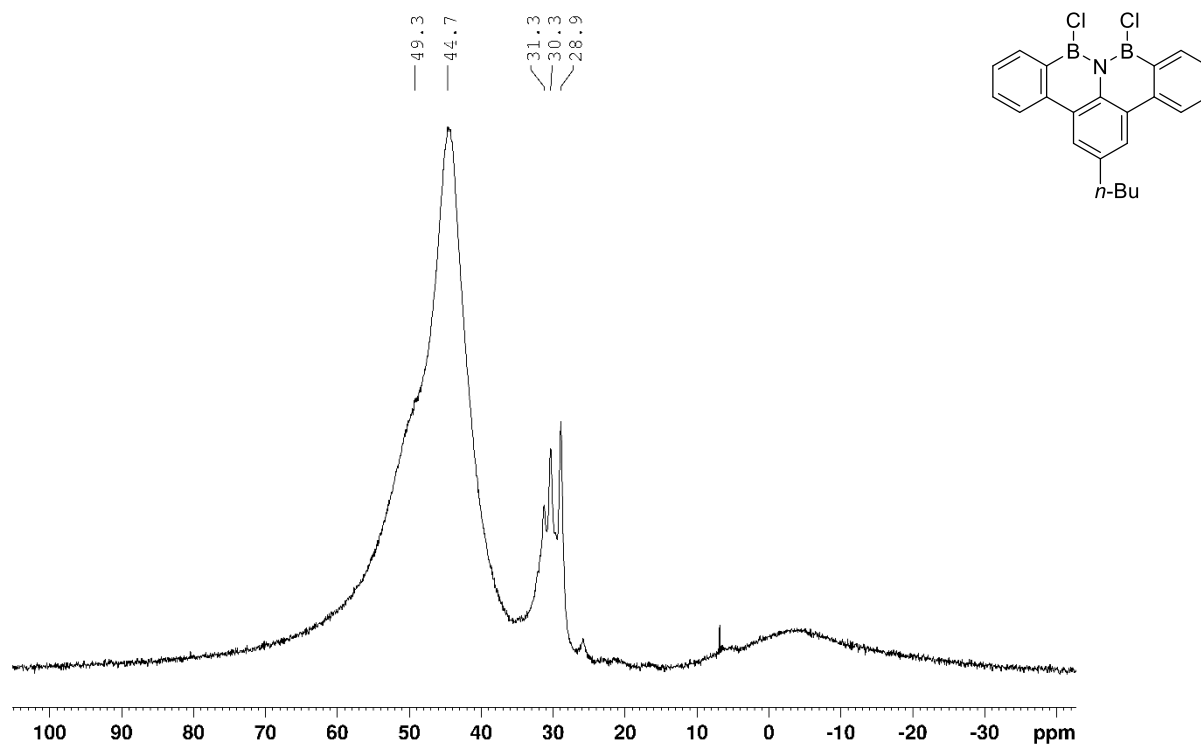


Figure S12: ^{11}B -NMR of **4** (crude product) in CD_2Cl_2

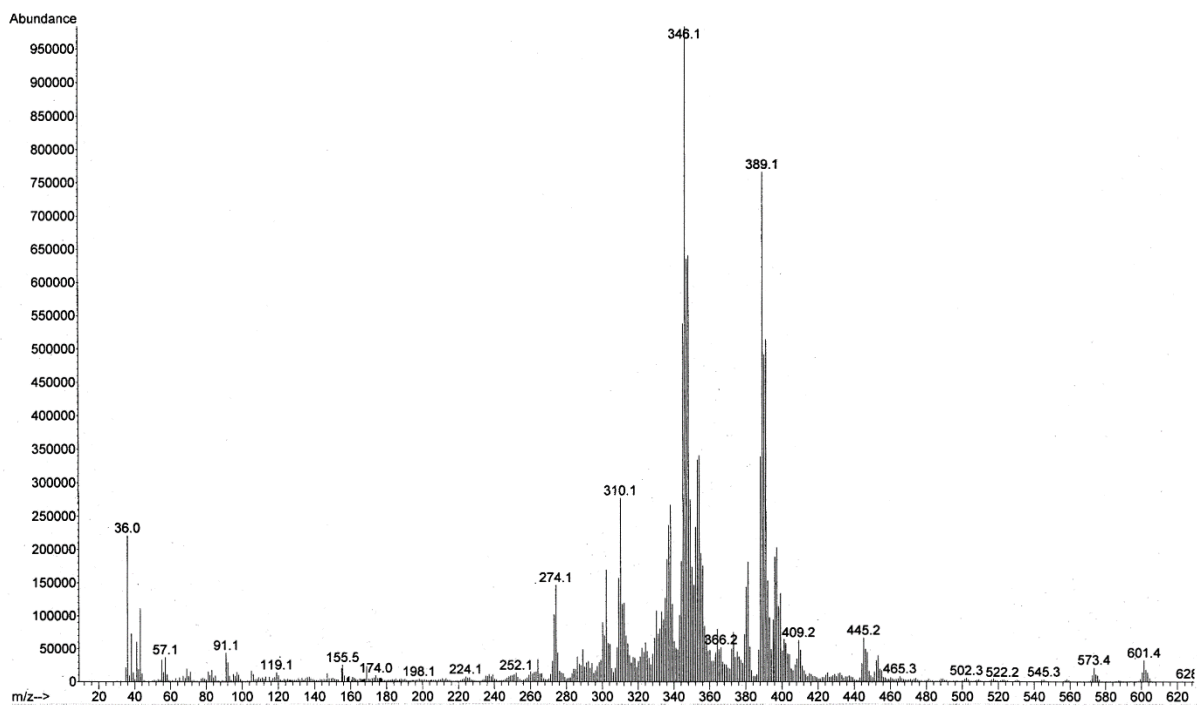


Figure S13: EI-MS of **4** (crude product)

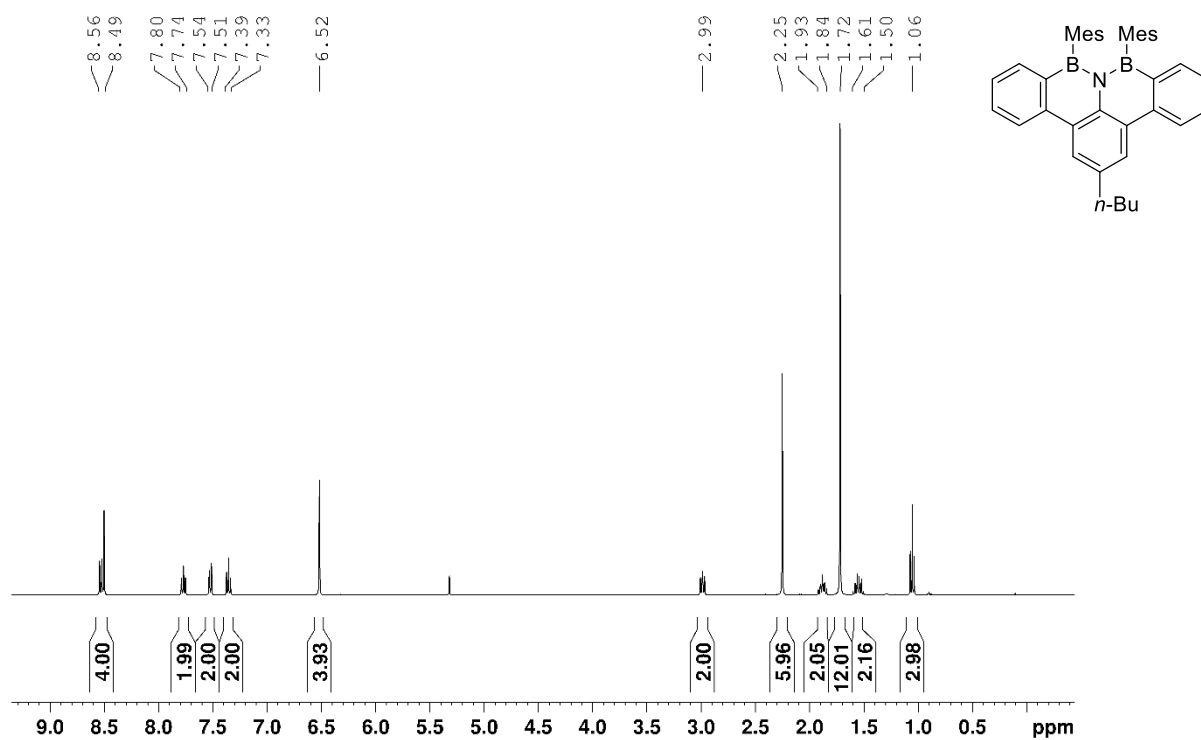


Figure S14: $^1\text{H-NMR}$ of **5** in CD_2Cl_2

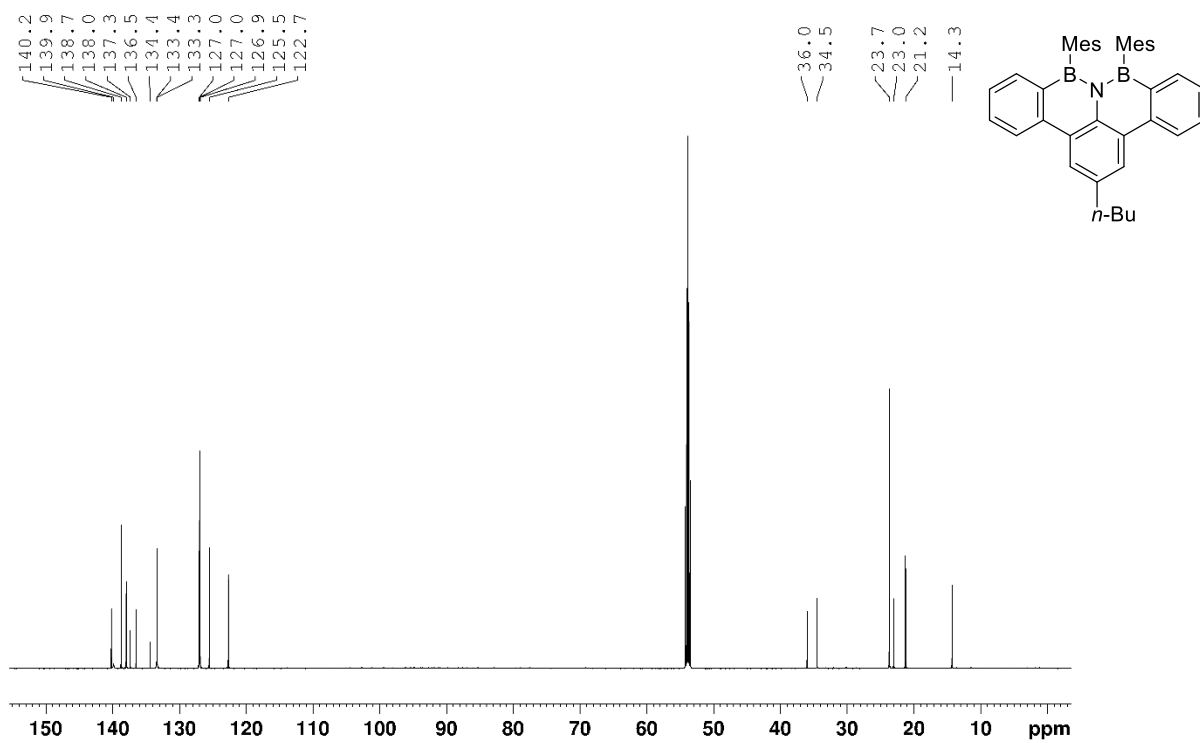


Figure S15: ¹³C-NMR of **5** in CD₂Cl₂

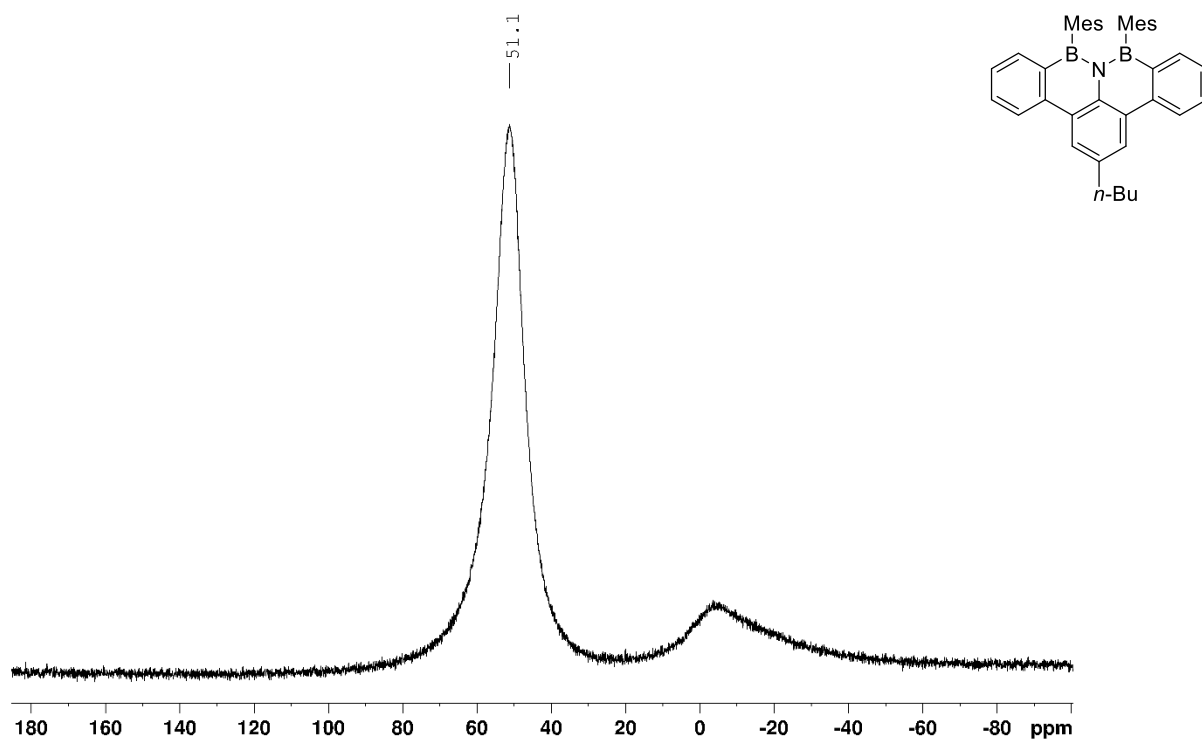


Figure S16: ¹¹B-NMR of **5** in CD₂Cl₂

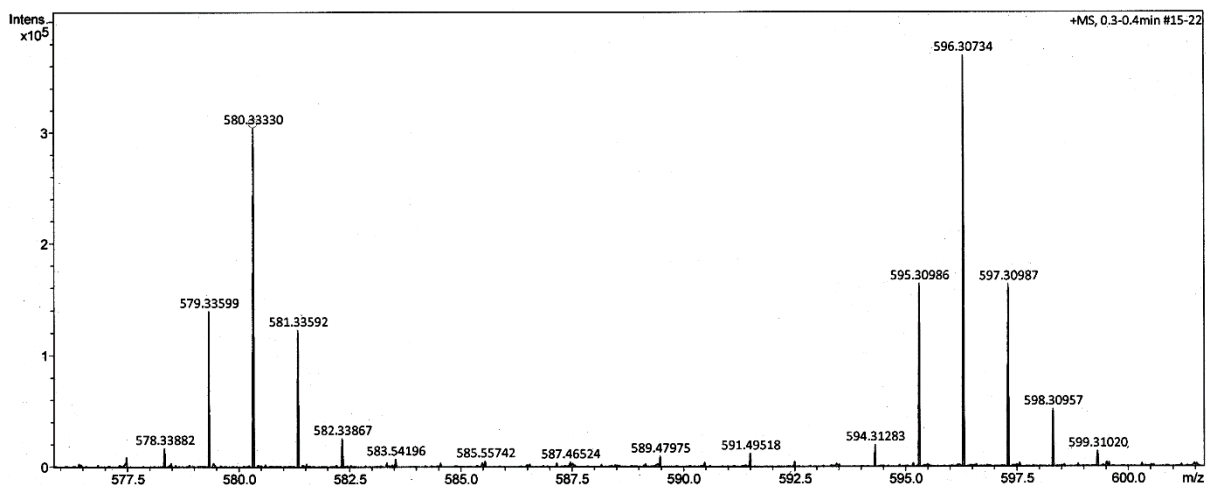


Figure S17: HR-ESI of **5** in acetonitrile

REFERENCES

- (1) Melhuish, W. H. *J. Phys. Chem.* **1961**, *65*, 229.
- (2) Inc., B. A.; Bruker AXS Inc.: Madison, WI, 2012.
- (3) Inc., B. A.; Bruker AXS Inc.: Madison, WI, 2012.
- (4) Inc., B. A.; Bruker AXS Inc.: Madison, WI, 2010.
- (5) Inc., B. A.; Sheldrick, G. M., Bruker AXS Inc.: Madison, WI, 2012.
- (6) Inc., B. A.; Sheldrick, G. M., Bruker AXS Inc.: Madison, WI, 2012.
- (7) Hubschle, C. B.; Sheldrick, G. M.; Dittrich, B. *J. Appl. Crystallogr.* **2011**, *44*, 1281.
- (8) Zewail, A. H. *J. Phys. Chem. A* **2000**, *104*, 5660.
- (9) Lee, C.; Yang, W.; Parr, R. G. *Phys. Rev. B* **1988**, *37*, 785.
- (10) M. J. Frisch et al.; *Gaussian 09*, Revision A.02; Gaussian, Inc.: Wallingford CT, 2009.
- (11) Weiner, A. M. *Ultrafast optics*; Wiley: Hoboken, N.J., 2009.
- (12) Stratmann, R. E.; Scuseria, G. E.; Frisch, M. J. *J. Chem. Phys.* **1998**, *109*, 8218.
- (13) B. Gollas, B. Krauß, B. Speiser, H. Stahl, *Curr. Sep.*, **1994**, *13*, 42.

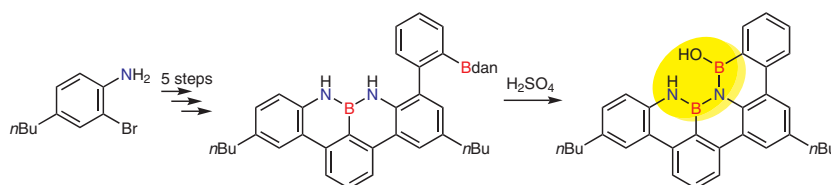
New Synthesis of a Dibenzoperylene Motif Featuring a Doubly Boron–Nitrogen-Doped Bay Region

Michael Fingerle

Simon Stocker

Holger F. Bettinger* 

Institut für Organische Chemie, Universität Tübingen,
Auf der Morgenstelle 18, 72076 Tübingen, Germany
holger.bettinger@uni-tuebingen.de



Received: 16.07.2019

Accepted after revision: 04.09.2019

Published online: 01.10.2019

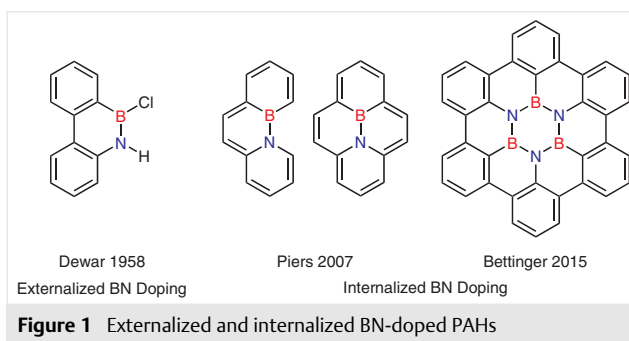
DOI: 10.1055/s-0039-1690687; Art ID: ss-2019-z0397-fa

Abstract A dibenzoperylene motif featuring a doubly boron–nitrogen-doped bay region is accessible from an aniline derivative in six steps in good overall yield. Two *n*-butyl groups provide the BN-doped polycyclic aromatic hydrocarbon with sufficient solubility in common organic solvents. The synthesis sequence allows installation of a second boron atom next to a weakly nucleophilic nitrogen by using a protected boron species. The title compound shows blue fluorescence, an extremely high fluorescence quantum yield, and an interesting doped bay region.

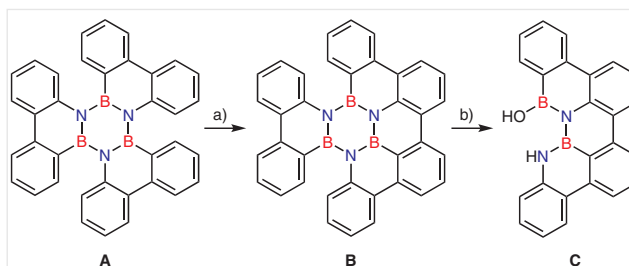
Key words boron, chromophores, nitrogen, azaborinines, polycycles

Modification of polycyclic aromatic hydrocarbons (PAHs) by substitution of pairs of carbon atoms by isosteric and isoelectronic BN (boron–nitrogen) units has received considerable attention over the last decade due to the potential as optoelectronic materials and organic semiconductors.^{1–12} Present challenges lie in the development of strategies that allow efficient and scalable syntheses of one-fold and multiple BN-doped PAHs, in particular if the BN group is fully embedded within a PAH scaffold. In 2007, the Piers group reported the BN-pyrene (Figure 1) as the first example of a BN-doped PAH with a BN unit fully surrounded by a conjugated carbon framework. The BN group is remarkably stable if embedded within the PAH framework, in contrast to the generally observed reactivity of aminoboranes. Similarly, the BN-phenanthrene isomer with the BN unit at the ring fusion centers 4a,4b is much less reactive than Dewar's structural isomer that has the BN unit at the 10,9-positions.¹³

In our efforts to achieve the synthesis of the triply BN-doped hexa-*peri*-hexabenzocoronene (BN-HBC), which were finally successful in 2015,¹⁴ we also described the synthesis of a BN–BN substituted dibenzoperylene **C**¹⁵ (Scheme 1). Irradiation of the borazine derivative of hexabenzotriph-



enylene **A**^{16–18} with UV light in the presence of iodine yields compound **B** by photocyclization and dehydrogenation. Hydrolysis of **B** results in the B₂N₂ dibenzoperylene **C**. A related doubly BN-substituted derivative of perylene was very recently reported by the Wagner group.⁹



The dibenzoperylene molecule **C** provides the interesting structural motif of a (BN)₂-doped bay region that is without precedence in the literature (an NBNBN motif was reported as by-product in the synthesis of a substituted BN-HBC molecule).¹⁹ For studying the chemical and physical properties of compound **C**, we decided to develop a new synthetic route that provides access in the gram scale. The

previously reported protocol requires irradiation of a 0.6 mM solution, and as often encountered with photochemical reactions, scale-up is not readily achieved. Introduction of two boron atoms in one (BN)₂ PAH system require step-wise reactions.²⁰ The synthetic challenge is the introduction of the second boron atom to the NBN unit, as the nucleophilicity of the N atom is reduced and thus electrophilic borylation is hindered. Also, we deemed it desirable to introduce alkyl groups for enhanced solubility.

We started the synthesis from the well-known 2-bromo-4-butylaniline (**1**), which can be synthesized by bromination of 4-butylaniline with NBS.²¹ In a Suzuki coupling reaction, the terphenyl motif **3** can be formed (Scheme 2). Following Hatakeyama et al., the electrophilic borylation using boron tribromide and sodium tetraphenylborate as a non-coordinating base leads to NBN-benzo[*f,g*]tetracene **4**.¹⁰ The NBN-benzotetracene motif has recently received some interest.^{11,12} The commonly used *o*-dichlorobenzene

solvent can be substituted for toluene without change in yield, which is easier to remove after the reaction. The resulting NBN-benzotetracene **4** undergoes a single bromination with NBS to give **5**. The conversion of this reaction is 80% but using more NBS to achieve a higher degree of conversion results in a two-fold bromination. Because **5** turned out to have low reactivity in cross-coupling reactions, we decided to reverse the polarity and introduced a Bpin group using bis(pinacolato)diboron, potassium acetate, and Pd(dppf)Cl₂. While this allows introduction of a phenyl group by a subsequent Suzuki reaction, the installation of the second boron atom of the bay region by electrophilic borylation with BCl₃ or BBr₃ fails. We thus resorted to Br-Bdan-benzene, as this contains a protected boron atom that does not interfere in the Suzuki reaction which is used to construct **7** (Scheme 2). The dansyl group protects the boron atom towards reaction with oxygen and water, so that purification of **7** by column chromatography can be done.

Biographical Sketches



Holger Bettinger was born in Nördlingen in 1970. He studied chemistry at the Friedrich Alexander University Erlangen-Nuremberg and completed doctoral research under the direction of Prof. P. v. R. Schleyer in 1998. Following postdoctoral research at the University of Georgia, Ruhr-University Bo-

chum, and Rice University, he started independent research at Ruhr University Bochum in 2001. After Habilitation in 2005, he was appointed as Professor of Organic Chemistry at Tübingen University in 2008. He was awarded with the Liebig Fellowship, the Heisenberg Fellowship, and recently with the

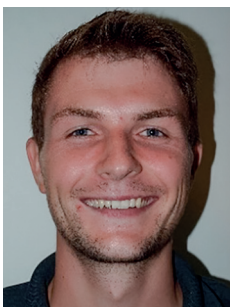
Forschungspreis of the Dr. Eberle Stiftung. His research interests focus on reactive intermediates, their electronic structure and reactivity, and on reactive polycyclic aromatic hydrocarbons (in particular acenes) and the influence of heteroatom doping.



Michael Fingerle studied chemistry at the Eberhard-Karls Universität Tübingen and com-

pleted his master thesis in 2016 in the laboratories of Prof. Dr. Holger Bettinger. His current re-

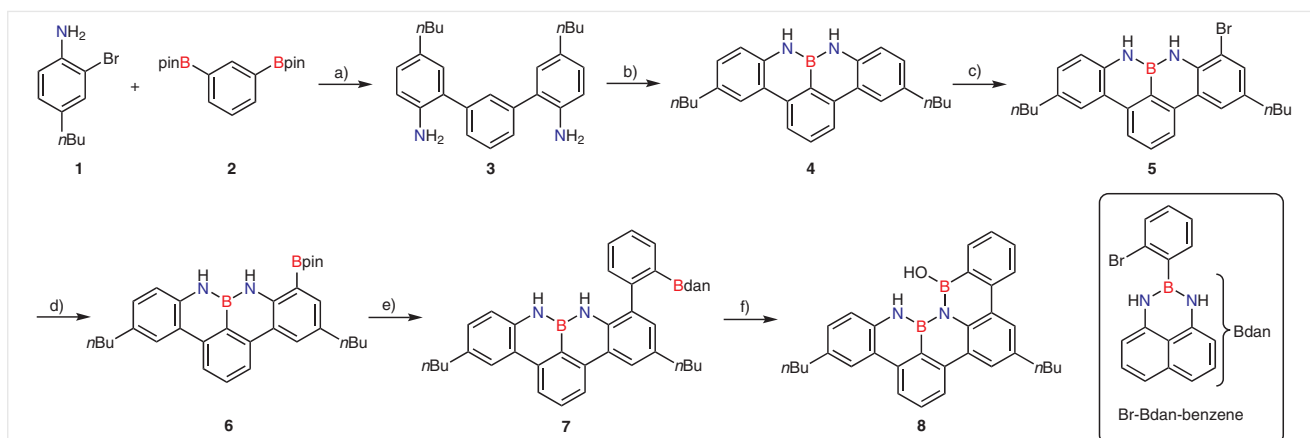
search focuses on BN-doped PAHs.



Simon Stocker studied chemistry at the Eberhard-Karls Universität Tübingen and received

a B. Sc. degree in 2018. He is currently in the M. Sc. program at the same institution and is

working in the Bettinger research group on BN-doped PAH molecules.



Scheme 2 Synthesis sequence of the dibenzoperylene motif **8**. *Reagents and conditions:* a) **1** (2.4 equiv), **2** (1 equiv), Pd(PPh₃)₄ (5 mol%), K₂CO₃ (6.6 equiv), mixture of DME and H₂O, reflux, 18 h, 92%; b) **3** (1 equiv), BBr₃ (1 equiv), NaBPh₄ (1.5 equiv), toluene, reflux, 18 h, 65%; c) **4** (1 equiv), NBS (1 equiv), mixture of CH₂Cl₂, CHCl₃, MeCN, 0 °C, 2 h, 48%; d) **5** (1 equiv), B₂Pin₂ (2.5 equiv), KOAc (6 equiv), Pd(dppf)Cl₂ (10 mol%), 1,4-dioxane, 90 °C, 18 h, 61%; e) **6** (1 equiv), Br-Bdan-benzene (1 equiv), K₂CO₃ (4 equiv), Pd(PPh₃)₄ (10 mol%), mixture of toluene, EtOH, H₂O, reflux, 18 h, 73%; f) **7** (1 equiv), H₂SO₄ (2 M in H₂O; 24 equiv), THF, 50 °C, 5 d, 92%.

The final step is the deprotection of the boron species and formation of the perylene motif **8**. Initial deprotection experiments were done with hydrochloric acid under ambient conditions, but **8** was not formed.²² Instead, the Bdan-group was substituted under B–C bond breaking with a hydroxy group in an oxidation process. Changing hydrochloric acid as reactant with PTSA under an inert atmosphere gave **8** in a yield of 20%. Following Hattori et al., degassed 2 M sulfuric acid increased the yield up to 92%²³ (Scheme 2). The ¹¹B NMR spectrum of **8** shows a broad signal at 31 ppm. Calculations (M062X/6-31G*) of the ¹¹B chemical shift agrees within 1 ppm with experiment. All products were characterized by multinuclear (¹H, ¹³C, ¹¹B) and correlated NMR spectroscopy (H–H–COSY, HSQC, HMBC, NOESY) as well as high-resolution mass spectrometry. Our synthesis provides access from **1** to **8** in six steps with an overall yield of 12%.

The absorption spectrum (Figure 2) of **8** shows two main absorption features in the wavelength region of 250–320 nm and 325–390 nm. In comparison with the unsubstituted perylene motif **C**, the bands show a similar pattern.¹⁵ The influence of the butyl groups is merely a small bathochromic shift.

Also, the fluorescence spectrum of compound **8**, which was recorded with an excitation wavelength of 377 nm (Figure 2), shifted slightly to red compared to **C** and similarly shows an emission band with partly resolved vibrational fine structure. The Stokes shifts of **8** (1209 cm⁻¹) and of **C** (1194 cm⁻¹) are of comparable size, too. The fluorescence quantum yield of **8** in CH₂Cl₂, measured with reference to 9,10-diphenylanthracene in ethanol, ($\phi_{\text{F}} = 0.95$), is large, $\phi_{\text{F}} = 0.84$.^{24,25}

For further investigations, we computed the nucleus-independent chemical shift [NICS(0) and NICS(1) values] at the M062X/6-31G* level of theory of our perylene motif **C** in comparison with the perylene scaffold **D** and the dibenzoperylene **E** (Figure 3).^{26–28}

Perylene **D** shows two combined naphthalene units with an inner nonaromatic ring.²⁶ Dibenzoperylene **E** seems to resemble two combined phenanthrene units with the same nonaromatic central ring. The middle ring of the phenanthrene unit shows as expected less aromaticity.^{26,27} For comparison, the aromaticity pattern of **C** is that of a quaterphenyl with an interconnecting BNBN linkage.

In summary, we have shown that the dibenzoperylene motif featuring a doubly alternating boron–nitrogen-doped bay region is accessible synthetically in six steps from 2-

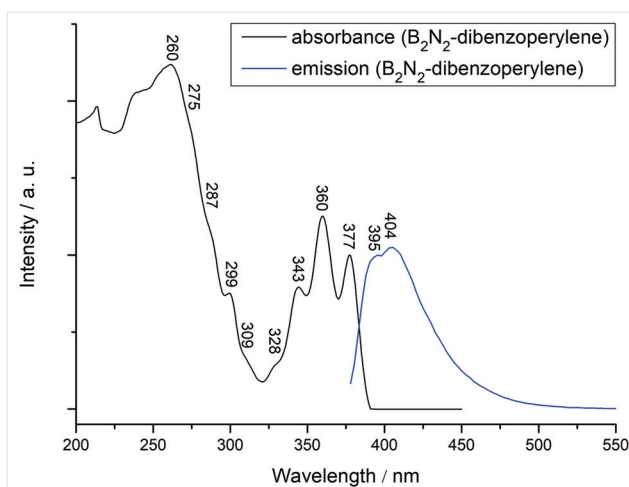


Figure 2 Absorption (black) and fluorescence (blue, $\lambda_{\text{ex}} = 377$ nm) spectrum of **8** (4×10^{-5} M in CH₂Cl₂).

bromo-4-butylaniline. Employing alkyl groups at the quaterphenyl increases the solubility of the perylene **8**. The key step of the synthesis is the insertion of the second boron atom via a protected boron species. Its deprotection could be optimized to proceed with a high conversion and high yield. The protocols developed here allow synthetic access to **8** in a gram scale. As expected, **8** shows absorption and fluorescence properties similar to the unsubstituted dibenzoperylene **C** as the butyl groups only cause a small bathochromic shift. The fluorescence quantum yield ($\phi_{FI} = 0.84$) of **8**, not determined for **C**, is unexpectedly high suggesting that the BNBN-substituted dibenzoperylene may be a platform for developing blue emitting materials. The perylene unit present in **8** is best considered to be comprised of a quaterphenyl moiety with a BNBN interconnecting bay region. The introduction of other groups than butyl at the quaterphenyl is expected to be straightforward. This allows the tuning of the (optical) properties as well as the synthesis of larger BNBN-doped PAH molecules.

Unless otherwise indicated, all reactions were carried out under dry and inert conditions by flaming all glassware with a heat gun (at 630 °C) under vacuum and purging with argon. All chemicals and solvents were purchased from commercial suppliers in anhydrous form or were dried by known methods. For column chromatography, a medium pressure liquid chromatography (MPLC) system (PuriFlash 430 evo, Interchim) was used, with Si-IR 20 μm columns. TLC was done using pre-coated polyester sheets (40 \times 80 mm) from Machery-Nagel (POLYGAM® SIL G/UV254) with 0.2 mm silica gel 60 with fluorescent indicator. A UV light source (254 nm and 366 nm) was used for visualization. Melting points were measured with a Büchi B-540 melting point apparatus. NMR spectroscopy was done on a Bruker Avance III 400, on a Bruker Avance III HDX 600, or on a Bruker Avance III HDX 700 spectrometer (equipped with a dual ($^1\text{H}/^{13}\text{C}$) probe head. Chemical shifts (δ) are given in ppm, coupling constants J in hertz (Hz) and standard abbreviations are designated to the multiplicities of the signals. The solvent signals were calibrated ($^1\text{H}/^{13}\text{C}$): CD_2Cl_2 5.32/53.84

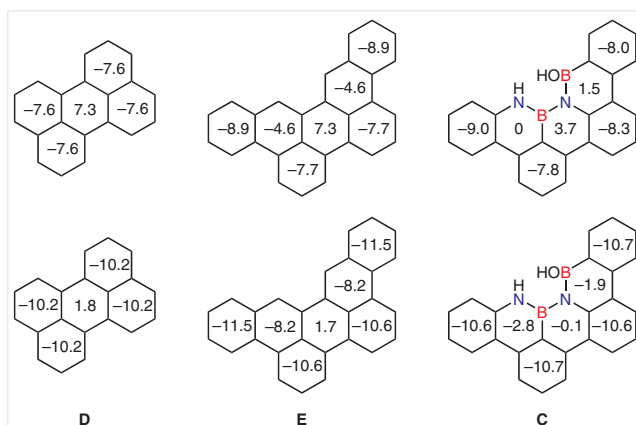


Figure 3 NICS(0) (above) and NICS(1) (below) values of perylene **D**, dibenzoperylene **E** and the BN-doped dibenzoperylene motif **C** computed at the M062X/6-31G* level of theory. Butyl groups are omitted. NICS(0) of benzene is -9.2 and NICS(1) -11.6 .

ppm, C_6D_6 7.16/128.06 ppm, CDCl_3 7.26/77.16 ppm, and $\text{THF-}d_8$ 3.58/67.21 ppm. Reference for ^1H and ^{13}C is TMS and for ^{11}B $\text{BF}_3\cdot\text{OEt}_2$ in CDCl_3 . H- and C-shift values are assigned and the corresponding numbering schemes are given in the Supporting Information. High-resolution mass spectrometry was done with electron spray ionization time of flight mass spectrometry (ESI-TOF-MS) on a maXis 4G Bruker system or EI on a MAT 95. Low-resolution electron impact mass spectrometry was done on a MSD 5977 (Agilent Technology) with a direct inlet probe (DIP) system (EI-MS, 70 eV).

Geometry optimizations on the S_0 potential energy surfaces were performed using the M062X²⁹ functional as implemented in Gaussian 09³⁰ in conjunction with the 6-31G* basis set.³¹ NICS(0) and NICS(1)^{27,28} were computed at the M062X/6-31G* level using the GIAO method.³²

Optical spectra were recorded on a PerkinElmer Lambda 1050 spectrometer with a PerkinElmer 3D WB Det Module. Excitation and emission spectra were recorded on a Cary Variant SPVF spectrometer using Hellma Analytics quartz cuvettes. All measurements were done in spectroscopy grade solvents. The fluorescence quantum yield of **8** in CH_2Cl_2 was measured with an excitation wavelength $\lambda_{\text{exc}} = 387$ nm (9,10-diphenylanthracene in EtOH as reference).

Terphenyl 3

A solution of 1,3-benzenediboronic acid bis(pinacol) ester (**2**; 5.7 g, 17.2 mmol, 1 equiv), 2-bromo-4-butylaniline (**1**; 8.8 g, 38.5 mmol, 2.4 equiv), $\text{Pd}(\text{PPh}_3)_4$ (1.1 g, 0.9 mmol, 5 mol%), and K_2CO_3 (15.5 g, 112.2 mmol, 6.5 equiv) in a mixture of 1,2-dimethoxyethane (500 mL) and H_2O (100 mL) was stirred under reflux (100 °C oil bath temp) for 18 h. DME was removed under reduced pressure and the residual mixture was extracted with CH_2Cl_2 (3 \times 100 mL). The combined organic layers were washed with brine (3 \times 50 mL) and dried (anhyd MgSO_4). All volatiles were removed under reduced pressure. The remaining solid was purified by column chromatography ($\text{CH}_2\text{Cl}_2/\text{EtOAc}$ 30:1, $R_f = 0.35$) and recrystallized from *n*-hexane (10 mL) to afford the desired compound **3** as pale yellow crystals; yield: 5.9 g (15.8 mmol, 92%); mp 79.6 °C (*n*-hexane).

^1H NMR (C_6D_6 , 700 MHz): $\delta = 7.76$ (m, 1 H, H-1), 7.45 (dd, $J = 7.6$, 1.7 Hz, 2 H, H-11, H-9), 7.25 (m, 1 H, H-10), 7.08 (d, $J = 2.1$ Hz, 2 H, H-18, H-4), 6.95 (dd, $J = 8.1$, 2.1 Hz, 2 H, H-16, H-6), 6.44 (d, $J = 8.1$ Hz, 2 H, H-15, H-7), 3.18 (br s, 4 H, 2 \times NH_2), 2.51–2.49 (m, 4 H, H-19, H-23), 1.55–1.52 (m, 4 H, H-20, H-24), 1.30–1.29 (m, 4 H, H-21, H-25), 0.87 (t, $J = 7.4$ Hz, 6 H, H-22, H-26).

^{13}C NMR (C_6D_6 , 176 MHz): $\delta = 142.1$ (C-14, C-8), 141.3 (C-2, C-12), 133.0 (C-17, C-5), 130.8 (C-18, C-4), 130.3 (C-1), 129.4 (C-10), 128.9, 128.3 (C-16, C-6), 128.0 (C-9, C-11), 127.5 (C-13, C-3), 116.1 (C-15, C-7), 35.3 (C-23, C-19), 34.5 (C-20, C-24), 22.7 (C-21, C-25), 14.2 (C-22, C-26).

HRMS (ESI): m/z [$\text{M} + \text{H}$]⁺ calcd for $\text{C}_{26}\text{H}_{33}\text{N}_2$: 373.26383; found: 373.26404 (Δ : 0.57 ppm).

NBN-Benzotetracene 4

Terphenyl **3** (3.2 g, 8.6 mmol, 1 equiv) and sodium tetraphenylborate (3.6 g, 10.4 mmol, 1.5 equiv) were dissolved in anhyd toluene (75 mL) under an inert atmosphere and cooled in an ice-bath. BBr_3 (2.2 g, 8.7 mmol, 1 equiv) was added slowly to the mixture in the ice-cooled flask and the mixture was then stirred under reflux (120 °C, oil bath temperature) for 18 h. The mixture was poured into sat. aq NaHCO_3 (100 mL) and THF was added until all particles had dissolved. The layers were separated, and the aqueous layer was extracted with CH_2Cl_2 (3 \times 50 mL). THF (30 mL) was added again to the aqueous layer and

the extraction step was repeated one more time. After drying (anhyd Na_2SO_4), all volatiles were removed under reduced pressure. The remaining solid was purified by column chromatography (CH_2Cl_2 , $R_f = 0.9$) and recrystallization from benzene (150 mL) afforded the desired compound **4** as colorless needles; yield: 2.1 g (5.6 mmol, 65%); mp 249 °C (benzene).

^1H NMR (CDCl_3 , 400 MHz): $\delta = 8.18$ (d, $J = 7.9$ Hz, 2 H, H-9, H-7), 8.05 (br s, 2 H, H-12, H-4), 7.82–7.78 (m, 1 H, H-8), 7.15 (dd, $J = 8.2$, 1.7 Hz, 2 H, H-2, H-14), 6.94 (d, $J = 8.2$ Hz, 2 H, H-15, H-1), 6.16 (br s, 2 H, H-NH), 2.71 (t, $J = 7.7$ Hz, 4 H, H-23, H-19), 1.71–1.67 (m, 4 H, H-24, H-20), 1.46–1.40 (m, 4 H, H-25, H-21), 0.98 (t, $J = 7.3$ Hz, 6 H, H-26, H-22).

^{13}C NMR (CDCl_3 , 101 MHz): $\delta = 139.0$ (C-10, C-6), 138.4 (C-16, C-17), 134.1 (C-13, C-3), 130.8 (C-8), 128.6 (C-14, C-2), 123.9 (C-12, C-4), 122.0 (C-11, C-5), 118.8 (C-9, C-7), 118.0 (C-15, C-1), 35.4 (C-23, C-19), 34.2 (C-24, C-20), 22.4 (C-21, C-25), 14.0 (C-26, C-22). C-B cannot be detected due to the quadrupole moment of B.

^{11}B NMR (CDCl_3 , 128 MHz): $\delta = 26.9$.

HRMS (EI): m/z [M] $^+$ calcd for $\text{C}_{26}\text{H}_{29}\text{BN}_2$: 380.24183; found: 380.24263 (Δ : 0.8 mmu).

Compound 5

To an ice-cold solution of compound **4** (3.6 g, 9.4 mmol, 1 equiv) in a mixture of $\text{HCl}_3/\text{CH}_2\text{Cl}_2$ (1:1, 500 mL in total) was added over 2 h a solution of NBS (1.7 g, 9.4 mmol, 1 equiv) in MeCN (60 mL). After complete addition, the mixture was stirred at r.t. for 12 h and all volatiles were removed under reduced pressure. Flash-chromatography [*n*-hexane/ CH_2Cl_2 8:1, R_f (2:1) = 0.57] afforded the desired product **5** as a colorless crystalline solid; yield: 2.1 g (4.5 mmol, 48%); mp 154 °C.

^1H NMR (CD_2Cl_2 , 700 MHz): $\delta = 8.19$ (d, $J = 8.0$ Hz, 1 H, H-10), 8.14 (d, $J = 8.0$ Hz, 1 H, H-8), 8.04 (d, $J = 1.3$ Hz, 1 H, H-13), 8.01 (s, 1 H, H-5), 7.80 (t, $J = 8.0$ Hz, 1 H, H-9), 7.46 (d, $J = 1.7$ Hz, 1 H, H-3), 7.17 (dd, $J = 8.1$, 1.8 Hz, 1 H, H-16), 7.00 (d, $J = 8.1$ Hz, 1 H, H-15), 6.92 (br s, 1 H, NH 1), 6.44 (br s, 1 H, NH 2), 2.72–2.67 (m, 4 H, H-23, H-19), 1.70–1.68 (m, 4 H, H-24, H-20), 1.44–1.43 (m, 4 H, H-25, H-21), 0.99–0.97 (m, 6 H, H-26, H-22).

^{13}C NMR (CD_2Cl_2 , 176 MHz): $\delta = 139.7$ (C-2), 139.1 (C-6), 139.0 (C-12), 136.6 (C-14), 135.5 (C-17), 135.1 (C-4), 132.2 (C-3), 131.6 (C-9), 129.5 (C-16), 127.6 (C-18), 124.4 (C-13), 124.2 (C-5), 124.2 (C-7), 122.3 (C-11), 120.0 (C-10), 119.6 (C-8), 118.8 (C-15), 113.5 (C-1), 35.9 (C-19), 35.6 (C-23), 34.8 (C-20), 34.5 (C-24), 23.0 (C-21), 22.9 (C-25), 14.4 (C-22), 14.3 (C-26).

^{11}B NMR (CD_2Cl_2 , 128 MHz): $\delta = 26.9$.

HRMS (EI): m/z [M] $^+$ calcd for $\text{C}_{26}\text{H}_{28}\text{BBrN}_2$: 458.15234; found: 458.15160 (Δ : 0.7 mmu).

Compound 6

Under an inert atmosphere compound **5** (1.4 g, 3.1 mmol, 1 equiv), bis(pinacolato)diboron (2.0 g, 7.8 mmol, 2.5 equiv), KOAc (1.8 g, 19 mmol, 6 equiv), and Pd(dppf) Cl_2 (0.2 g, 0.3 mmol, 10 mol%) were dissolved in anhyd 1,4-dioxane (180 mL) and the reaction mixture was stirred at 90 °C for 18 h. After cooling down, the mixture was washed with H_2O (3 \times 50 mL) and the combined organic layers were dried (anhyd Na_2SO_4). The solvent was removed under reduced pressure. Column chromatography (*n*-hexane/ CH_2Cl_2 3:1, $R_f = 0.1$) furnished the desired compound **6**; yield: 0.9 g (1.8 mmol, 61%); mp not determined due to decomposition of **6**.

^1H NMR (CD_2Cl_2 , 600 MHz): $\delta = 8.43$ (br s, 1 H, NH 2), 8.20 (d, $J = 2.0$ Hz, 1 H, H-5), 8.17 (t, $J = 8.0$ Hz, 2 H, H-10, H-8), 8.05 (d, $J = 1.5$ Hz, 1 H, H-13), 7.79 (t, $J = 8.0$ Hz, 1 H, H-9), 7.66 (d, $J = 2.0$ Hz, 1 H, H-3), 7.16 (dd, $J = 8.0$, 1.5 Hz, 1 H, H-15), 7.02 (d, $J = 8.0$ Hz, 1 H, H-16), 6.45 (br s, 1 H, NH 1), 2.72–2.68 (m, 4 H, H-19, H-23), 1.70–1.65 (m, 4 H, H-20, H-24), 1.45–1.39 (m, 16 H, H-32, H-31, H-30, H-29, H-21, H-25), 0.97 (t, $J = 7.4$ Hz, 6 H, H-22, H-26).

^{13}C NMR (CD_2Cl_2 , 151 MHz): $\delta = 145.7$ (C-1), 139.9 (C-14), 139.5 (C-4), 139.4 (C-12), 137.5 (C-3), 134.7 (C-17), 133.6 (C-6), 131.3 (C-9), 129.3 (C-15), 128.5 (C-5), 127.6 (C-18), 124.4 (C-13), 122.3 (C-11), 122.1 (C-7), 119.3 (C-8)*, 119.1 (C-10)*, 118.5 (C-16), 115.5 (C-2), 84.7 (C-28, C-27), 35.8 (C-19), 35.8 (C-23), 34.9 (C-20), 34.8 (C-24), 25.3 (C-32, C-31, C-30, C-29), 23.1 (C-21), 23.0 (C-25), 14.4 (C-22, C-26). * Signals may be swapped due to overlap in the ^1H NMR spectrum.

^{11}B NMR (CD_2Cl_2 , 128 MHz): $\delta = 31.2$, 26.8.

HRMS (EI): m/z [M] $^+$ calcd for $\text{C}_{32}\text{H}_{40}\text{B}_2\text{N}_2\text{O}_2$: 506.32704; found: 506.32966 (Δ : 2.6 mmu).

Compound 7

Compound **6** (0.9 g, 1.8 mmol, 1 equiv), Br-Bdan-benzene (0.6 g, 1.8 mmol, 1 equiv), K_2CO_3 (1.0 g, 7.2 mmol, 4 equiv), and Pd(PPh $_3$) $_4$ (0.2 g, 0.2 mmol, 10 mol%) were dissolved in a mixture of toluene (150 mL), EtOH (40 mL) and H_2O (75 mL), and the reaction mixture was stirred under reflux (100 °C oil bath temp) for 12 h. After cooling down, the mixture was washed with H_2O (3 \times 30 mL) and the aqueous layer was extracted with CH_2Cl_2 (3 \times 30 mL). The combined organic layers were dried (anhyd Na_2SO_4) and all volatiles were removed under reduced pressure. Flash chromatography [*n*-hexane/ CH_2Cl_2 3:1, R_f (2:1) = 0.49] afforded the desired compound **7** as a colorless solid; yield: 819 mg (1.31 mmol, 73%); mp not determined due to decomposition of **7**.

^1H NMR (CD_2Cl_2 , 600 MHz): $\delta = 8.27$ (d, $J = 8.1$ Hz, 1 H, H-8), 8.19–8.18 (m, 2 H, H-10, H-5), 8.02 (d, $J = 1.7$ Hz, 1 H, H-13), 7.87 (dd, $J = 7.5$, 1.1 Hz, 1 H, H-31), 7.83 (t, $J = 8.1$ Hz, 1 H, H-9), 7.65–7.62 (m, 1 H, H-29), 7.59–7.57 (m, 1 H, H-30), 7.48 (dd, $J = 7.4$, 0.8 Hz, 1 H, H-28), 7.15 (d, $J = 2.0$ Hz, 1 H, H-3), 7.10 (dd, $J = 8.1$, 1.7 Hz, 1 H, H-15), 6.94–6.92 (m, 2 H, H-40, H-36), 6.88 (d, $J = 8.1$ Hz, 1 H, H-15), 6.86 (dd, $J = 8.3$, 0.8 Hz, 2 H, H-39, H-37), 6.25 (s, 1 H, NH 2), 6.20 (s, 1 H, NH 1), 5.98 (dd, $J = 7.3$, 0.8 Hz, 2 H, H-41, H-35), 5.70 (s, 2 H, NH 1 , NH 2), 2.73 (td, $J = 7.6$, 1.3 Hz, 2 H, H-23), 2.69–2.66 (m, 2 H, H-19), 1.67–1.62 (m, 4 H, H-24, H-20), 1.43–1.38 (m, 2 H, H-25), 1.37–1.32 (m, 2 H, H-21), 0.95 (t, $J = 7.3$ Hz, 3 H, H-26), 0.82 (t, $J = 7.3$ Hz, 3 H, H-22).

^{13}C NMR (CD_2Cl_2 , 151 MHz): $\delta = 143.7$ (C-27), 141.5 (C-42, C-34), 139.7 (C-11), 139.6 (C-7), 139.0 (C-17), 136.7 (C-38, C-6), 134.8 (C-14), 134.4 (C-4), 133.9 (C-31), 131.6 (C-1), 131.5 (C-9), 131.3 (C-28), 131.0 (C-29), 130.3 (C-3), 129.3 (C-15), 128.3 (C-30), 128.0 (C-40, C-36), 124.4 (C-5), 124.4 (C-13), 122.8 (C-12), 122.2 (C-2), 120.0 (C-33), 119.7 (C-8), 119.5 (C-10), 118.5 (C-16), 117.8 (C-39, C-37), 106.2 (C-41, C-35), 35.8 (C-23), 35.8 (C-19), 34.9 (C-24), 34.7 (C-20), 23.0 (C-25), 22.9 (C-21), 14.3 (C-26), 14.2 (C-22). C-B cannot be detected due to the quadrupole moment of B.

^{11}B NMR (CD_2Cl_2 , 128 MHz): $\delta = 29.0$ (br s).

HRMS (ESI): m/z [$M + \text{H}$] $^+$ calcd for $\text{C}_{42}\text{H}_{41}\text{B}_2\text{N}_4$: 623.35118; found: 623.35153 (Δ : 0.6 ppm).

Dibenzoperylene 8

Under an inert atmosphere compound **7** (0.3 g, 0.5 mmol, 1 equiv) was dissolved in degassed THF (100 mL). To this solution was added dropwise a degassed H_2SO_4 solution (6.0 mL, 2 M in H_2O , 12 mmol, 24 equiv). The mixture was stirred at 50 °C for 5 days. The solution was extracted with CH_2Cl_2 (4 \times 25 mL) and the combined organic layers

were washed with sat. aq NaHCO₃ (3 × 25 mL), H₂O (3 × 25 mL) and brine (2 × 25 mL). After drying (MgSO₄), all volatiles were removed under reduced pressure. Column chromatography (*n*-hexane/CH₂Cl₂ 1:1, *R_f* = 0.5) furnished the desired compound as a colorless solid; yield: 222 mg (0.46 mmol, 92%); mp 207 °C.

¹H NMR (THF-*d*₈, 700 MHz): δ = 9.78 (br s, 1 H, OH), 9.06 (br s, 1 H, NH), 8.45 (d, *J* = 8.4 Hz, 1 H, H-4), 8.34–8.29 (m, 4 H, H-9, H-7, H-12, H-14), 8.23 (dd, *J* = 7.5, 1.1 Hz, 1 H, H-1), 8.17 (s, 1 H, H-17), 7.81–7.79 (m, 1 H, H-13), 7.70–7.69 (m, 1 H, H-3), 7.48–7.46 (m, 1 H, H-2), 7.20 (dd, *J* = 8.1, 1.8 Hz, 1 H, H-19), 7.14 (d, *J* = 8.1 Hz, 1 H, H-20), 2.86 (t, *J* = 7.7 Hz, 2 H, H-25), 2.74 (t, *J* = 7.7 Hz, 2 H, H-29), 1.82–1.77 (m, 2 H, H-26), 1.71–1.69 (m, 2 H, H-30), 1.51–1.47 (m, 2 H, H-27), 1.46–1.41 (m, 2 H, H-31), 1.00 (t, *J* = 7.4 Hz, 3 H, H-28), 0.98 (t, *J* = 7.4 Hz, 3 H, H-32).

¹³C NMR (THF-*d*₈, 176 MHz): δ = 142.6 (C-5), 140.6 (C_q-?), 140.2 (C_q-?), 139.5 (C-21), 137.2 (C_q-?), 135.7 (C-8), 135.1 (C-18), 132.4 (C-3, C-1), 131.9 (C-13), 129.4 (C-19), 128.5 (C-24), 127.4 (C-22), 126.9 (C-2), 126.7 (C_q-?), 125.9 (C-H_m), 125.7 (C_q-?), 125.4 (C-H_m), 124.4 (C-17), 123.8 (C-4), 122.6 (C-16), 120.4 (C-H_m), 120.0 (C-20, C-H_m), 36.4 (C-25, C-29), 35.3 (C-26), 35.1 (C-30), 23.4 (C-27), 23.3 (C-31), 14.5 (C-32), 14.5 (C-28). All 'C-H_m' belong to the proton multiplet of 8.34–8.29 ppm and cannot be completely assigned. All quaternary 'C_q-?' cannot be completely assigned.

¹¹B NMR (THF-*d*₈, 128 MHz): δ = 31.1.

HRMS (EI): *m/z* [M]⁺ calcd for C₃₂H₃₂B₂N₂O: 482.26953; found: 482.27274 (Δ: 3.2 mmu).

Funding Information

This research was funded by the Vector foundation. The authors acknowledge support by the state of Baden-Württemberg through bwHPC and the DFG through grant no INST 40/467-1 FUGG.

Acknowledgment

The computations were performed on the BwForCluster JUSTUS.

Supporting Information

Supporting information for this article is available online at <https://doi.org/10.1055/s-0039-1690687>.

References

- Bosdet, M. J. D.; Piers, W. E. *Can. J. Chem.* **2009**, *87*, 8.
- Campbell, P. G.; Marwitz, A. J. V.; Liu, S.-Y. *Angew. Chem. Int. Ed.* **2012**, *51*, 6074.
- Helten, H. *Chem. Eur. J.* **2016**, *22*, 12972.
- Jiang, W.; Li, Y.; Wang, Z. *Chem. Soc. Rev.* **2013**, *42*, 6113.
- Stępień, M.; Gońka, E.; Żyła, M.; Sprutta, N. *Chem. Rev.* **2017**, *117*, 3479.
- Wang, X.-Y.; Wang, J.-Y.; Pei, J. *Chem. Eur. J.* **2015**, *21*, 3528.
- Morgan, M. M.; Piers, W. E. *Dalton Trans.* **2016**, *45*, 5920.
- Giustra, Z. X.; Liu, S.-Y. *J. Am. Chem. Soc.* **2018**, *140*, 1184.
- Kaehler, T.; Bolte, M.; Lerner, H.-W.; Wagner, M. *Angew. Chem. Int. Ed.* **2019**, *58*, 11379.
- Numano, M.; Nagami, N.; Nakatsuka, S.; Katayama, T.; Nakajima, K.; Tatsumi, S.; Yasuda, N.; Hatakeyama, T. *Chem. Eur. J.* **2016**, *22*, 11574.
- Yang, D.-T.; Nakamura, T.; He, Z.; Wang, X.; Wakamiya, A.; Peng, T.; Wang, S. *Org. Lett.* **2018**, *20*, 6741.
- Wang, X.; Zhang, F.; Schellhammer, K. S.; Machata, P.; Ortmann, F.; Cuniberti, G.; Fu, Y.; Hunger, J.; Tang, R.; Popov, A. A.; Berger, R.; Müllen, K.; Feng, X. *J. Am. Chem. Soc.* **2016**, *138*, 11606.
- Dewar, M. J. S.; Kubba, V. P.; Pettit, R. *J. Chem. Soc.* **1958**, 3073.
- Krieg, M.; Reicherter, F.; Haiss, P.; Ströbele, M.; Eichele, K.; Treanor, M.-J.; Schaub, R.; Bettinger, H. F. *Angew. Chem. Int. Ed.* **2015**, *54*, 8284.
- Müller, M.; Behnle, S.; Maichle-Mössmer, C.; Bettinger, H. F. *Chem. Commun.* **2014**, *50*, 7821.
- Biswas, S.; Müller, M.; Tönshoff, C.; Eichele, K.; Maichle-Mössmer, C.; Ruff, A.; Speiser, B.; Bettinger, H. F. *Eur. J. Org. Chem.* **2012**, 4634.
- Köster, R.; Hattori, S.; Morita, Y. *Angew. Chem. Int. Ed. Engl.* **1965**, *4*, 695; *Angew. Chem.* **1965**, *77*, 719.
- Müller, M.; Maichle-Mössmer, C.; Sirsch, P.; Bettinger, H. F. *ChemPlusChem* **2013**, *78*, 988.
- Dosso, J.; Tasseroul, J.; Fasano, F.; Marinelli, D.; Biot, N.; Fermi, A.; Bonifazi, D. *Angew. Chem. Int. Ed.* **2017**, *56*, 4483.
- Fingerle, M.; Maichle-Mössmer, C.; Schundelmeier, S.; Speiser, B.; Bettinger, H. F. *Org. Lett.* **2017**, *19*, 4428.
- Lee, C.-I.; Zhou, J.; Ozerov, O. V. *J. Am. Chem. Soc.* **2013**, *135*, 3560.
- Noda, H.; Furutachi, M.; Asada, Y.; Shibasaki, M.; Kumagai, N. *Nat. Chem.* **2017**, *9*, 571.
- Hattori, Y.; Ogaki, T.; Ishimura, M.; Ohta, Y.; Kirihata, M. *Tetrahedron Lett.* **2017**, *17*, 2436.
- Brouwer, A. M. *Pure Appl. Chem.* **2011**, *83*, 2213.
- Lakowicz, J. R. *Principles of Fluorescence Spectroscopy*, 3rd ed; Springer: Berlin, **2006**.
- Chen, Z.; Wannere, C. S.; Corminboeuf, C.; Puchta, R.; Schleyer, P. v. R. *Chem. Rev.* **2005**, *105*, 3842.
- Schleyer, P. v. R.; Maerker, C.; Dransfeld, A.; Jiao, H.; van Eikema Hommes, N. J. R. *J. Am. Chem. Soc.* **1996**, *118*, 6317.
- Schleyer, P. v. R.; Jiao, H.; van Eikema Hommes, N. J. R.; Malkin, V. G.; Malkina, O. L. *J. Am. Chem. Soc.* **1997**, *119*, 12669.
- Zhao, Y.; Truhlar, D. G. *Theor. Chem. Acc.* **2008**, *120*, 215.
- Frisch, M. J.; Trucks, G. W.; Schlegel, H. B.; Scuseria, G. E.; Robb, W. A.; Cheeseman, J. R.; Scalmani, G.; Barone, V.; Petersson, G. A.; Nakatsuji, H.; Li, X.; Caricato, M.; Marenich, A.; Bloino, J.; Janesko, B. G.; Gomperts, R.; Mennucci, B.; Hratchian, H. P.; Ortiz, J. V.; Izmaylov, A. F.; Sonnenberg, J. L.; Williams-Young, D.; Ding, F.; Lipparini, F.; Egidi, F.; Goings, J.; Peng, B.; Petrone, A.; Henderson, T.; Ranasinghe, D.; Zakrzewski, V. G.; Gao, J.; Rega, N.; Zheng, G.; Liang, W.; Hada, M.; Ehara, M.; Toyota, K.; Fukuda, R.; Hasegawa, J.; Ishida, M.; Nakajima, T.; Honda, Y.; Kitao, O.; Nakai, H.; Vreven, T.; Throssell, K.; Montgomery, J. A. Jr.; Peralta, J. E.; Ogliaro, F.; Bearpark, M.; Heyd, J. J.; Brothers, E.; Kudin, K. N.; Staroverov, V. N.; Keith, T.; Kobayashi, R.; Normand, J.; Raghavachari, K.; Rendell, A.; Burant, J. C.; Iyengar, S. S.; Tomasi, J.; Cossi, M.; Millam, J. M.; Klene, M.; Adamo, C.; Cammi, R.; Ochterski, J. W.; Martin, R. L.; Morokuma, K.; Farkas, O.; Foresman, J. B.; Fox, D. J. *Gaussian 09, Revision A.02*; Gaussian Inc: Wallingford CT, **2009**.
- Hariharan, P. C.; Pople, J. A. *Theor. Chim. Acta* **1973**, *28*, 213.
- Wolinski, K.; Hinton, J. F.; Pulay, P. *J. Am. Chem. Soc.* **1990**, *112*, 8251.

Supporting Information

for DOI: 10.1055/s-0039-1690687

© 2019. Thieme. All rights reserved.

Georg Thieme Verlag KG, Rüdigerstraße 14, 70469 Stuttgart, Germany

Supporting Information (SI)

New Synthesis of a Dibenzoperylene Motif Featuring a Doubly Boron-Nitrogen Doped Bay Region

Michael Fingerle, Simon Stocker, Holger F. Bettinger

Institut für Organische Chemie, Auf der Morgenstelle 18, 72076 Tübingen, Germany

E-Mail: Holger.Bettinger@uni-tuebingen.de

Contents

- 1. Cartesian Coordinates of Stationary Points in ÅNGSTRÖM**
- 2. Spectra – NMR & mass**

1. Cartesian Coordinates of Stationary Points in ÅNGSTRÖM

a) Compound D (D_{2H}), S₀

32
scf done: -769.086611144

1	0.000000000	3.360522000	3.415764000
6	0.000000000	2.415719000	2.881252000
6	0.000000000	1.229902000	3.566613000
1	0.000000000	1.211282000	4.653013000
6	0.000000000	2.419905000	1.473931000
6	0.000000000	1.247749000	0.739478000
6	0.000000000	0.000000000	1.438398000
6	0.000000000	-1.247749000	0.739478000
6	0.000000000	-2.419905000	1.473931000
6	0.000000000	-2.415719000	2.881252000
6	0.000000000	-1.229902000	3.566613000
6	0.000000000	0.000000000	2.863903000
6	0.000000000	-1.247749000	-0.739478000
6	0.000000000	-2.419905000	-1.473931000
6	0.000000000	-2.415719000	-2.881252000
6	0.000000000	-1.229902000	-3.566613000
6	0.000000000	0.000000000	-2.863903000
6	0.000000000	0.000000000	-1.438398000
6	0.000000000	1.229902000	-3.566613000
6	0.000000000	2.415719000	-2.881252000
1	0.000000000	3.360522000	-3.415764000
1	0.000000000	1.211282000	-4.653013000
6	0.000000000	1.247749000	-0.739478000
6	0.000000000	2.419905000	-1.473931000
1	0.000000000	-1.211282000	-4.653013000
1	0.000000000	-3.360522000	-3.415764000
1	0.000000000	-3.380328000	-0.972038000
1	0.000000000	3.380328000	-0.972038000
1	0.000000000	-1.211282000	4.653013000
1	0.000000000	-3.380328000	0.972038000
1	0.000000000	-3.360522000	3.415764000
1	0.000000000	3.380328000	0.972038000

b) Compound E (C₂), S₀

44
scf done: -1076.25632364

6	-0.412350000	-3.548535000	-2.852745000
6	-0.255911000	-2.869401000	-1.623590000
6	-0.109085000	-3.605414000	-0.425703000
6	-0.113604000	-5.014702000	-0.507244000
6	-0.262686000	-5.660184000	-1.716321000
6	-0.416069000	-4.922727000	-2.903798000
6	-0.225814000	-1.443119000	-1.587551000
6	-0.058991000	-0.736598000	-0.431889000
6	0.009196000	-1.454784000	0.822274000
6	0.057806000	-0.738236000	2.049207000
6	0.206118000	-1.448048000	3.232847000
6	0.255911000	-2.843931000	3.236964000
6	0.146909000	-3.547035000	2.058149000
6	0.019909000	-2.875356000	0.827010000
6	-0.057806000	0.738236000	2.049207000
6	-0.206118000	1.448048000	3.232847000
6	-0.255911000	2.843931000	3.236964000
6	-0.146909000	3.547035000	2.058149000
6	-0.019909000	2.875356000	0.827010000
6	-0.009196000	1.454784000	0.822274000
6	0.109085000	3.605414000	-0.425703000
6	0.255911000	2.869401000	-1.623590000
6	0.412350000	3.548535000	-2.852745000
6	0.416069000	4.922727000	-2.903798000
6	0.262686000	5.660184000	-1.716321000
6	0.113604000	5.014702000	-0.507244000
6	0.058991000	0.736598000	-0.431889000
6	0.225814000	1.443119000	-1.587551000
1	-0.166649000	4.629749000	2.088804000

1	-0.372796000	3.373260000	4.177388000
1	-0.297503000	0.927734000	4.178672000
1	0.343369000	0.929396000	-2.536395000
1	0.166649000	-4.629749000	2.088804000
1	0.297503000	-0.927734000	4.178672000
1	0.372796000	-3.373260000	4.177388000
1	0.524979000	2.961493000	-3.760752000
1	0.535262000	5.436055000	-3.852715000
1	0.263227000	6.745208000	-1.749674000
1	0.001185000	5.613925000	0.389019000
1	-0.001185000	-5.613925000	0.389019000
1	-0.263227000	-6.745208000	-1.749674000
1	-0.535262000	-5.436055000	-3.852715000
1	-0.524979000	-2.961493000	-3.760752000
1	-0.343369000	-0.929396000	-2.536395000

c) Compound C (C₁), S₀

45
scf done: -1158.43144079

6	3.584183000	-2.797797000	0.095460000
6	2.920399000	-1.561124000	0.050100000
6	3.663562000	-0.363811000	-0.033085000
6	5.064555000	-0.466717000	-0.059331000
6	5.714016000	-1.687386000	-0.012690000
6	4.963664000	-2.864181000	0.063825000
7	1.534990000	-1.541835000	0.085573000
5	0.763799000	-0.353827000	0.061391000
6	1.550329000	0.954245000	-0.011403000
6	0.840092000	2.166754000	-0.039907000
6	1.553596000	3.359818000	-0.191092000
6	2.941704000	3.336090000	-0.273442000
6	3.647348000	2.144314000	-0.212268000
6	2.961897000	0.929202000	-0.085468000
6	-0.636510000	2.132911000	0.079253000
6	-1.328067000	3.338967000	0.214475000
6	-2.707867000	3.391623000	0.305821000
6	-3.425937000	2.214351000	0.229250000
6	-2.795972000	0.972044000	0.093684000
6	-1.373475000	0.913822000	0.073812000
6	-3.628066000	-0.243008000	-0.023887000
6	-3.012348000	-1.504192000	0.010310000
6	-3.798463000	-2.661708000	-0.097923000
6	-5.172609000	-2.594895000	-0.240838000
6	-5.780952000	-1.338405000	-0.294318000
6	-5.024455000	-0.183640000	-0.193768000
7	-0.704967000	-0.334470000	0.068273000
5	-1.472840000	-1.555568000	0.114171000
1	-4.504867000	2.261433000	0.305168000
1	-3.215661000	4.341520000	0.434342000
1	-0.772287000	4.265847000	0.276742000
8	-0.806664000	-2.756853000	0.232650000
1	4.728614000	2.173907000	-0.280393000
1	1.053476000	4.317396000	-0.268436000
1	3.481362000	4.271152000	-0.392925000
1	-3.332184000	-3.646561000	-0.086360000
1	-5.766760000	-3.499358000	-0.323452000
1	-6.856115000	-1.261736000	-0.426830000
1	-5.536243000	0.767536000	-0.274121000
1	5.664139000	0.435172000	-0.112512000
1	6.797997000	-1.726938000	-0.034082000
1	5.458708000	-3.829752000	0.101176000
1	2.990230000	-3.706419000	0.156049000
1	1.089473000	-2.448487000	0.137379000
1	-1.415261000	-3.502439000	0.292904000

2. Spectra – NMR & mass

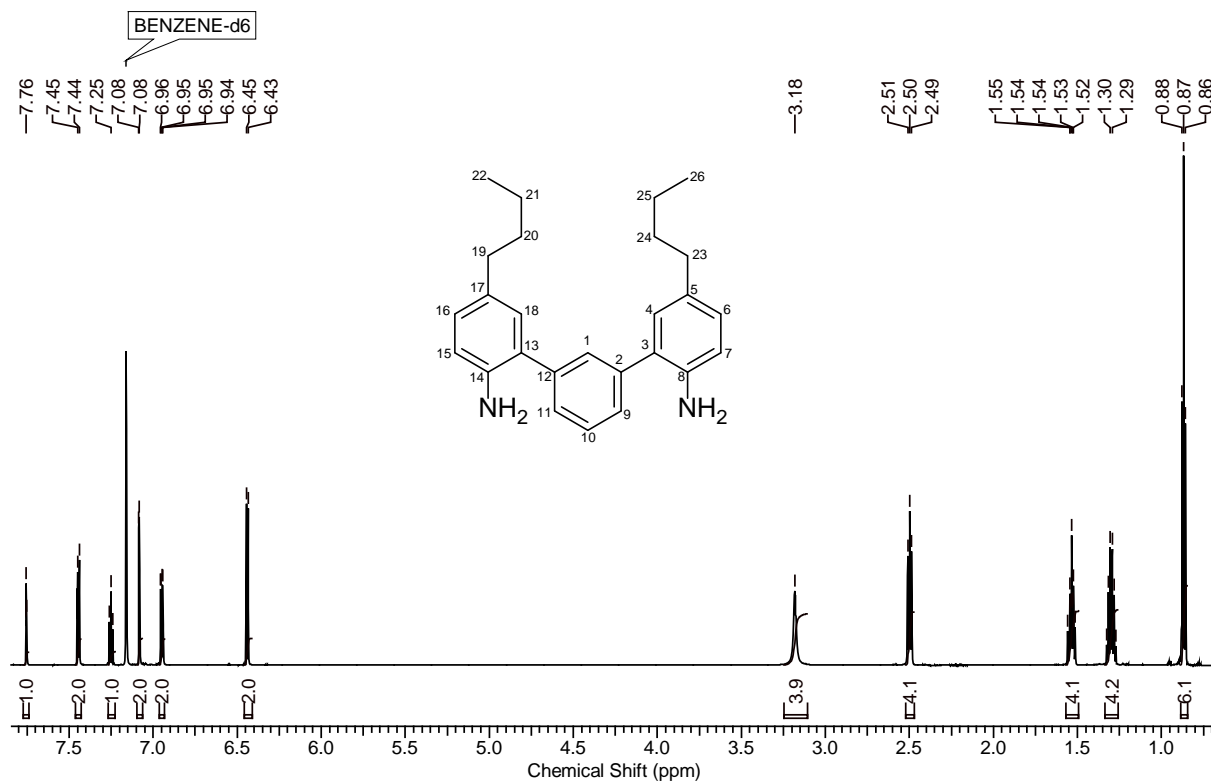


Figure S1: ¹H-NMR of **3** in C₆D₆.

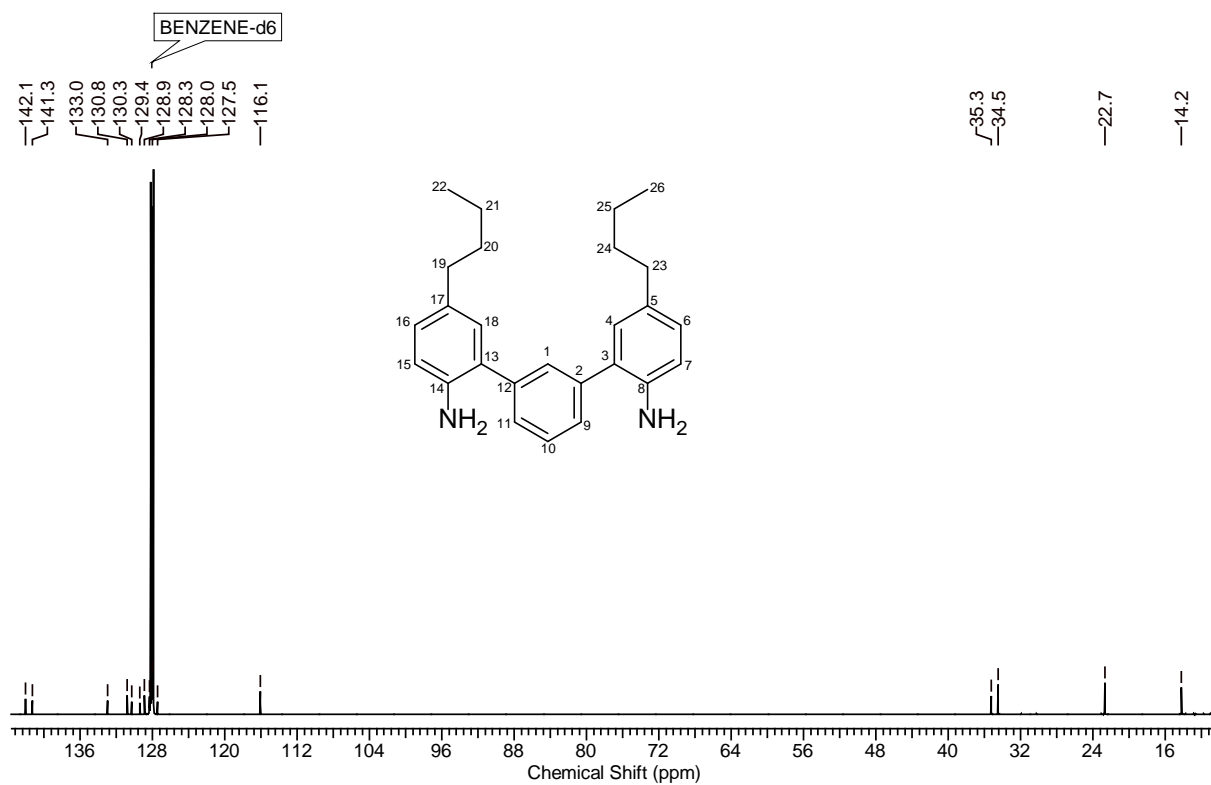
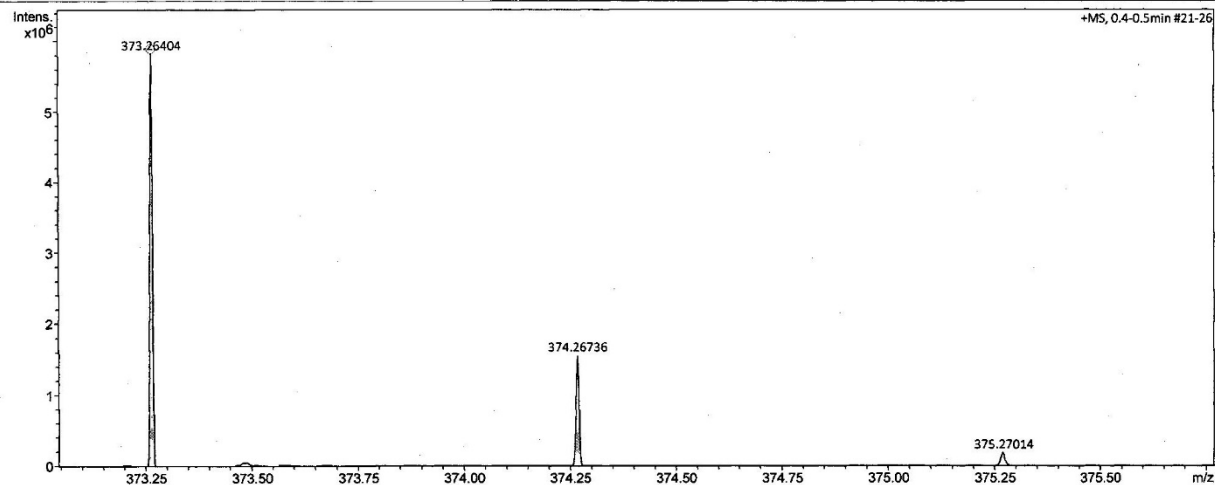


Figure S2: ¹³C-NMR of **3** in C₆D₆.

Display Report

Analysis Info	D:\Data\oi\Fingerle_MF 76_GC6_01_17849.d	Acquisition Date	9/8/2017 12:27:45 PM
Analysis Name	fia_ms_80-1000_pos_neu.m	Operator	BDAL@DE
Method	Fingerle_MF 76	Instrument	maXis
Sample Name			288882.21253
Comment			

Acquisition Parameter					
Source Type	ESI	Ion Polarity	Positive	Set Nebulizer	1.2 Bar
Focus	Active	Set Capillary	4500 V	Set Dry Heater	200 °C
Scan Begin	80 m/z	Set End Plate Offset	-500 V	Set Dry Gas	5.0 l/min
Scan End	1000 m/z	Set Charging Voltage	0 V	Set Divert Valve	Waste
		Set Corona	0 nA	Set APCI Heater	0 °C



Fingerle_MF 76_GC6_01_17849.d
Bruker Compass DataAnalysis 4.2

printed: 9/8/2017 2:13:17 PM

by: BDAL@DE

Page 1 of 1

Figure S3: High resolution ESI mass spectrum of **3**.

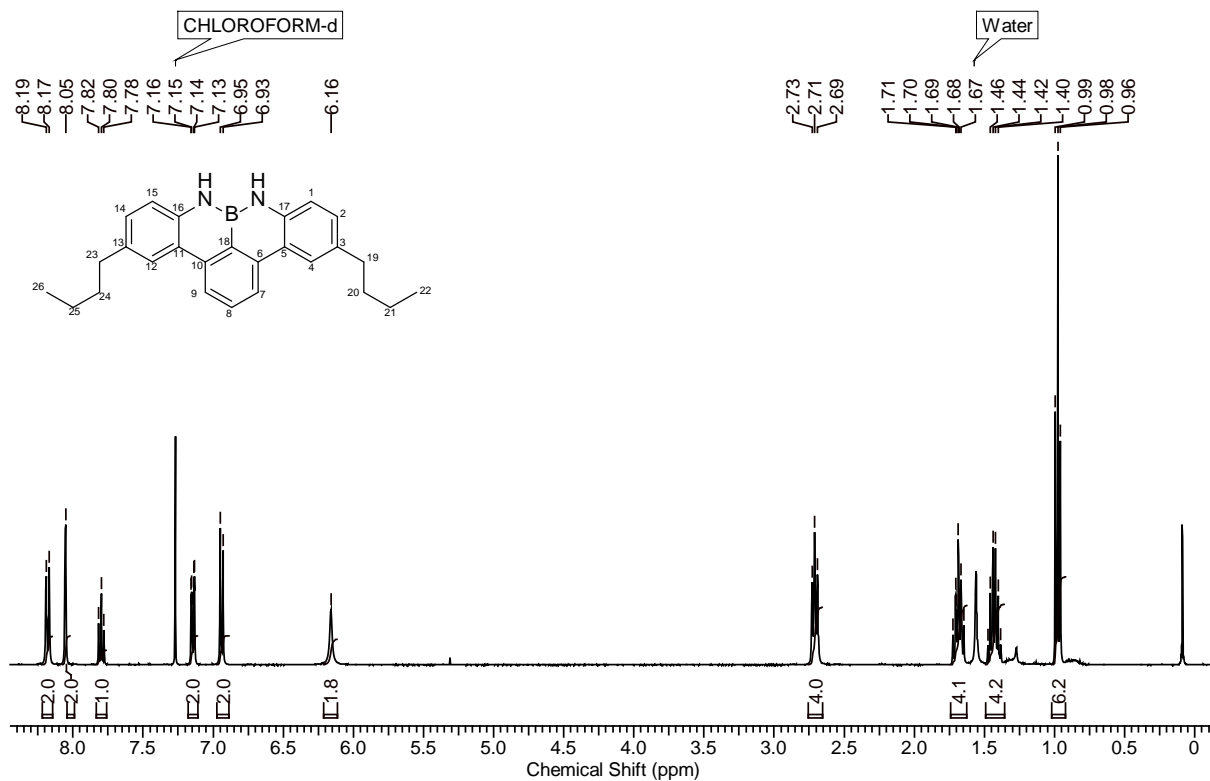


Figure S4: ¹H-NMR of **4** in CDCl₃.

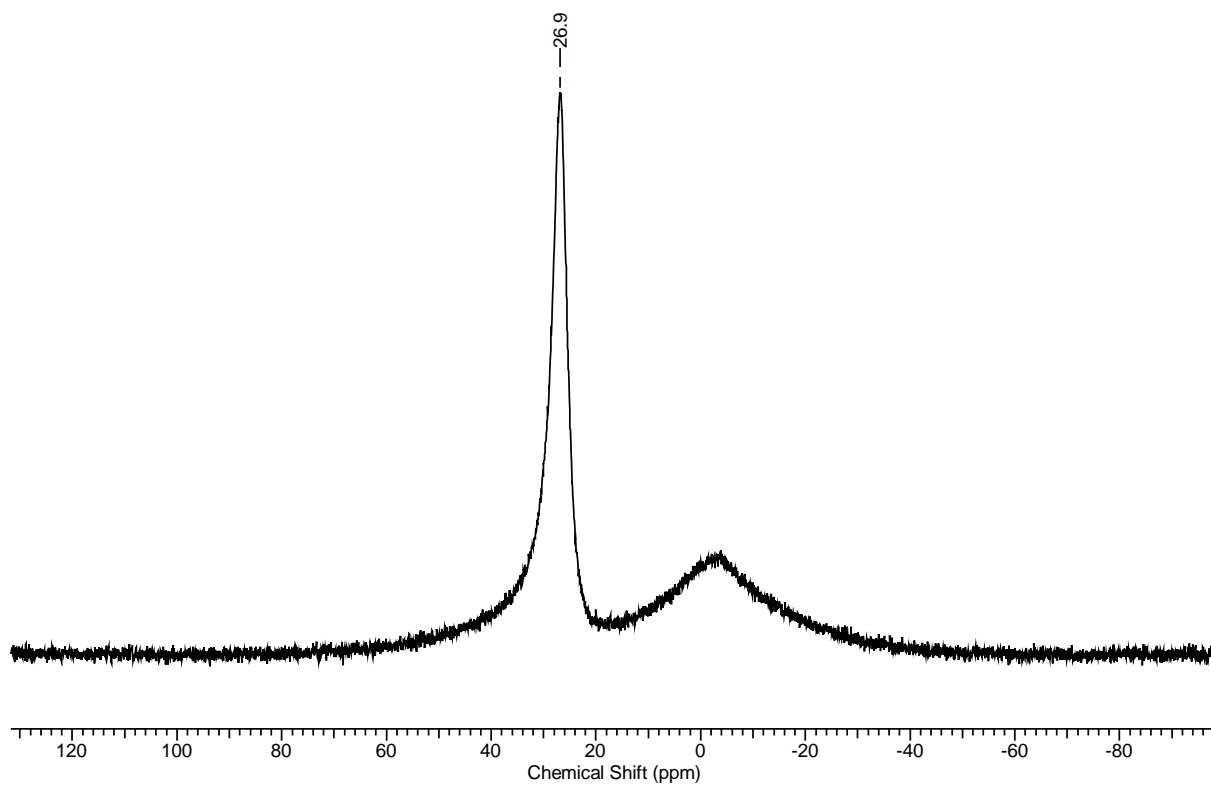


Figure S5: ^{11}B -NMR of **4** in CDCl_3 .

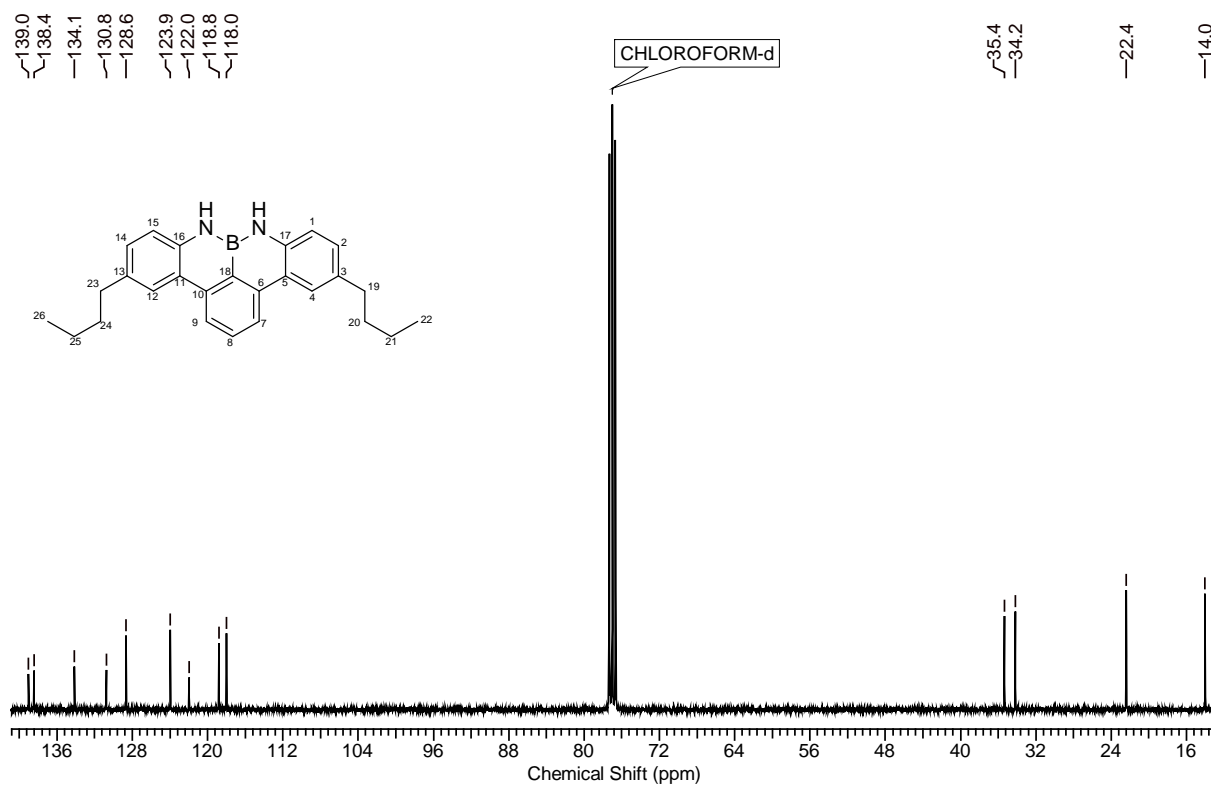


Figure S6: ^{13}C -NMR of **4** in CDCl_3 .

File :D:\MassHunter\GCMS\1\data\Fingerle MF 79_01.D
Operator :
Acquired : 11 Sep 2017 11:33 using AcqMethod EI_30-1000.M
Instrument : MSD 5977
Sample Name: Fingerle MF 79
Misc Info : EI-Quelle; 230°C; 70 eV
Vial Number: 1

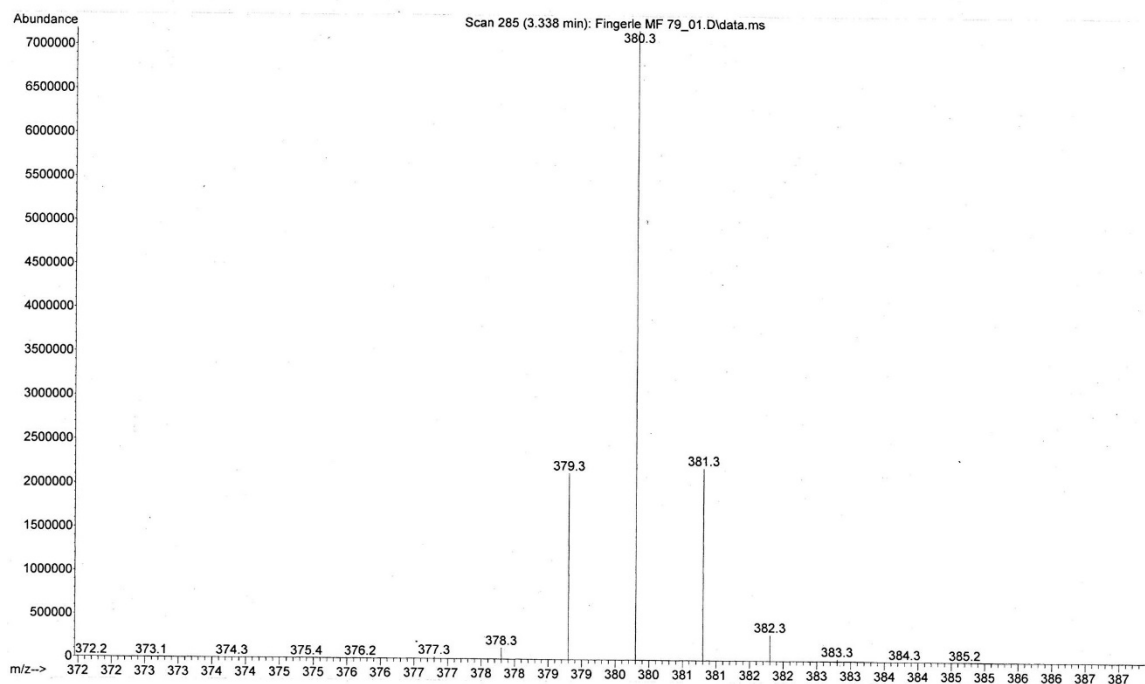


Figure S7: EI mass spectrum of 4.

M a s s e n f e i n b e s t i m m u n g

Name: Fingerle Probenbezeichnung: MF 79

Ionisierungsmethode: EI ..X...

Massenspektrometer: MAT 95 Quelle: 250 °C und 70eV

Referenz - Ion und seine exakte Masse:

$C_9F_{15}^+$ 393 392,97549

die **gefundene exakte Masse** erhält man zu : **380,24263**

damit ergibt/ergeben sich folgende **Elementkombination(en)** :

Measured Mass	Tolerance (mmu)	Charge on Molecule		Min	Max
380.24263	10	1	C	0	40
			[13]C	0	0
			H	0	80
			D	0	0
			N	1	3
			[15]N	0	0
			O	0	0
			F	0	0
			Na	0	0
			Si	0	0
			P	0	0
			S	0	0
			Cl	0	0
			B	1	1

Formula:	RDB	Calc Mass	Deviation mmu
C26H29N2B	14.0	380.241831	0.799

Searched: 6407
Hits: 1

Datum: 12. Sep. 2017

MS - Nummer:

170196

Figure S8: HR-EI of 4

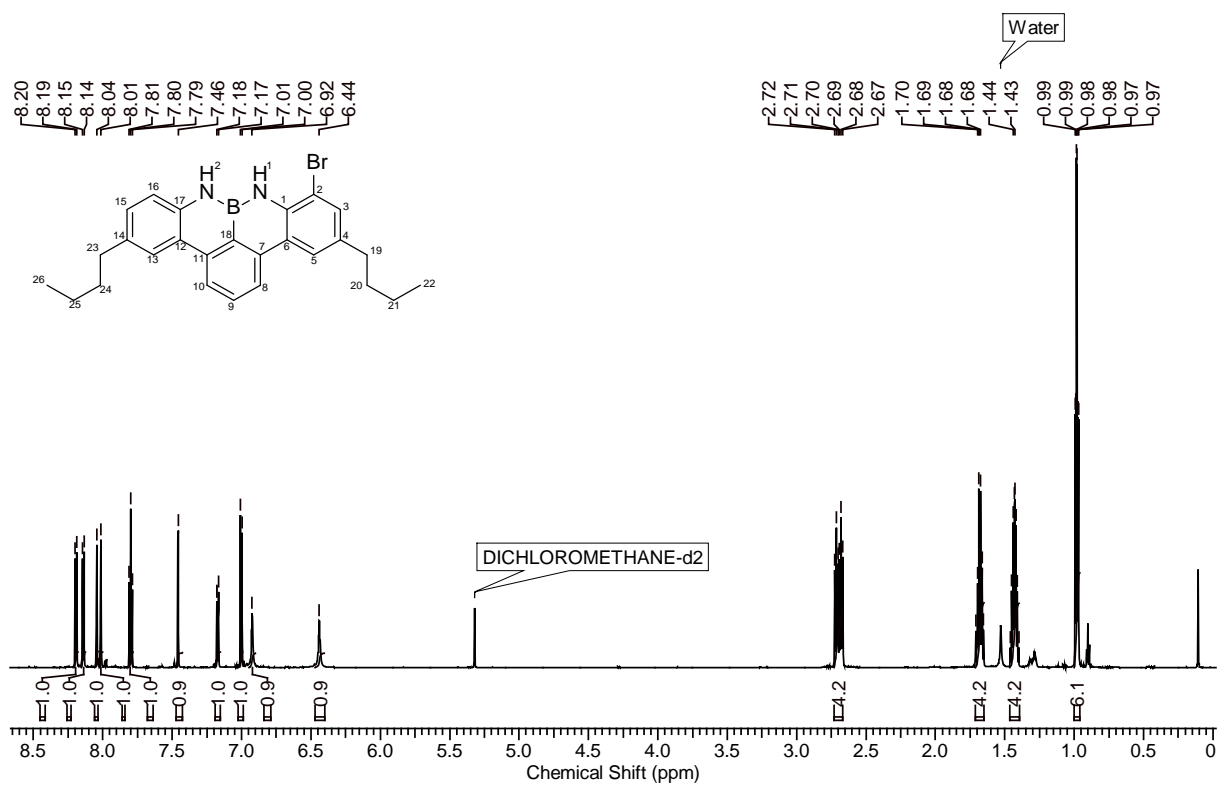


Figure S9: $^1\text{H-NMR}$ of **5** in CD_2Cl_2 .

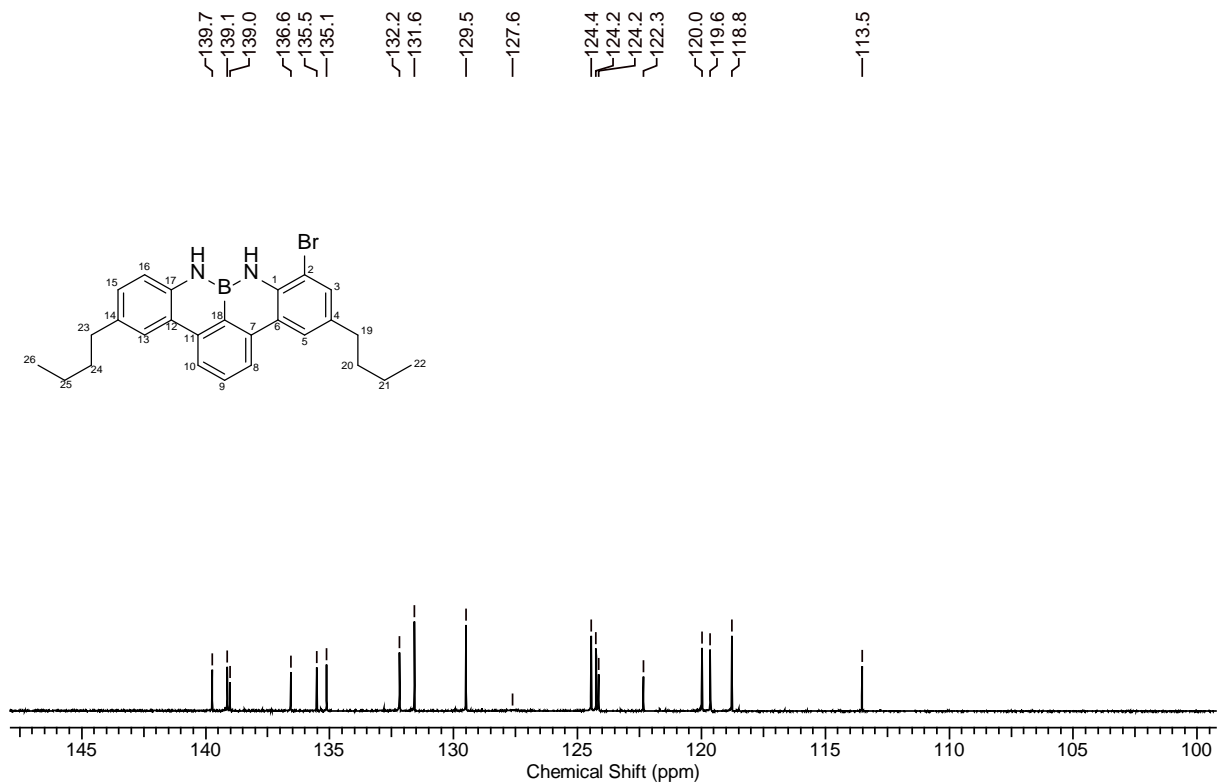


Figure S10: $^{13}\text{C-NMR}$ (aromatic) of **5** in CD_2Cl_2 .

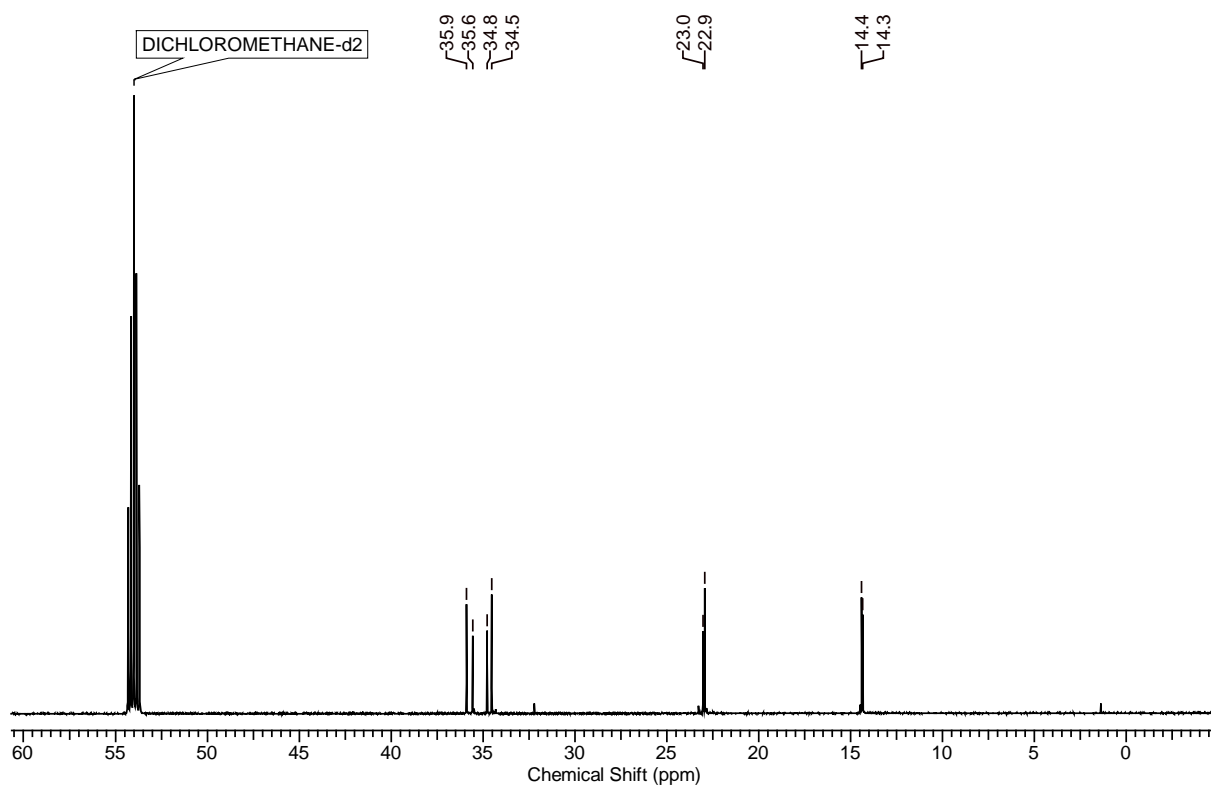


Figure S11: ¹³C-NMR (non-aromatic) of **5** in CD₂Cl₂.

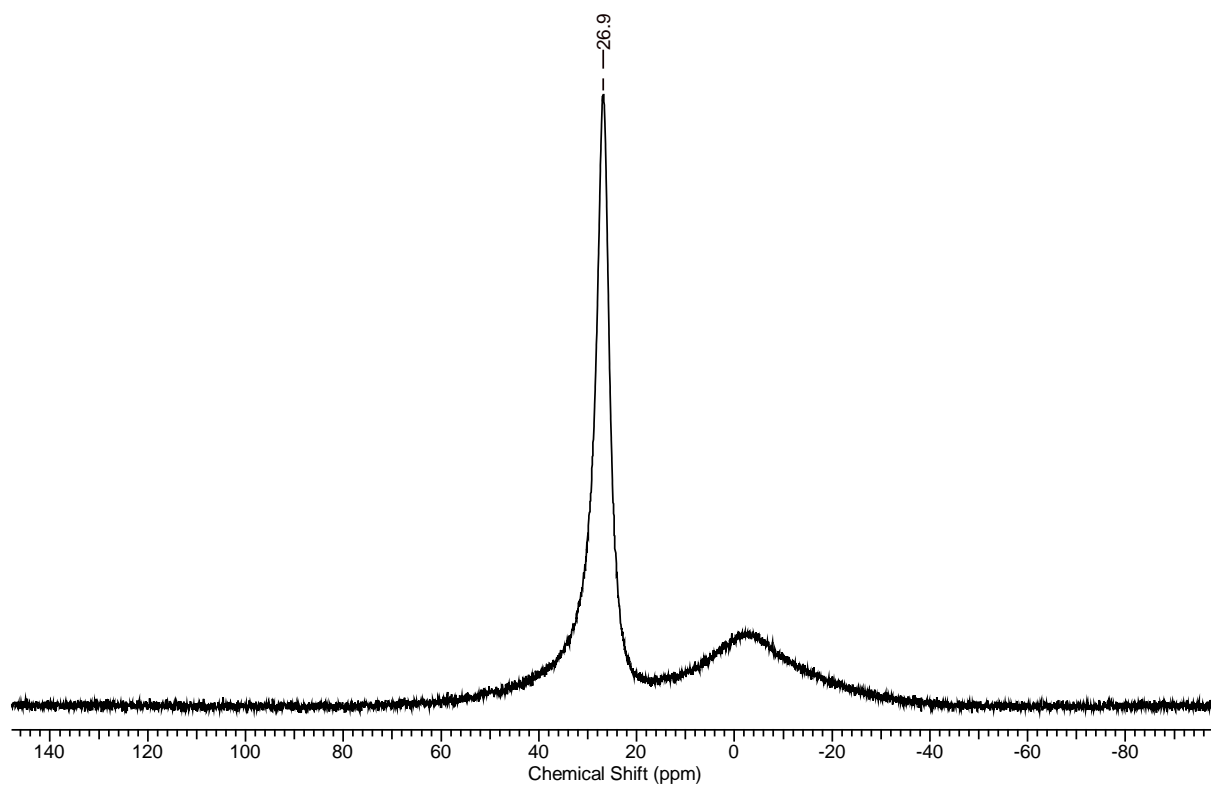


Figure S12: ¹¹B-NMR of **5** in CD₂Cl₂.

File :D:\MassHunter\GCMS\1\data\Fingerle MF 134_1.D
Operator :
Acquired : 04 Dec 2018 12:07 using AcqMethod DIP_EI_CI_source_230.M
Instrument : MSD 5977
Sample Name: Fingerle MF 134
Misc Info : EI mit CI Source; 230°C
Vial Number: 1

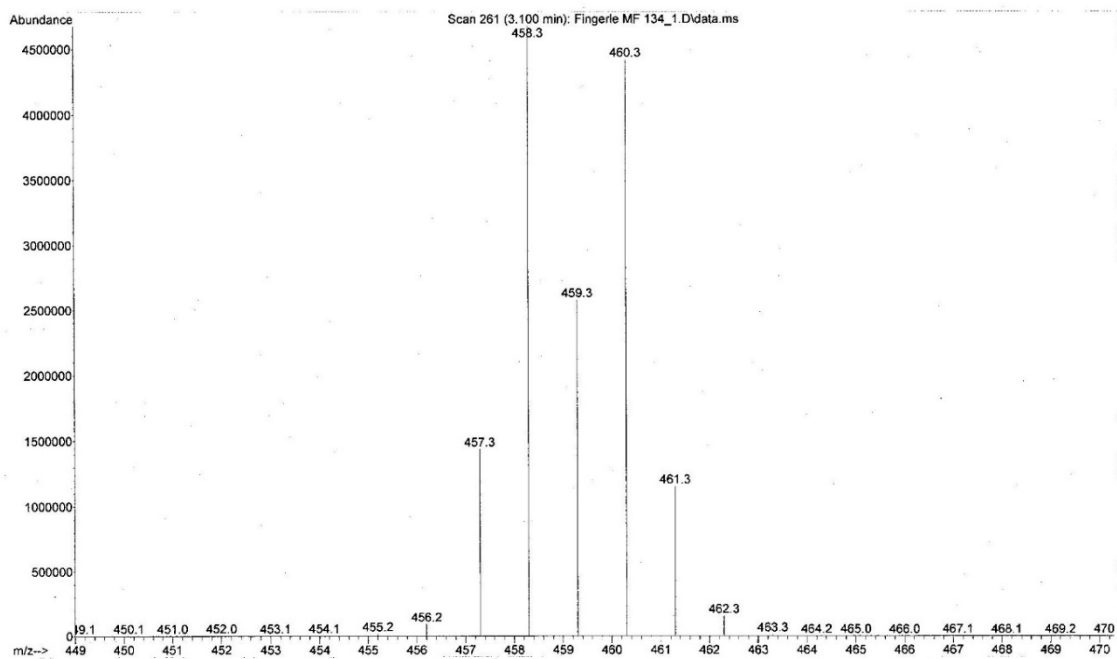


Figure S13: EI mass spectrum of **5**.

M a s s e n f e i n b e s t i m m u n g

Name: Fingerle Probenbezeichnung: MF 134

Ionisierungsmethode: EI ..X... FAB

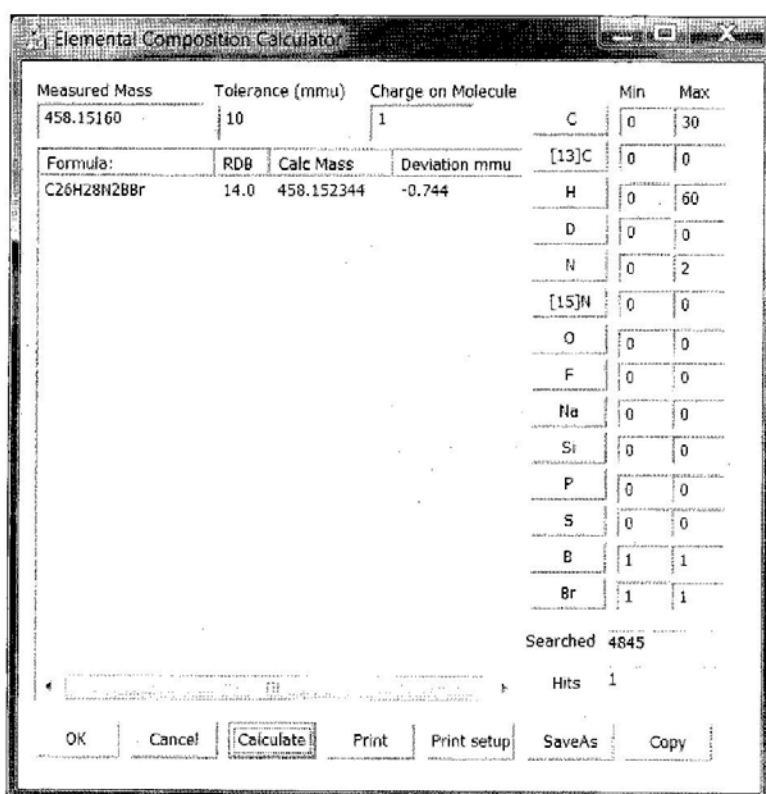
Massenspektrometer: MAT 95

Referenz - Ion und seine **exakte Masse**:

$C_9F_{18}N^+$ 464 463,97376

die **gefundene exakte Masse** erhält man zu: 458,15160

damit ergibt/ergeben sich folgende **Elementkombination(en)** :



Datum: 10. Dez. 2018

MS - Nummer:

180290

Figure S14: HR-EI of 5.

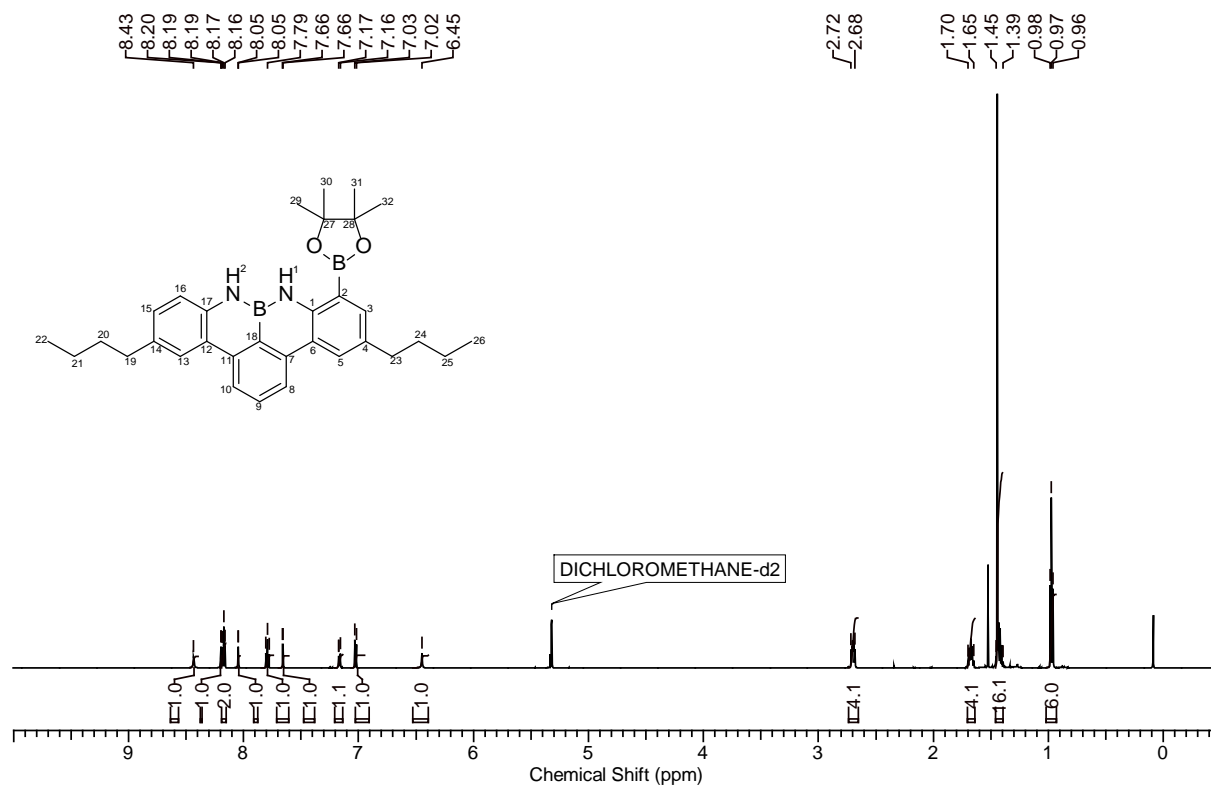


Figure S15: $^1\text{H-NMR}$ of **6** in CD_2Cl_2 .

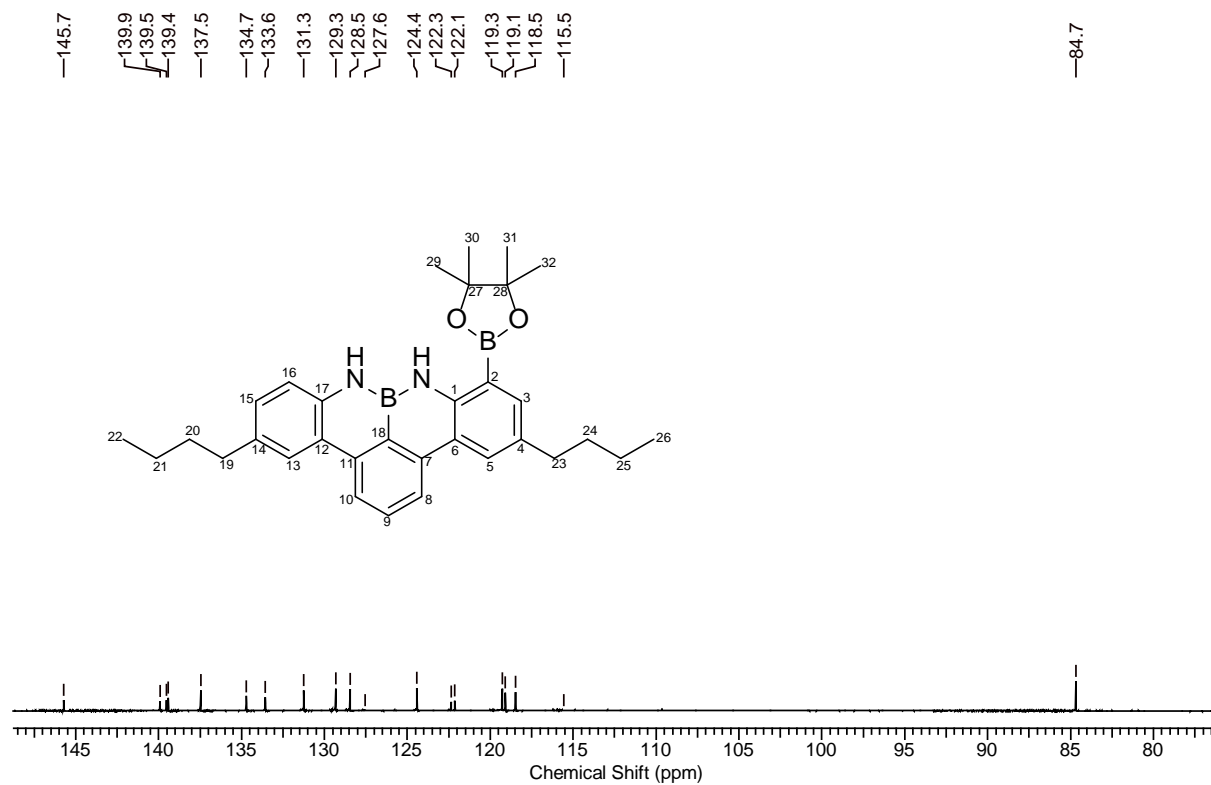


Figure S16: $^{13}\text{C-NMR}$ (aromatic) of **6** in CD_2Cl_2 .

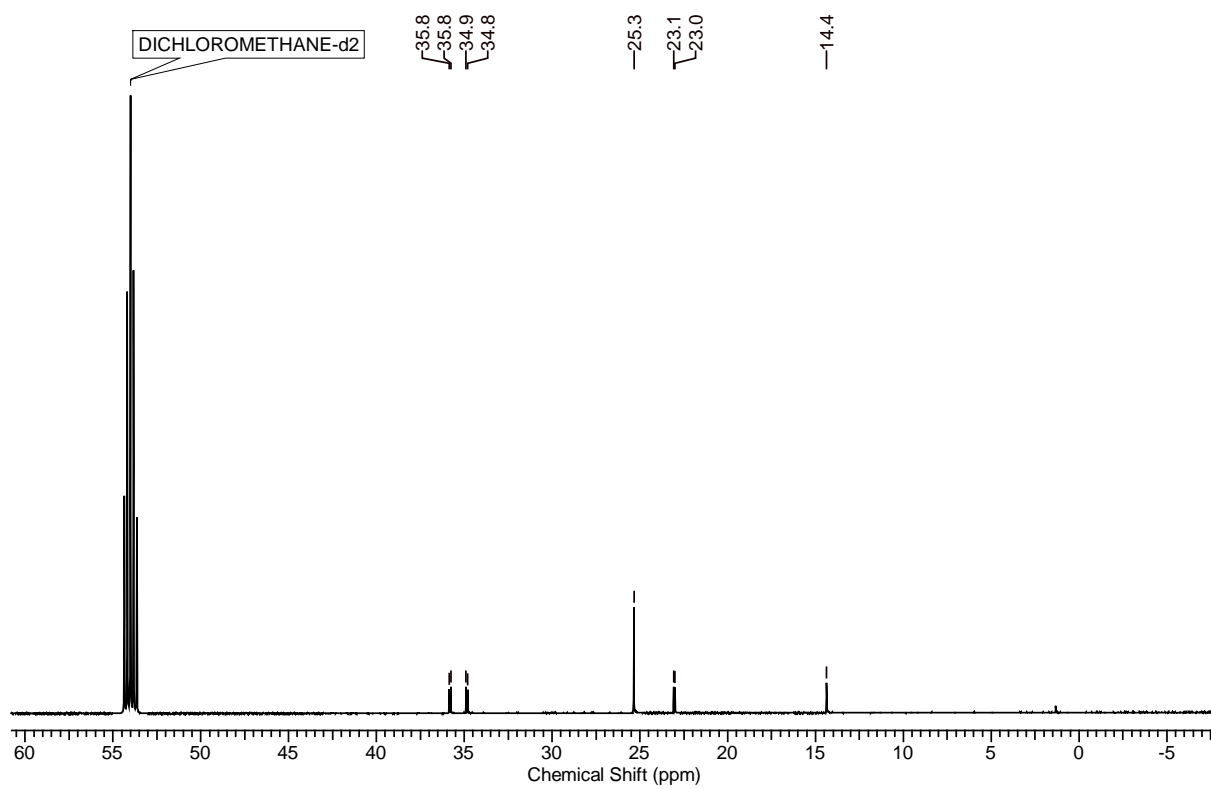


Figure S17: ¹³C-NMR (non-aromatic) of **6** in CD₂Cl₂.

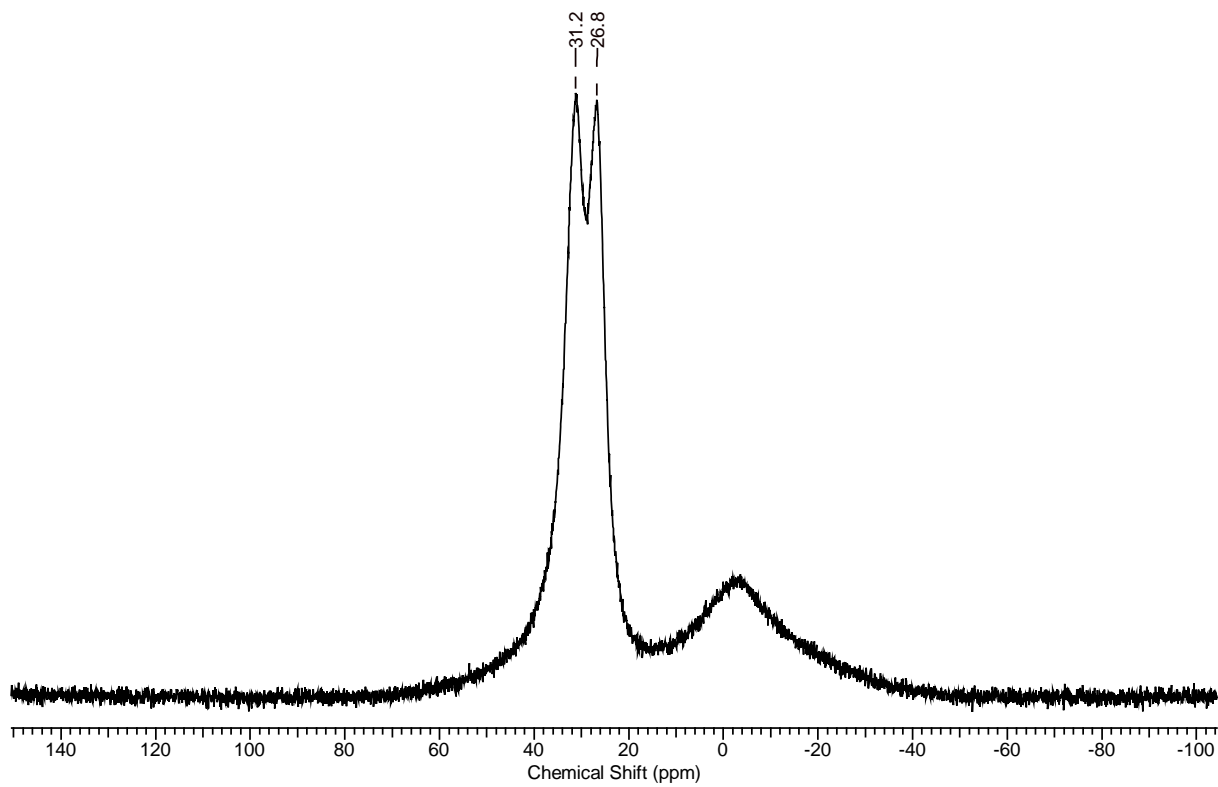


Figure S18: ¹¹B-NMR of **6** in CD₂Cl₂.

File :D:\MassHunter\GCMS\1\data\Fingerle MF146_1.D
Operator :
Acquired : 08 Apr 2019 16:28 using AcqMethod EI_30-1000_B_M
Instrument : MSD 5977
Sample Name: Fingerle MF146
Misc Info : EI-Source; 230°C; 70 eV
Vial Number: 1

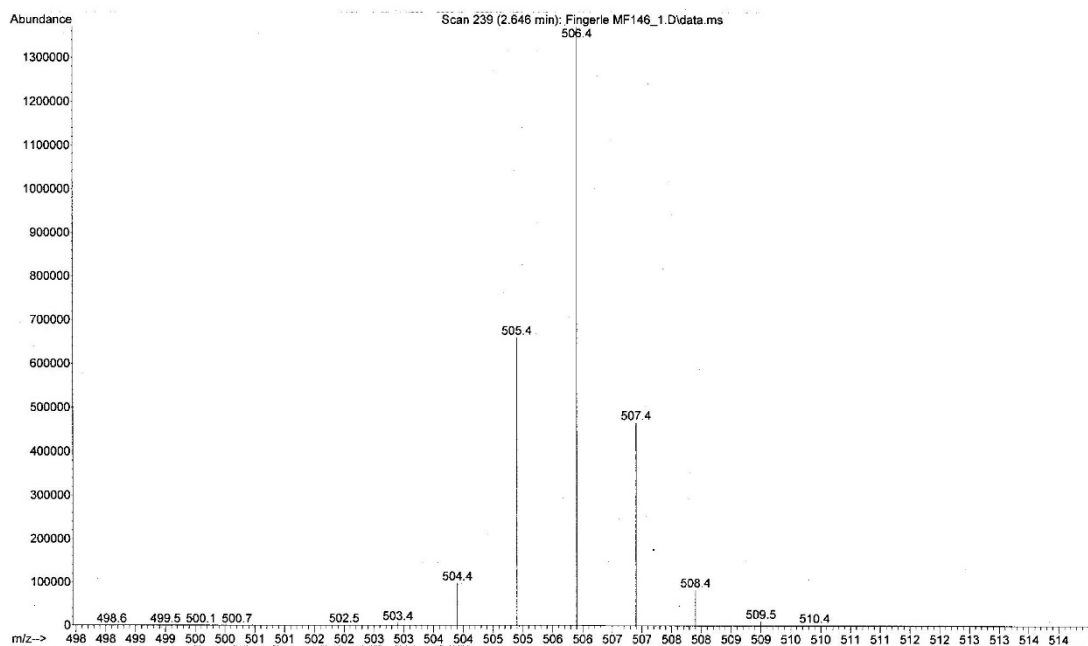


Figure S19: EI mass spectrum of **6**.

M a s s e n f e i n b e s t i m m u n g

Name: Fingerle Probenbezeichnung: MF 146

Ionisierungsmethode: EI ..X... FAB

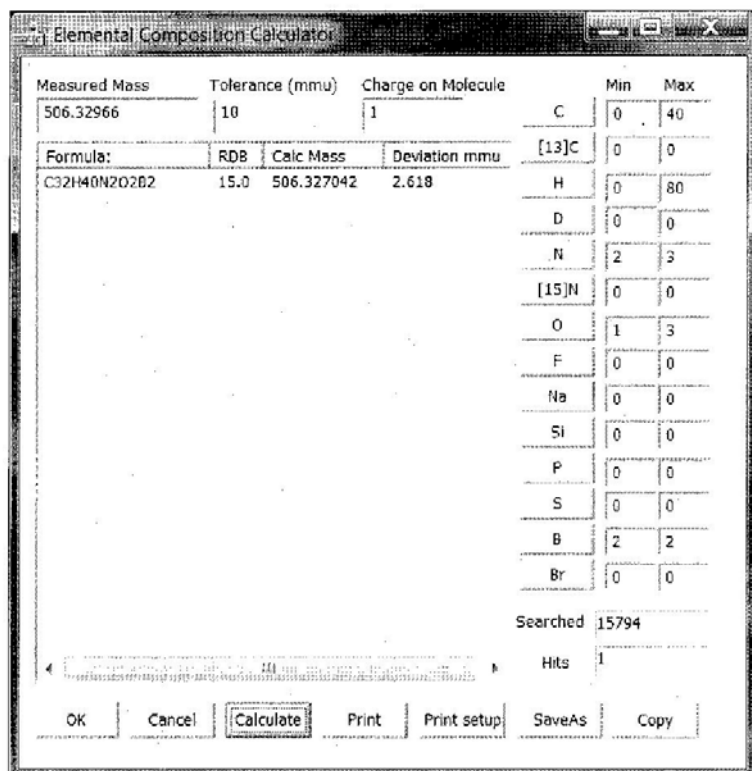
Massenspektrometer: MAT 95

Referenz - Ion und seine **exakte Masse**:

$C_9F_{20}N^+$ 502 501,97057

die **gefundene exakte Masse** erhält man zu: 506,32966

damit ergibt/ergeben sich folgende **Elementkombination(en)** :



Datum: 10. April 2019

MS - Nummer: 190199

Figure S20: HR-EI of 6.

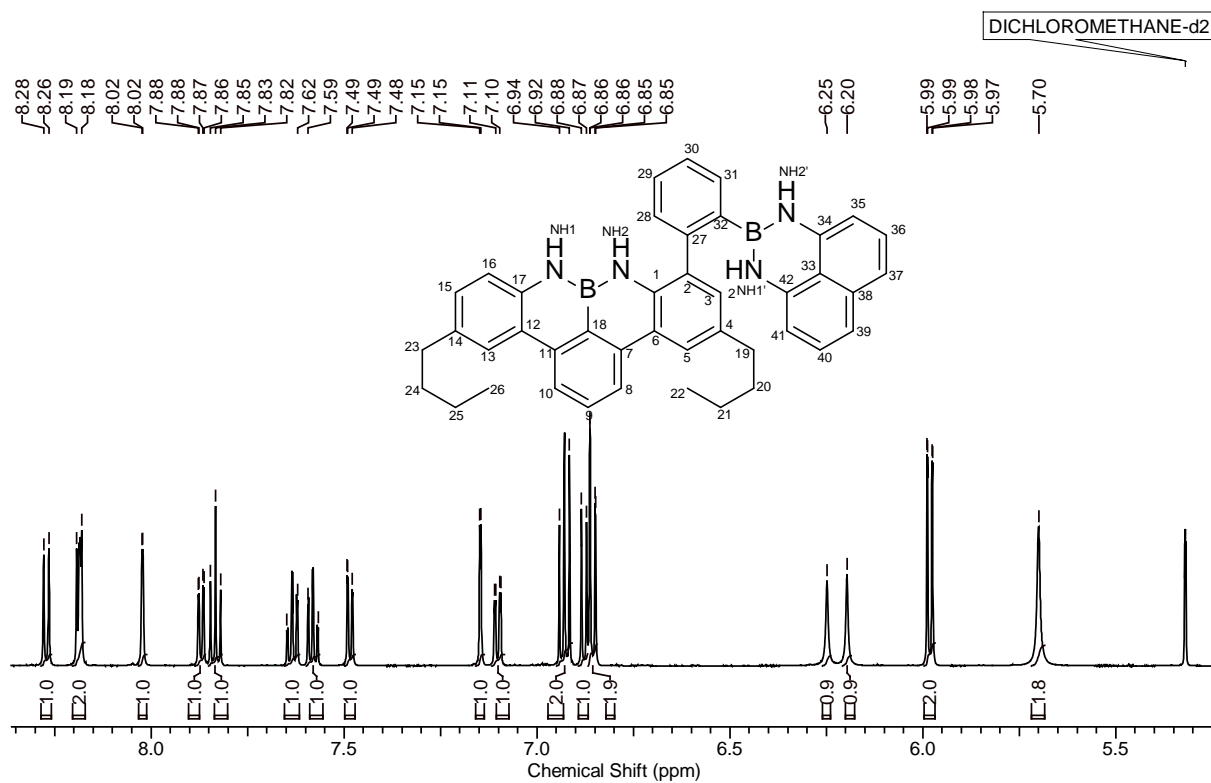


Figure S21: ¹H-NMR (aromatic) of **7** in CD₂Cl₂.

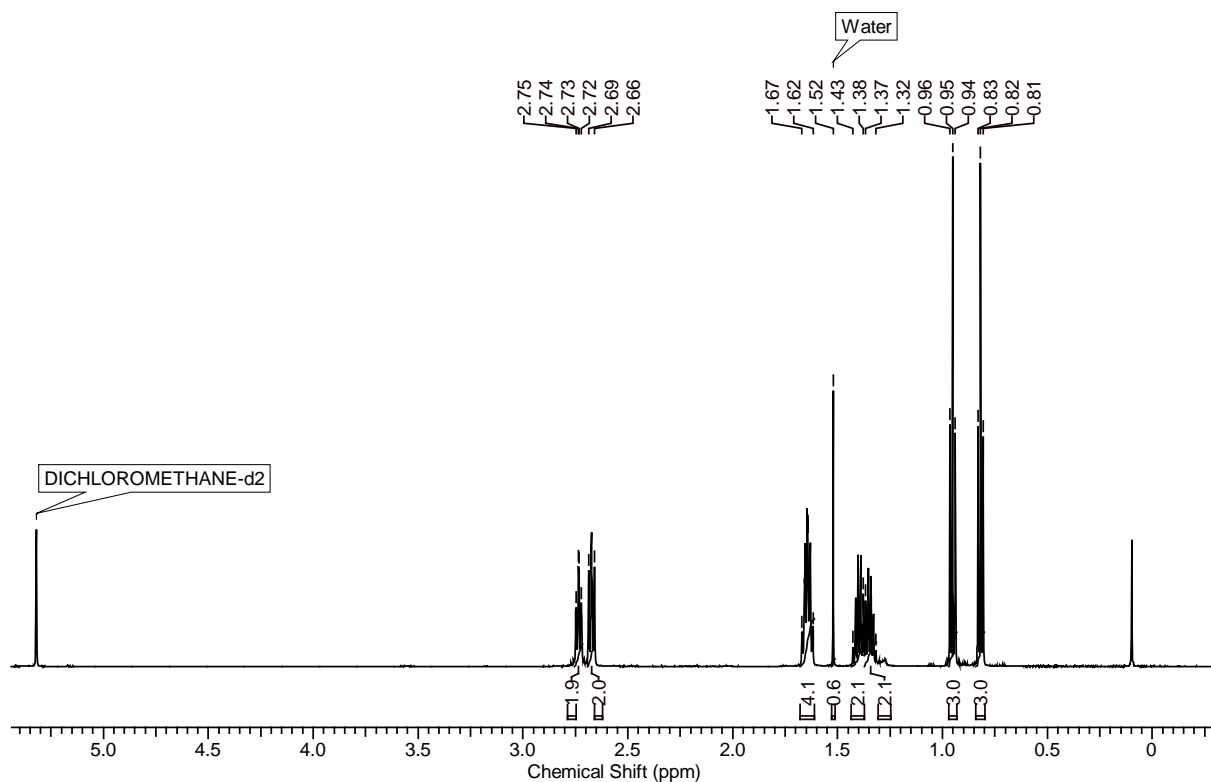


Figure S22: ¹H-NMR (non-aromatic) of **7** in CD₂Cl₂.

—143.7
 —141.5
 —139.7
 —139.6
 —139.0
 —136.7
 —134.8
 —134.4
 —133.9
 —131.6
 —131.5
 —131.3
 —131.0
 —130.3
 —129.3
 —128.3
 —128.0
 —124.4
 —122.8
 —122.2
 —120.0
 —119.7
 —119.5
 —118.5
 —117.8

—106.2

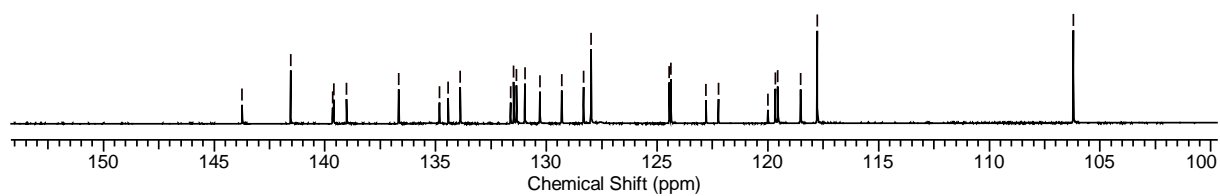
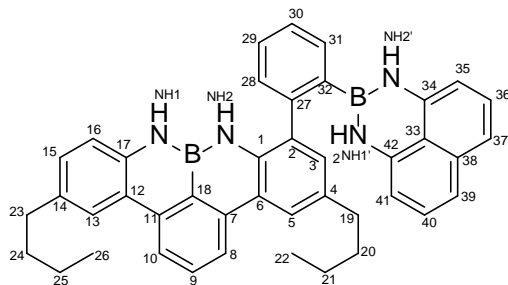


Figure S23: ^{13}C -NMR (aromatic) of **7** in CD_2Cl_2 .

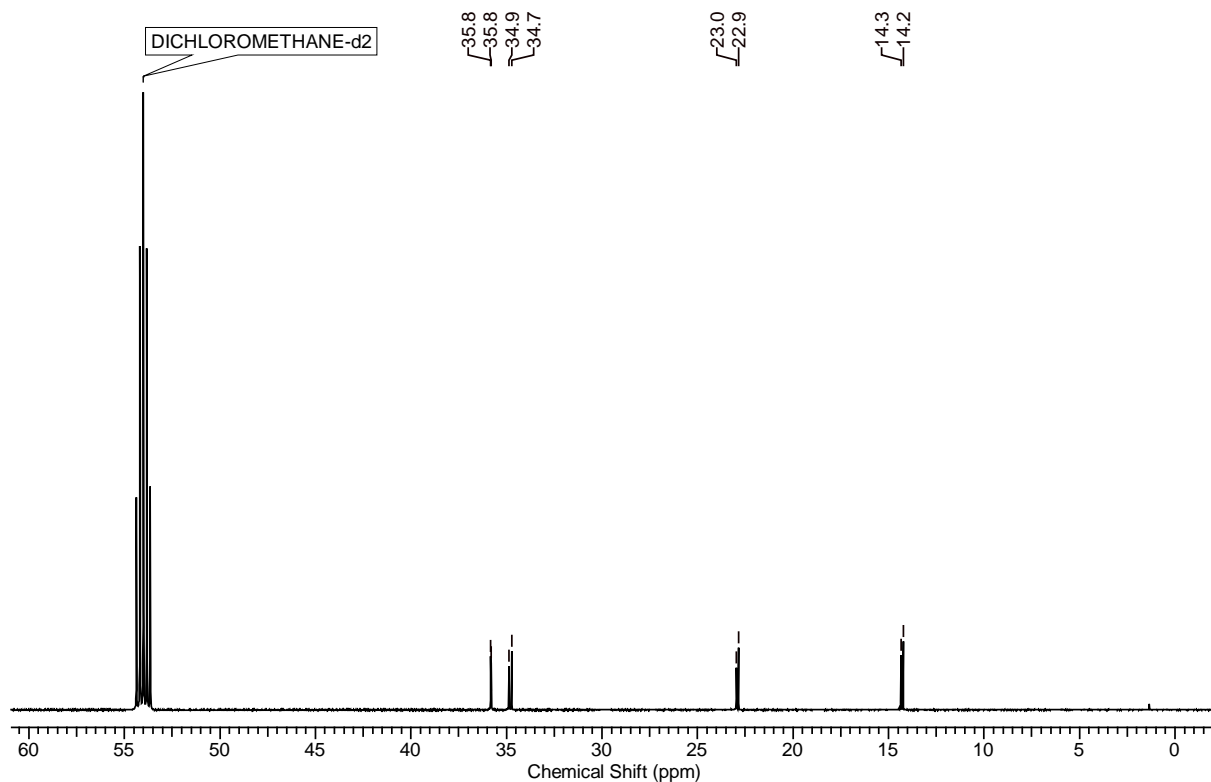


Figure S24: ^{13}C -NMR (non-aromatic) of **7** in CD_2Cl_2 .

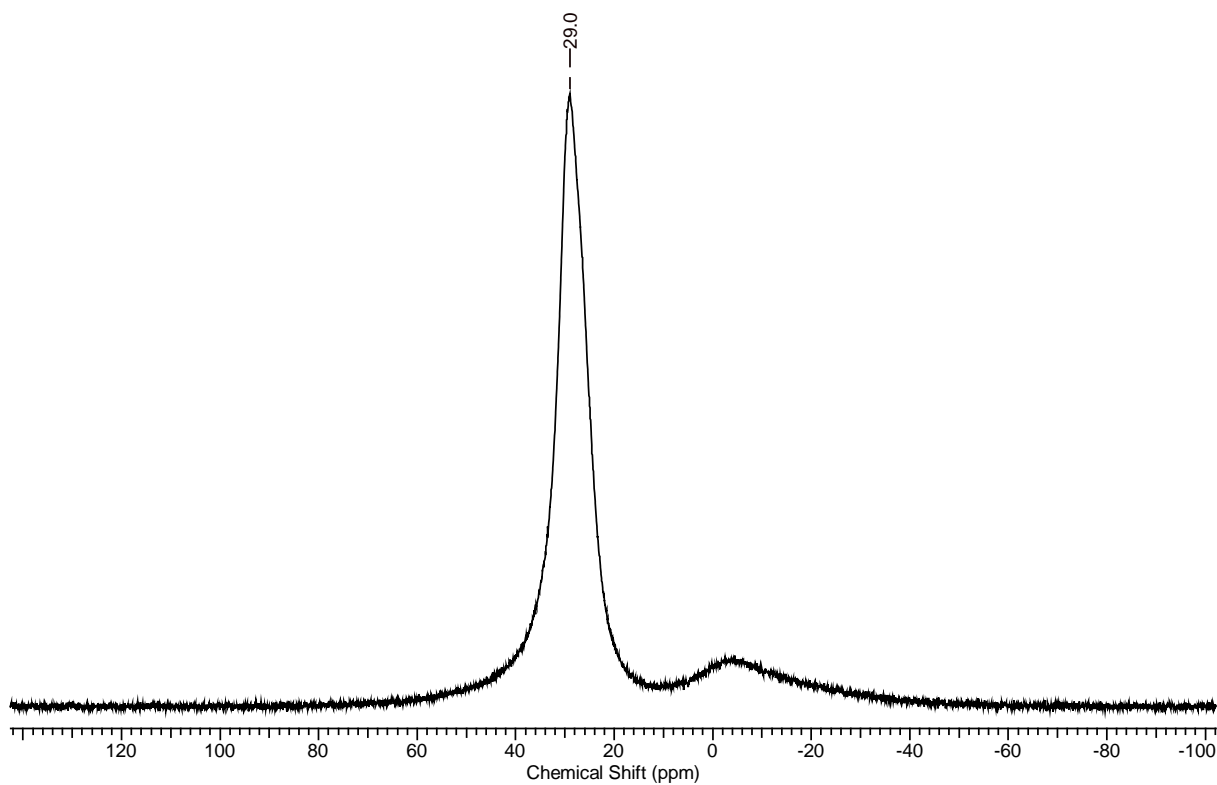


Figure S25: ^{11}B -NMR of **7** in CD_2Cl_2 .

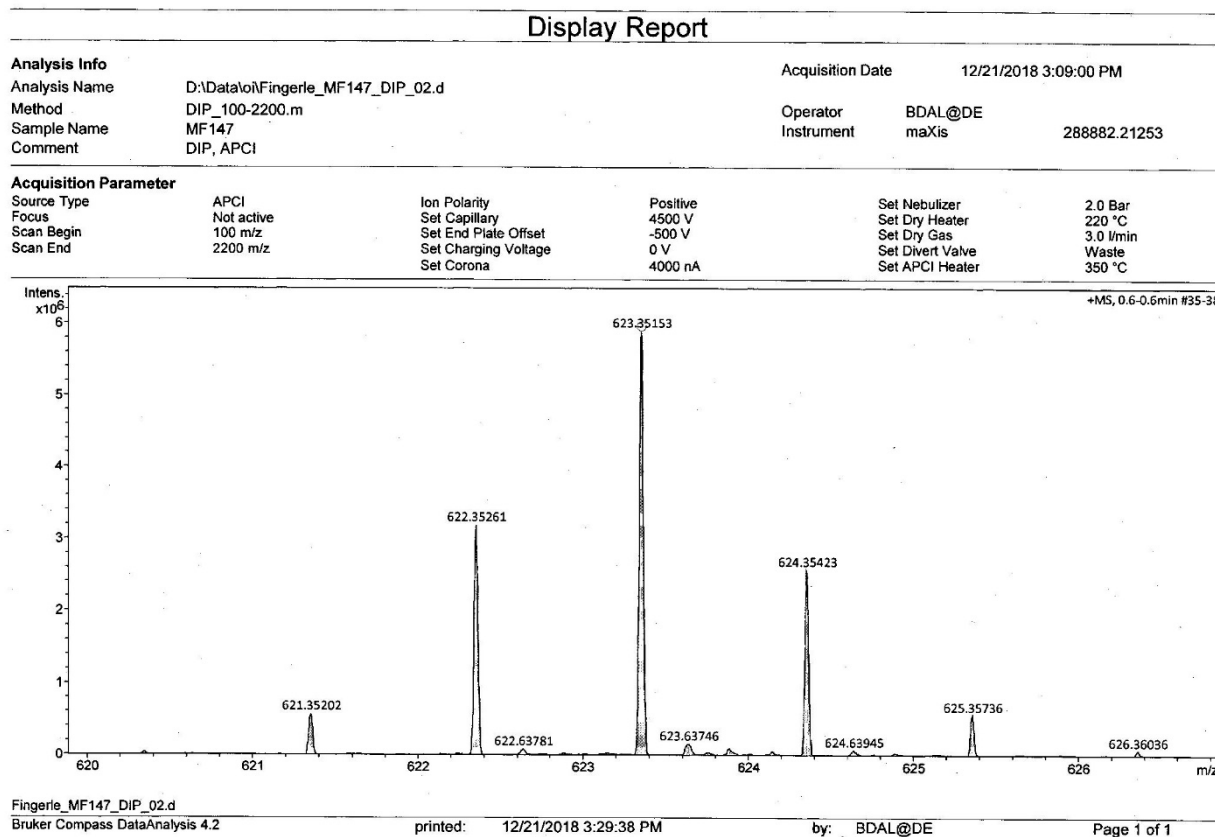


Figure S26: HR-APCI mass spectrum of **7**.

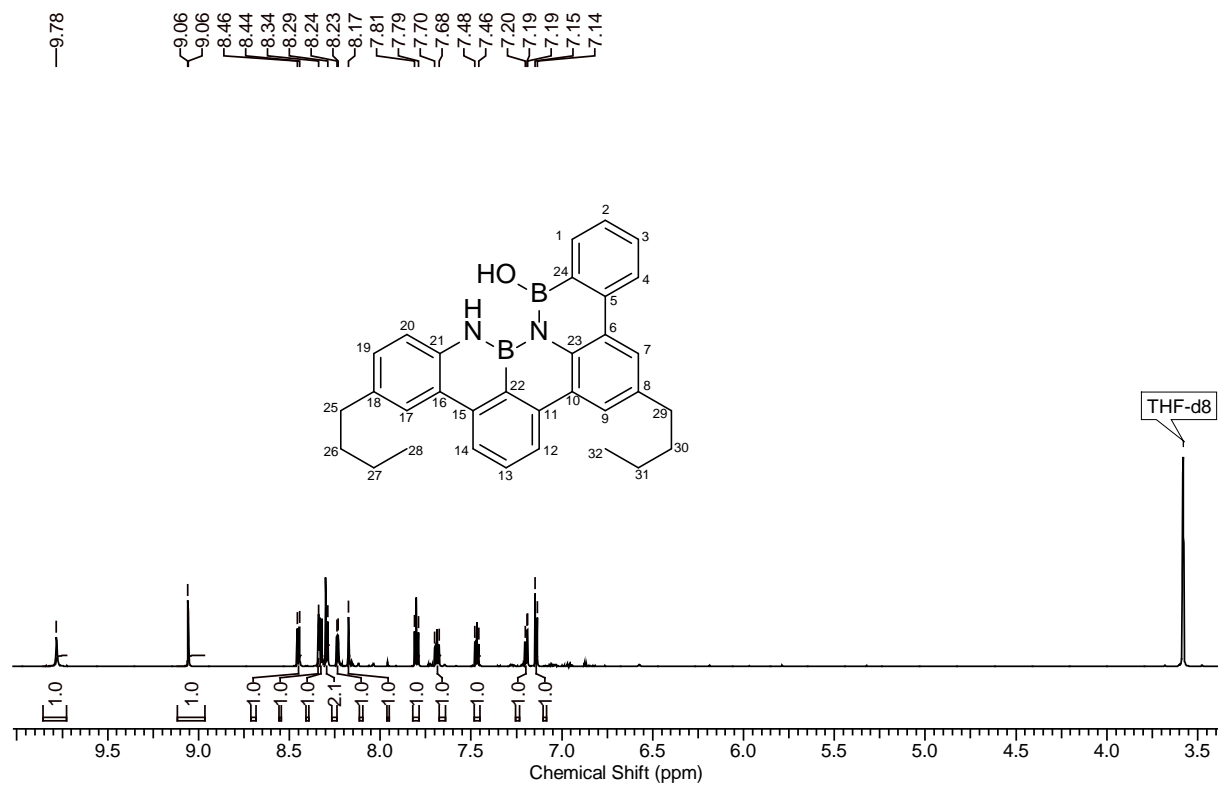


Figure S27: $^1\text{H-NMR}$ (aromatic) of **8** in thf-d_8 .

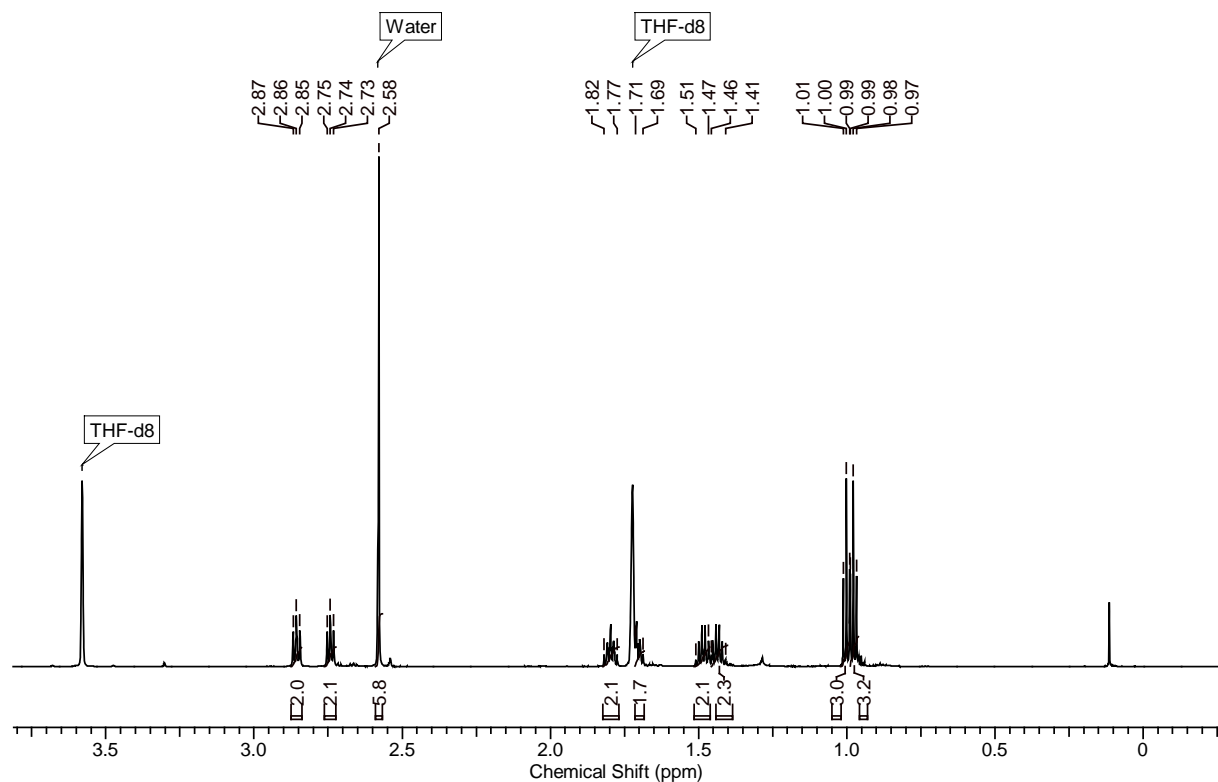


Figure S28: $^1\text{H-NMR}$ (non-aromatic) of **8** in thf-d_8 .

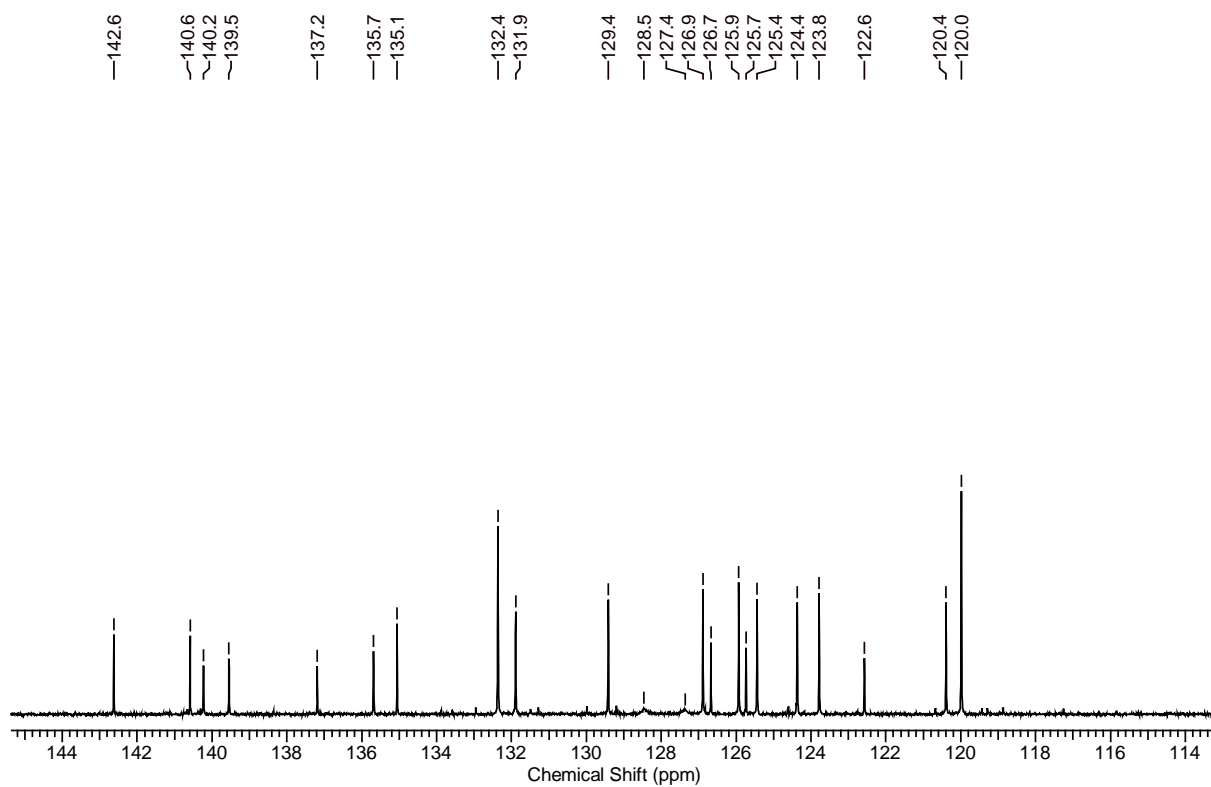


Figure S29: ^{13}C -NMR (aromatic) of **8** in thf-d_8 .

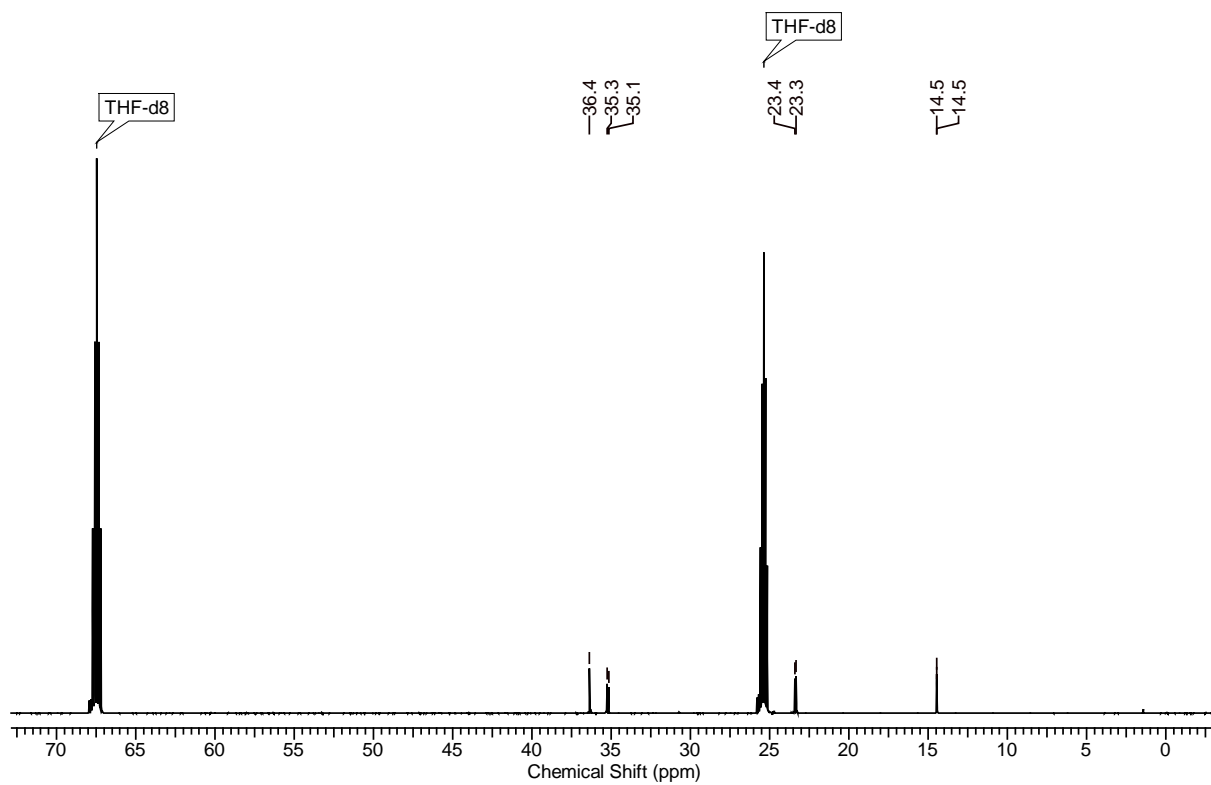


Figure S30: ^{13}C -NMR (non-aromatic) of **8** in thf-d_8 .

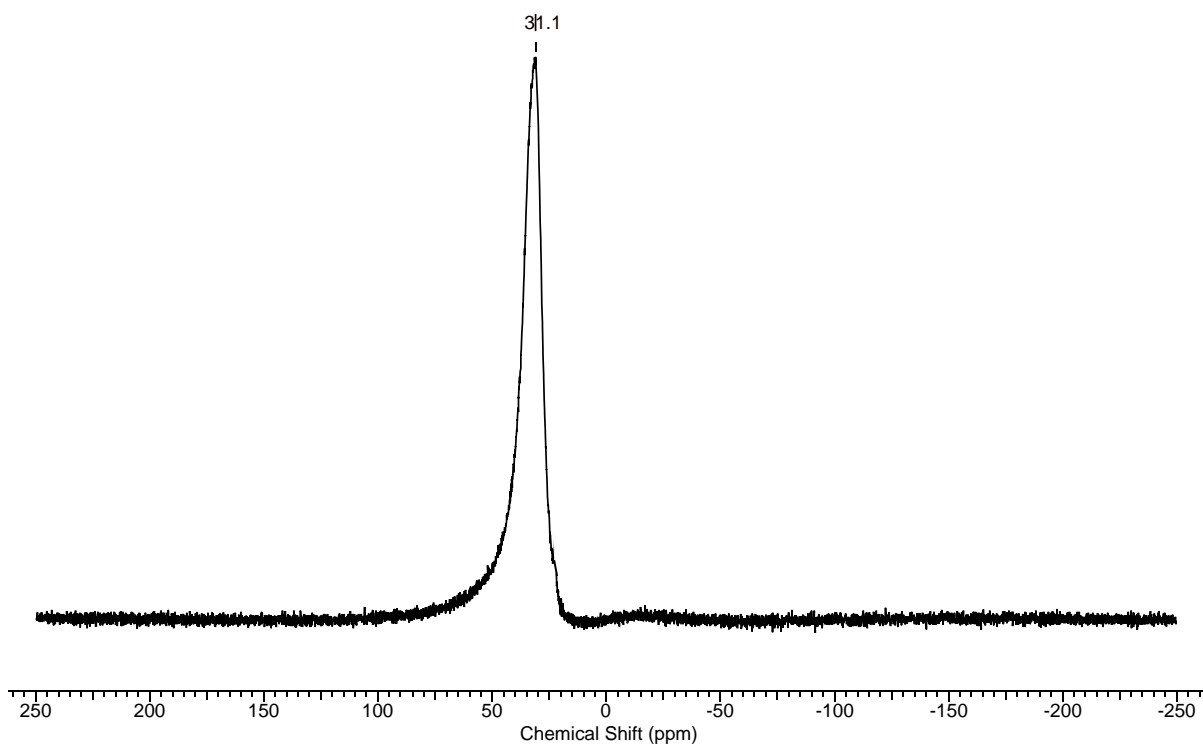


Figure S31: ^{11}B -NMR of **8** in thf-d_8 .

File :D:\MassHunter\GCMS\1\data\Fingerle MF 149_1.D
Operator :
Acquired : 07 Mar 2019 08:35 using AcqMethod EI_30-1000_B_M
Instrument : MSD 5977
Sample Name: Fingerle MF 149
Misc Info : EI-Quelle 230°C
Vial Number: 1

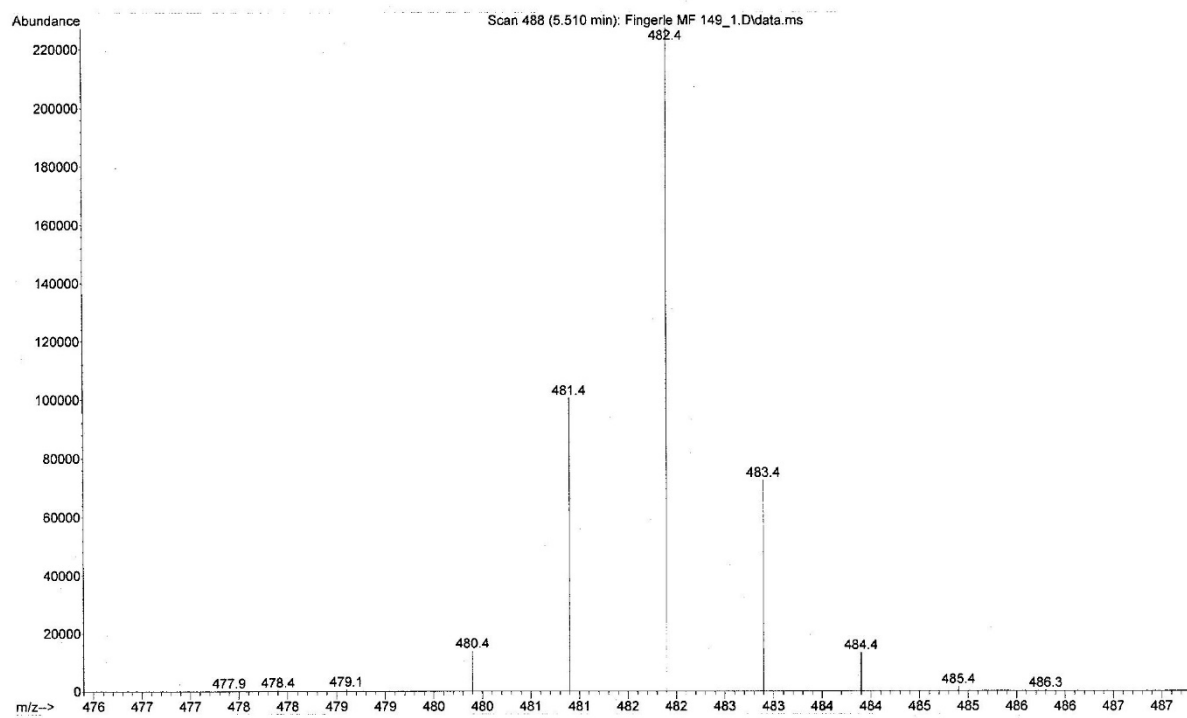


Figure S32: EI mass spectrum of **8**.

M a s s e n f e i n b e s t i m m u n g

Name: Fingerle Probenbezeichnung: MF 149

Ionisierungsmethode: EI ..X... FAB

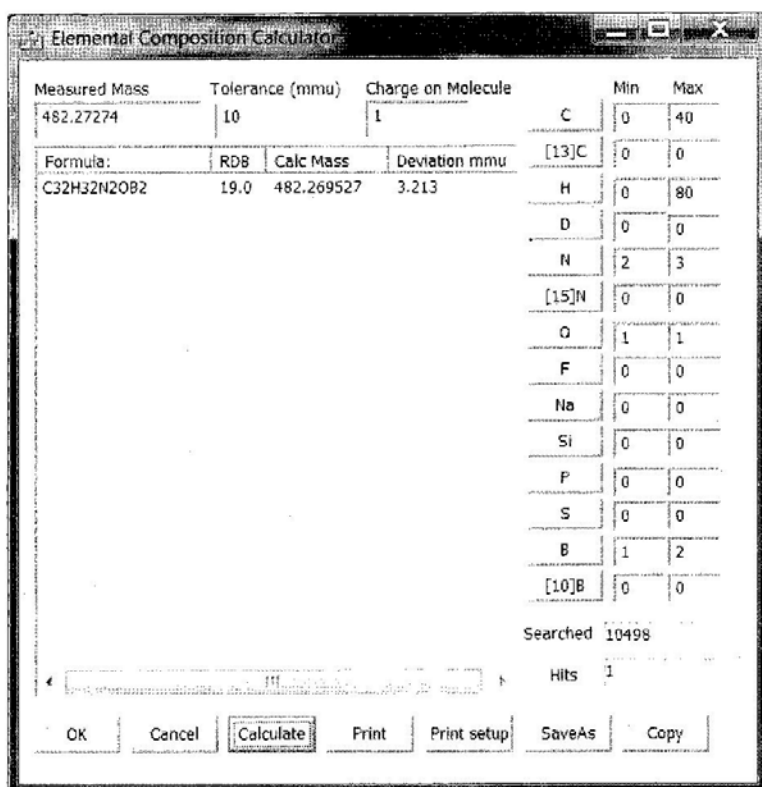
Massenspektrometer: MAT 95

Referenz - Ion und seine exakte Masse:

$C_9F_{20}N^+$ 502 501,97057

die gefundene exakte Masse erhält man zu: 482,27274

damit ergibt/ergeben sich folgende Elementkombination(en) :



Datum: 07. März 2019

MS - Nummer: 190069

Figure S33: HR-EI of 8.


 Cite this: *Chem. Commun.*, 2020, 56, 3847

 Received 17th January 2020,
Accepted 6th February 2020

DOI: 10.1039/d0cc00471e

rsc.li/chemcomm

Embedding a boroxazine ring into a nanographene scaffold by a concise bottom-up synthetic strategy†

 Michael Fingerle and Holger F. Bettinger *

Embedding a boroxazine (B₃N₂O) heterocycle by a *m*-quinquephenyl scaffold renders a B/N/O substituted nanographene molecule. The target compound can be synthesized in four steps and in good overall yield. The incorporation of a boroxazine core modifies the electronic structure and results in high fluorescence quantum yield.

Polycyclic aromatic hydrocarbons (PAHs) are indispensable active materials in organic electronic devices.^{1,2} A strategy to modify the electronic properties of a given PAH scaffold without compromising favorable structural and intermolecular packing properties is the exchange of carbon atoms by heteroatoms.³ Depending on their position in the periodic table, such modifications can result in “hole” or “electron” doping of the PAH. The pairwise exchange of carbon atoms by isoelectronic and isosteric boron–nitrogen (BN) couples received particular attention.^{4–11} Indeed, boron–nitrogen containing PAHs, in particular those with a 1,4-azaborine motif,^{12–22} have been identified as promising materials for OLED applications.^{23–33}

Interestingly, the quite unusual boroxazine (oxadiazatriborine) heterocycle (Fig. 1) also attracted attention in the context of OLED applications.³⁴ However, robust syntheses of this hybrid of borazine and boroxin heterocycles (Fig. 1) have not been reported. After early mass spectroscopic evidence of the existence of the boroxazine ring system,³⁵ Meller *et al.*^{36–38} observed formation of derivatives that could however not be separated from by-products. A targeted synthesis was described later by Niedenzu *et al.*,³⁹ while structural characterization of the parent (obtained as a mixture with the dioxazatriborine B₃NO₂ ring) was achieved by microwave spectroscopy.⁴⁰

Challenges for possible applications of boroxazines are developing scalable and efficient syntheses, as stressed by Morgan and Piers in the context of BN-PAHs,⁸ and ensuring

hydrolytic stability of the heterocycle. Previous experience with borazine substituted hexa-*peri*-hexabenzocoronene (BN-HBC)^{41,42} suggests that the incorporation of the boroxazine core into a stiff nanographene scaffold would stabilize the otherwise readily hydrolyzed heterocycle.

Herein, we describe the concise synthesis and characterization of a nanographene molecule **A** that features a central B₃N₂O ring and show that the resulting heteroatom doped nanographene displays interesting photophysical properties (Scheme 1).

We started the synthesis from a recently published NBN-benzotetracene motif **1** that carries two *n*-butyl groups for enhanced solubility.⁴³ During the last years, such NBN-benzotetracenes have received interest as scaffolds for further synthetic elaboration and as organic materials.^{44–47} In a first step, a two-fold electrophilic aromatic bromination of **1** with NBS was carried out at the positions ortho to the nitrogen atoms in yields of 80%. As the conversion with NBS is slow and incomplete, unreacted **1** and the product of single bromination⁴³ have to be separated by column chromatography.

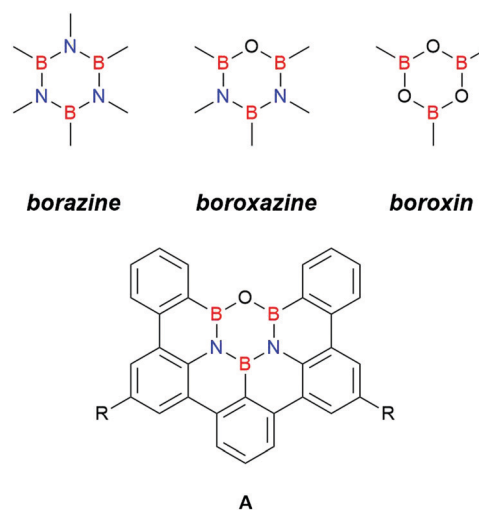
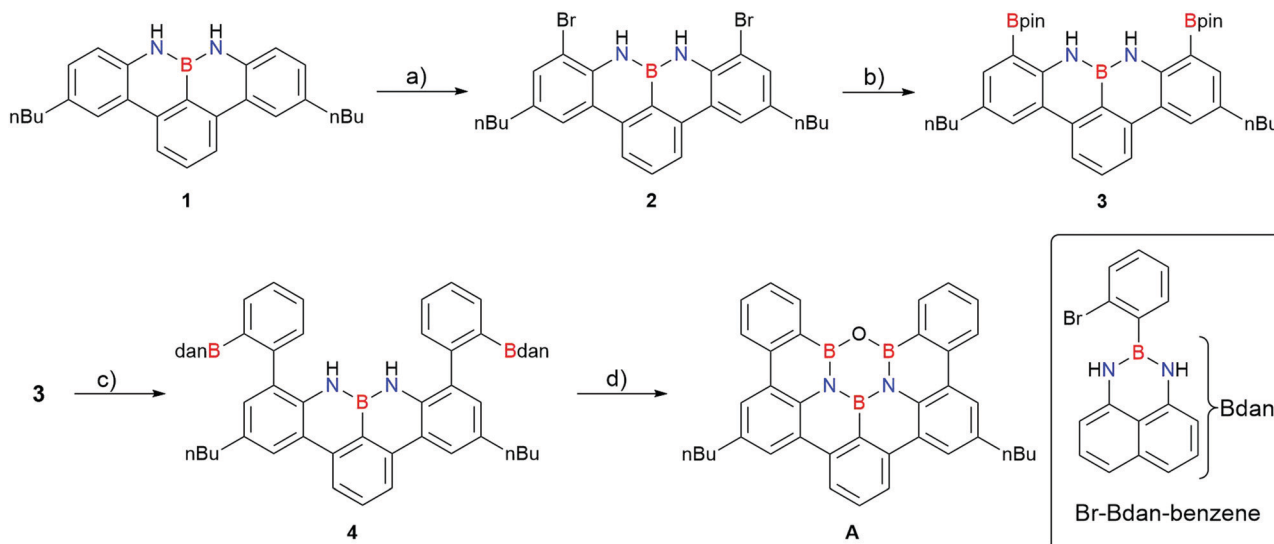


Fig. 1 The B/N/O containing heterocycles and the target compound **A** (R = *n*Bu).

Institut für Organische Chemie, Auf der Morgenstelle 18, 72076 Tübingen, Germany. E-mail: holger.bettinger@uni-tuebingen.de

† Electronic supplementary information (ESI) available: Synthesis protocols and spectra, computational details, and Cartesian coordinates. See DOI: 10.1039/d0cc00471e



Scheme 1 Synthesis sequence of the B_3N_2O PAHs; (a) 1 equiv. **1**, 2 equiv. NBS, mixture of dichloromethane, chloroform, acetonitrile, RT, 18 h, 80%; (b) 1 equiv. **2**, 5 equiv. B_2Pin_2 , 12 equiv. KOAc, 0.1 equiv. $Pd(dppf)Cl_2$, dioxane, 90 °C, 18 h, 68%; (c) 1 equiv. **3**, 2.5 equiv. Br-Bdan-benzene, 10 equiv. K_2CO_3 , 0.1 equiv. $Pd(PPh_3)_4$, mixture of toluene, ethanol, water, reflux, 18 h, 70%; (d) 1 equiv. **4**, 48 equiv. H_2SO_4 (2 M in H_2O), thf, 50 °C, 3 d, 90%.

Using Br_2 instead of NBS leads to a triple bromination. The next rings are installed by a Suzuki cross-coupling reaction, but due to our experience with the monobrominated derivative,⁴³ we opted for a preceding umpolung using bis(pinacolato)diboron, potassium acetate, and $Pd(dppf)Cl_2$ in 1,4-dioxane giving **3** in 68% yield. The following double Suzuki cross coupling reactions of **3** with the phenyl bromide, which carries a dansyl protected boron center at the *ortho* position, proceeds smoothly to **4** in yields of 70%.⁴⁸ Following Hattori *et al.*,⁴⁹ 2 M sulfuric acid deprotects the Bdan species and the B_3N_2O ring of **A** is formed with yields of 90%. Due to the low solubility, **A** can be purified by washing with THF, water, acetone, and dichloromethane, as well as by sublimation. NMR data of **A** were measured in 1,4-dioxane- d_8 at 80 °C. All products were characterized by

multinuclear (1H , ^{13}C , ^{11}B) and correlated NMR spectroscopy (H–H–COSY, HSQC, HMBC, NOESY) as well as by high resolution mass spectrometry. The ^{11}B spectrum of **A** shows a broad signal at 30.5 ppm that is in between the typical range of borazines and boroxines. In summary, our synthetic protocols provide access to **A** in four steps with an overall yield of 34%.

Single crystals were obtained by sublimation in a quartz tube at 10^{-3} mbar and 300 °C. Unfortunately, X-ray data could be collected only to a resolution limit of 1 Å. However, the data obtained suffice to confirm the expected connectivity of **A** (see Fig. S25, ESI†). The unit cell lengths ($a = 18.67$ Å, $b = 4.93$ Å, $c = 31.56$ Å) suggest that the compound crystallizes in a β motif⁵⁰ with an intermolecular π – π stacking distance of about 3.3 Å. Better quality crystals could not be grown, despite many attempts under varied sublimation conditions and from solution phase.

The absorption spectrum (Fig. 2) of **A** measured in solution phase shows three somewhat broad maxima in the 330–370 nm range as absorptions of longest wavelength. The parent all-carbon system (dibenzo[*fg,ij*]phenanthro[9,10,1,2,3-*pqrst*]pentaphene) has its lowest energy absorption at 430 nm (α band).^{51,52} This shows that the incorporation of the boroxazine ring significantly increases the optical gap. The all-carbon system also has a distinctively different absorption spectrum.^{51,52} In particular, the apparent vibrational fine structure present of **A** in the 330–370 nm range is absent in the all-carbon congener. These features sharpen and split into additional maxima if measured in an argon matrix at 10 K (Fig. 2) that is prepared by gas phase deposition of **A**, indicating that they do not arise from aggregation in solution. Increasing the concentration from 1.1×10^{-6} M to 8.0×10^{-6} M results in a new broad feature at longer wavelength (379 nm, see Fig. S23, ESI†) due to aggregation.

The fluorescence spectrum of **A** (Fig. 2) is insensitive to the excitation wavelength as expected based on Kasha's rule. The Stokes shift of 221 cm^{-1} is quite small, which is indicative of

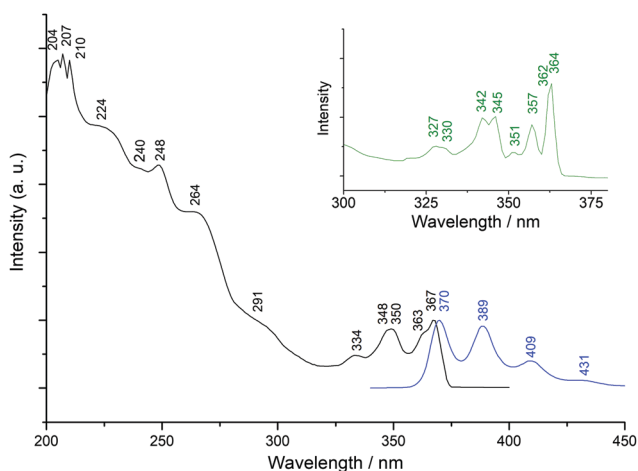


Fig. 2 Absorption (black) and fluorescence (blue, $\lambda_{ex} = 334$ nm) spectra of **A** (1.1×10^{-6} M in 1,4-dioxane). Inset: Absorption spectrum (green) measured in an argon matrix at 10 K.

the pronounced stiffness of the molecular structure in the excited state, and the fluorescence quantum yield, measured with the reference to anthracene in ethanol ($\phi_{\text{Fl}} = 0.27$), is quite large ($\phi_{\text{Fl}} = 0.58$).^{53,54}

Most remarkable of the fluorescence spectra is the vibrational fine structure that is evident from the continuous spacing of roughly 1270 cm^{-1} . This suggests that some of the bands in the 330–370 nm region of the absorption spectrum are the corresponding features of the vibrational progression. However, due to the missing mirror image behavior of absorption and fluorescence spectra, an additional excited state is likely involved in the absorption spectrum in this energy range. This expectation is confirmed by computational investigations (\mathbf{A}_{H} (R = H), TD-B3LYP/6-311+G**) that arrive at two excited states that are very close in energy (S_1 : 346 nm; S_2 : 341 nm; energy difference 0.05 eV) and have similar oscillator strengths ($f(S_1) = 0.17$; $f(S_2) = 0.14$). The natural transition orbitals⁵⁵ (NTOs, Fig. 3) reveal that the dominant single electron transitions to S_1 and S_2 involve the same hole, but different particle densities. This is due to the small energy difference of 0.1 eV between the lowest unoccupied molecular orbital (LUMO) and LUMO+1 that is small compared to the HOMO–LUMO energy gap of 3.4 eV.

The electronic structure of the target compound was further analyzed by computation of the magnetic properties, *i.e.*, nucleus independent chemical shift (NICS) and anisotropy of the current-induced density (ACID) plots,^{56,57} at the B3LYP/6-311+G** level theory. The NICS(1)^{58,59} values (Fig. 4) identify the heteroatom containing rings as being nonaromatic. In particular, the oxadiazatriborinine ring has a NICS value close to zero. The five benzene rings of the molecular perimeter, on the other hand, have large negative NICS values similar to those of benzene. This is in agreement with Clar's aromatic sextet and with the ACID plot (Fig. 4). The all-carbon rings sustain cyclic electron delocalization,

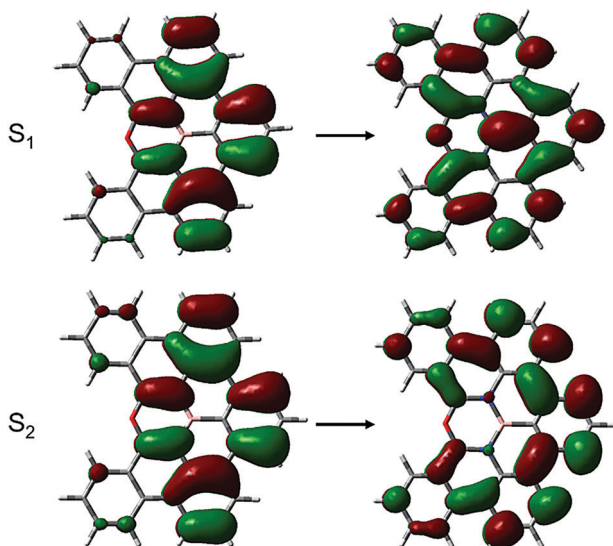


Fig. 3 Natural transition orbitals (NTOs) of the hole and particle densities of the two lowest energy excitations from the ground state to the S_1 and S_2 states of \mathbf{A}_{H} as computed at the TD-B3LYP/6-311+G** level.

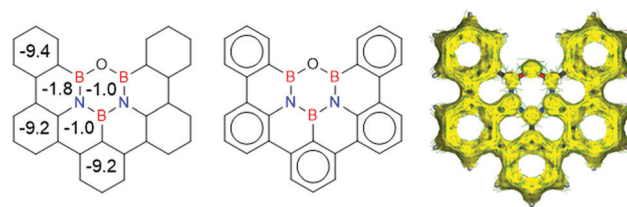


Fig. 4 NICS(1) (left) values of individual rings in \mathbf{A}_{H} (NICS(1) of benzene is -10.2), the Clar sextet (center) representation, and plot of the anisotropy of current-induced density (ACID, right) as computed at the B3LYP/6-311+G** level of theory. *n*-Butyl groups are omitted.

but this is interrupted by the heteroatoms in the four rings that contain two or three heteroatoms as well as in the boroxazine ring.

Based on these data, the target molecule appears as a planarized *m*-quinquephenyl that is interconnected by a boroxazine ring that precludes extended electron delocalization over the π -system. That this seemingly simple interpretation is an oversimplification is obvious when comparing the absorption spectra of \mathbf{A} ($\lambda_{\text{max}} = 367 \text{ nm}$ in 1,4-dioxane) and *m*-quinquephenyl ($\lambda_{\text{max}} = 249 \text{ nm}$ in cyclohexane),⁶⁰ and considering the computed hole and particle densities (Fig. 3) involving the first two electronic transitions of \mathbf{A} as these have significant contributions of the heteroatoms.

In summary, our study shows that the boroxazine ring can be incorporated into the backbone of an extended organic π system by a concise synthetic strategy. The fixation of the boroxazine ring within the PAH scaffold renders it stable towards hydrolysis. The substitution of a benzene by a boroxazine ring significantly changes the electronic structure of the organic π system and widens the electronic gap. The high fluorescence quantum yield of the system turns it an interesting platform for luminescence applications.

We are grateful to Dr Christina Tönshoff for matrix isolation spectroscopy and Dr Hartmut Schubert for X-ray diffraction. This work was supported in part by Vector Foundation. The authors acknowledge support by the State of Baden-Württemberg through bwHPC and the German Research Foundation (DFG) through grant no. INST 40/467-1 FUGG (JUSTUS cluster).

Note added in proof: Recently, Bonifazi *et al.* obtained a derivative of \mathbf{A} (R = 2,6-dimethylphenyl) as by-product of borazine synthesis, see ref. 61.

Conflicts of interest

There are no conflicts to declare.

Notes and references

- 1 F. Ortmann, K. S. Radke, A. Günther, D. Kasemann, K. Leo and G. Cuniberti, *Adv. Funct. Mater.*, 2015, **25**, 1933–1954.
- 2 M. Bendikov, F. Wudl and D. F. Perepichka, *Chem. Rev.*, 2004, **104**, 4891–4945.
- 3 M. Stępień, E. Gońka, M. Żyła and N. Sprutta, *Chem. Rev.*, 2016, **117**, 3479–3716.
- 4 M. J. D. Bosdet and W. E. Piers, *Can. J. Chem.*, 2009, **87**, 8–29.
- 5 P. G. Campbell, A. J. V. Marwitz and S.-Y. Liu, *Angew. Chem., Int. Ed.*, 2012, **51**, 6074–6092.
- 6 Z. X. Giustra and S.-Y. Liu, *J. Am. Chem. Soc.*, 2018, **140**, 1184–1194.
- 7 H. Helten, *Chem. – Eur. J.*, 2016, **22**, 12972.

- 8 M. M. Morgan and W. E. Piers, *Dalton Trans.*, 2016, **45**, 5920–5924.
- 9 X.-Y. Wang, J.-Y. Wang and J. Pei, *Chem. – Eur. J.*, 2015, **21**, 3528–3539.
- 10 H. Helten, *Chem. – Asian J.*, 2019, **14**, 919–935.
- 11 S. K. Møllerup and S. Wang, *Trends Chem.*, 2019, **1**, 77–89.
- 12 T. Agou, J. Kobayashi and T. Kawashima, *Chem. – Eur. J.*, 2007, **13**, 8051–8060.
- 13 T. Hatakeyama, K. Shiren, K. Nakajima, S. Nomura, S. Nakatsuka, K. Kinoshita, J. Ni, Y. Ono and T. Ikuta, *Adv. Mater.*, 2016, **28**, 2777–2781.
- 14 H. Nakanotani, T. Furukawa, T. Hosokai, T. Hatakeyama and C. Adachi, *Adv. Opt. Mater.*, 2017, **5**, 1700051.
- 15 S. Nakatsuka, H. Gotoh, K. Kinoshita, N. Yasuda and T. Hatakeyama, *Angew. Chem., Int. Ed.*, 2017, **56**, 5087–5090.
- 16 S. Oda, B. Kawakami, R. Kawasumi, R. Okita and T. Hatakeyama, *Org. Lett.*, 2019, **21**, 9311–9314.
- 17 J. Wu, Y. Kan, Z. Xue, J. Huang, P. Chen, X. Yu, Z. Guo and Z. Su, *J. Mater. Chem. C*, 2017, **5**, 9088–9097.
- 18 I. S. Park, K. Matsuo, N. Aizawa and T. Yasuda, *Adv. Funct. Mater.*, 2018, **28**, 1802031.
- 19 X. Liang, Z.-P. Yan, H.-B. Han, Z.-G. Wu, Y.-X. Zheng, H. Meng, J.-L. Zuo and W. Huang, *Angew. Chem., Int. Ed.*, 2018, **57**, 11316–11320.
- 20 J. A. Knöller, G. Meng, X. Wang, D. Hall, A. Pershin, D. Beljonne, Y. Olivier, S. Laschat, E. Zysman-Colman and S. Wang, *Angew. Chem., Int. Ed.*, 2020, **59**, 3156–3160.
- 21 S. H. Han, J. H. Jeong, J. W. Yoo and J. Y. Lee, *J. Mater. Chem. C*, 2019, **7**, 3082–3089.
- 22 M. Ando, M. Sakai, N. Ando, M. Hirai and S. Yamaguchi, *Org. Biomol. Chem.*, 2019, **17**, 5500–5504.
- 23 T. Kaehler, M. Bolte, H.-W. Lerner and M. Wagner, *Angew. Chem., Int. Ed.*, 2019, **58**, 11379–11384.
- 24 S. Nakatsuka, N. Yasuda and T. Hatakeyama, *J. Am. Chem. Soc.*, 2018, **140**, 13562–13565.
- 25 H. Fukagawa, T. Oono, Y. Iwasaki, T. Hatakeyama and T. Shimizu, *Mater. Chem. Front.*, 2018, **2**, 704–709.
- 26 C. J. Saint-Louis, R. N. Shavnore, C. D. C. McClinton, J. A. Wilson, L. L. Magill, B. M. Brown, R. W. Lamb, C. E. Webster, A. K. Schrock and M. T. Huggins, *Org. Biomol. Chem.*, 2017, **15**, 10172–10183.
- 27 W. Zhang, F. Zhang, R. Tang, Y. Fu, X. Wang, X. Zhuang, G. He and X. Feng, *Org. Lett.*, 2016, **18**, 3618–3621.
- 28 S. Wang, D.-T. Yang, J. Lu, H. Shimogawa, S. Gong, X. Wang, S. K. Møllerup, A. Wakamiya, Y.-L. Chang, C. Yang and Z.-H. Lu, *Angew. Chem., Int. Ed.*, 2015, **54**, 15074–15078.
- 29 G. Li, Y. Zhao, J. Li, J. Cao, J. Zhu, X. W. Sun and Q. Zhang, *J. Org. Chem.*, 2015, **80**, 196–203.
- 30 S. Hashimoto, T. Ikuta, K. Shiren, S. Nakatsuka, J. Ni, M. Nakamura and T. Hatakeyama, *Chem. Mater.*, 2014, **26**, 6265–6271.
- 31 Y.-L. Chang, Y.-L. Rao, S. Gong, G. L. Ingram, S. Wang and Z.-H. Lu, *Adv. Mater.*, 2014, **26**, 6729–6733.
- 32 X. Wang, F. Zhang, J. Liu, R. Tang, Y. Fu, D. Wu, Q. Xu, X. Zhuang, G. He and X. Feng, *Org. Lett.*, 2013, **15**, 5714–5717.
- 33 N. Ishida, M. Narumi and M. Murakami, *Helv. Chim. Acta*, 2012, **95**, 2474–2480.
- 34 G. Fitzgerald, C. Lin, A. B. Dyatkin and P. M. Lahti, US20180226580A1, 2018.
- 35 K. F. Hoffmann and U. Engelhardt, *Z. Naturforsch.*, 1970, **25b**, 317.
- 36 A. Møller, C. Habben, M. Noltemeyer and G. M. Sheldrick, *Z. Naturforsch.*, 1982, **37b**, 1504–1506.
- 37 A. Møller and C. Habben, *Monatsh. Chem.*, 1982, **113**, 139–153.
- 38 R. Oesterle, W. Maringgele and A. Møller, *J. Organomet. Chem.*, 1985, **284**, 281–289.
- 39 M. Komorowska, K. Niedenzu and W. Weber, *Inorg. Chem.*, 1990, **29**, 289–294.
- 40 Y. Kawashima, H. Takeo and C. Matsumura, *Inorg. Chem.*, 1989, **28**, 666–669.
- 41 M. Krieg, F. Reicherter, P. Haiss, M. Ströbele, K. Eichele, M.-J. Treanor, R. Schaub and H. F. Bettinger, *Angew. Chem., Int. Ed.*, 2015, **54**, 8284–8286.
- 42 J. Dosso, J. Tasseroul, F. Fasano, D. Marinelli, N. Biot, A. Fermi and D. Bonifazi, *Angew. Chem., Int. Ed.*, 2017, **56**, 4483–4487.
- 43 M. Fingerle, S. Stocker and H. F. Bettinger, *Synthesis*, 2019, 4147–4152.
- 44 M. Numano, N. Nagami, S. Nakatsuka, T. Katayama, K. Nakajima, S. Tatsumi, N. Yasuda and T. Hatakeyama, *Chem. – Eur. J.*, 2016, **22**, 11574–11577.
- 45 D.-T. Yang, T. Nakamura, Z. He, X. Wang, A. Wakamiya, T. Peng and S. Wang, *Org. Lett.*, 2018, **20**, 6741–6745.
- 46 X. Wang, F. Zhang, K. S. Schellhammer, P. Machata, F. Ortman, G. Cuniberti, Y. Fu, J. Hunger, R. Tang, A. A. Popov, R. Berger, K. Müllen and X. Feng, *J. Am. Chem. Soc.*, 2016, **138**, 11606–11615.
- 47 Z. Sun, C. Yi, Q. Liang, C. Bingli, W. Zhu, P. Qiang, D. Wu and F. Zhang, *Org. Lett.*, 2020, **22**, 209–213.
- 48 H. Noda, M. Furutachi, Y. Asada, M. Shibasaki and N. Kumagai, *Nat. Chem.*, 2017, **9**, 571–577.
- 49 Y. Hattori, T. Ogaki, M. Ishimura, Y. Ohta and M. Kirihata, *Tetrahedron Lett.*, 2017, **17**, 2436.
- 50 G. R. Desiraju and A. Gavezzotti, *Acta Crystallogr., Sect. B: Struct. Sci.*, 1989, **45**, 473–482.
- 51 E. Clar, C. T. Ironside and M. Zander, *J. Chem. Soc.*, 1959, 142–147.
- 52 C. Kübel, K. Eckhardt, V. Enkelmann, G. Wegner and K. Müllen, *J. Mater. Chem.*, 2000, **10**, 879–886.
- 53 M. Brouwer Albert, *Pure Appl. Chem.*, 2011, **83**, 2213.
- 54 J. R. Lakowicz, *Principles of Fluorescence Spectroscopy*, Springer, Berlin, 3rd edn, 2006.
- 55 A. Dreuw and M. Head-Gordon, *Chem. Rev.*, 2005, **105**, 4009–4037.
- 56 R. Herges and D. Geuenich, *J. Phys. Chem. A*, 2001, **105**, 3214–3220.
- 57 D. Geuenich, K. Hess, F. Köhler and R. Herges, *Chem. Rev.*, 2005, **105**, 3758–3772.
- 58 P. v. R. Schleyer, C. Maerker, A. Dransfeld, H. Jiao and N. J. R. van Eikema Hommes, *J. Am. Chem. Soc.*, 1996, **118**, 6317–6318.
- 59 P. v. R. Schleyer, H. Jiao, N. J. R. v. E. Hommes, V. G. Malkin and O. L. Malkina, *J. Am. Chem. Soc.*, 1997, **119**, 12669–12670.
- 60 S. Ozasa, Y. Fujioka, M. Fujiwara and E. Ibuki, *Chem. Pharm. Bull.*, 1980, **28**, 3210–3222.
- 61 J. Dosso, T. Battisti, B. D. Ward, N. Demitri, C. Hughes, A. P. Williams, K. D. M. Harris and D. Bonifazi, *Chem. – Eur. J.*, 2020, DOI: 10.1002/chem.201905794.

Electronic Supporting Information (ESI)

Embedding a boroxazine ring into a nanographene scaffold by a concise bottom-up synthetic strategy

Michael Fingerle, Holger F. Bettinger

Institut für Organische Chemie, Auf der Morgenstelle 18, 72076 Tübingen, Germany

E-Mail: Holger.Bettinger@uni-tuebingen.de

Contents

- 1. Experimental and Computational Details**
- 2. Synthesis**
- 3. Cartesian Coordinates of Stationary Points**
- 4. Spectra**

1. Experimental and Computational Details

Experimental Details

Unless otherwise indicated, all reactions were done under inert conditions by flaming all glassware with a heat gun (at 630 °C) under vacuum and purging with argon. All chemicals and solvents were dried by known methods or were purchased from commercial suppliers in anhydrous form. Column chromatography were done with a medium pressure liquid chromatography (MPLC) system (PuriFlash 430 evo, Interchim), with Si-IR 20 μm columns in size of 12 g up to 120 g. Thin layer chromatography (TLC) was done using pre-coated polyester sheets (40 x 80 mm) from Machery-Nagel (POLYGAM®SIL G/UV254) with 0.2 mm silica gel 60 with fluorescence indicator. For visualization, UV light source (254 nm and 366 nm) was used. Melting points were measured with a Büchi B-540 apparatus. Nuclear magnetic resonance spectroscopy (NMR) was done on a Bruker Avance III HDX 600 (equipped with a dual ($^1\text{H}/^{13}\text{C}$) probe head. Chemical shifts (δ) are given in ppm, coupling constants in Hertz (Hz) and the multiplicities of the signals are designated as follows: s = singlet, br s = broad singlet, d = doublet, dd = doublet of doublet, t = triplet and m = multiplet. The signals of NMR solvents were calibrated ($^1\text{H}/^{13}\text{C}$): CD_2Cl_2 5.32/53.84 ppm and thf-d_8 3.58/67.21 ppm. Reference for ^1H and ^{13}C were tetramethyl silane (TMS) and for ^{11}B $\text{BF}_3\cdot\text{OEt}_3$ in CDCl_3 . High resolution mass spectrometry was done with electron spray ionization time of flight mass spectrometry (ESI-TOF-MS) on a maXis 4G Bruker system or with an APCI source combined with a direct inlet probe (DIP) system. EI high resolution mass spectrometry was done on a Finnigan/MasCom MAT95. Optical spectra were recorded on a PerkinElmer Lambda 1050 spectrometer with a PerkinElmer 3D WB Det Module. Excitation and emission spectra were recorded on a Cary Variant SPVF spectrometer using Hellma Analytics quartz cuvettes. All measurements were done in spectroscopy grade solvents. The fluorescence quantum yield of **A** in 1,4-dioxane was measured with an excitation wavelength $\lambda_{\text{ex}} = 362$ nm (anthracene in ethanol as reference). Infrared spectroscopy was measured on a Bruker Tensor 27 with KBr pellets. The single crystal of **A** was measured on a Bruker Apex II with Cu K_α radiation.

Computational Details

Geometry optimizations of **A** on the S_0 potential energy surface (PES) were performed using the B3LYP^{1, 2} functional as implemented in Gaussian 09³ in conjunction with the 6-311+G** basis set.⁴ Computation of the harmonic vibrational frequencies confirms that the resulting geometry corresponds to a minimum on the PES. Excited state energies and natural transition orbitals (NTO) were computed using the time-dependent (TD)⁵ method in conjunction with the B3LYP functional and the 6-311+G** basis set. Nuclear-independent chemical shifts⁶⁻⁸ were computed at the B3LYP/6-311+G** level using the GIAO method.⁹ The anisotropy of current-induced density (ACID)^{10, 11} was computed at the B3LYP/6-311+G** level using the AICD-2.0.0 program kindly provided by Professor Herges.

2. Synthesis

Synthesis of 2

To an ice-cold solution of **1** (1.9 g, 5.0 mmol, 1 equiv.) in a mixture of chloroform/DCM (1:1) (500 mL in total) was added over 2 h a solution of NBS (1.8 g, 10 mmol, 2 equiv.) in acetonitrile (120 mL). After complete addition the mixture was stirred at room temperature. After 12 h, all volatiles were removed under reduced pressure. Flash-chromatography (*n*-hexane/DCM 9:1, $R_f = 0.21$) yielded the desired product **2** as a colourless solid (2.1 g, 4.0 mmol, 80 %).

$^1\text{H-NMR}$ (600 MHz, CD_2Cl_2): 8.14 (d, $J = 8.0$ Hz, 2H, H-3), 7.99 (d, $J = 1.5$ Hz, 2H, H-2), 7.79 (t, $J = 8.0$ Hz, 1H, H-4), 7.45 (d, $J = 1.5$ Hz, 2H, H-1), 7.05 (br s, H-5, 2H), 2.67 (t, $J = 7.8$ Hz, 4H, H-6), 1.70-1.63 (m, 4H, H-7), 1.45-1.37 (m, 4H, H-8), 0.97 (t, $J = 7.4$ Hz, 6H, H-9).

$^{11}\text{B-NMR}$ (128 MHz, CD_2Cl_2): 27.0

$^{13}\text{C-NMR}$ (151 MHz, CD_2Cl_2): 138.9 (C-7), 136.2 (C-5), 135.5 (C-2), 132.1 (C-1), 131.5 (C-10), 127.2 (br s, C-8), 124.0 (C-3), 123.8 (C-4), 120.0 (C-9), 113.4 (C-6), 35.4 (C-11), 34.3 (C-12), 22.7 (C-13), 14.2 (C-14).

HRMS (ESI): m/z $[\text{M}+\text{H}]^+$ calcd. for $\text{C}_{26}\text{H}_{27}\text{BBr}_2\text{N}_2$: 537.07144; found 537.07219 ($\Delta = 1.95$ ppm)

Mp: 215 °C

Synthesis of 3

Under an inert atmosphere **2** (2.1 g, 4.0 mmol, 1 equiv.), bis(pinacolato) diboron (5.1 g, 20 mmol, 5 equiv.), potassium acetate (4.7 g, 48 mmol, 12 equiv.) and $\text{Pd}(\text{dppf})\text{Cl}_2$ (0.3 g, 0.4 mmol, 0.1 equiv.) were dissolved in dry dioxane (250 mL) and stirred under reflux (90 °C oil bath temp.) for 18 h. After cooling down, 100 mL ethyl acetate were added and the mixture was washed with water (3 x 50 mL). The aqueous layer was extracted with dichloromethane (3 x 50 mL). All combined organic layers were dried over anhydrous sodium sulphate. All volatiles were removed under reduced pressure. Column chromatography (*n*-hexane/DCM 2:1, $R_f = 0.2$) yielded the desired compound **3** (1.7 g, 2.7 mmol, 68 %).

$^1\text{H-NMR}$ (600 MHz, CD_2Cl_2): 8.58 (br s, 2H, H-5), 8.19 (d, $J = 1.9$ Hz, 2H, H-2), 8.17 (d, $J = 8.0$ Hz, 2H, H-3), 7.78 (t, $J = 8.0$ Hz, 1H, H-4), 7.64 (d, $J = 1.9$ Hz, 2H, H-1), 2.70 (t, $J = 7.9$ Hz, 4H, H-7), 1.71-1.65 (m, 4H, H-8), 1.48-1.39 (m, 4H, H-9), 1.46 (s, 24H, H-6), 0.98 (t, $J = 7.4$ Hz, 6H, H-10).

$^{11}\text{B-NMR}$ (128 MHz, CD_2Cl_2): 31.4, 26.6.

^{13}C -NMR (151 MHz, CD_2Cl_2): 145.9 (C-5), 139.6 (C-9), 137.1 (C-1), 133.2 (C-2), 131.0 (C-12), 128.3 (C-3), 127.4 (C-10), 122.0 (C-4), 118.9 (C-11), 115.5 (C-6), 84.4 (C-7), 35.6 (C-13), 34.8 (C-14), 25.3 (C-8), 22.9 (C-15), 14.2 (C-16).

HRMS (EI): m/z $[\text{M}]^+$ calcd. for $\text{C}_{38}\text{H}_{51}\text{B}_3\text{N}_2\text{O}_4$: 632.412252; found: 632.40571 ($\Delta = 6.54$ mmu)

Mp: decomposition

Synthesis of 4

3 (1.7 g, 2.7 mmol, 1 equiv.), Br-Bdan-benzene (2.2 g, 6.8 mmol, 2.5 equiv.), potassium carbonate (4.5 g, 32 mmol, 12 equiv.) and $\text{Pd}(\text{PPh}_3)_4$ (0.3 g, 0.3 mmol, 0.1 equiv.) were dissolved in a mixture of toluene (150 mL), ethanol (40 mL) and water (75 mL) and stirred under reflux (100 °C oil bath temp.) for 12 h. After cooling to rt, the reaction mixture was washed with water (3 x 30 mL) and the aqueous layer was extracted with DCM (4 x 50 mL). All combined organic layers were dried over anhydrous sodium sulphate and all volatiles were removed under reduced pressure. Flash chromatography (n-hexane/DCM 3:1 gradient to 3:2; R_f (3:2) = 0.1) yielded the desired compound **4** as a colourless solid (1.6 g, 1.9 mmol, 70 %).

^1H -NMR (600 MHz, CD_2Cl_2): 8.31-8.28 (m, 2H, H-3), 8.18-8.16 (m, 2H, H-2), 7.89-7.85 (m, 1H, H-4), 7.81-7.77 (m, 2H, H-8), 7.58-7.48 (m, 4H, H-6, H-7), 7.42 (dd, $J = 7.5$ Hz, $J = 1.0$ Hz, 1H, H-12), 7.37 (dd, $J = 7.3$ Hz, $J = 1.1$ Hz, 1H, H-5), 7.08-7.06 (m, 2H, H-1), 6.95-6.92 (m, 2H, H-10), 6.87-6.79 (m, 6H, H-11, H-18, H-19), 6.18 (s, 1H, NH1), 6.16 (s, 1H, NH2), 5.97 (dd, $J = 7.3$ Hz, $J = 0.7$ Hz, 2H, H-9), 5.89 (dd, $J = 7.3$ Hz, $J = 0.8$ Hz, 2H, H-13), 5.65 (s, 2H, NH3), 5.58 (s, 2H, NH4), 2.73-2.67 (m, 4H, H-14), 1.64-1.55 (m, 4H, H-15), 1.35-1.26 (m, 4H, H-16), 0.81-0.74 (m, 6H, H-17).

^{11}B -NMR (128 MHz, CD_2Cl_2): 29.1, 26.6.

^{13}C -NMR (151 MHz, CD_2Cl_2): 143.6 (C-11), 143.5 (C-10), 141.4 (C-19), 141.3 (C-18), 139.5 (C-5), 139.4 (C-6), 136.5 (C-), 136.4 (C-), 135.2 (C-13), 134.9 (C-12), 134.2 (C-3), 133.7 (C-17), 133.6 (C-16), 131.5 (C-), 131.4 (C-8), 131.3 (C-14), 131.1 (C-15), 130.7 (C-), 130.6 (C-), 130.5 (C-1), 130.3 (C-2), 128.0 (C-), 127.8 (C-22), 127.8 (C-), 127.3 (C-9), 124.2 (C-4), 122.6 (C-), 122.6 (C-), 119.8 (C-), 119.8 (C-7), 119.7 (C-), 117.6 (C-), 117.5 (C-), 106.0 (C-20), 106.0 (C-21), 35.6 (C-23), 34.6 (C-24), 22.6 (C-25), 14.0 (C-26). All other signals could not be assigned due to the two multiplet signals in the ^1H NMR with 4H and 6H.

HRMS (EI): m/z $[\text{M}]^+$ calcd. for $\text{C}_{58}\text{H}_{51}\text{B}_3\text{N}_6\text{Na}$: 887.43717; found: 887.43794 ($\Delta = 0.8$ mmu)

Mp: decomposition

Synthesis of A

Under an inert atmosphere **4** (112 mg, 0.13 mmol, 1 equiv.) was dissolved in degassed THF (50 mL). A degassed H₂SO₄ solution (3.1 mL, 2 M in water, 6.28 mmol, 48 equiv.) was added dropwise. The mixture was stirred for 3 days at 50 °C. After cooling to rt, the obtained solid was filtered and washed with concentrated NaHCO₃ solution, water, acetone and thf until a white solid was obtained. Sublimation in a quartz ampule (10⁻³ mbar, 300 °C) yielded the desired compound **A** as colourless needles (66.2 mg, 0.12 mmol, 90 %).

¹H-NMR (600 MHz, 80 °C, dioxane-d₈): 8.74-8.72 (m, 2H, H-1), 8.55 (d, *J* = 8.0 Hz, 2H, H-4), 8.48-8.42 (m expected as d + s; d, 2H, H-7; s, 4H, H-5, H-6), 7.98-7.94 (m, 1H, H-8), 7.84-7.79 (m, 2H, H-3), 7.66-7.61 (m, 2H, H-2), 2.98 (t, *J* = 7.7 Hz, 4H, H-9), 1.95-1.86 (m, 4H, H-10), 1.63-1.53 (m, 4H, H-11), 1.07 (t, *J* = 7.4 Hz, 6H, H-12).

¹¹B-NMR (128 MHz, 80 °C, dioxane-d₈): 30.5 (br s).

¹³C-NMR (151 MHz, 80 °C, dioxane-d₈): 142.4 (C-5), 140.4 (C-12), 138.1 (C-6), 136.6 (C-8), 134.5 (C-11), 133.4 (C-1), 132.9 (C-14), 132.3 (C-3), 126.9 (C-2), 126.0 (C-10), 125.0 (C*-7), 124.9 (C*-9), 123.1 (C-4), 120.8 (C-13), 36.0 (C-15), 34.3 (C-16), 22.7 (C-17), 13.8 (C-18). C* could be interchanged due to overlap in ¹H-NMR. C-B are not found due to quadrupole moment.

IR (KBr) ν (cm⁻¹): 3069, 3037, 2951, 2926, 2869, 2853, 1602, 1585, 1573, 1556, 1547, 1483, 1460, 1430, 1395, 1380, 1328, 1294, 1251, 813, 780, 459, 738, 675, 621.

UV/vis (1,4-dioxane) λ_{\max} (log ϵ): 204 (5.16), 207 (5.17), 210 (5.17), 224 (5.07), 240 (4.99), 248 (5.00), 264 (4.90), 291 (4.48), 334 (4.16), 348 (4.42), 350 (4.42), 363 (4.39), 367 (4.48).

HRMS (DIP-APCI): *m/z* [M+H]⁺ calcd. for C₃₈H₃₃B₃N₂O: 567.29627; found 567.29583 (Δ = 0.81 ppm)

EA: calcd. for C₃₈H₃₃B₃N₂O: N 4.95 %, C 80.62 %, H 5.88 %; found: N 4.96, C 80.97, H 5.89 %.

Mp: 320 °C

3. Cartesian Coordinates of Stationary Points

Given in Å and computed at B3LYP/6-311+G**

Compound **A_H** (C_{2v})

```
53
scf done: -1413.43740047

6      0.000000000      2.532604000      2.190431000
6      0.000000000      2.551803000      3.596188000
6      0.000000000      0.000000000     -2.268365000
6      0.000000000      1.236596000     -2.950048000
6      0.000000000      2.490197000     -2.165773000
6      0.000000000      2.482153000     -0.739258000
6      0.000000000      3.711852000     -0.014551000
6      0.000000000      3.743902000      1.464606000
6      0.000000000     -2.551803000      3.596188000
6      0.000000000     -2.532604000      2.190431000
6      0.000000000     -3.743902000      1.464606000
6      0.000000000     -3.711852000     -0.014551000
6      0.000000000     -2.482153000     -0.739258000
6      0.000000000     -1.236596000     -2.950048000
6      0.000000000     -2.490197000     -2.165773000
6      0.000000000      3.726754000     -2.824494000
1      0.000000000      3.758515000     -3.905093000
6      0.000000000      4.909189000     -0.743251000
1      0.000000000      5.855227000     -0.220441000
6      0.000000000      1.214504000     -4.352375000
1      0.000000000      2.126224000     -4.934050000
6      0.000000000     -1.214504000     -4.352375000
1      0.000000000     -2.126224000     -4.934050000
6      0.000000000     -3.726754000     -2.824494000
1      0.000000000     -3.758515000     -3.905093000
6      0.000000000     -4.909189000     -0.743251000
1      0.000000000     -5.855227000     -0.220441000
6      0.000000000     -4.951431000      2.193546000
1      0.000000000     -5.907766000      1.688366000
6      0.000000000     -3.747272000      4.295260000
1      0.000000000     -3.755672000      5.379624000
6      0.000000000      3.747272000      4.295260000
1      0.000000000      3.755672000      5.379624000
6      0.000000000      4.951431000      2.193546000
1      0.000000000      5.907766000      1.688366000
6      0.000000000      4.923774000     -2.128198000
1      0.000000000      5.866344000     -2.663380000
6      0.000000000      0.000000000     -5.029783000
1      0.000000000      0.000000000     -6.114808000
6      0.000000000     -4.923774000     -2.128198000
1      0.000000000     -5.866344000     -2.663380000
6      0.000000000     -4.950151000      3.579888000
1      0.000000000     -5.895836000      4.111765000
6      0.000000000      4.950151000      3.579888000
1      0.000000000      5.895836000      4.111765000
5      0.000000000      0.000000000     -0.761165000
5      0.000000000     -1.222483000      1.401360000
5      0.000000000      1.222483000      1.401360000
7      0.000000000      1.256642000     -0.040863000
7      0.000000000     -1.256642000     -0.040863000
8      0.000000000      0.000000000      2.034216000
1      0.000000000     -1.606988000      4.128519000
1      0.000000000      1.606988000      4.128519000
```


4. Spectra

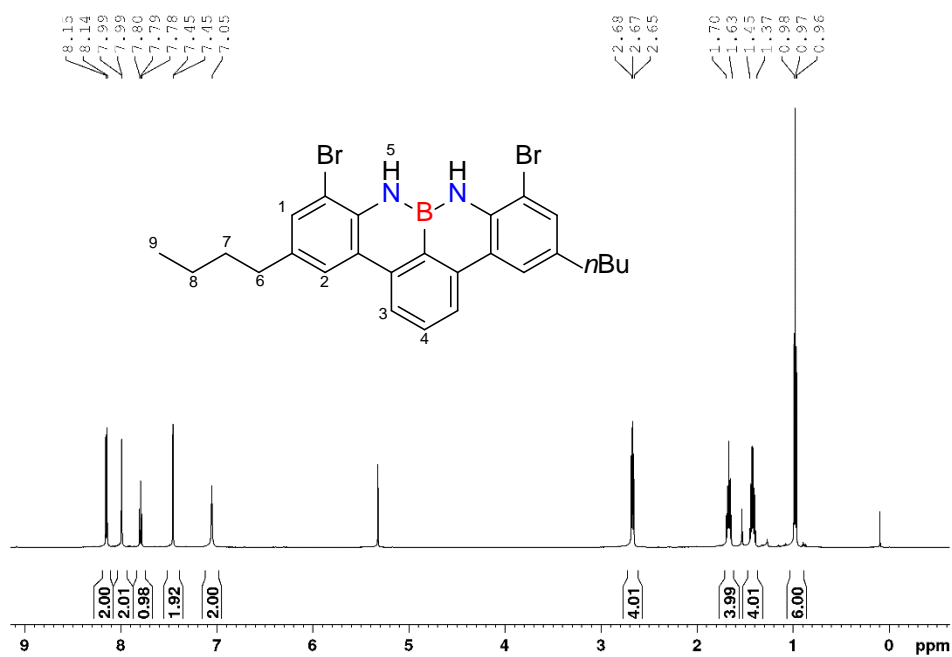


Figure S1: ¹H-NMR of **2** in CD₂Cl₂.

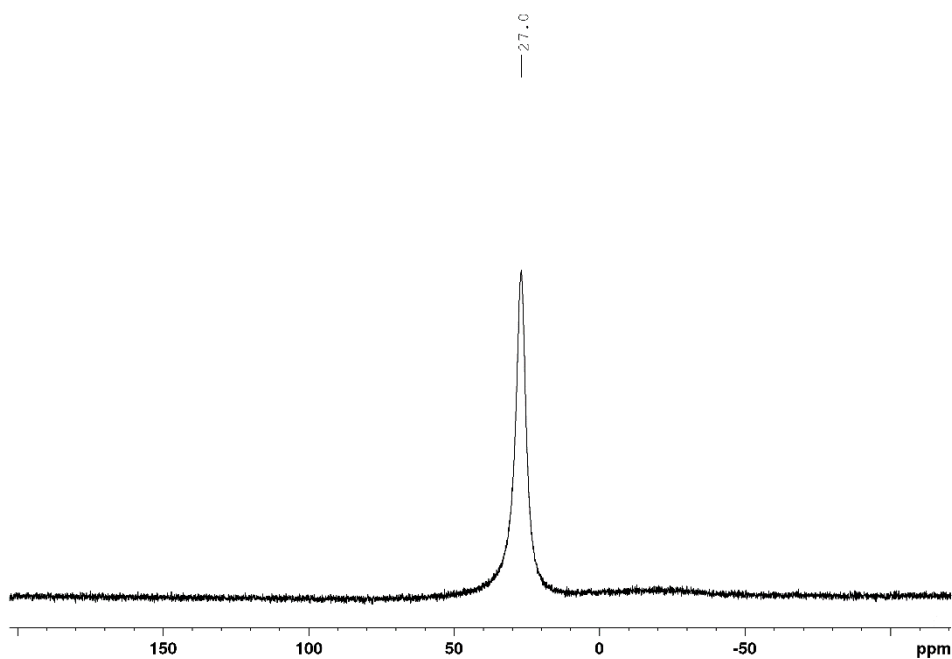


Figure S2: ¹¹B-NMR of **2** in CD₂Cl₂.

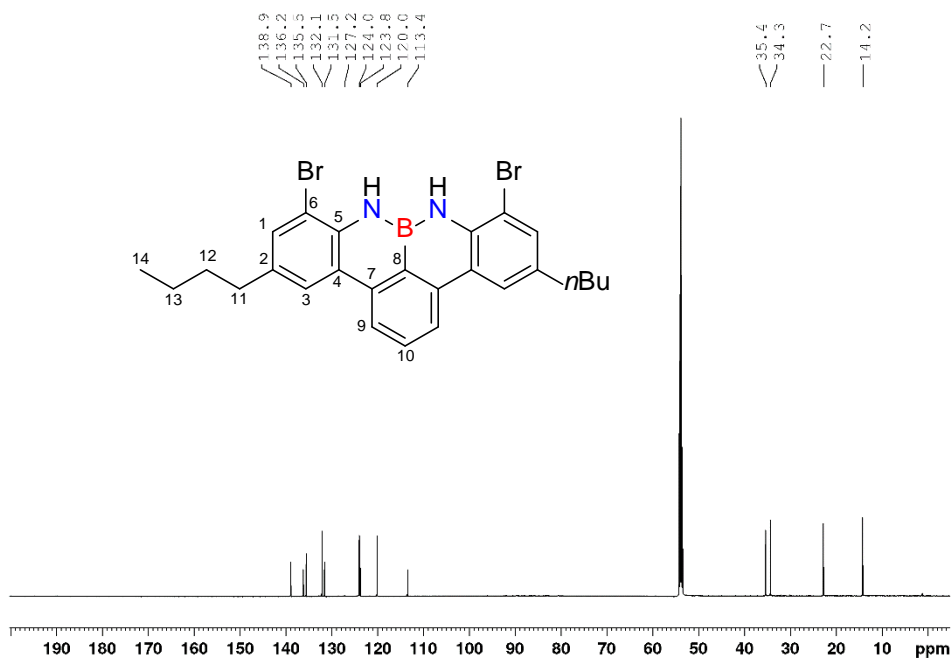
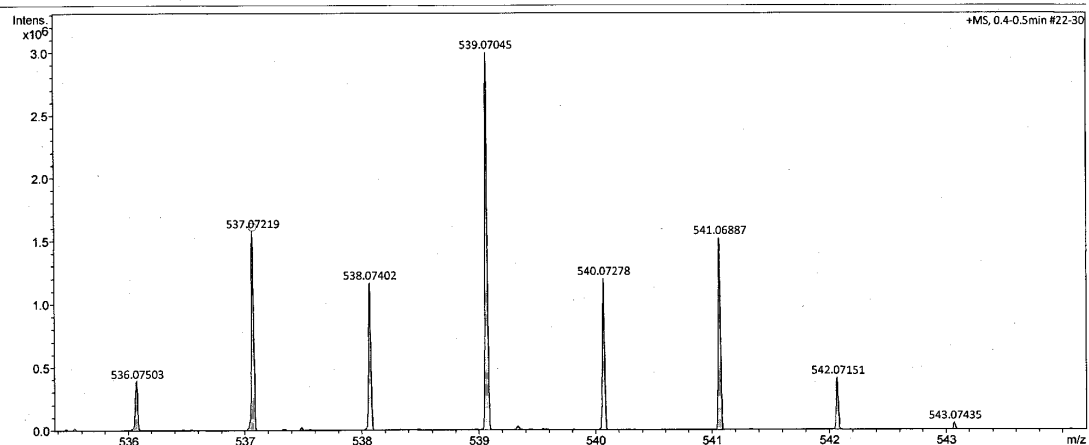


Figure S3: ^{13}C -NMR of **2** in CD_2Cl_2 .

Display Report

Analysis Info	D:\Data\oil\Fingerle MF 150_GB5_01_33040.d	Acquisition Date	7/11/2019 11:39:55 AM
Analysis Name	fia_ms_50-1300_pos_apci_neu.m	Operator	BDAL@DE
Method	Fingerle MF 150	Instrument	maXis
Sample Name			288882.21253
Comment			

Acquisition Parameter	APCI	Ion Polarity	Positive	Set Nebulizer	2.5 Bar
Source Type	Not active	Set Capillary	2000 V	Set Dry Heater	250 °C
Focus	50 m/z	Set End Plate Offset	-500 V	Set Dry Gas	4.0 l/min
Scan Begin	1300 m/z	Set Charging Voltage	0 V	Set Divert Valve	Waste
Scan End		Set Corona	3000 nA	Set APCI Heater	400 °C



Fingerle MF 150_GB5_01_33040.d
Bruker Compass DataAnalysis 4.2

printed: 7/11/2019 12:49:00 PM

by: BDAL@DE

Page 1 of 1

Figure S4: HR-APCI of **2**.

High Resolution MS

- FT-ICR-MS
 ESI- oder APCI-TOF-MS (MS/MS möglich)
 egal (je nach freien Kapazitäten)

Name: Fingerle

AK: Bettinger

Tel.

email:

Datum:

Probenbezeichnung: MF150 nominelle Masse:

Falls Masse nicht bekannt, welcher Massenbereich soll gemessen werden:

Summenformel (falls bekannt): $C_{26}H_{27}Br_2N_2$

Strukturformel (falls bekannt):

Einwaage (zwischen 0,1 mg und 2 mg):

Löslich in:

Falls schon gelöst, in welchem Lösemittel und in welcher Konzentration:

Hinweise bezüglich Zersetzlichkeit:

Hinweise bezüglich Toxizität (wenn bekannt):

Hohe Massengenauigkeit erwünscht? ja/nein

Massenanalyse erwünscht?

Wenn ja, welche Elemente sollen berücksichtigt werden?

MS/MS erwünscht?:

Ergebnis:

$[M+H]^+$ (theor.) = $537,07068$ ¹¹⁴

Gemessen = $537,07219$

Relative Massenabweichung = $1,95$ ppm

Figure S5: Data sheet of HR-APCI of 2.

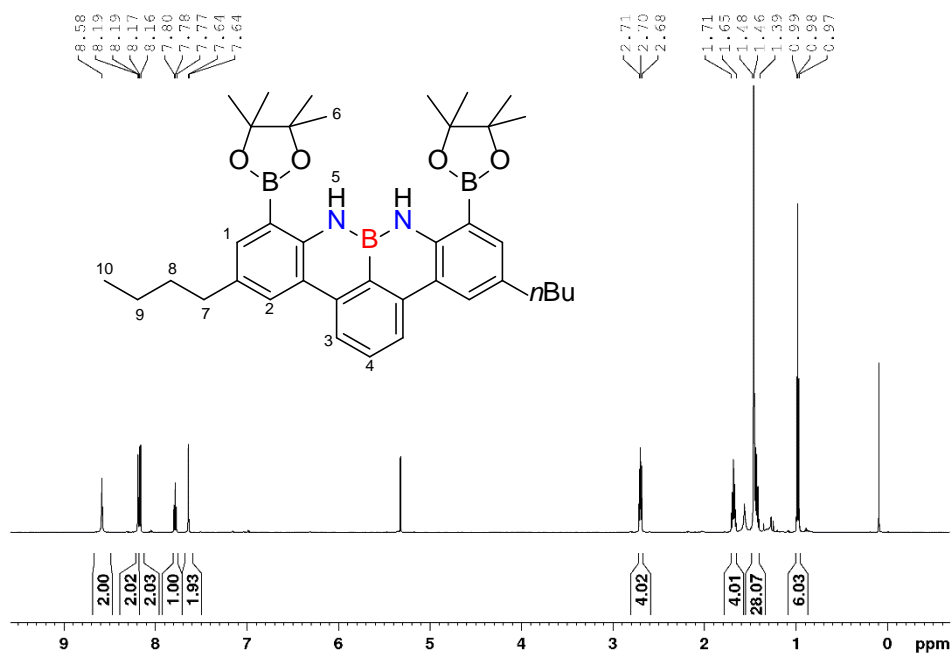


Figure S6: $^1\text{H-NMR}$ of **3** in CD_2Cl_2 .

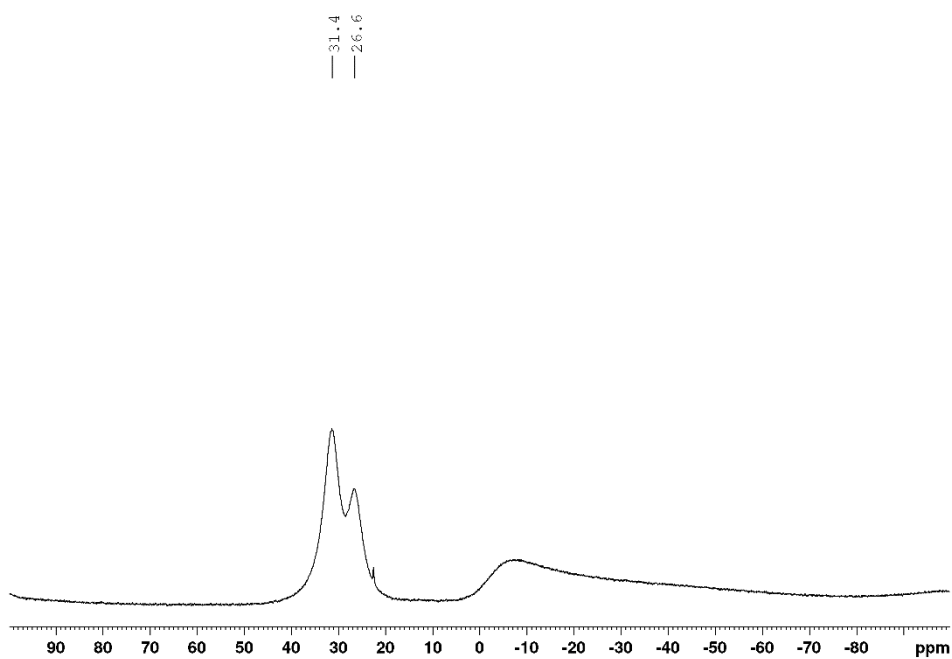


Figure S7: $^{11}\text{B-NMR}$ of **3** in CD_2Cl_2 .

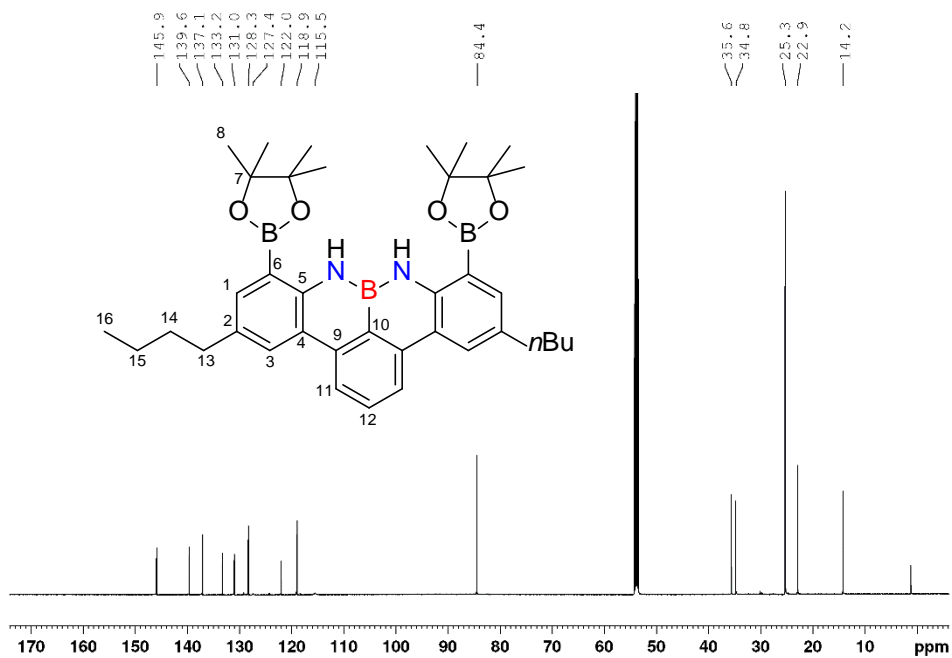


Figure S8: ^{13}C -NMR of **3** in CD_2Cl_2 .

File :D:\MassHunter\GCMS\1\data\Fingerle MF 151_1.D
 Operator :
 Acquired : 15 Feb 2019 12:02 using AcqMethod EI_30-1000_B_M
 Instrument : MSD 5977
 Sample Name: Fingerle MF 151
 Misc Info : EI-Quelle; 230°C
 Vial Number: 1

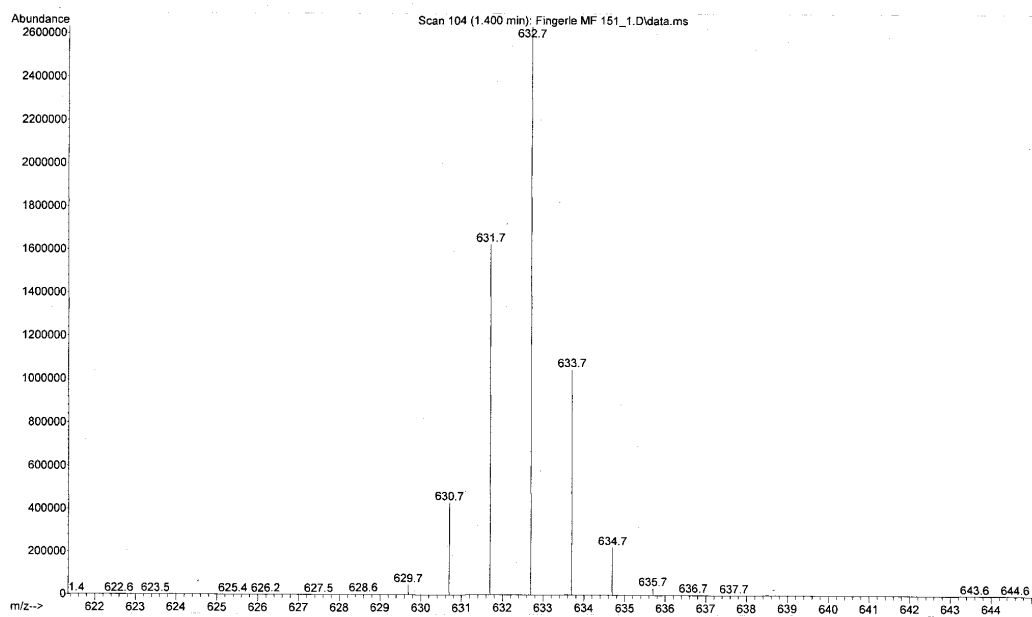


Figure S9: EI-MS spectra of **3**.

M a s s e n f e i n b e s t i m m u n g

Name: Fingerle Probenbezeichnung: MF 151

Ionisierungsmethode: EI ..X... FAB

Massenspektrometer: MAT 95

Referenz - Ion und seine exakte Masse:

$C_{12}F_{24}N^+$ 614 613,96418

die gefundene exakte Masse erhält man zu: 632,40571

damit ergibt/ergeben sich folgende Elementkombination(en) :

Measured Mass	Tolerance (mmu)	Charge on Molecule	Min	Max
632.40571	10	1	C	0 45
			[13]C	0 0
			H	0 90
			D	0 0
			N	0 2
			[15]N	0 0
			O	3 4
			F	0 0
			Na	0 0
			Si	0 0
			P	0 0
			S	0 0
			B	3 3
			Br	0 0

Formula: RDB Calc Mass Deviation mmu
C38H51N204B3 16.0 632.412252 -6.542

Searched 21060
Hits 1

OK Cancel Calculate Print Print setup SaveAs Copy

Datum: 25. Feb. 2019

MS - Nummer:

190054

Figure S10: Data sheet of HR-EI of 3.

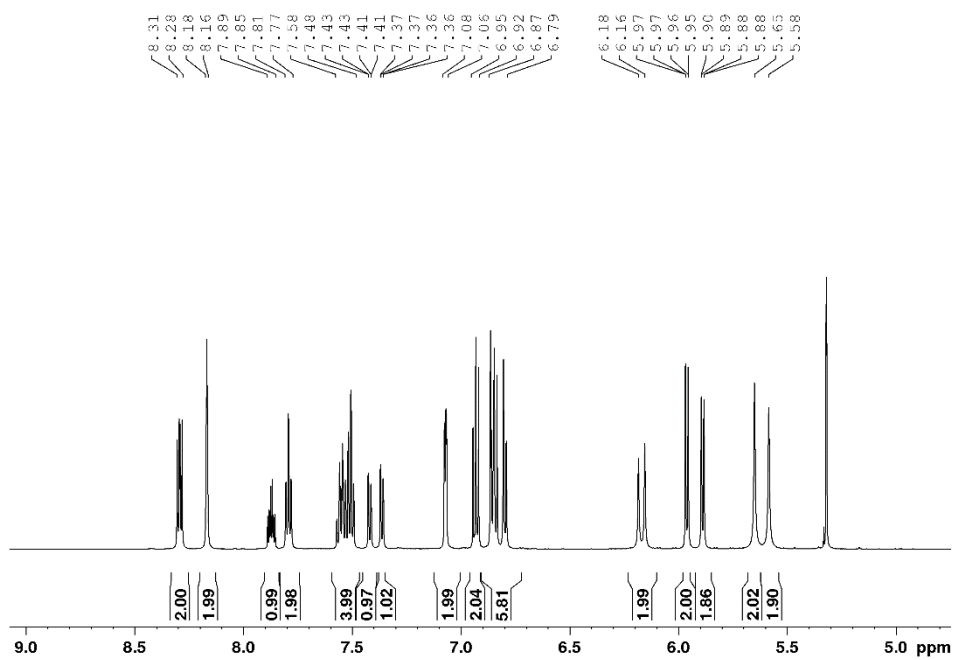


Figure S11: $^1\text{H-NMR}$ (aromatic signals) of **4** in CD_2Cl_2 .

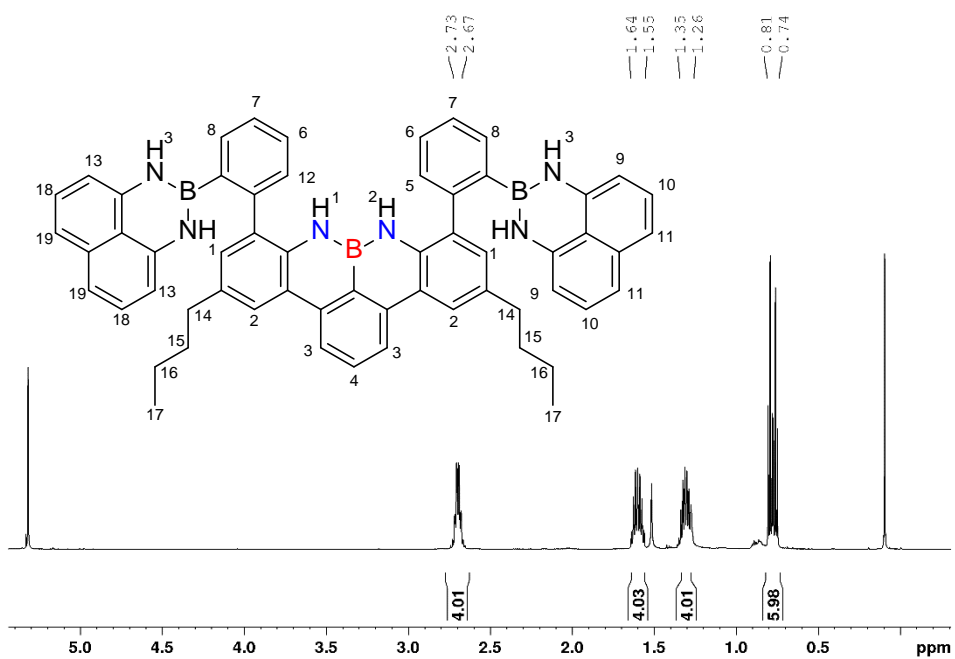
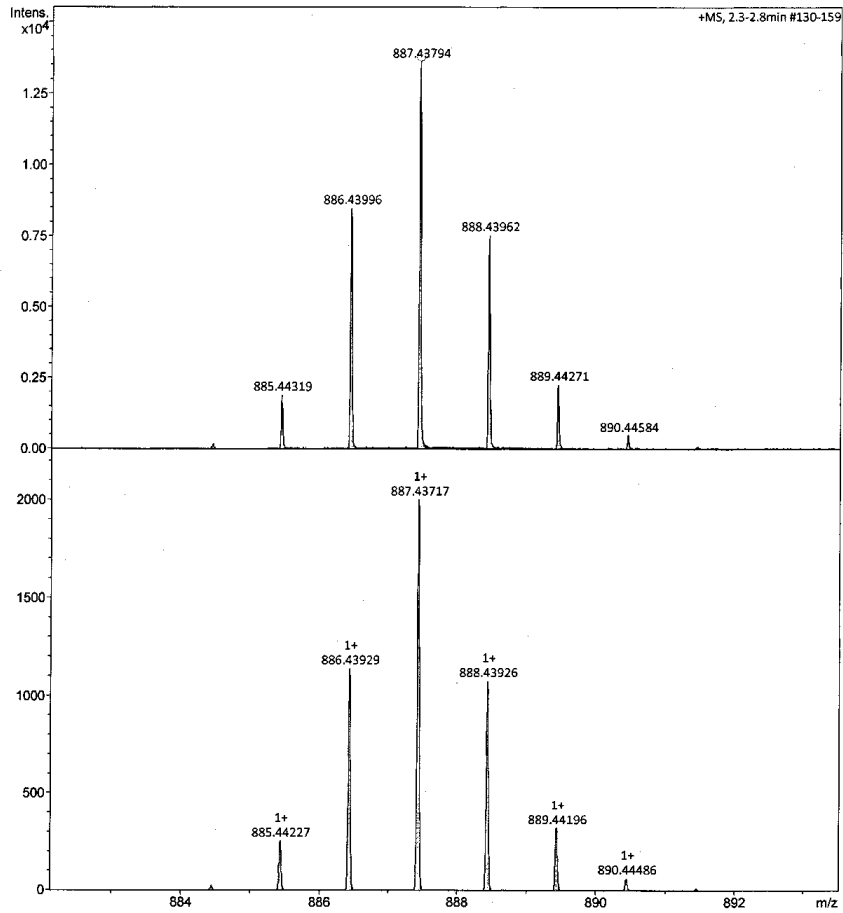


Figure S12: $^1\text{H-NMR}$ (non-aromatic signals) of **4** in CD_2Cl_2 .

Display Report

Analysis Info
Analysis Name D:\Data\01\Bettinger_Fingerle_MF152000001.d
Method tune_low_neu.m
Sample Name MF152
Comment
Acquisition Date 2/14/2019 3:44:48 PM
Operator BDAL@DE
Instrument maXis 288882.21253

Acquisition Parameter
Source Type ESI
Focus Active
Scan Begin 50 m/z
Scan End 1250 m/z
Ion Polarity Positive
Set Capillary 4500 V
Set End Plate Offset -500 V
Set Charging Voltage 0 V
Set Corona 0 nA
Set Nebulizer 1.0 Bar
Set Dry Heater 200 °C
Set Dry Gas 3.0 l/min
Set Divert Valve Waste
Set APCI Heater 0 °C



Bettinger_Fingerle_MF152000001.d
Bruker Compass DataAnalysis 4.2
printed: 2/19/2019 2:25:01 PM
by: BDAL@DE
Page 1 of 1

Figure S13: HR-APCI of 4.

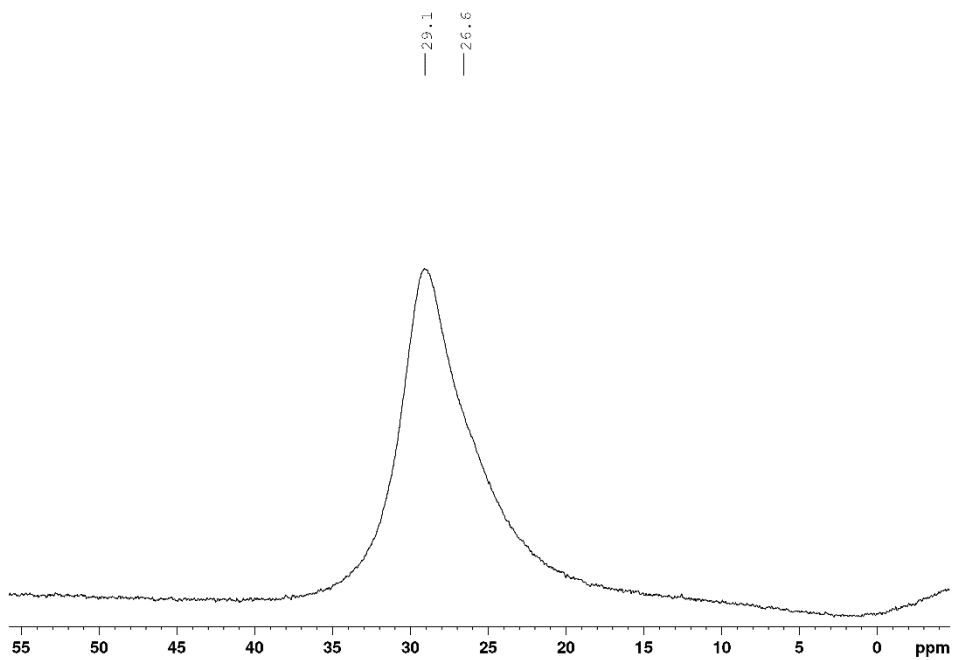


Figure S14: ^{11}B -NMR of **4** in CD_2Cl_2 .

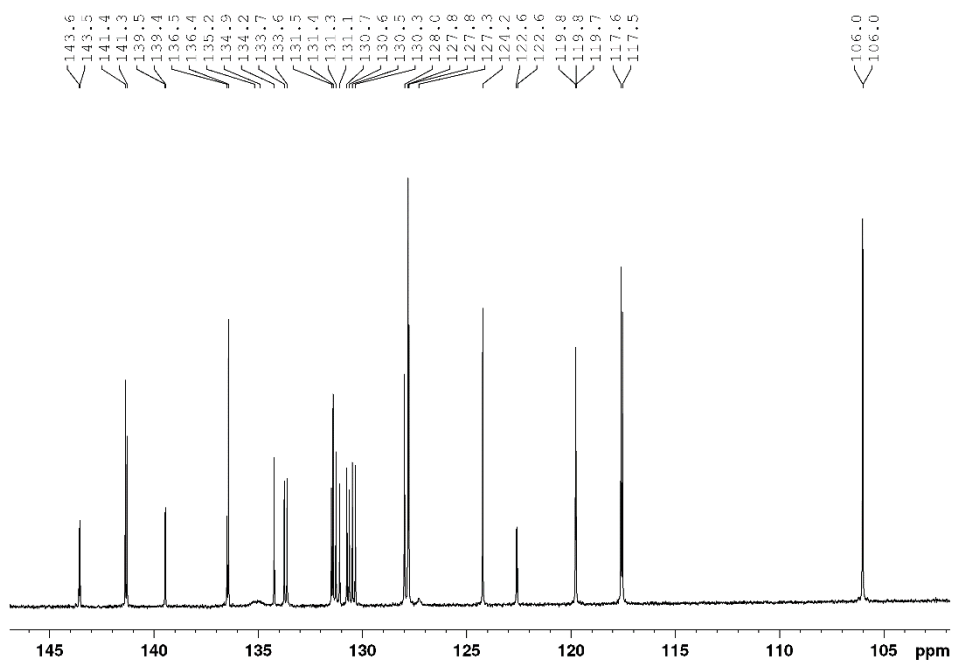


Figure S15: ^{13}C -NMR (aromatic signals) of **4** in CD_2Cl_2 .

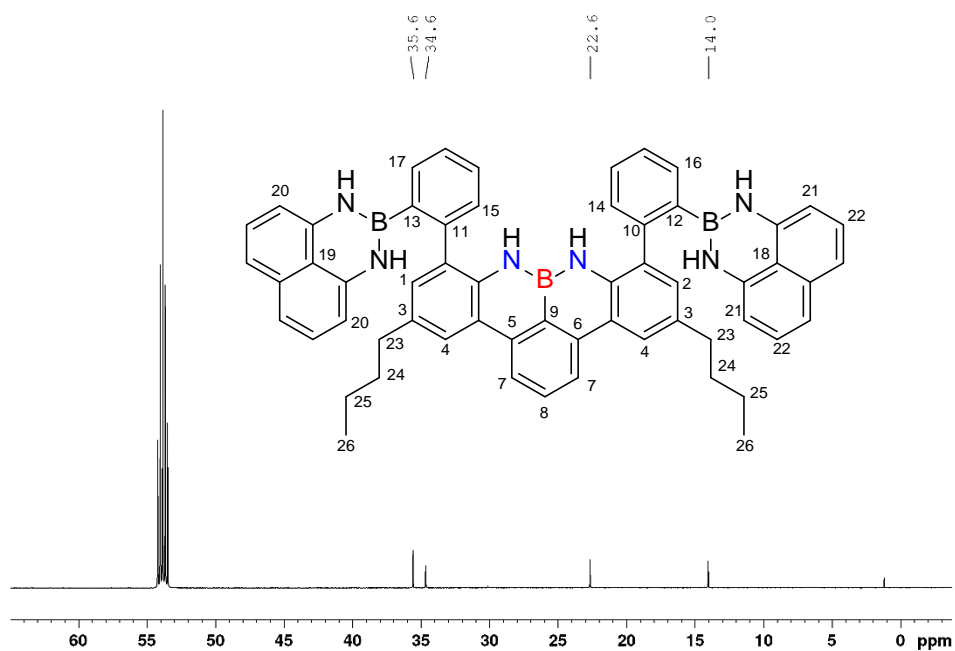


Figure S16: ^{13}C -NMR (non-aromatic signals) of **4** in CD_2Cl_2 .

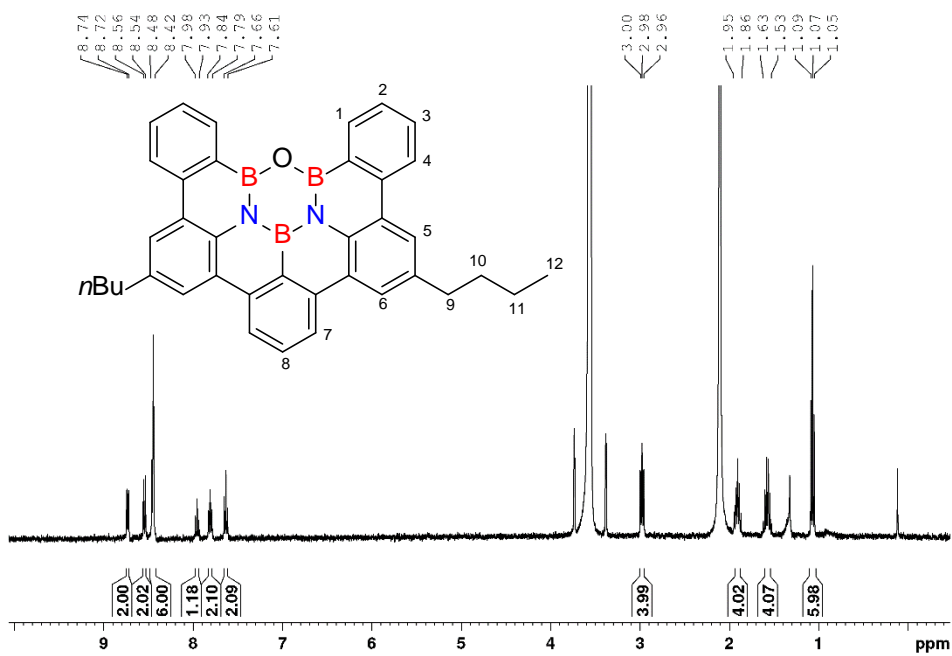


Figure S17: ^1H -NMR (aromatic signals) of **A** in dioxane- d_8 at 80 $^\circ\text{C}$.

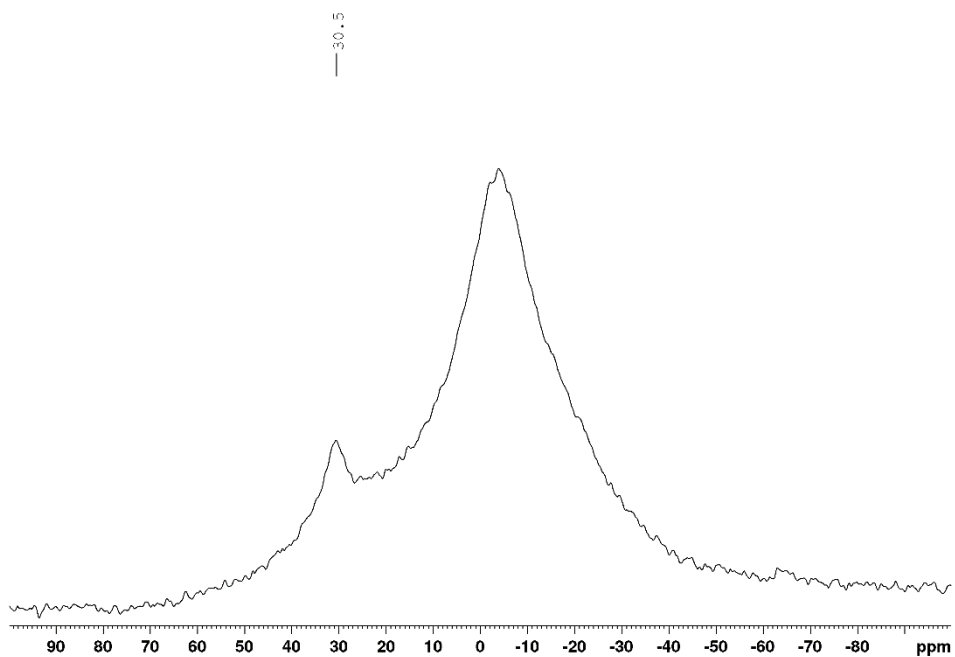


Figure S18: ^{11}B -NMR of A in dioxane- d_8 at 80 °C.

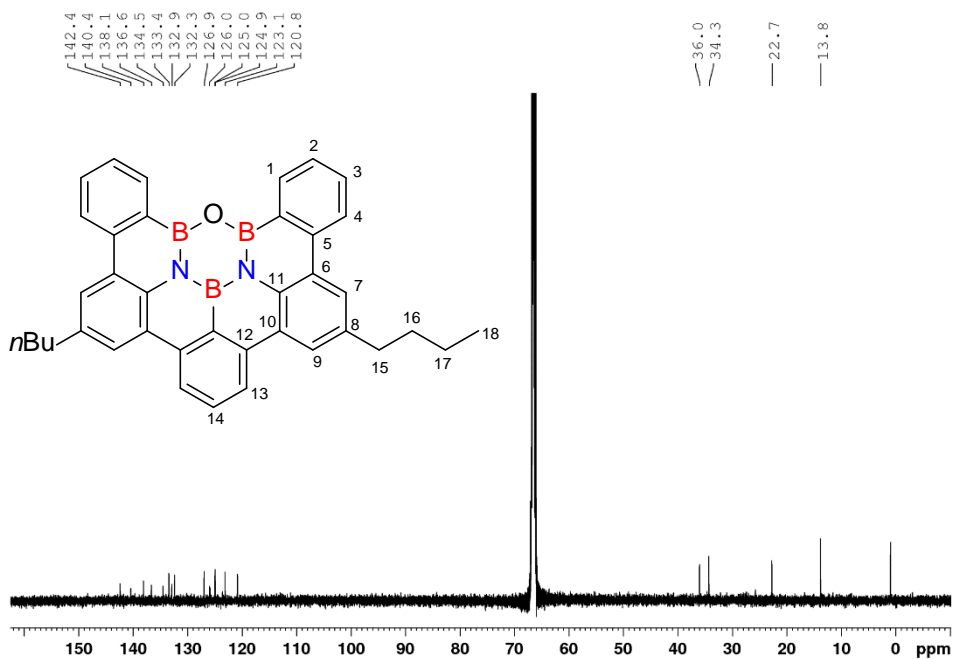


Figure S19: ^{13}C -NMR of A in dioxane- d_8 at 80 °C.

EuroEA Elemental Analyser



AutoRun name : AG Bettinger-052219 (125)
Date of Analysis : 22 May 2019
Time of Analysis : 13:16:11
Analysed by : ea

Signed By : ea
Operator Group : GRP1
Configuration : CHNS

Calibration Type : K-Factor

Results Summary for Element %

#	Type	Name	N %	C %	H %	S %	O %	Weight (mg)
1	Blk	Blank	-	-	-	-	-	-
2	Blk	Blank	-	-	-	-	-	-
3	Std	Sulphanilamide	16.430	42.021	4.718	18.641	-	1.724
4	Std	Sulphanilamide	16.107	41.677	4.649	18.601	-	1.139
5	Smp	MF 153	5.118	80.879	5.900	-	-	1.078
6	Smp	MF 153	4.960	80.969	5.889	-	-	1.053

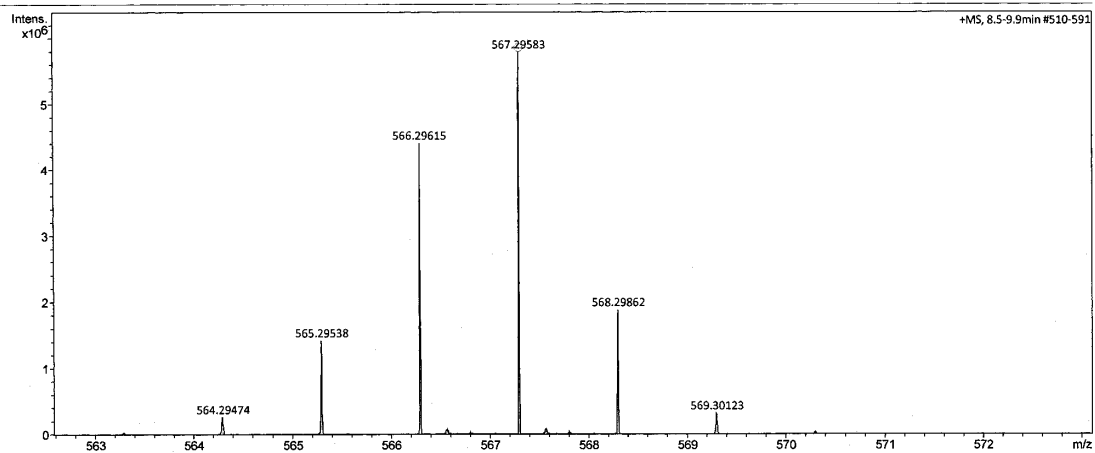
berchnet: 4,95 80,62 5,88 %

Figure S20: Elementary analysis of A.

Display Report

Analysis Info		Acquisition Date 1/13/2020 2:26:56 PM	
Analysis Name	D:\Data\oil\Fingerle_MF 153000001.d	Operator	BDAL@DE
Method	tune_low_apci_DIP_neu.m	Instrument	maXis 288882.21253
Sample Name			
Comment			

Acquisition Parameter			
Source Type	APCI	Ion Polarity	Positive
Focus	Active	Set Capillary	4500 V
Scan Begin	100 m/z	Set End Plate Offset	-500 V
Scan End	2200 m/z	Set Charging Voltage	0 V
		Set Corona	4000 nA
		Set Nebulizer	2.0 Bar
		Set Dry Heater	220 °C
		Set Dry Gas	3.0 l/min
		Set Divert Valve	Waste
		Set APCI Heater	400 °C



Fingerle_MF 153000001.d
 Bruker Compass DataAnalysis 4.2 printed: 1/13/2020 2:52:22 PM by: BDAL@DE Page 1 of 1

Figure S21: HR-APCI of A.

High Resolution MS

- FT-ICR-MS
- ESI- oder APCI-TOF-MS (MS/MS möglich)
- egal (je nach freien Kapazitäten)

Name: _____ AK: _____
Tel. _____ email: _____
Datum: _____
Probenbezeichnung: **MF153** nominelle Masse: _____
Falls Masse nicht bekannt, welcher Massenbereich soll gemessen werden:
Summenformel (falls bekannt): _____
Strukturformel (falls bekannt): _____

Einwaage (zwischen 0,1 mg und 2 mg): _____

Löslich in: _____

Falls schon gelöst, in welchem Lösemittel und in welcher Konzentration: _____

Hinweise bezüglich Zersetzlichkeit: _____

Hinweise bezüglich Toxizität (wenn bekannt): _____

Hohe Massengenauigkeit erwünscht? _____ ja/nein

Massenanalyse erwünscht? _____

Wenn ja, welche Elemente sollen berücksichtigt werden? _____

MS/MS erwünscht?: _____

Ergebnis:

$$[M + H]^+_{(\text{theor.})} = 567,29448 \quad \underline{\underline{567,29627}}$$

$$\text{Gemessen} = 567,29583$$

$$\text{Relative Massenabweichung} = 0,81 \text{ ppm}$$

Figure S22: Data sheet of HR-APCI of A.

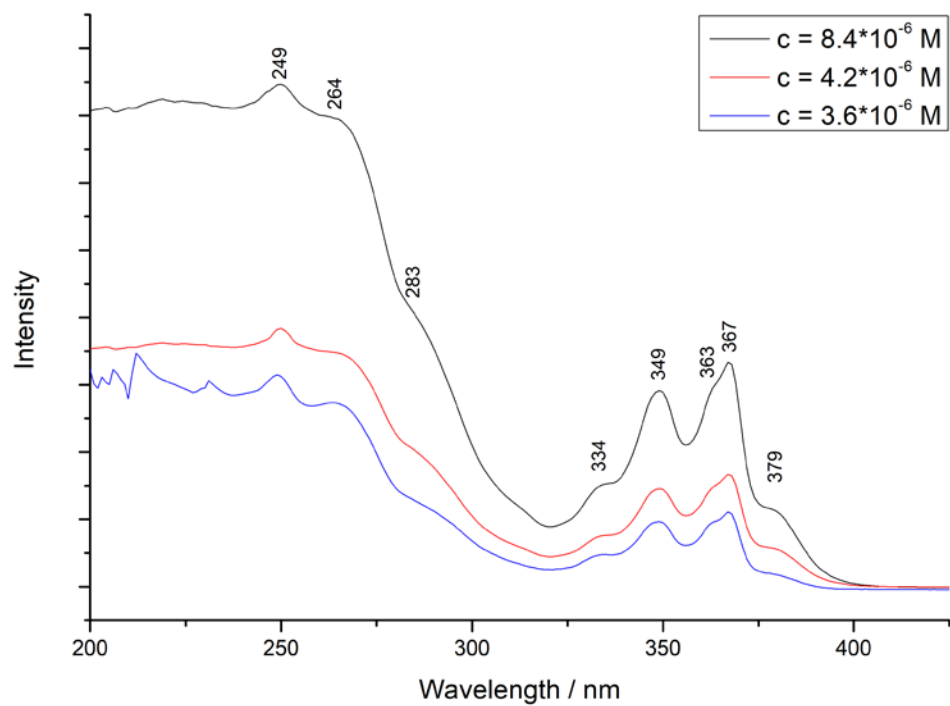


Figure S23: UV-Vis spectra of **A** in dioxane (various concentrations).

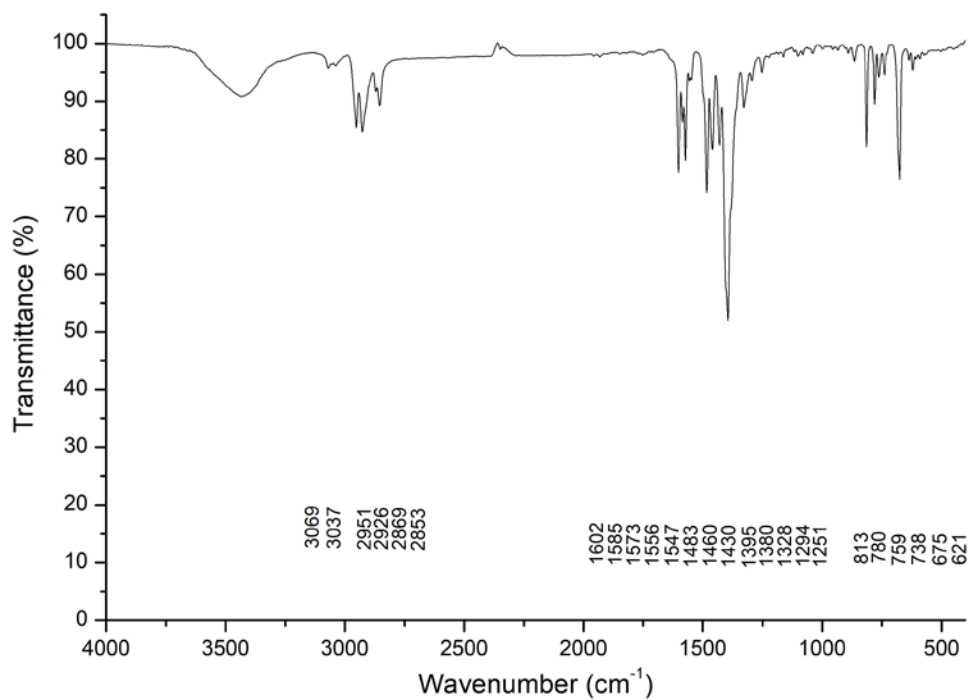


Figure S24: IR (KBr) spectra of **A**.

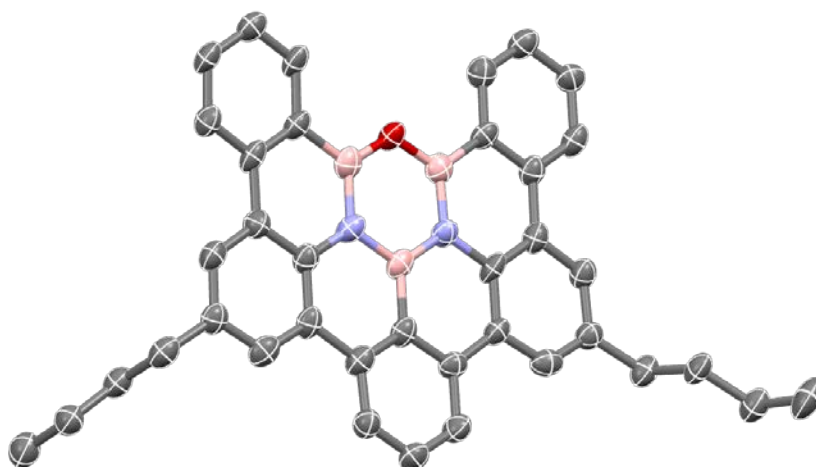


Figure S25: Molecular structure of **A** (hydrogens are omitted for clarity).

References

1. K. Kim and K. D. Jordan, *J. Phys. Chem.*, 1994, **98**, 10089-10094.
2. P. J. Stephens, F. J. Devlin, C. F. Chabalowski and M. J. Frisch, *J. Phys. Chem.*, 1994, **98**, 11623-11627.
3. M. J. Frisch, G. W. Trucks, H. B. Schlegel, G. E. Scuseria, W. A. Robb, J. R. Cheeseman, G. Scalmani, V. Barone, G. A. Petersson, H. Nakatsuji, X. Li, M. Caricato, A. Marenich, J. Bloino, B.

- G. Janesko, R. Gomperts, B. Mennucci, H. P. Hratchian, J. V. Ortiz, A. F. Izmaylov, J. L. Sonnenberg, D. Williams-Young, F. Ding, F. Lipparini, F. Egidi, J. Goings, B. Peng, A. Petrone, T. Henderson, D. Ranasinghe, V. G. Zakrzewski, J. Gao, N. Rega, G. Zheng, W. Liang, M. Hada, M. Ehara, K. Toyota, R. Fukuda, J. Hasegawa, M. Ishida, T. Nakajima, Y. Honda, O. Kitao, H. Nakai, T. Vreven, K. Throssell, J. A. Montgomery, J. E. P. Jr., F. Ogliaro, M. Bearpark, J. J. Heyd, E. Brothers, K. N. Kudin, V. N. Staroverov, T. Keith, R. Kobayashi, J. Normand, K. Raghavachari, A. Rendell, J. C. Burant, S. S. Iyengar, J. Tomasi, M. Cossi, J. M. Millam, M. Klene, C. Adamo, R. Cammi, J. W. Ochterski, R. L. Martin, K. Morokuma, O. Farkas, J. B. Foresman and D. J. Fox, *Gaussian 09*, Revision A.02; Gaussian, Inc.: Wallingford CT, 2009.
4. R. Krishnan, J. S. Binkley, R. Seeger and J. A. Pople, *J. Chem. Phys.*, 1980, **72**, 650-654.
 5. R. E. Stratmann, G. E. Scuseria and M. J. Frisch, *J. Chem. Phys.*, 1998, **109**, 8218-8224.
 6. Z. Chen, C. S. Wannere, C. Corminboeuf, R. Puchta and P. v. R. Schleyer, *Chem. Rev.*, 2005, **105**, 3842-3888.
 7. P. v. R. Schleyer, H. Jiao, N. J. R. v. E. Hommes, V. G. Malkin and O. L. Malkina, *J. Am. Chem. Soc.*, 1997, **119**, 12669-12670.
 8. G. E. Herberich, H.-W. Marx, S. Moss, P. v. R. Schleyer and T. Wagner, *Chem. Eur. J.*, 1996, **2**, 458-461.
 9. K. Wolinski, J. F. Hinton and P. Pulay, *J. Am. Chem. Soc.*, 1990, **112**, 8251-8260.
 10. D. Geuenich, K. Hess, F. Köhler and R. Herges, *Chem. Rev.*, 2005, **105**, 3758-3772.
 11. R. Herges and D. Geuenich, *J. Phys. Chem. A*, 2001, **105**, 3214-3220.

Synthetic Methods

Heteroatom Cycloaddition at the (BN)₂ Bay Region of Dibenzoperylene

Michael Fingerle, Juliane Dingerkus, Hartmut Schubert, Kai M. Wurst, Marcus Scheele, and Holger F. Bettinger*

Abstract: Cycloaddition-dehydration involving a BNBN-butadiene analogue at the bay region of a dibenzoperylene and a non-enolizable aldehyde provides a novel strategy for incorporation of the oxadiazaborinane (B₂N₂CO) ring into the scaffold of a polycyclic aromatic hydrocarbon resulting in highly emissive compounds.

The introduction of heteroatoms is a very popular strategy to modify the electronic properties of polycyclic aromatic hydrocarbons (PAHs) for application as organic electronic materials.^[1] In particular, the isoelectronic and isosteric exchange of carbon-carbon (CC) by boron and nitrogen pairs (BN) opened a huge field of novel organic materials since the report of the first BN doped PAH in 1958.^[2] In addition to BN substitution, the incorporation of oxygen atoms is a useful approach to develop new compounds for material applications and catalysis.^[1,3]

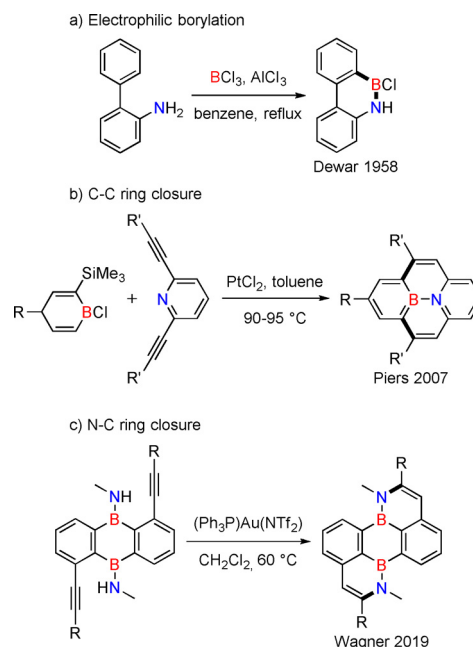
Among the available methods for synthesizing 1,2-azaborine containing PAHs, the electrophilic borylation, introduced by Dewar^[2a] and optimized further, is attractive as both B–N and B–C bonds are constructed in one synthetic step (Scheme 1 a).^[2h,3a,4] Alternatively, the coupling of carbon-carbon (CC) bonds around existing BN units has occasionally been employed, e.g., by Piers,^[5] Bonifazi,^[3b,6] and our group (Scheme 1 b).^[7] The Wagner group^[8] described the Au catalyzed NC bond formation as the final step of the synthesis of a doubly BN substituted perylene (Scheme 1 c).^[8,9]

Perylenes and dibenzoperylenes with BN doping have been synthesized by Wagner, Bonifazi and our group.^[3b,4j,8,10] We have developed a multistep synthesis of a dibenzoperylene

How to cite: *Angew. Chem. Int. Ed.* **2021**, *60*, 15798–15802

International Edition: doi.org/10.1002/anie.202016699

German Edition: doi.org/10.1002/ange.202016699



Scheme 1. Selected representative examples of available methods for synthesis of 1,2-azaborine containing PAHs.

1 that features a BNBN unit at its bay region.^[4j] It would be interesting to use this heterodiene as functional group for widening the chemical space in heteroatom doped PAH synthesis by cycloaddition reactions. Cycloaddition reactions at the bay region of perylene are well known (Scheme 2),^[11] and they were even suggested for growth of carbon nanotubes by reaction of armchair rims with acetylene.^[12] However, the analogous cycloaddition reaction of heteroatom bay region substituted PAHs are unknown. The closest to this are cycloaddition reactions of diazadiboretidines, which are the quite reactive BN analogs of antiaromatic cyclobutadiene. Paetzold postulated hetero-Diels–Alder reactions of diazadiboretidines with ketones and aldehydes forming 1,3,5,2,4-oxadiazaborinane (B₂N₂CO) rings under ring extension (Scheme 2).^[13]

The cycloaddition of **A** (a model for **1** without the n-Bu groups) with typical electron rich (TCNE, TME) or electron poor dienophiles (methyl vinyl ether, see Figure 1) is unfavorable as revealed by quantum chemical calculations (M062X/6–311 + G**), even after dehydration. However, the reaction **A** → **C** + H₂O becomes mildly exergonic if the polar carbonyl group of benzaldehyde is employed as

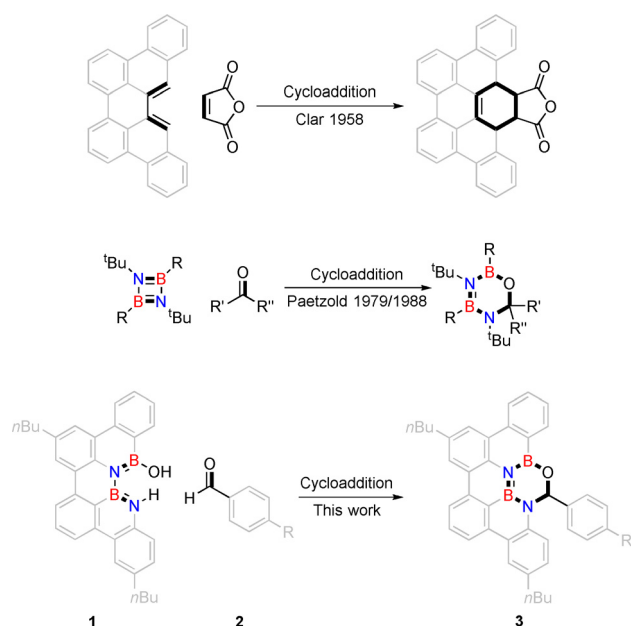
*] M. Fingerle, J. Dingerkus, Prof. Dr. H. F. Bettinger
Institut für Organische Chemie, Universität Tübingen
Auf der Morgenstelle 18, 72076 Tübingen (Germany)
E-mail: holger.bettinger@uni-tuebingen.de

Dr. H. Schubert
Institut für Anorganische Chemie, Universität Tübingen
Auf der Morgenstelle 18, 72076 Tübingen (Germany)

K. M. Wurst, Prof. Dr. M. Scheele
Institut für Physikalische und Theoretische Chemie
Universität Tübingen
Auf der Morgenstelle 18, 72076 Tübingen (Germany)

Supporting information and the ORCID identification number(s) for the author(s) of this article can be found under:
https://doi.org/10.1002/anie.202016699.

© 2021 The Authors. Angewandte Chemie International Edition published by Wiley-VCH GmbH. This is an open access article under the terms of the Creative Commons Attribution Non-Commercial License, which permits use, distribution and reproduction in any



Scheme 2. Cycloaddition reactions of dibenzoperylene (top), diazaboretidines (center) and BN bay region doped dibenzoperylene (bottom).

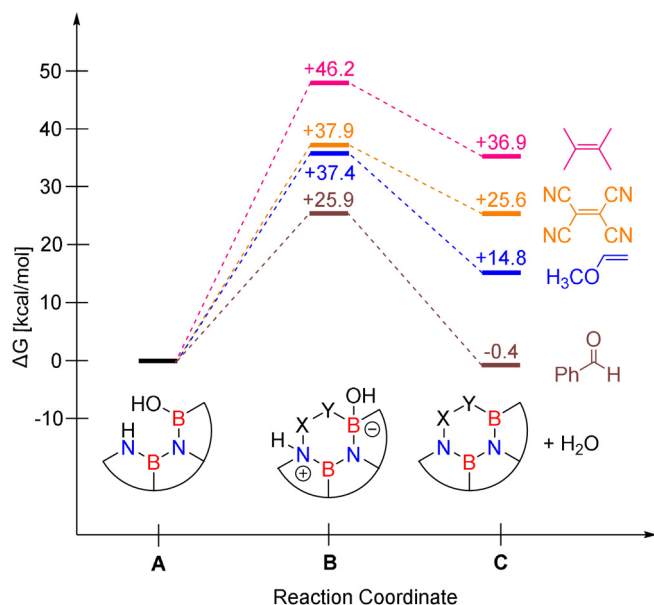


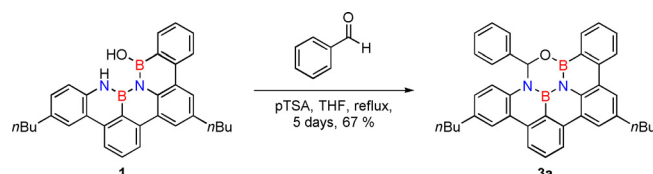
Figure 1. Free energy differences for different dienophiles calculated at the M062X/6-311+G** level of theory ($T=298.15$ K); (BN)₂ dibenzoperylene scaffolds **A**, **B** and **C** are abbreviated for clarity.

dienophile. For reactions with other hetero dienophiles, see Supporting Information (SI).

Heating **1** and benzaldehyde in THF even for a long period of time does not result in any reaction. To facilitate the dehydration that is necessary to have an exergonic reaction, we added an excess of para-toluenesulfonic acid (pTSA) in order to induce an acid catalyzed dehydration. To remove emerging water from equilibrium, we heated the mixture in the presence of molecular sieve in a Soxhlet extractor. Then, a slow reaction proceeds and after 5 days of reaction time, the

product **3a**, which is stable against oxygen and moisture, can be isolated in a good yield of 67% by column chromatography.

Compound **3a** (Scheme 3) can be characterized by multinuclear (¹H, ¹³C, ¹¹B) and correlated NMR spectroscopy (2D spectra) as well as by high resolution mass spectrometry. Notably, the ¹H NMR shows one singlet for the benzylic proton in the ON₂B₂C-ring that experiences significant deshielding and resonates at 7.02 ppm (see SI, Figure S1). The ¹¹B spectrum of **3a** shows a broad signal at 28.3 ppm for both boron atoms (see SI, Figure S3).



Scheme 3. Heteroatom cycloaddition reaction with benzaldehydes; 1 equiv **1**, 10 equiv benzaldehyde, 10 equiv pTSA, THF, Soxhlet extractor with 3 Å molecular sieve, reflux, 5 days.

Single crystals for X-ray crystallography were obtained by recrystallization from THF (for crystallographic data see SI). Compound **3a** crystallizes in the triclinic space group $P\bar{1}$ with two enantiomeric molecules due to the asymmetric sp³ carbon in the B₂N₂CO ring (see Figure 2). The dibenzoperylene motif is responsible for intermolecular π - π stacking with a distance of 3.5 Å between molecular planes, while the single phenyl groups as well as one butyl group feature towards the next molecular layer. The BN bond lengths average 1.43 Å, slightly shorter than analogous bond lengths in typical BN doped PAHs (1.45–1.47 Å).^[5a,14] The CO, BO and NC bond length are in good agreement with the literature.^[15] The newly formed heterocycle adopts a puckered geometry with a tilt angle of 18.15° involving the BNB and NCO planes. This ring

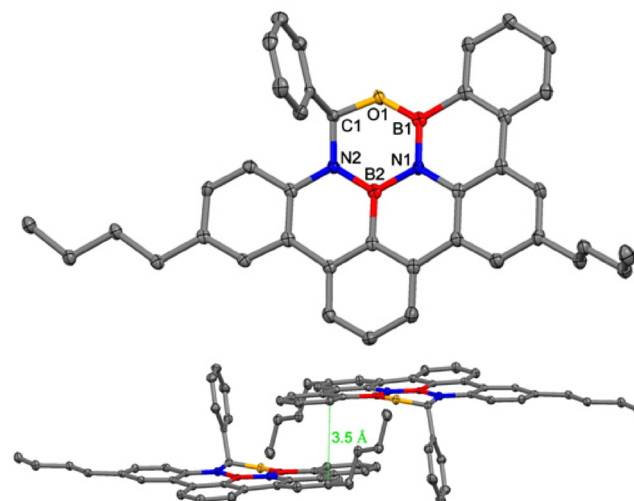


Figure 2. Molecular structure of **3a** (hydrogen atoms omitted for clarity (top), ellipsoids set at 50% probability; selected bond length of **3a** in Å: O1-B1 1.376, B1-N1 1.420, N1-B2 1.444, B2-N2 1.422, N2-C1 1.468, C1-O1 1.430; packing of **3a** (bottom).^[20]

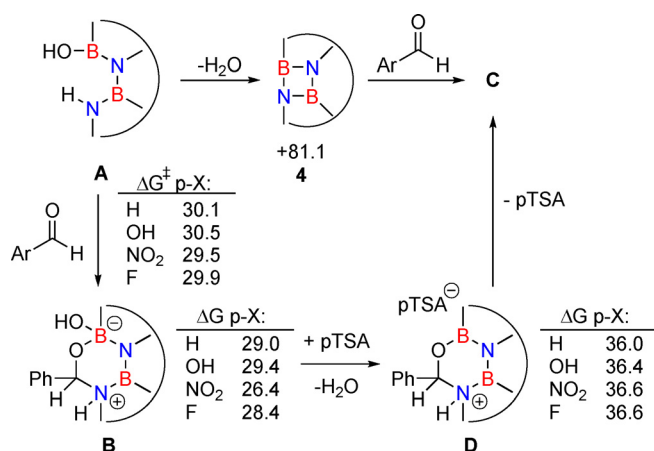
has a sp^3 hybridized carbon center and is expected to be non-aromatic as confirmed by NICS(1) computations (see SI, Figure S40).^[16] While the four all-carbon rings of the PAH backbone have large negative NICS(1), the heteroatom containing rings have small NICS(1) values, reminiscent of the related boroxazine derivative.^[3c]

In order to investigate substituent effects, a number of aryl aldehydes were employed in the reaction (Table 1). The reaction time and yield are not affected significantly by the electronic nature of the substituent (Table 1, entries 1–4) as revealed by TLC monitoring of the disappearance of **1**. Mesitaldehyde can also be used as a dienophile, but provides lower yields due to steric hindrance (Table 1, entry 5). The product with the sterically more encumbered pivalaldehyde can only be detected in low yields (Table 1, entry 6) and with some impurities (see SI Figure S32). The α,β -unsaturated cinnamaldehyde undergoes this cycloaddition reaction in good yields (Table 1, entry 7) and selectively at the aldehyde function as no product resulting from cycloaddition to the $C=C$ double bond is observed. All dehydrated cycloaddition products are stable against oxygen and moisture and can be purified by column chromatography.

Table 1: Screening of different dienophiles in cycloaddition reaction with $(BN)_2$ -dibenzoperylene and yield values. Conditions as in Scheme 3.

Entry	Dienophile	Product	Yield [%]
1			67
2			74
3			73
4			80
5			40
6			15
7			77

The influence of pTSA on the reagents was investigated by NMR spectroscopy in $[D_8]THF$. A mixture of pTSA and benzaldehyde gives unchanged 1H NMR spectra compared to individual compounds. This observation is in line with the pK_a values of pTSA (-2.8)^[17] and of protonated benzaldehyde (-7.1).^[18] On the other hand, the signal of the OH group of **1** at 9.06 ppm (assignment based on 2D NMR) turns broad at low concentrations of pTSA and becomes weaker and broader with increasing the pTSA concentration, indicating rapid exchange between the OH proton and the acidic proton of pTSA. The NH proton is not affected by the presence of pTSA and its signal remains sharp at 9.78 ppm. These results indicate that the OH group is involved in dynamic proton exchange with pTSA in THF solution. The action of pTSA could result in acid catalyzed dehydration of **1** to give the diazadiboretidine intermediate **4** (Scheme 4). Recall that



Scheme 4. Possible mechanisms as computed at the M062X/6–311 + G** level of theory in THF solution ($T = 339$ K). Energy data is given in $kcal\ mol^{-1}$.

these species were previously reported to undergo cycloaddition reactions with aldehydes (see Scheme 2).^[13a,b] Computations on the model system **A** without the n-Bu groups at the M062X/6–311 + G** level of theory with a continuum model to mimic the THF solvent effect show that formation of **4** is a very high energy process, $\Delta G(THF) = +81.1\ kcal\ mol^{-1}$ (Scheme 4). Therefore, **4** cannot be relevant for the mechanism of the dehydrative cycloaddition reaction. However, neutral **A** can undergo the concerted cycloaddition with benzaldehyde with a barrier of $30.1\ kcal\ mol^{-1}$, and this barrier is changed by at most $0.4\ kcal\ mol^{-1}$ in the presence of para substituents (p-OH, p- NO_2 , p-F) on the aryl group of the aldehyde (Scheme 4). The cycloaddition product **B** is a very shallow minimum on the potential energy surface as the barrier for the back reaction to the reagents is merely 1–3 $kcal\ mol^{-1}$ depending on p-X (Scheme 4). The pTSA could then cause acid catalyzed dehydration of **B** to give intermediate **D** (Scheme 4) that is higher in energy than **B** by roughly 8 $kcal\ mol^{-1}$. The energy barriers of the cycloaddition step and its insensitivity to electronic substituent effects of the aryl aldehydes are in qualitative agreement with the experimental observations that the reaction rate is independent of

the benzaldehyde concentration but that addition of acid is essential. Alternatively, the OH protonated form of **1**, a borenium ion, could undergo the cycloaddition presumably with a decreased activation barrier, but the Gibbs free energy ($T = 339\text{ K}$) of this borenium ion is higher than that of **D** by roughly 12 kcal mol^{-1} .

The absorption and fluorescence spectra of compounds **3a–e** and **3g** were recorded in dichloromethane solutions (see Figure 3). The spectra resemble each other and are quite similar to those of **1**. The substituents in **3b–e** or the presence of the C=C bridge in **3g** turned out to result in shifts of peak maxima of 1–2 nm. The Stokes shifts are small throughout (600 cm^{-1} – 755 cm^{-1} , see SI for details). The fluorescence quantum yields of all products except for **3c** is 78% and higher using 9,10-diphenylanthracene in ethanol as reference (see SI). The cycloaddition product with p-nitrobenzaldehyde **3c** only shows a low fluorescence quantum yield of 7%. The decrease of the fluorescence quantum yield of aromatic compounds upon introduction of a nitro groups is well known.^[19]

The electrochemical properties of **3a** were investigated by cyclic voltammetry. At scan rates greater than 2 V s^{-1} , we find a quasi-reversible reduction signal at $E^0 = -2.724\text{ V vs. Fc/}$

Fc^+ . At slow scan rates, the associated oxidation peak of this reduction signal is less pronounced, suggesting a slow chemical follow-up reaction of the reduced species of **3a** (EC mechanism). Two further signals with peak potentials at approx. -3.0 V and -3.1 V vs. Fc/ were found in the forward scan at 50 mV s^{-1} within our electrochemical window (see Supporting Information for details).

In summary, we described the first cycloaddition-dehydration reaction of a BNB bay region doped dibenzoperylene with different non-enolizable aldehydes forming new BN doped PAHs with an 1,3,5,2,4-oxadiazadiborinan ($\text{B}_2\text{N}_2\text{CO}$) ring. The reaction is robust towards the electronic structure of the aldehydes, but is affected by steric effects. The novel reaction products, PAH with an embedded oxadiazadiborinane ring, show very high fluorescence quantum yields ($>78\%$), which make this conjugation of BN-doped PAH with aldehydes a promising strategy towards enlarging the chemical scope in heteroatom doped PAH chemistry.

Acknowledgements

We thank Dr. P. Wagner for helpful discussions. This work was supported by the Vector Foundation. The authors acknowledge support by the state of Baden-Württemberg through bwHPC and the German Research Foundation (DFG) through grant no INST 40/575-1 FUGG (JUSTUS 2 cluster). Open access funding enabled and organized by Projekt DEAL.

Conflict of interest

The authors declare no conflict of interest.

Keywords: boron · cycloaddition · dibenzoperylene · nitrogen · polycycles

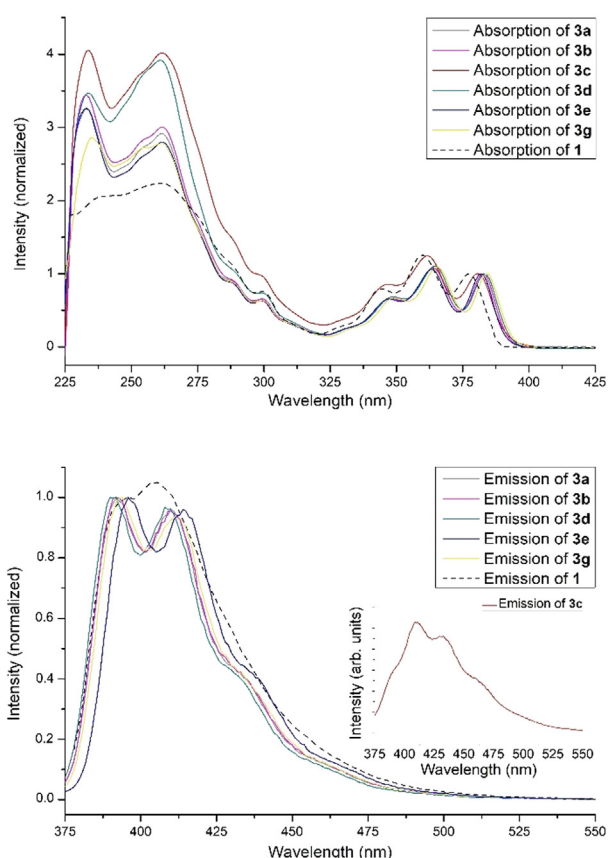


Figure 3. Absorption (normalized on maxima with longest wavelength, top) and fluorescence spectra ($\lambda_{\text{ex}} = 347\text{ nm}$, normalized on maxima with shortest wavelength, bottom) of the cycloaddition products in dichloromethane including absorption and fluorescence spectra of **1** (dashed line) for comparison. Inset: fluorescence spectrum of **3c** ($\Phi_{\text{f}} = 0.07$).

- [1] M. Stępień, E. Gońka, M. Żyła, N. Sprutta, *Chem. Rev.* **2017**, *117*, 3479–3716.
- [2] a) M. J. S. Dewar, V. P. Kubba, R. Pettit, *J. Chem. Soc.* **1958**, 3073–3076; b) M. J. D. Bosdet, W. E. Piers, *Can. J. Chem.* **2009**, *87*, 8–29; c) P. G. Campbell, A. J. V. Marwitz, S.-Y. Liu, *Angew. Chem. Int. Ed.* **2012**, *51*, 6074–6092; *Angew. Chem.* **2012**, *124*, 6178–6197; d) X.-Y. Wang, J.-Y. Wang, J. Pei, *Chem. Eur. J.* **2015**, *21*, 3528–3539; e) H. Helten, *Chem. Eur. J.* **2016**, *22*, 12972–12982; f) M. M. Morgan, W. E. Piers, *Dalton Trans.* **2016**, *45*, 5920–5924; g) Z. X. Giustra, S.-Y. Liu, *J. Am. Chem. Soc.* **2018**, *140*, 1184–1194; h) P. B. Pati, E. Jin, Y. Kim, Y. Kim, J. Mun, S. J. Kim, S. J. Kang, W. Choe, G. Lee, H.-J. Shin, Y. S. Park, *Angew. Chem. Int. Ed.* **2020**, *59*, 14891–14895; *Angew. Chem.* **2020**, *132*, 15001–15005; i) A. S. Scholz, J. G. Massoth, M. Bursch, J.-M. Mewes, T. Hetzke, B. Wolf, M. Bolte, H.-W. Lerner, S. Grimme, M. Wagner, *J. Am. Chem. Soc.* **2020**, *142*, 11072–11083.
- [3] a) H. Noda, M. Furutachi, Y. Asada, M. Shibusaki, N. Kumagai, *Nat. Chem.* **2017**, *9*, 571–577; b) J. Dosso, T. Battisti, B. D. Ward, N. Demitri, C. E. Hughes, P. A. Williams, K. D. M. Harris, D. Bonifazi, *Chem. Eur. J.* **2020**, *26*, 6608–6621; c) M. Fingerle, H. F. Bettinger, *Chem. Commun.* **2020**, *56*, 3847–3850.

- [4] a) M. J. S. Dewar, W. H. Poesche, *J. Am. Chem. Soc.* **1963**, *85*, 2253–2256; b) M. J. S. Dewar, W. H. Poesche, *J. Org. Chem.* **1964**, *29*, 1757–1762; c) T. Hatakeyama, S. Hashimoto, S. Seki, M. Nakamura, *J. Am. Chem. Soc.* **2011**, *133*, 18614–18617; d) T. Hatakeyama, S. Hashimoto, T. Oba, M. Nakamura, *J. Am. Chem. Soc.* **2012**, *134*, 19600–19603; e) X. Wang, F. Zhang, K. S. Schellhammer, P. Machata, F. Ortmann, G. Cuniberti, Y. Fu, J. Hunger, R. Tang, A. A. Popov, R. Berger, K. Müllen, X. Feng, *J. Am. Chem. Soc.* **2016**, *138*, 11606–11615; f) M. Fingerle, C. Maichle-Mössmer, S. Schundelmeier, B. Speiser, H. F. Bettinger, *Org. Lett.* **2017**, *19*, 4428–4431; g) D.-T. Yang, T. Nakamura, Z. He, X. Wang, A. Wakamiya, T. Peng, S. Wang, *Org. Lett.* **2018**, *20*, 6741–6745; h) Y. Fu, K. Zhang, E. Dmitrieva, F. Liu, J. Ma, J. J. Weigand, A. A. Popov, R. Berger, W. Pisula, J. Liu, X. Feng, *Org. Lett.* **2019**, *21*, 1354–1358; i) M. Numano, N. Nagami, S. Nakatsuka, T. Katayama, K. Nakajima, S. Tatsumi, N. Yasuda, T. Hatakeyama, *Chem. Eur. J.* **2016**, *22*, 11574–11577; j) M. Fingerle, S. Stocker, H. F. Bettinger, *Synthesis* **2019**, *51*, 4147–4152; k) Z. Sun, C. Yi, Q. Liang, C. Bingi, W. Zhu, P. Qiang, D. Wu, F. Zhang, *Org. Lett.* **2020**, *22*, 209–213; l) X.-Y. Wang, F.-D. Zhuang, X.-C. Wang, X.-Y. Cao, J.-Y. Wang, J. Pei, *Chem. Commun.* **2015**, *51*, 4368–4371; m) G. Li, Y. Zhao, J. Li, J. Cao, J. Zhu, X. W. Sun, Q. Zhang, *J. Org. Chem.* **2015**, *80*, 196–203.
- [5] a) M. J. D. Bosdet, W. E. Piers, T. S. Sorensen, M. Parvez, *Angew. Chem. Int. Ed.* **2007**, *46*, 4940–4943; *Angew. Chem.* **2007**, *119*, 5028–5031; b) B. Neue, J. F. Araneda, W. E. Piers, M. Parvez, *Angew. Chem. Int. Ed.* **2013**, *52*, 9966–9969; *Angew. Chem.* **2013**, *125*, 10150–10153; c) M. J. D. Bosdet, C. A. Jaska, W. E. Piers, T. S. Sorensen, M. Parvez, *Org. Lett.* **2007**, *9*, 1395–1398; d) C. A. Jaska, W. E. Piers, R. McDonald, M. Parvez, *J. Org. Chem.* **2007**, *72*, 5234–5243.
- [6] J. Dosso, J. Tasseroul, F. Fasano, D. Marinelli, N. Biot, A. Fermi, D. Bonifazi, *Angew. Chem. Int. Ed.* **2017**, *56*, 4483–4487; *Angew. Chem.* **2017**, *129*, 4554–4558.
- [7] M. Krieg, F. Reichert, P. Haiss, M. Ströbele, K. Eichele, M.-J. Treanor, R. Schaub, H. F. Bettinger, *Angew. Chem. Int. Ed.* **2015**, *54*, 8284–8286; *Angew. Chem.* **2015**, *127*, 8402–8404.
- [8] T. Kaehler, M. Bolte, H.-W. Lerner, M. Wagner, *Angew. Chem. Int. Ed.* **2019**, *58*, 11379–11384; *Angew. Chem.* **2019**, *131*, 11501–11506.
- [9] F. Alonso, I. P. Beletskaya, M. Yus, *Chem. Rev.* **2004**, *104*, 3079–3160.
- [10] M. Müller, S. Behnle, C. Maichle-Mössmer, H. F. Bettinger, *Chem. Commun.* **2014**, *50*, 7821–7823.
- [11] a) E. Clar, M. Zander, *J. Chem. Soc.* **1957**, 4616–4619; b) E. Clar, M. Zander, *J. Chem. Soc.* **1958**, 1861–1865; c) K. F. Lang, H. Buffleb, J. Kalowy, *Chem. Ber.* **1960**, *93*, 303–309; d) S. Tokita, K. Hiruta, S. Ishikawa, K. Kitahara, H. Nishi, *Synthesis* **1982**, 854–855; e) S. Tokita, K. Hiruta, K. Kitahara, H. Nishi, *Synthesis* **1982**, 229–231; f) S. Tokita, K. Hiruta, Y. Yaginuma, S. Ishikawa, H. Nishi, *Synthesis* **1984**, 270–271; g) M. Glodek, A. Makal, D. Plazuk, *J. Org. Chem.* **2018**, *83*, 14165–14174; h) A. Kurpanik, M. Matussek, G. Szafraniec-Gorol, M. Filapek, P. Lodowski, B. Marcol-Szumilas, W. Ignasiak, J. G. Małecki, B. Machura, M. Małecka, W. Danikiewicz, S. Pawlus, S. Krompiec, *Chem. Eur. J.* **2020**, *26*, 12150–12157.
- [12] a) E. H. Fort, P. M. Donovan, L. T. Scott, *J. Am. Chem. Soc.* **2009**, *131*, 16006–16007; b) E. H. Fort, L. T. Scott, *J. Mater. Chem.* **2011**, *21*, 1373–1381.
- [13] a) P. Paetzold, A. Richter, T. Thijssen, S. Wuertenberg, *Chem. Ber.* **1979**, *112*, 3811–3827; b) P. Schreyer, P. Paetzold, R. Boese, *Chem. Ber.* **1988**, *121*, 195–205; c) P. Paetzold, J. Kiesgen, K. Krahé, H.-U. Meier, R. Boese, *Z. Naturforsch. B* **1991**, *46*, 853–860.
- [14] Z. Liu, T. B. Marder, *Angew. Chem. Int. Ed.* **2008**, *47*, 242–244; *Angew. Chem.* **2008**, *120*, 248–250.
- [15] F. H. Allen, D. G. Watson, L. Brammer, A. G. Orpen, R. Taylor, *International Tables for Crystallography*, IUCr, Chester, **2006**, pp. 790–811.
- [16] a) P. v. R. Schleyer, C. Maerker, A. Dransfeld, H. Jiao, N. J. R. van Eikema Hommes, *J. Am. Chem. Soc.* **1996**, *118*, 6317–6318; b) P. v. R. Schleyer, H. Jiao, N. J. R. van Eikema Hommes, V. G. Malkin, O. L. Malkina, *J. Am. Chem. Soc.* **1997**, *119*, 12669–12670.
- [17] J. P. Guthrie, *Can. J. Chem.* **1978**, *56*, 2342–2354.
- [18] H. J. P. de Lijser, N. A. Rangel, *J. Org. Chem.* **2004**, *69*, 8315–8322.
- [19] a) A. Catalfo, M. E. Serrentino, V. Librando, G. Perrini, G. de Guidi, *Appl. Spectrosc.* **2008**, *62*, 1233–1237; b) C. Reichardt, R. A. Vogt, C. E. Crespo-Hernández, *J. Chem. Phys.* **2009**, *131*, 224518; c) O. F. Mohammed, E. Vauthey, *J. Phys. Chem. A* **2008**, *112*, 3823–3830; d) R. A. Vogt, C. Reichardt, C. E. Crespo-Hernández, *J. Phys. Chem. A* **2013**, *117*, 6580–6588.
- [20] Deposition Number 2050368 contains the supplementary crystallographic data for this paper. These data are provided free of charge by the joint Cambridge Crystallographic Data Centre and Fachinformationszentrum Karlsruhe Access Structures service www.ccdc.cam.ac.uk/structures.

Manuscript received: December 16, 2020
Accepted manuscript online: April 2, 2021
Version of record online: June 11, 2021

Supporting Information

Heteroatom Cycloaddition at the (BN)₂ Bay Region of Dibenzoperylene

*Michael Fingerle, Juliane Dingerkus, Hartmut Schubert, Kai M. Wurst, Marcus Scheele, and Holger F. Bettinger**

anie_202016699_sm_miscellaneous_information.pdf

Supporting Information (SI)

Table Of Contents

1. General	S2
2. Syntheses	S5
3. Spectra	S11
4. X-Ray Crystallographic Data	S35
5. Computational Investigations	S36
6. Cyclic Voltammetry	S38
7. Cartesian Coordinates of Stationary Points in Å	S40
8. References	S75

1. General

Experimental details. All reactions were done under inert conditions by flaming the glassware with a heat gun (630 °C) under vacuum, following purging with argon. Molecular sieve was dried under vacuum and with a temperature profile from 150 °C to 300 °C over 5 hours. Chemicals and solvents were purchased from commercial suppliers in anhydrous form or were dried by known methods. Column chromatography were done using a medium pressure liquid chromatography (MPLC) system (PuriFlash 430 evo, Interchim) with Si-IR 20 μm columns in size of 12 g up to 120 g. Pre-coated polyester sheets (40 x 80 mm) from Machery-Nagel (POLYGAM@SIL G/UV254) with 0.2 mm silica gel 60 with fluorescent indicator were used for thin layer chromatography (TLC). For visualization, UV light source (254 nm and 366 nm) was used. Nuclear magnetic resonance spectroscopy (NMR) was done on a Bruker Avance III HDX 600 equipped with a dual ($^1\text{H}/^{13}\text{C}$) probe head. Chemical shifts (δ) are given in ppm, coupling constants in Hertz (Hz) and the multiplicities of the signals are designated as follows: s = singlet, br s = broad singlet, d = doublet, dd = doublet of doublet, t = triplet and m = multiplet. The signals of NMR solvents were calibrated ($^1\text{H}/^{13}\text{C}$): CD_2Cl_2 5.32/53.84 ppm and thf- d_8 3.58/67.21 ppm. Reference for ^1H and ^{13}C were tetramethyl silane (TMS), for ^{11}B $\text{BF}_3\cdot\text{OEt}_3$ in CDCl_3 and CFCl_3 for ^{19}F . High resolution mass spectrometry was done on a maXis 4G Bruker system with an APCI source combined with a direct inlet probe (DIP) system. Optical spectra were recorded on a PerkinElmer Lambda 1050 spectrometer with a PerkinElmer 3D WB Det Module. Excitation and emission spectra were recorded on a Cary Variant SPVF spectrometer using Hellma Analytics quartz cuvettes. All measurements were done in spectroscopy grade solvents. The fluorescence quantum yields were measured with an excitation wavelength $\lambda_{\text{ex}} = 370$ nm (diphenylanthracene in ethanol as reference).

X-Ray crystallography. X-ray data were collected with a Bruker Smart APEX II diffractometer with graphite-monochromated Mo K_α radiation. The programs used were

Bruker's APEX2v2011.8-0, including SADABS for absorption correction, SAINT for data reduction and SHELXS for structure solution, as well as the WinGX suite of programs version 1.70.01 or the GUI ShelXle, including SHELXL for structure refinement.^[1]

Cyclic voltammetry. Cyclic voltammetry (CV) was carried out using a CHI760E Bipotentiostat (CH-Instruments) controlled by the CHI760E software (version 20.04). The full-glass electrochemical measurement cell was placed in a faraday cage in a nitrogen filled glovebox. A platinum disc electrode (3 mm diameter, Metrohm part no. 6.1204.310) served as the working electrode and a coiled platinum wire (30 cm length, 3 mm diameter) as the counter electrode. As a reference electrode, a Haber-Luggin double-reference system, consisting of a Ag/Ag⁺ redox couple (a silver wire placed in a 0.01 M AgClO₄ solution in 0.1 M tetrabutylammonium hexafluorophosphate (TBAHFP)/acetonitrile (MeCN)) capacitively connected to a platinum wire immersed in the electrolyte of the sample compartment, is employed.^[2] The reference electrode chamber is further separated from the Haber-Luggin capillary by a spacer frit filled with 0.1 M TBAHFP/MeCN. In this way, contamination of the sample compartment and vice versa of the Ag/Ag⁺ reference electrode chamber can be prevented. The sample chamber was filled with 0.1 M TBAHFP in tetrahydrofuran (THF). CV measurements were performed at scan rates between 20 mV/s and 5 V/s. The voltage drop, caused by the resistance of the electrolyte, was corrected by positive feedback iR-compensation. If not stated otherwise, all cyclic voltammograms are corrected by the capacitive background currents. All potentials are given versus the formal potential of the ferrocene/ferrocenium (Fc/Fc⁺) couple, which was determined by cyclic voltammetry to be at 185 ± 2 mV vs. the Ag/Ag⁺ reference system.

All chemicals were handled under inert conditions and stored inside a nitrogen filled glovebox. THF (HPLC-grade) was distilled from Na three times, degassed via freeze-pump-thaw and stored over activated 4 Å molecular sieve. Acetonitrile (HPLC-grade) was subsequent

distilled from P_2O_5 , CaH_2 and again P_2O_5 , followed by degassing via freeze-pump-thaw and storing over activated 3 Å molecular sieve. Prior to use, both solvents were run through a column filled with activated neutral alumina. The electrolyte TBAHFP (98%, Alfa Aesar) was recrystallized five times in 3:1 EtOH/H₂O, followed by drying 7 d at 105 °C and 2-3 mbar. Ferrocene (98%, Acros Organics) and $AgClO_4$ ($\geq 97\%$, anhydrous, Alfa Aesar) were used as received.

Computational Details. Geometry optimizations were performed using the M062X functional^[3] as implemented in Gaussian 16^[4] in conjunction with the 6-311+G** basis set.^[5] Harmonic vibrational frequencies were computed to confirm the nature of stationary points as minima or first-order saddle points, and to obtain Gibbs free energies at $T = 298.15$ K and $T = 339$ K. The influence of THF solvent was considered during geometry optimization and harmonic vibrational frequency computations using the polarizable continuum model with the integral equation formalism implemented in Gaussian 16.^[6] The NICS values were computed using the GIAO^[7] method at the M062X/6-311+G** level of theory.

2. Syntheses

General synthesis of cycloaddition reactions

In a dried flask equipped with a Soxhlet extractor filled with 3 Å molecular sieve, 145 mg (BN)₂ dibenzoperylene **1** (0.3 mmol, 1 equiv.) were dissolved in dry thf (30 mL). 5 mL of a *p*-toluenesulfonic acid solution (0.6 M in thf, 10 equiv., stored over 3 Å molecular sieve) and 10 equiv. of the benzaldehyde derivative were added, and the mixture stirred under reflux (95 °C oil bath temperature) for 5 days. After cooling down to room temperature, the reaction mixture was quenched with sat. NaHCO₃ solution (20 mL) and extracted with ethylacetate (3 x 20 mL). All combined organic layers were washed with brine (3 x 20 ml) and dried over MgSO₄. All volatiles were removed under reduced pressure. Column chromatography yielded the desired compound.

Synthesis of **3a** (with BA-H):

Column Chromatography: n-hexane/DCM 4:1, R_f = 0.13, colorless solid, yield: 115 mg (0.20 mmol, 67 %).

¹H NMR (CD₂Cl₂, 600 MHz): δ = 8.30 (d, *J* = 8.0 Hz, 1H, H-4), 8.17-8.12 (m, 3H, H-22, H-16, H-14), 8.12-8.09 (m, 2H, H-10, H-8), 8.05 (dd, *J* = 7.3 Hz, *J* = 1.4 Hz, 1H, H-1), 7.76 (t, *J* = 7.8 Hz, 1H, H-15), 7.69-7.66 (m, 1H, H-3), 7.45-7.42 (m, 1H, H-2), 7.39-7.36 (m, 2H, H-28, H-26), 7.24-7.21 (m, 3H, H-30, H-29, H-25), 7.09 (dd, *J* = 8.5 Hz, *J* = 2.0 Hz, 1H, H-24), 7.02 (s, 1H, H-31), 6.86 (d, *J* = 8.5 Hz, 1H, H-19), 2.80 (t, *J* = 7.9 Hz, 2H, H-32), 2.71-2.68 (m, 2H, H-36), 1.80-1.75 (m, 2H, H-33), 1.71-1.66 (m, 2H, H-37), 1.52-1.47 (m, 2H, H-34), 1.47-1.41 (m, 2H, H-38), 1.02 (t, *J* = 7.4 Hz, 3H, H-35), 0.99 (t, *J* = 7.4 Hz, 3H, H-39).

¹¹B NMR (CD₂Cl₂, 193 MHz): δ = 28.3.

¹³C NMR (CD₂Cl₂, 151 MHz): δ = 141.8 (C-5), 141.1 (C-27), 139.8 (C-13), 139.2 (C-17), 136.8 (C-20), 136.0 (C-9), 135.5 (C-23), 133.7 (C-12), 132.5 (C-1), 132.3 (C-15), 132.1 (C-3), 129.1 (C-30), 129.1 (C-29, C-25), 129.0 (C-24), 127.2 (C-6), 126.7 (C-2), 126.5 (C-28, C-26), 124.7 (C-8), 124.7 (C-10), 124.7 (C-22), 124.6 (C-11), 124.5 (C-7), 124.4 (C-18), 123.8 (C-21), 122.9 (C-4), 120.1 (C-16)*, 119.8 (C-14)*, 116.1 (C-19), 84.0 (C-), 36.1 (C-), 35.5 (C-), 34.6 (C-), 34.3 (C-), 22.9 (C-), 14.3 (C-), 14.2 (C-). C*s belong to the multiplet in the ¹H-NMR (8.17-8.12 ppm) and can be interchanged.

HR-MS (APCI-DIP): *m/z* [M+H]⁺ calcd. for C₃₉H₃₇B₂N₂O: 571.30993; found: 571.30996.

UV/Vis (dichloromethane) λ (log ε): 383 (4.31), 364 (4.34), 348 (4.13), 334 (3.77), 299 (4.13), 287 (4.27), 261 (4.78), 256 (4.75), 233 (4.83).

Fluorescence quantum yield: 88 %.

Synthesis of 3b (with BA-OH)

Column Chromatography: n-hexane/DCM 1:3, $R_f = 0.29$, colorless solid, yield: 130 mg (0.22 mmol, 74 %).

^1H NMR (CD_2Cl_2 , 600 MHz): $\delta = 8.33$ (d, $J = 8.3$ Hz, 1H, H-4), 8.20 (d, $J = 8.0$ Hz, 2H, H-14, H-16), 8.17-8.15 (m, 3H, H-8, H-10, H-22), 8.08 (dd, $J = 7.4$ Hz, $J = 1.3$ Hz, 1H, H-1), 7.81 (t, $J = 8.0$ Hz, 1H, H-15), 7.70-7.67 (m, 1H, H-3), 7.46-7.42 (m, 1H, H-2), 7.28-7.26 (m, 2H, H-26, H-28), 7.12 (dd, $J = 8.4$ Hz, $J = 1.9$ Hz, 1H, H-24), 7.08 (s, 1H, H-32), 6.92 (d, $J = 8.4$ Hz, 1H, H-19), 6.69-6.66 (m, 2H, H-25, H-29), 4.93 (s, 1H, H-31), 2.83 (t, $J = 7.9$ Hz, 2H, H-33), 2.71-2.68 (m, 2H, H-37), 1.81-1.75 (m, 2H, H-34), 1.71-1.65 (m, 2H, H-38), 1.52-1.46 (m, 2H, H-35), 1.46-1.39 (m, 2H, H-39), 1.02 (t, $J = 7.4$ Hz, 3H, H-36), 0.98 (d, $J = 7.4$ Hz, 3H, H-40).

^{11}B NMR (CD_2Cl_2 , 193 MHz): $\delta = 29.2$.

^{13}C NMR (CD_2Cl_2 , 151 MHz): $\delta = 156.4$ (C-30), 141.8 (C-5), 139.9 (Cq), 139.3 (Cq), 136.9 (C-20), 136.1 (C-9), 135.5 (C-23), 133.9 (C-27), 133.8 (Cq), 132.6 (C-1), 132.4 (C-15), 132.2 (C-3), 129.1 (C-24), 128.1 (C-26, C-28), 127.3 (C-6), 126.8 (C-2), 124.8 (C-8), 124.8 (C-10), 124.7 (C-22), 124.6 (Cq), 124.6 (Cq), 124.4 (C-18), 123.8 (C-21), 122.9 (C-4), 120.1 (C-16)*, 119.9 (C-14)*, 116.2 (C-), 115.8 (C-25, C-29), 83.7 (C-32), 36.1 (C-33), 35.5 (C-37), 34.6 (C-34), 34.3 (C-38), 22.9 (C-39, C-35), 14.3 (C-36), 14.2 (C-40).

C*s belong to the duplet in the ^1H -NMR at 8.20 ppm and can be interchanged, Cq cannot completely assigned due to the multiplet signal in the ^1H NMR.

HR-MS (APCI-DIP): m/z $[\text{M}+\text{H}]^+$ calcd. for $\text{C}_{39}\text{H}_{37}\text{B}_2\text{N}_2\text{O}_2$: 587.30485; found: 571.30405.

UV/Vis (dichloromethane) λ (log ϵ): 383 (4.28), 364 (4.31), 348 (4.11), 334 (3.75), 229 (4.10), 286 (4.26), 262 (4.76), 256 (4.74), 233 (4.82).

Fluorescence quantum yield: 80 %

Synthesis of 3c (with BA-NO₂)

Column Chromatography: n-hexane/DCM 1:1, $R_f = 0.25$ yellow solid, yield: 137 mg (0.22 mmol, 73 %).

^1H NMR (CD_2Cl_2 , 600 MHz): δ = 8.31 (d, J = 8.2 Hz, 1H, H-4), 8.18-8.14 (m, 3H, H-14, H-16, H-22), 8.11 (s, 2H, H-8, H-10), 8.07-8.03 (m, 3H, H-1, H-25, H-29), 7.79 (t, J = 7.7 Hz, 1H, H-15), 7.71-7.67 (m, 1H, H-3), 7.56-7.53 (m, 2H, H-26, H-28), 7.46-7.43 (m, 1H, H-2), 7.10 (dd, J = 8.5 Hz, J = 2.0 Hz, 1H, H-24), 7.08 (s, 1H, H-31), 6.72 (d, J = 8.5 Hz, 1H, H-19), 2.82 (t, J = 7.9 Hz, 2H, H-32), 2.71-2.68 (m, 2H, H-36), 1.79-1.74 (m, 2H, H-33), 1.71-1.65 (m, 2H, H-37), 1.52-1.46 (m, 2H, H-34), 1.46-1.40 (m, 1H, H-38), 1.02 (t, J = 7.4 Hz, 3H, H-35), 0.98 (t, J = 7.4 Hz, 3H, H-39).

^{11}B NMR (CD_2Cl_2 , 193 MHz): δ = 28.9.

^{13}C NMR (CD_2Cl_2 , 151 MHz): δ = 148.5 (C-30), 147.9 (C-27), 141.9 (C-5), 139.9 (C-13), 139.2 (C-17), 136.3 (C-20), 136.3 (C-9), 136.0 (C-23), 133.4 (C-), 132.6 (C-15), 132.5 (C-1), 132.4 (C-3), 129.1 (C-24), 127.7 (C-26, C-28), 126.8 (C-2), 125.0 (C-22), 124.9 (C-8/10), 124.8 (C-8/10), 124.6 (C-7/11), 124.5 (C-7/11), 124.4 (C-25, C-29), 124.1 (C-18), 123.9 (C-21), 123.0 (C-4), 120.3 (C-14/16), 120.0 (C-14/16), 115.9 (C-19), 82.9 (C-31), 36.1 (C-32), 35.5 (C-36), 34.6 (C-33), 34.3 (C-37), 22.9 (C-34), 22.9 (C-38), 14.3 (C-35), 14.2 (C-39).

HR-MS (APCI-DIP): m/z $[\text{M}+\text{H}]^+$ calcd. for $\text{C}_{39}\text{H}_{36}\text{B}_2\text{N}_3\text{O}_3$: 616.29501; found: 616.29395.

UV/Vis (dichloromethane) λ (log ϵ): 381 (4.18), 362 (4.27), 348 (4.11), 332 (3.79), 298 (4.17), 284 (4.40), 261 (4.78), 255 (4.76), 233 (4.78).

Fluorescence quantum yield: 7 %.

Synthesis of 3d (with BA-F)

Column Chromatography: n-hexane/DCM 85:15, R_f = 0.21, colorless solid, yield: 141 mg (0.24 mmol, 80 %).

^1H NMR (CD_2Cl_2 , 600 MHz): δ = 8.33-8.30 (m, 1H, H-4), 8.19-8.16 (m, 2H, H-14, H-16), 8.16 (d, J = 1.7 Hz, 1H, H-22), 8.13 (s, 2H, H-8, H-10), 8.06 (dd, J = 7.4 Hz, J = 1.4, 1H, H-1), 7.79 (t, J = 7.9 Hz, 1H, H-15), 7.70-7.67 (m, 1H, H-3), 7.46-7.43 (m, 1H, H-2), 7.39-7.35 (m, 2H, H-26, H-28), 7.11 (dd, J = 8.4 Hz, J = 1.7 Hz, 1H, H-24), 7.06 (s, 1H, H-32), 6.93-6.90 (m, 2H, H-29, H-25), 6.84 (d, J = 8.4 Hz, 1H, H-19), 2.81 (t, J = 7.9 Hz, 2H, H-33), 2.72-2.68 (m, 2H, H-37), 1.80-1.74 (m, 2H, H-34), 1.71-1.66 (m, 2H, H-38), 1.52-1.46 (m, 2H, H-35), 1.46-1.40 (m, 2H, H-39), 1.02 (t, J = 7.4 Hz, 3H, H-36), 0.98 (t, J = 7.4 Hz, 3H, H-40).

^{11}B NMR (CD_2Cl_2 , 193 MHz): δ = 28.5

^{13}C NMR (CD_2Cl_2 , 151 MHz): $\delta = 163.1$ (d, $J = 246$ Hz, C-30), 141.8 (C-5), 139.9 (C-13), 139.2 (C-17), 137.4 (d, $J = 3$ Hz, C-27), 136.6 (C-20), 136.2 (C-9), 135.6 (C-23), 133.6 (C-12), 132.5 (C-1), 132.4 (C-15), 132.2 (C-3), 129.1 (C-24), 128.5 (d, $J = 9$ Hz, C-28, C-26), 127.1 (C-6), 126.8 (C-2), 124.8 (C-8), 124.8 (C-10), 124.8 (C-22), 124.6 (C-7), 124.5 (C-11), 124.3 (C-18), 123.8 (C-21), 122.9 (C-4), 120.2 (C-16)*, 119.9 (C-14)*, 116.1 (C-19), 116.0 (d, $J = 22$ Hz, C-29, C-25), 83.3 (C-32), 36.1 (C-33), 35.5 (C-37), 34.6 (C-34), 34.3 (C-38), 22.9 (C-35, C-39), 14.3 (C-36), 14.2 (C-40).

C*s belong to the multiplet in the ^1H -NMR (8.19-8.16 ppm) and can be interchanged.

^{19}F NMR (CD_2Cl_2 , 564 MHz): $\delta = -113.84$.

HR-MS (APCI-DIP): m/z $[\text{M}+\text{H}]^+$ calcd. for $\text{C}_{39}\text{H}_{36}\text{B}_2\text{FN}_2\text{O}$: 589.30051; found: 589.29964.

UV/Vis (dichloromethane) λ (log ϵ): 382 (4.32), 363 (4.34), 348 (4.13), 334 (3.78), 299 (4.12), 286 (4.28), 262 (4.77), 255 (4.74), 233 (4.83).

Fluorescence quantum yield: 78 %.

Synthesis of 3e (with Mesitaldehyde)

Column Chromatography: n-hexane/DCM 84:16, $R_f = 0.3$, colorless solid, yield: 74.0 mg (0.12 mmol, 40 %).

^1H NMR (CD_2Cl_2 , 600 MHz): $\delta = 8.26$ -8.24 (m, 1H, H-4), 8.07-8.01 (m, 4H, H-8, H-14, H-16, H-22), 7.98 (d, $J = 1.3$ Hz, 1H, H-10), 7.88 (dd, $J = 7.3$ Hz, $J = 1.3$ Hz, 1H, H-1), 7.69 (t, $J = 7.9$ Hz, 1H, H-15), 7.67-7.64 (m, 1H, H-3), 7.39-7.36 (m, 1H, H-2), 6.97 (s, 2H, H-29, H-34), 6.95 (dd, $J = 8.4$ Hz, $J = 2.0$ Hz, 1H, H-24), 6.48-6.46 (m, 2H, H-19, H-25), 2.79-2.75 (m, 2H, H-35), 2.72 (s, 3H, H-32), 2.68-2.64 (m, 2H, H-39), 2.17 (s, 3H, H-33), 1.79-1.73 (m, 2H, H-36), 1.70-1.65 (m, 2H, H-40), 1.62 (s, 3H, H-31), 1.54-1.48 (m, 2H*, H-41), 1.48-1.41 (m, 2H, H-37), 1.03 (t, $J = 7.4$ Hz, 3H, H-38), 0.99 (t, $J = 7.4$ Hz, 3H, H-42).

*signal overlaps with water

^{11}B NMR (CD_2Cl_2 , 193 MHz): $\delta = 28.4$.

^{13}C NMR (CD_2Cl_2 , 151 MHz): $\delta = 141.8$ (C-5), 139.7 (C-13), 139.1 (C-17), 138.1 (C-q), 137.1 (C-q), 136.3 (C-20), 135.8 (C-q), 135.7 (C-9), 135.2 (C-23), 134.8 (C-q), 133.6 (C-12), 132.5 (C-1), 132.1 (C-15), 132.0 (C-25), 131.9 (C-3), 130.3 (C-29), 128.6 (C-24), 127.1 (C-6), 126.6 (C-2), 124.6 (C-7), 124.6 (C-10), 124.5 (C-8), 124.5 (C-22), 124.4 (C-11), 124.2 (C-18), 123.7 (C-21), 122.7 (C-4), 120.0 (C-16*), 119.6 (C-14*), 115.5 (C-19), 82.6 (C-34), 36.2

(C-35), 35.5 (C-39), 34.6 (C-36), 34.2 (C-40), 23.0 (C-41), 23.0 (C-37), 21.1 (C-31), 20.9 (C-33), 20.6 (C-32), 14.3 (C-38), 14.2 (C-42).

All C-q's are quaternary carbons of the mesityl group and cannot completely assigned. C-16 and C-14 can be interchanged due to the proton multiplet at 8.07-8.01 ppm.

HR-MS (APCI-DIP): m/z $[M+H]^+$ calcd. for $C_{42}H_{43}B_2N_2O$: 613.35697; found: 613.35570.

UV/Vis (dichloromethane) λ (log ϵ): 384 (4.29), 365 (4.32), 349 (4.11), 336 (3.74), 300 (4.08), 287 (4.24), 262 (4.73), 255 (4.71), 235 (4.74).

Fluorescence quantum yield: 84 %.

Synthesis of 3f (with Pivalaldehyde)

Column Chromatography: n-hexane/DCM 4:1, $R_f = 0.2$, colorless solid, yield: 24.8 mg (45.0 μ mol, 15 %) with impurities.

1H NMR (CD_2Cl_2 , 600 MHz): $\delta = 8.46-8.41$ (m, 1H), 8.30-8.22 (m, 5H), 8.17 (d, $J = 2$ Hz, 1H), 7.93-7.87 (m, 1H), 7.80-7.73 (m, 1H), 7.58-7.50 (m, 1H), 7.31-7.27 (m, 2H), 6.52 (s, 1H), 2.90-2.84 (m, 2H), 2.78-2.72 (m, 2H), 1.86-1.66 (m, 4H), 1.52-1.39 (m, 4H)*, 1.04-0.95 (m, 6H)*, 0.93 (s, 9H).

Signals which overlap with impurities are marked with * and are given with correct proton numbers.

Synthesis of 3g (with Cinnamaldehyde)

Column Chromatography: n-hexane/DCM 85:15, $R_f = 0.18$, colorless solid, yield: 137 mg (0.23 mmol, 77 %).

1H NMR ($THF-d_8$, 600 MHz): $\delta = 8.48-8.46$ (d, $J = 8.4$ Hz, 1H, H-4), 8.35-8.28 (m, 5H, H-8, H-10, H-14, H-16, H-22), 8.23 (dd, $J = 7.4$ Hz, $J = 1.4$ Hz, 1H, H-1), 7.84 (t, $J = 8.0$ Hz, 1H, H-15), 7.74-7.67 (m, 1H, H-3), 7.49-7.44 (m, 1H, H-2), 7.44-7.39 (m, 1H, H-19), 7.32-7.27 (m, 3H, H-24, H-29, H-33), 7.17-7.06 (m, 3H, H-30, H-31, H-32), 7.03 (d, $J = 5.4$ Hz, 1H, H-25), 6.84 (d, $J = 15.9$ Hz, 1H, H-27), 6.53 (dd, $J = 15.9$ Hz, $J = 5.4$ Hz, 1H, H-26), 2.87 (t, $J = 7.7$ Hz, 2H, H-34), 2.74 (t, $J = 7.7$ Hz, 2H, H-38), 1.84-1.66 (m, 4H, H-35, H-39), 1.53-1.39 (m, 4H, H-36, H-40), 1.03-0.95 (m, 6H, H-37, H-41).

^{11}B NMR ($THF-d_8$, 193 MHz): $\delta = 28.6$.

^{13}C NMR (THF- d_8 , 151 MHz): δ = 142.6 (C-5), 140.3 (C-q), 139.9 (C-q), 137.5 (C-20), 136.7 (C-28), 136.4 (C-9), 135.5 (C-23), 134.3 (C-q), 133.0 (C-27), 132.9 (C-1), 132.6 (C-15), 132.5 (C-3), 129.5 (C-24), 128.9 (C-30, C-32), 128.7 (C-26), 128.5 (C-31), 127.5 (C-29, C-33), 127.0 (C-2), 125.2 (C-m), 125.2 (C-m), 125.2 (C-q), 125.1 (C-m), 124.4 (C-q), 123.4 (C-4), 120.5 (C-m), 120.3 (C-m), 116.0 (C-19), 82.6 (C-25), 36.4 (C-34), 35.8 (C-38), 35.0 (C-35), 34.8 (C-39), 23.2 (C-36), 23.1 (C-40), 14.2 (C-37), 14.2 (C-41). The “C-m” signals belongs to the multiplet CHs at 8.35-8.28 ppm in the proton NMR and cannot completely assigned. Due to this multiplet, all quaternary “C-q” cannot completely assigned.

HR-MS (APCI-DIP): m/z $[\text{M}+\text{H}]^+$ calcd. for $\text{C}_{41}\text{H}_{39}\text{B}_2\text{N}_2\text{O}$: 597.32564; found: 571.32546.

UV/Vis (dichloromethane) λ (log ϵ): 383 (4.26), 364 (4.30), 349 (4.09), 335 (3.74), 299 (4.13), 286 (4.31), 261 (4.85), 254 (4.83), 233 (4.80).

Fluorescence quantum yield: 80 %.

3. Spectra

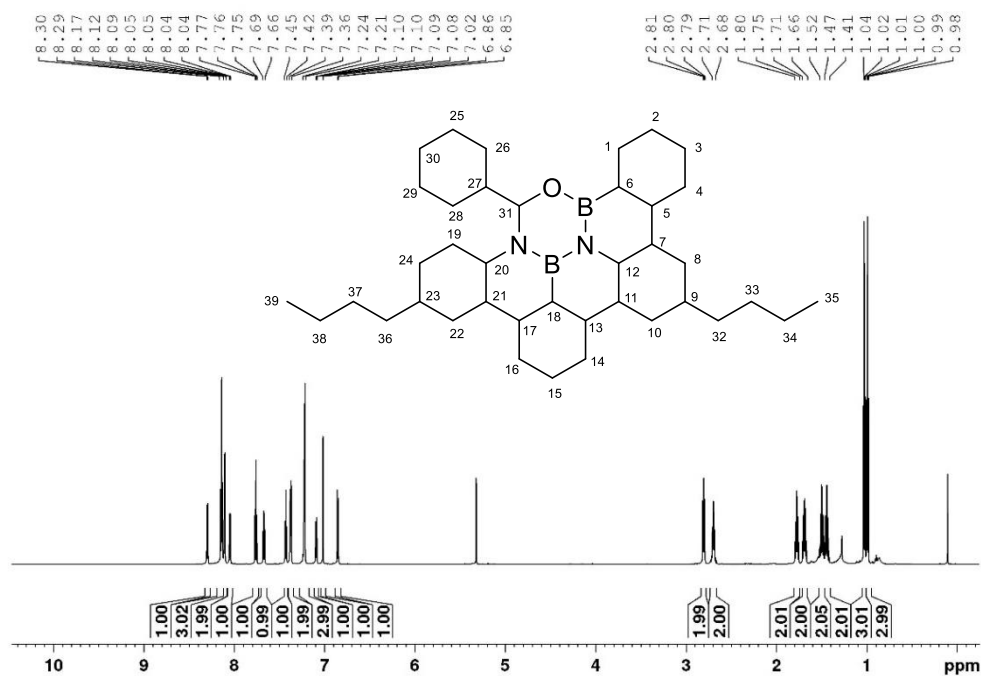


Figure S1: ¹H-NMR of **3a** in CD₂Cl₂.

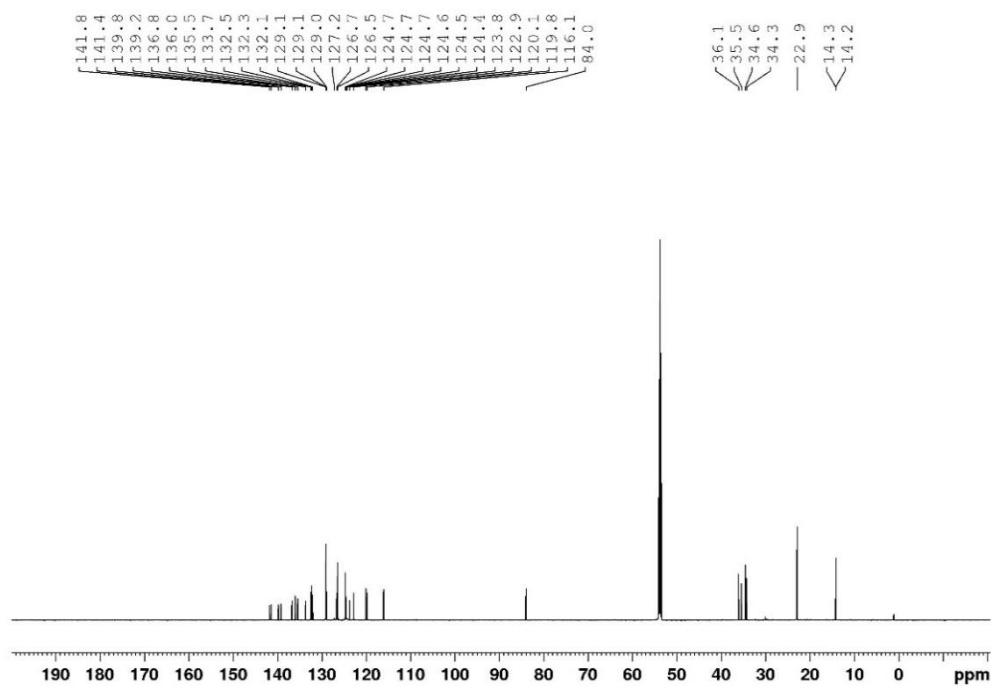


Figure S2: ¹³C-NMR of **3a** in CD₂Cl₂.

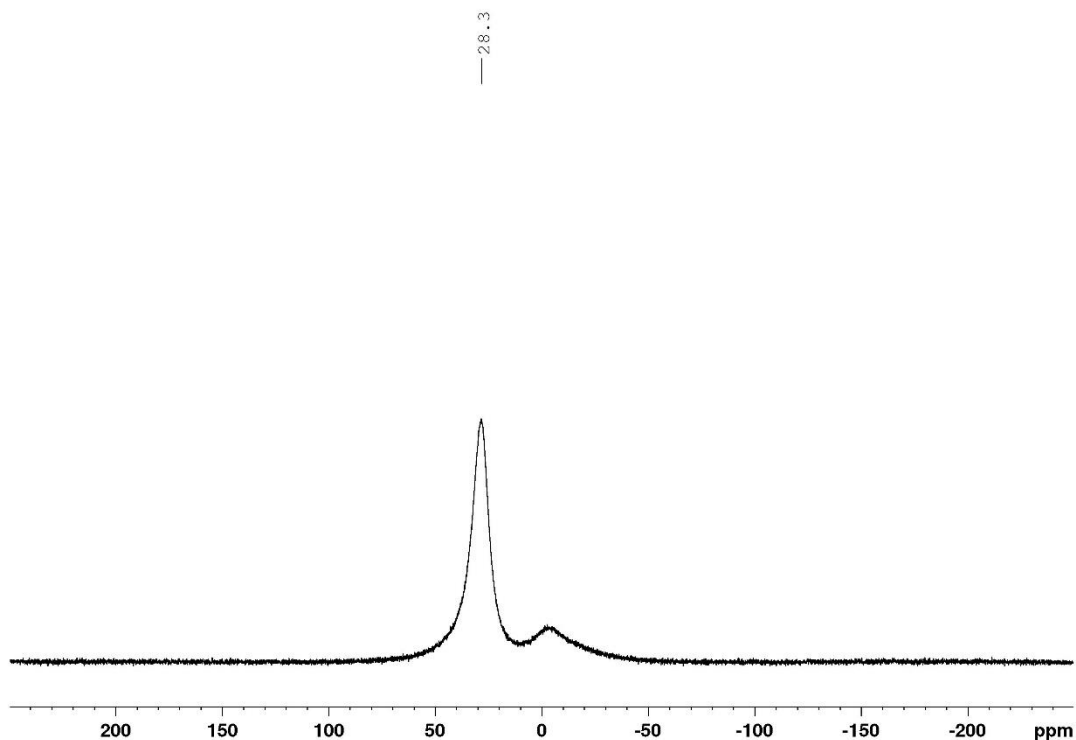


Figure S3: ^{11}B -NMR of **3a** in CD_2Cl_2 .

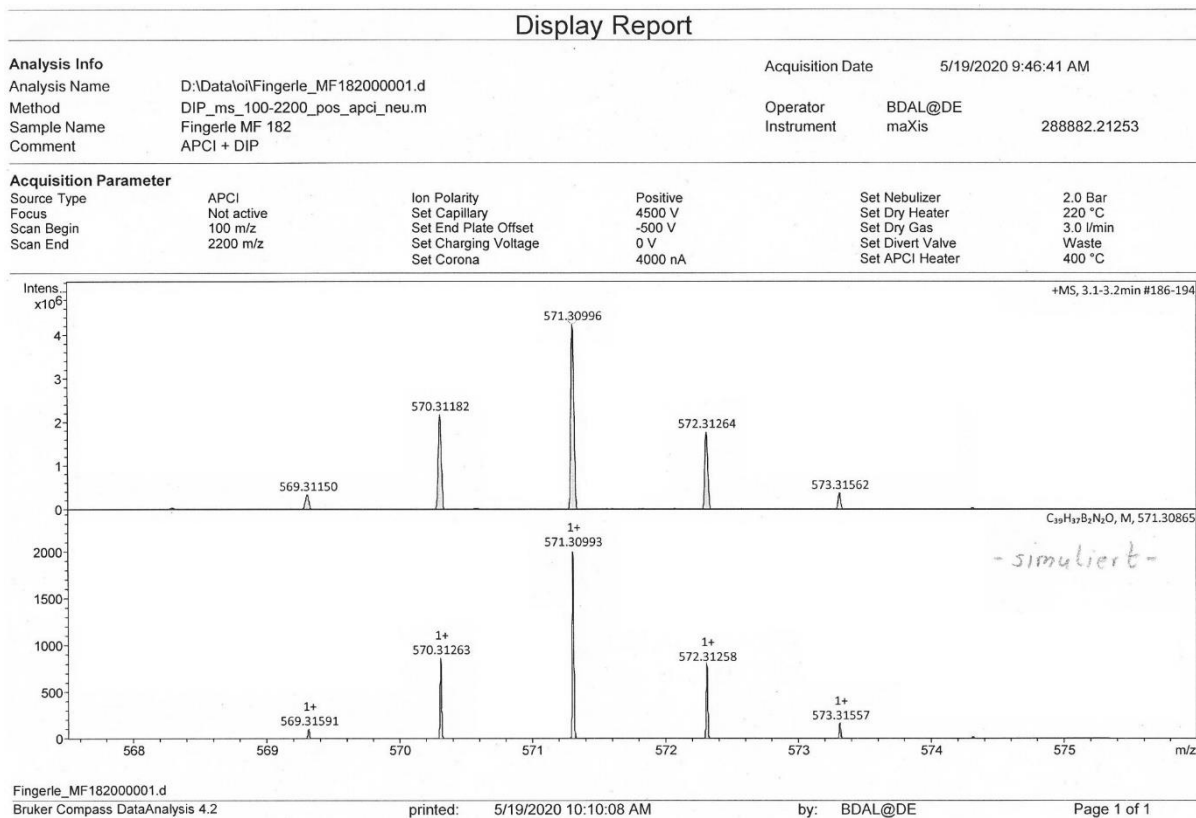


Figure S4: High resolution MS of **3a**.

High Resolution MS DIP-APCI

- FT-ICR-MS
- ESI- oder APCI-TOF-MS (MS/MS möglich)
- egal (je nach freien Kapazitäten)

Name: Michael Fingerle

AK: Bettinger

Tel. 76250

email:

Datum: 11.05.2020

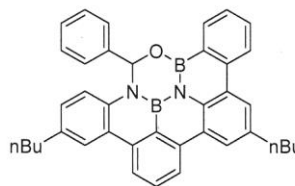
Probenbezeichnung: MF182

nominelle Masse: 570.30

Falls Masse nicht bekannt, welcher Massenbereich soll gemessen werden:

Summenformel (falls bekannt): $C_{39}H_{36}B_2N_2O$

Strukturformel (falls bekannt):



Einwaage (zwischen 0,1mg und 2 mg):

Löslich in:

Falls schon gelöst, in welchem Lösemittel und in welcher Konzentration:

Hinweise bezüglich Zersetzlichkeit:

Hinweise bezüglich Toxizität (wenn bekannt):

Hohe Massengenauigkeit erwünscht? ja/nein

Massenanalyse erwünscht?

Wenn ja, welche Elemente sollen berücksichtigt werden?

MS/MS erwünscht?:

Ergebnis:

$[M + H]^+_{(theor.)} = 571,30993$

Gemessen = 571,30996

Relative Massenabweichung = 0,05 ppm

Figure S5: Data sheet high resolution MS of **3a**.

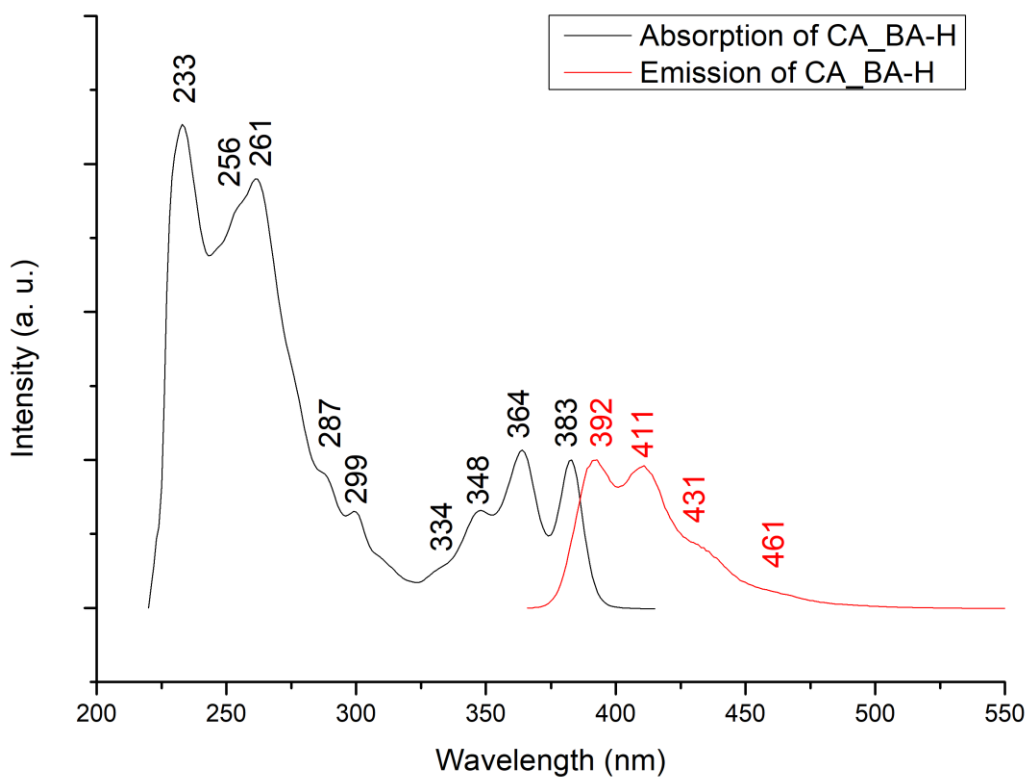


Figure S6: Absorption and emission spectra of **3a** (10^{-5} mol/L) in CD_2Cl_2 .

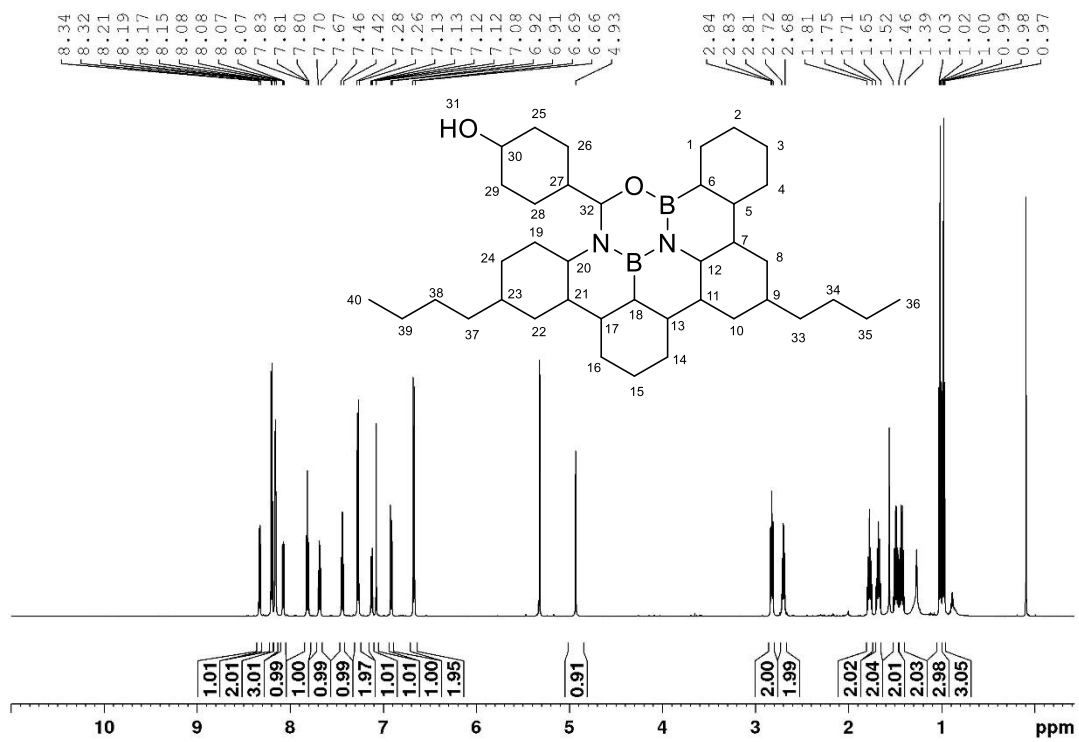


Figure S7: $^1\text{H-NMR}$ of **3b** in CD_2Cl_2 .

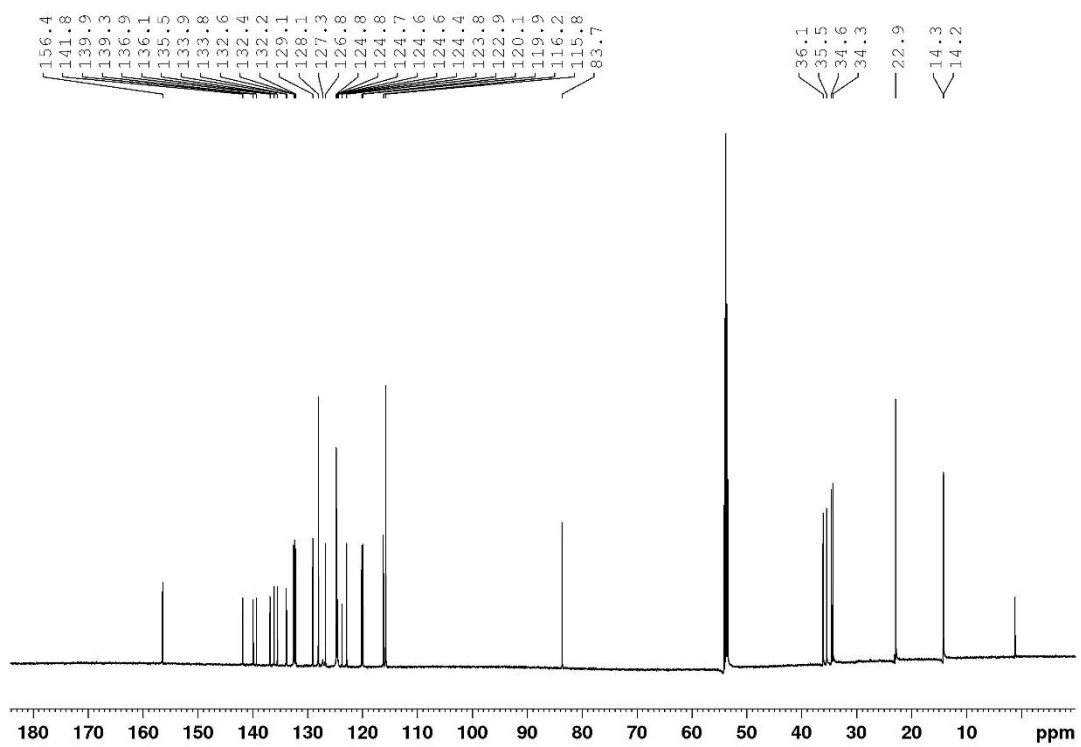


Figure S8: ^{13}C -NMR of **3b** in CD_2Cl_2 .

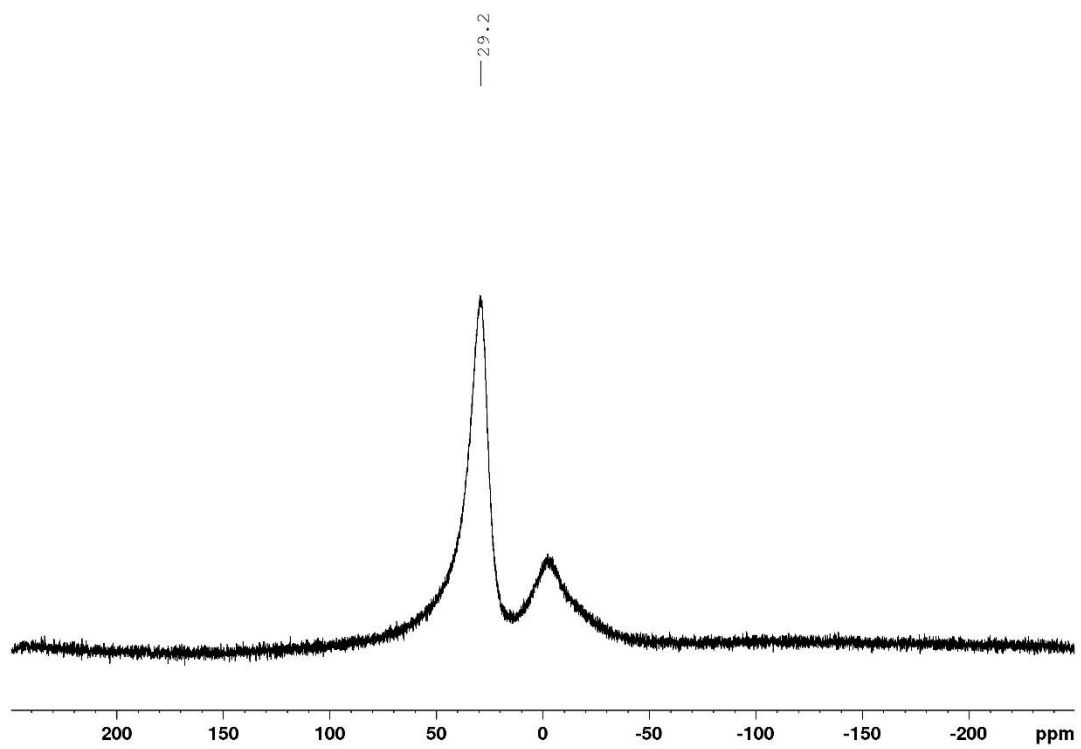
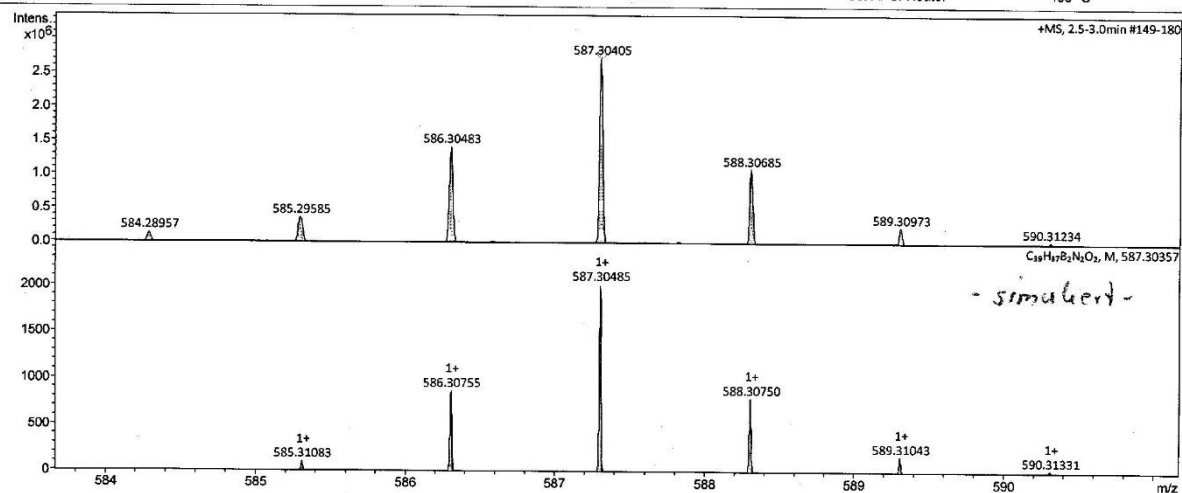


Figure S9: ^{11}B -NMR of **3b** in CD_2Cl_2 .

Display Report

Analysis Info		Acquisition Date	5/19/2020 11:34:22 AM
Analysis Name	D:\Data\ol\Fingerle_MF184000002.d	Operator	BDAL@DE
Method	DIP_ms_100-2200_pos_apci_neu.m	Instrument	maXis
Sample Name	Fingerle MF 184		288882.21253
Comment	APCI + DIP		

Acquisition Parameter					
Source Type	APCI	Ion Polarity	Positive	Set Nebulizer	2.0 Bar
Focus	Not active	Set Capillary	4500 V	Set Dry Heater	220 °C
Scan Begin	100 m/z	Set End Plate Offset	-500 V	Set Dry Gas	3.0 l/min
Scan End	2200 m/z	Set Charging Voltage	0 V	Set Divert Valve	Waste
		Set Corona	4000 nA	Set APCI Heater	400 °C



Fingerle_MF184000002.d
 Bruker Compass DataAnalysis 4.2 printed: 5/19/2020 11:51:47 AM by: BDAL@DE Page 1 of 1

Figure S10: High resolution MS of **3b**.

High Resolution MS DIP-APCI

- FT-ICR-MS
- ESI- oder APCI-TOF-MS (MS/MS möglich)
- egal (je nach freien Kapazitäten)

Name: Michael Fingerle

AK: Bettinger

Tel. 76250

email:

Datum: 11.05.2020

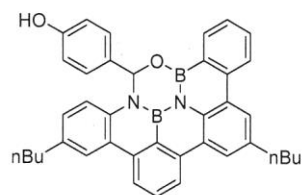
Probenbezeichnung: MF184

nominelle Masse: 586.30

Falls Masse nicht bekannt, welcher Massenbereich soll gemessen werden:

Summenformel (falls bekannt): $C_{39}H_{36}B_2N_2O_2$

Strukturformel (falls bekannt):



Einwaage (zwischen 0,1mg und 2 mg):

Löslich in:

Falls schon gelöst, in welchem Lösemittel und in welcher Konzentration:

Hinweise bezüglich Zersetzlichkeit:

Hinweise bezüglich Toxizität (wenn bekannt):

Hohe Massengenauigkeit erwünscht? ja/nein

Massenanalyse erwünscht?

Wenn ja, welche Elemente sollen berücksichtigt werden?

MS/MS erwünscht?:

Ergebnis:

$$[M + H]^+_{(theor.)} = 587,30485$$

$$\text{Gemessen} = 587,30405$$

$$\text{Relative Massenabweichung} = 1,37 \text{ ppm}$$

Figure S11: Data sheet high resolution MS of **3b**.

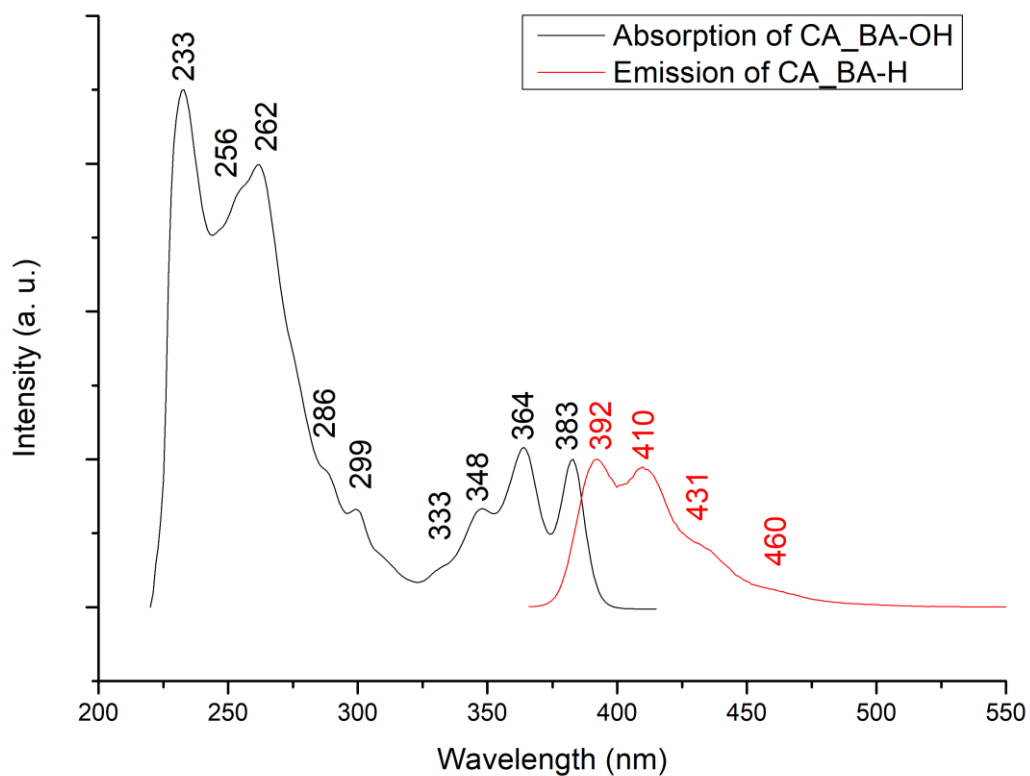


Figure S12: Absorption and emission spectra of **3b** (10^{-5} mol/L) in CD_2Cl_2 .

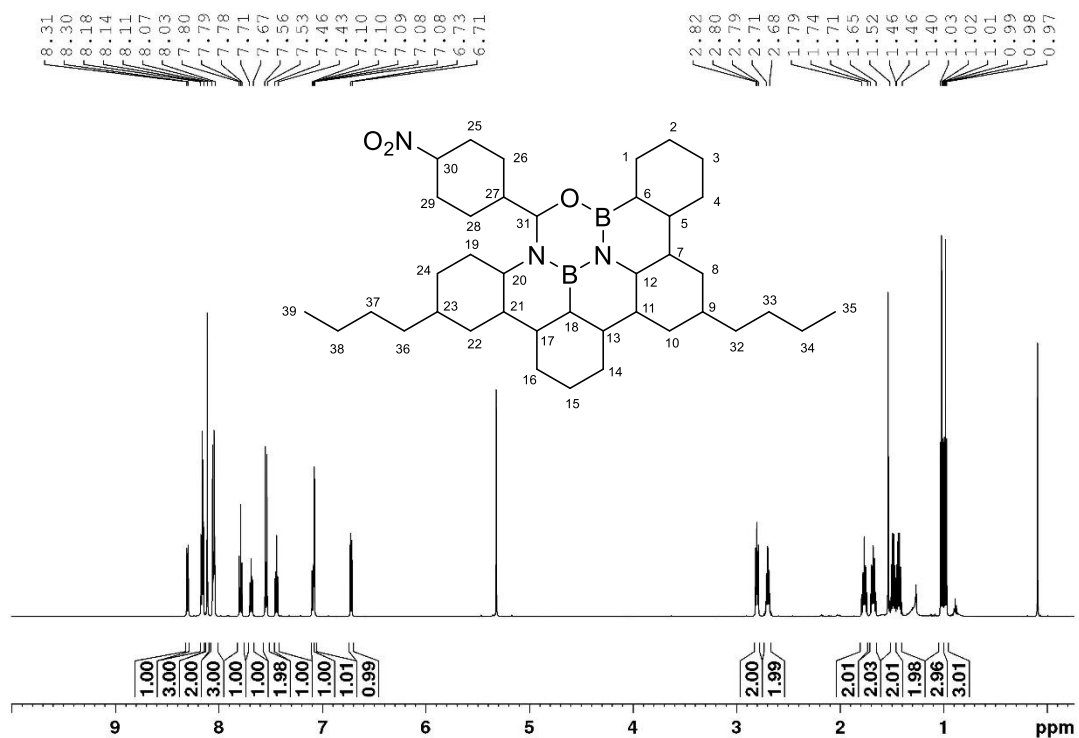


Figure S13: $^1\text{H-NMR}$ of **3c** in CD_2Cl_2 .

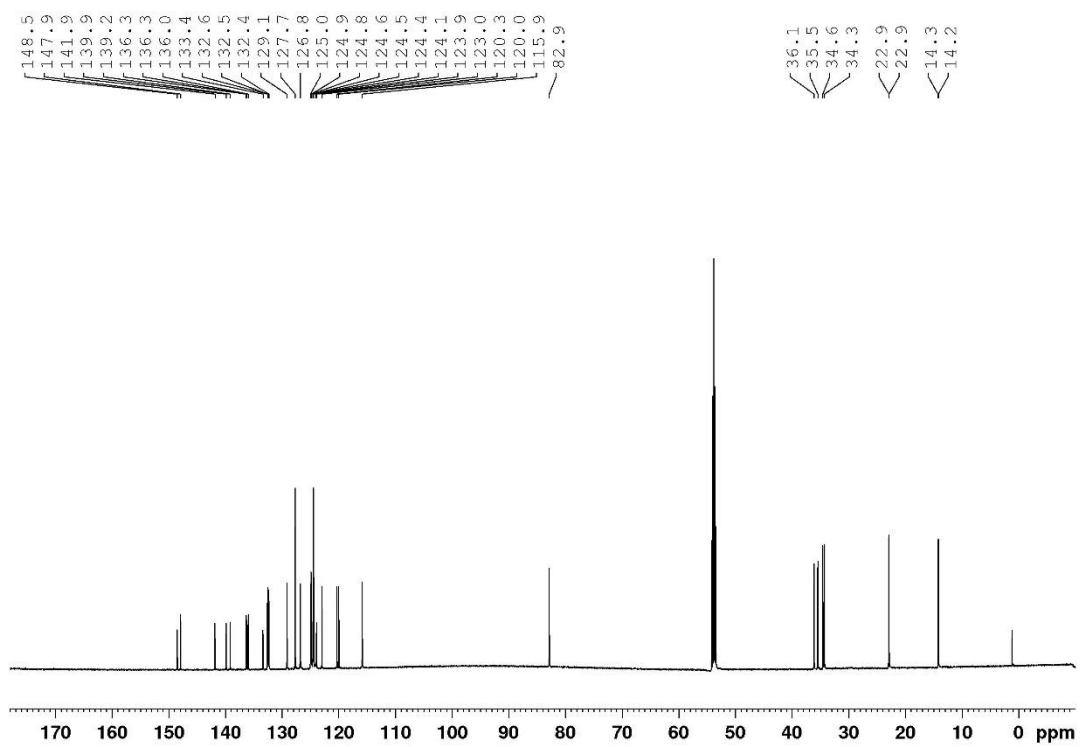


Figure S14: ^{13}C -NMR of **3c** in CD_2Cl_2 .

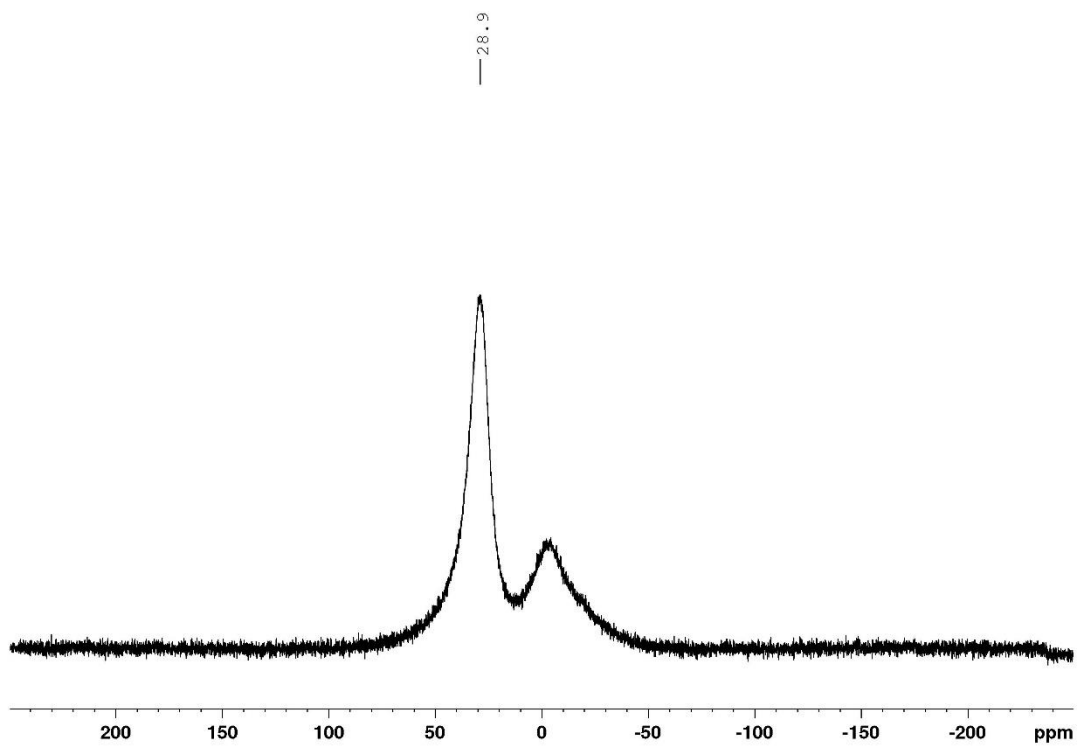
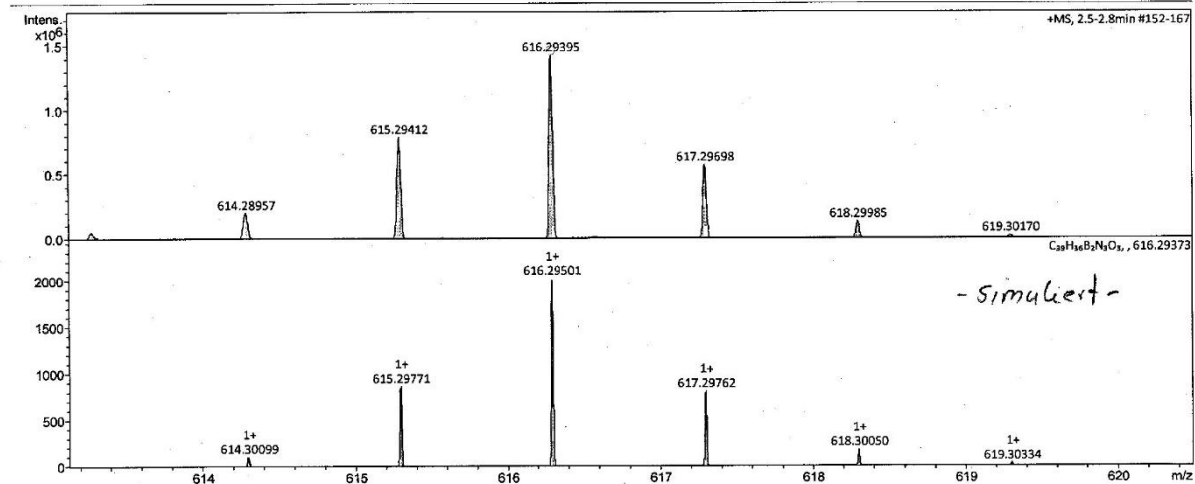


Figure S15: ^{11}B -NMR of **3c** in CD_2Cl_2 .

Display Report

Analysis Info	D:\Data\0\Fingerle_MF188000001.d	Acquisition Date	5/19/2020 12:43:29 PM
Analysis Name	DIP_ms_100-2200_pos_apci_neu.m	Operator	BDAL@DE
Method	Fingerle MF 188	Instrument	maXis
Sample Name	APCI + DIP		288882.21253
Comment			

Acquisition Parameter					
Source Type	APCI	Ion Polarity	Positive	Set Nebulizer	2.0 Bar
Focus	Not active	Set Capillary	4500 V	Set Dry Heater	220 °C
Scan Begin	100 m/z	Set End Plate Offset	-500 V	Set Dry Gas	3.0 l/min
Scan End	2200 m/z	Set Charging Voltage	0 V	Set Divert Valve	Waste
		Set Corona	4000 nA	Set APCI Heater	400 °C



Fingerle_MF188000001.d
 Bruker Compass DataAnalysis 4.2 printed: 5/19/2020 1:00:51 PM by: BDAL@DE Page 1 of 1

Figure S16: High resolution MS of **3c**.

High Resolution MS DIP-APCI

- FT-ICR-MS
- ESI- oder APCI-TOF-MS (MS/MS möglich)
- egal (je nach freien Kapazitäten)

Name: Michael Fingerle

AK: Bettinger

Tel. 76250

email:

Datum: 11.05.2020

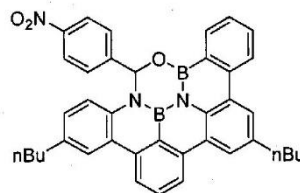
Probenbezeichnung: MF188

nomielle Masse: 615.29

Falls Masse nicht bekannt, welcher Massenbereich soll gemessen werden:

Summenformel (falls bekannt): $C_{39}H_{35}B_2N_3O_3$

Strukturformel (falls bekannt):



Einwaage (zwischen 0,1 mg und 2 mg):

Löslich in:

Falls schon gelöst, in welchem Lösemittel und in welcher Konzentration:

Hinweise bezüglich Zersetzlichkeit:

Hinweise bezüglich Toxizität (wenn bekannt):

Hohe Massengenauigkeit erwünscht? ja/nein

Massenanalyse erwünscht?

Wenn ja, welche Elemente sollen berücksichtigt werden?

MS/MS erwünscht?:

Ergebnis:

$[M + H]^+$ (theor.) = 616,29501

Gemessen = 616,29395

Relative Massenabweichung = 1,73 ppm

Figure S17: Data sheet high resolution MS of **3c**.

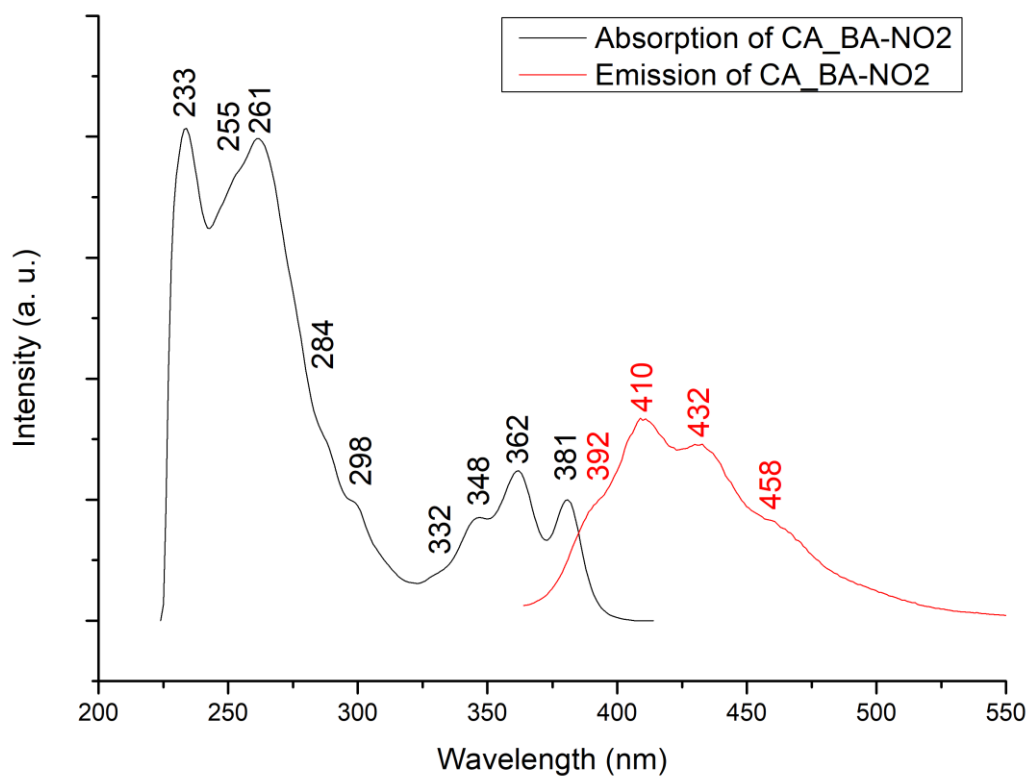


Figure S18: Absorption and emission spectra of **3c** (10^{-5} mol/L) in CD_2Cl_2 .

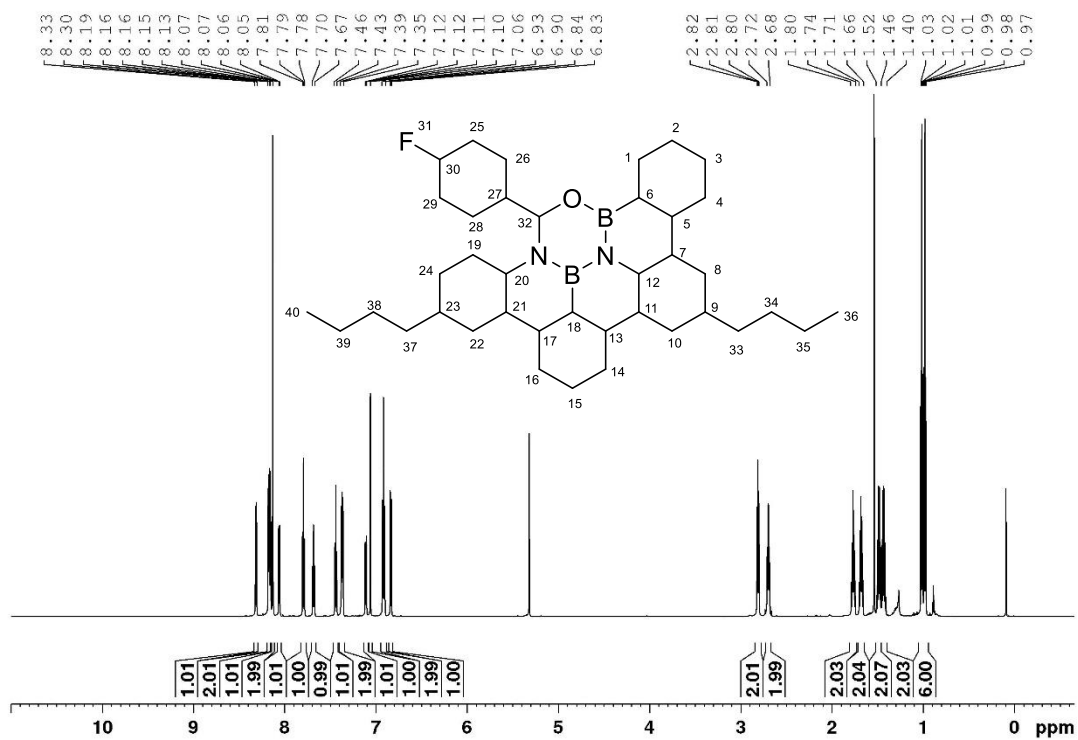


Figure S19: $^1\text{H-NMR}$ of **3d** in CD_2Cl_2 .

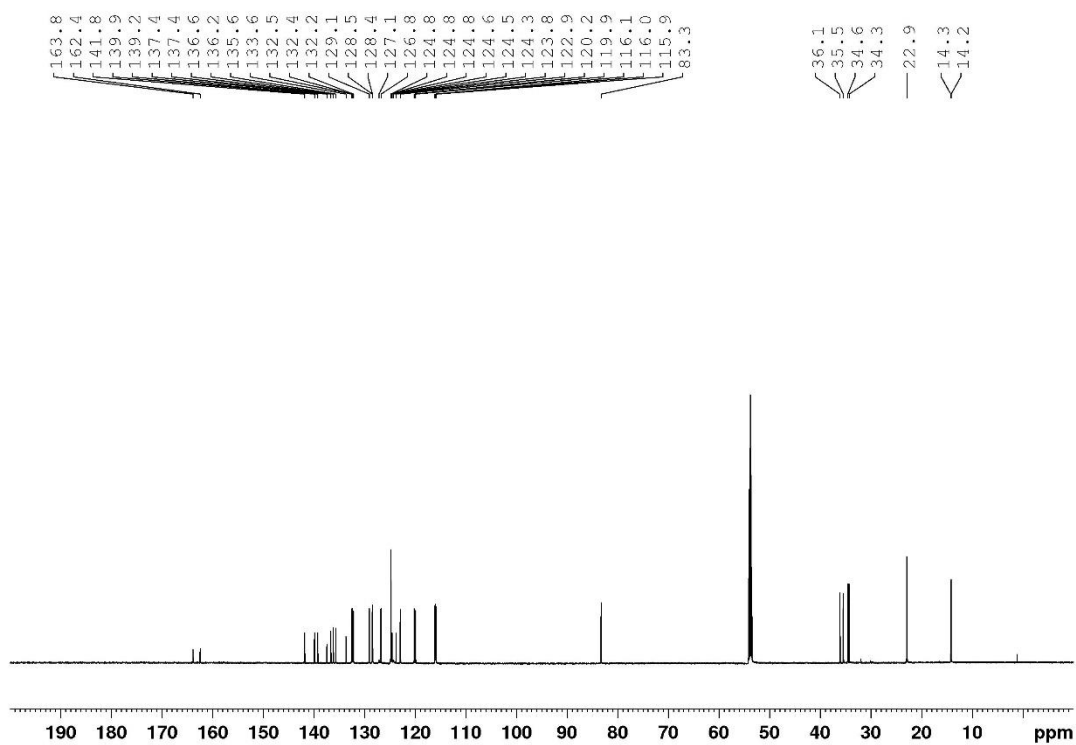


Figure S20: ^{13}C -NMR of **3d** in CD_2Cl_2 .

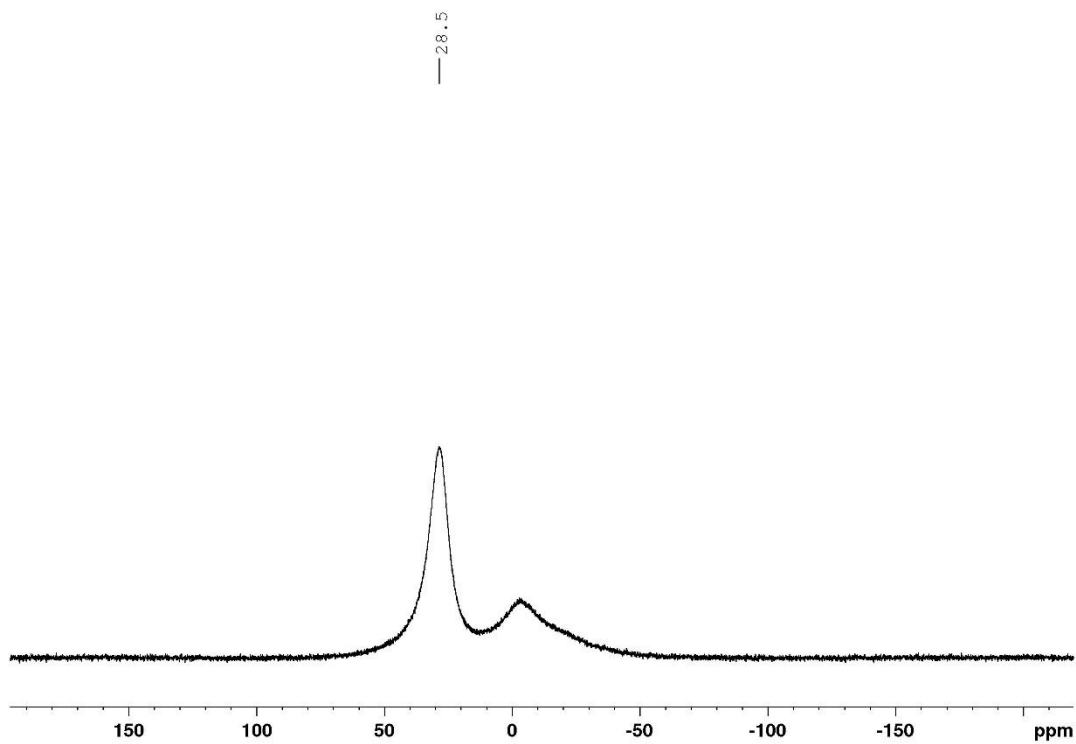


Figure S21: ^{11}B -NMR of **3d** in CD_2Cl_2 .

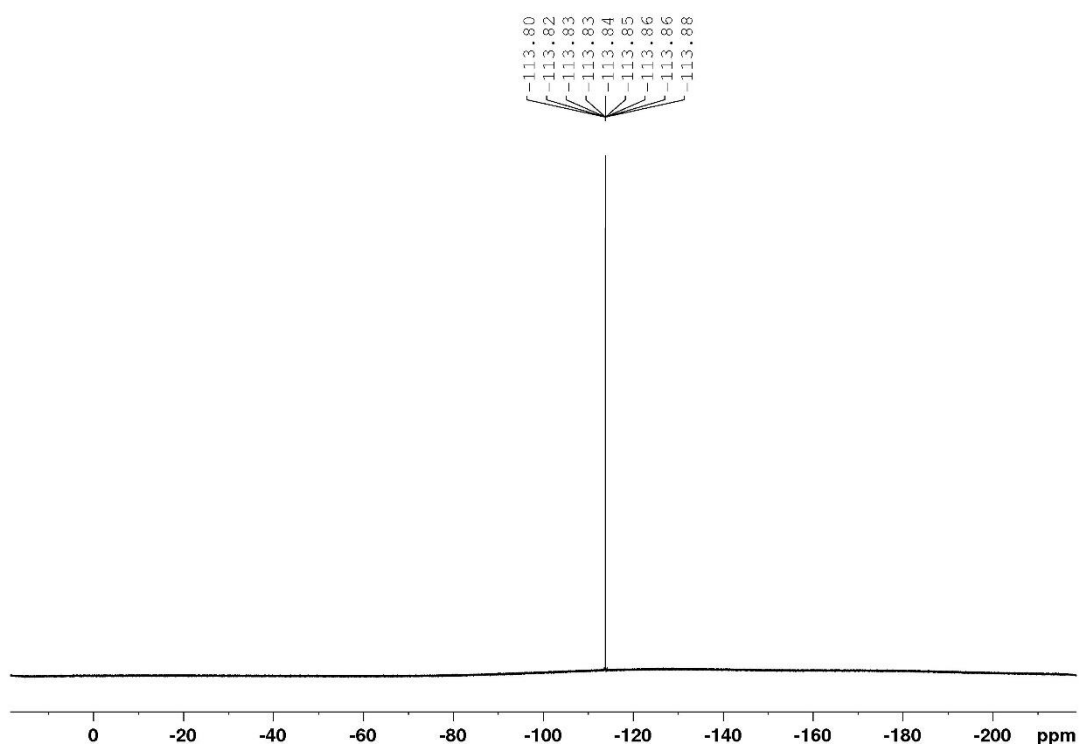


Figure S22: ^{19}F NMR of **3d** in CD_2Cl_2 .

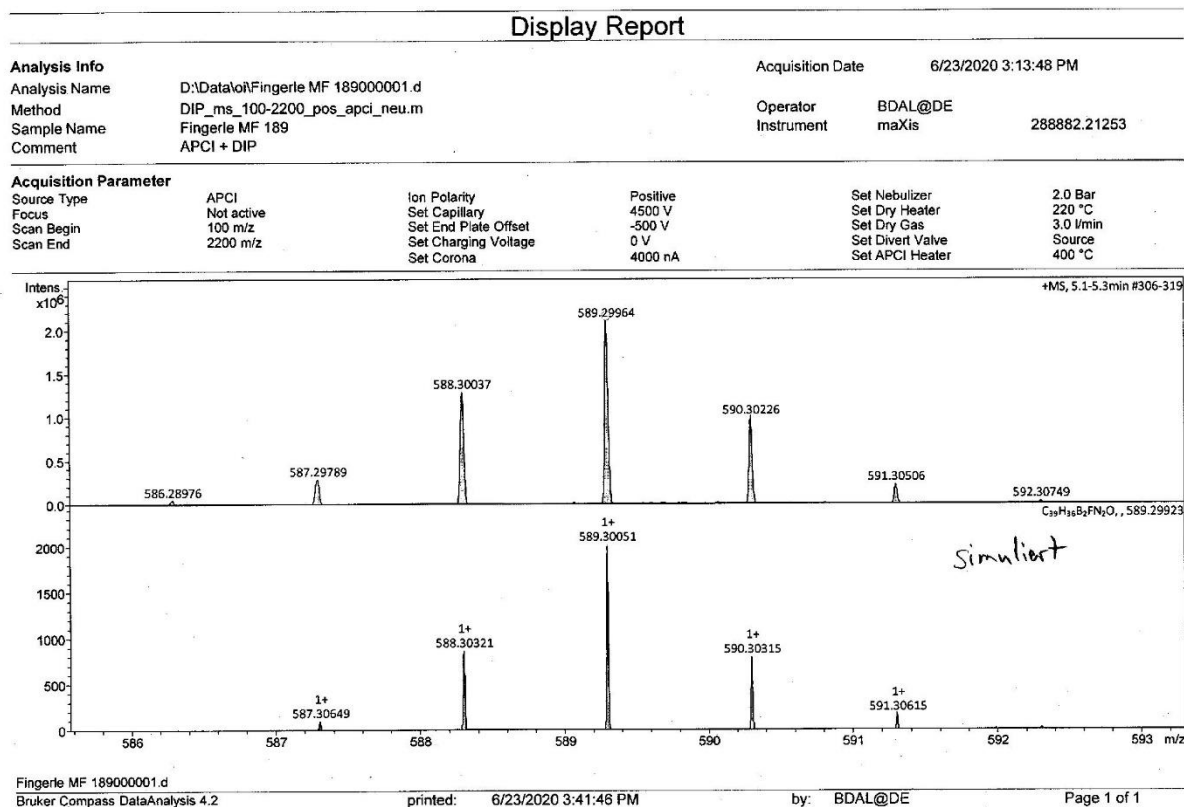


Figure S23: High resolution MS of **3d**.

High Resolution MS DIP-APCI

- FT-ICR-MS
- ESI- oder APCI-TOF-MS (MS/MS möglich)
- egal (je nach freien Kapazitäten)

Name: Michael Fingerle

AK: Bettinger

Tel. 76250

email:

Datum: 17.07.2020

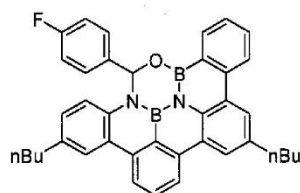
Probenbezeichnung: MF189

nominelle Masse:

Falls Masse nicht bekannt, welcher Massenbereich soll gemessen werden:

Summenformel (falls bekannt):

Strukturformel (falls bekannt):



Chemical Formula: $C_{39}H_{35}B_2FN_2O$
Exact Mass: 588,29

Einwaage (zwischen 0,1 mg und 2 mg):

Löslich in:

Falls schon gelöst, in welchem Lösemittel und in welcher Konzentration:

Hinweise bezüglich Zersetzlichkeit:

Hinweise bezüglich Toxizität (wenn bekannt):

Hohe Massengenauigkeit erwünscht? ja/nein

Massenanalyse erwünscht?

Wenn ja, welche Elemente sollen berücksichtigt werden?

MS/MS erwünscht?:

Ergebnis:

$[M+H]^+$ (theor.) = 589,30051

Gemessen = 589,29964

Relative Massenabweichung = 1,48 ppm

Figure S24: Data sheet high resolution MS of **3d**.

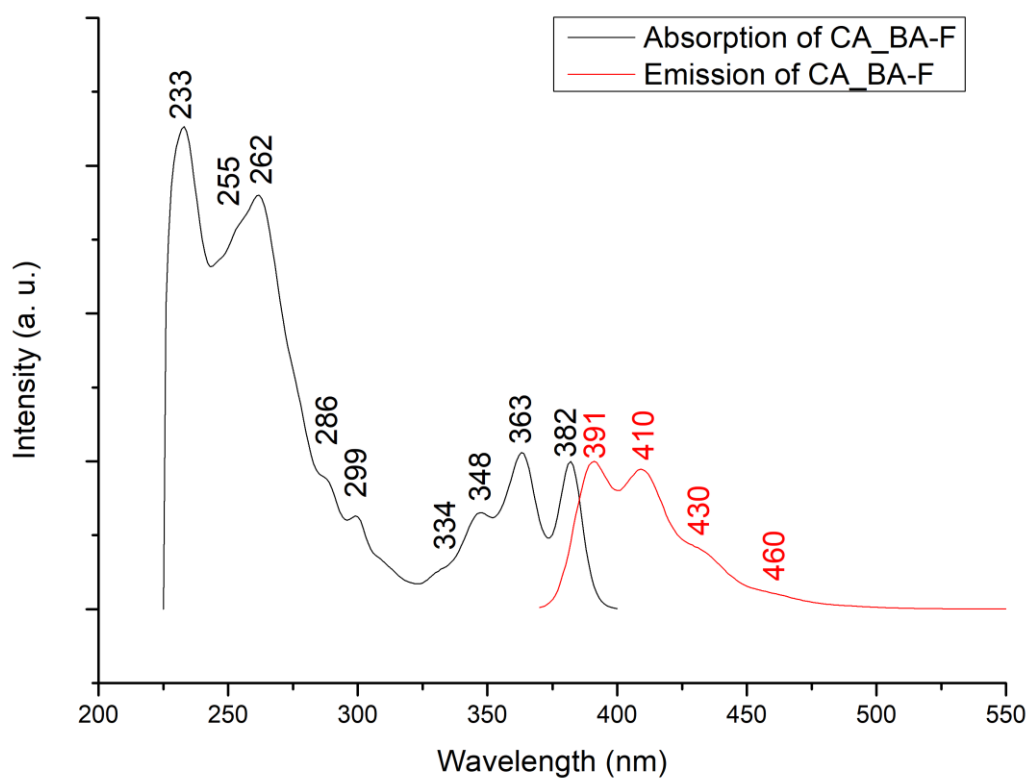


Figure S25: Absorption and emission spectra of **3d** (10⁻⁵ mol/L) in CD₂Cl₂.

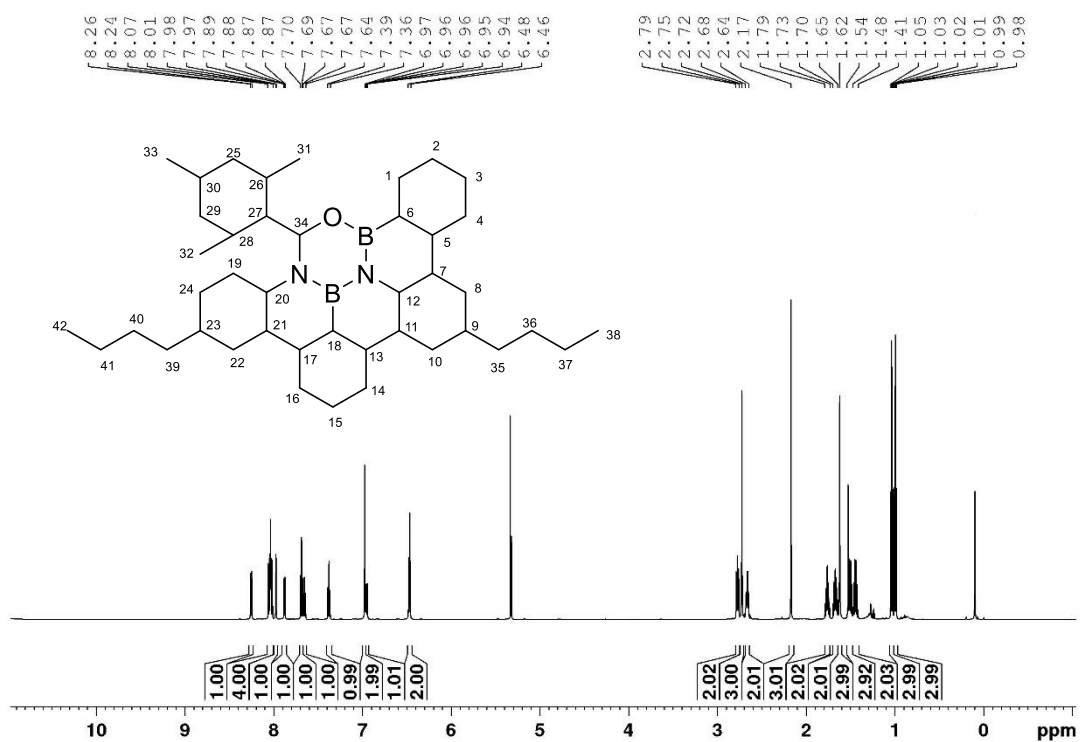


Figure S26: ¹H-NMR of **3e** in CD₂Cl₂.

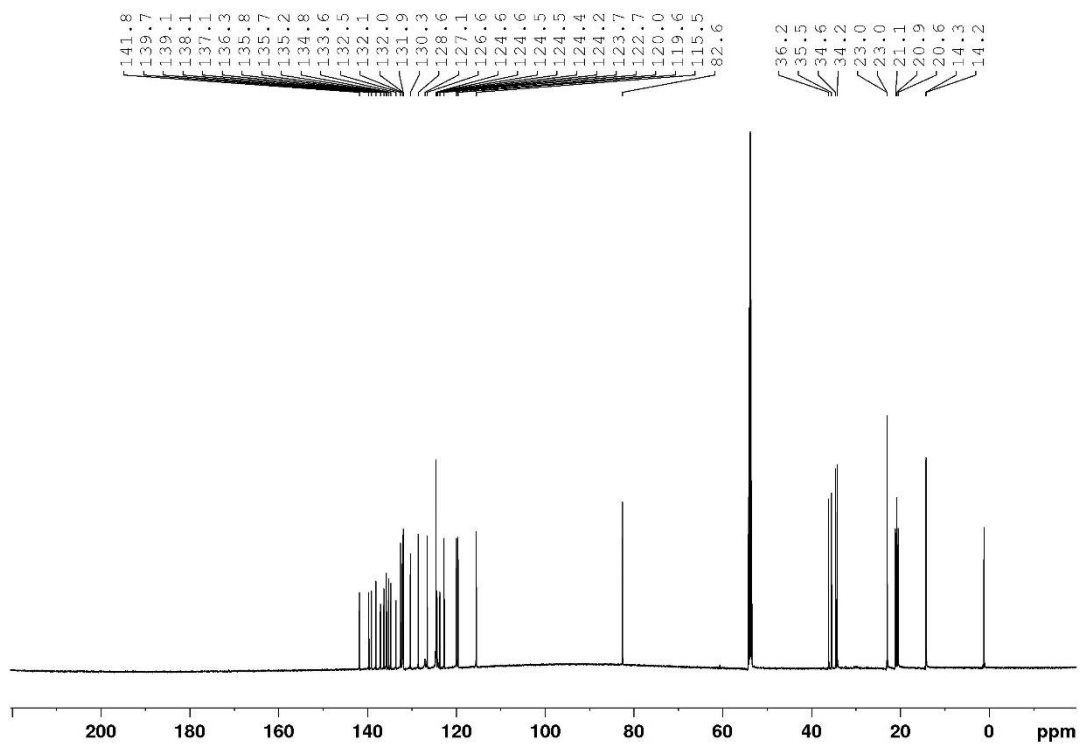


Figure S27: ^{13}C -NMR of **3e** in CD_2Cl_2 .

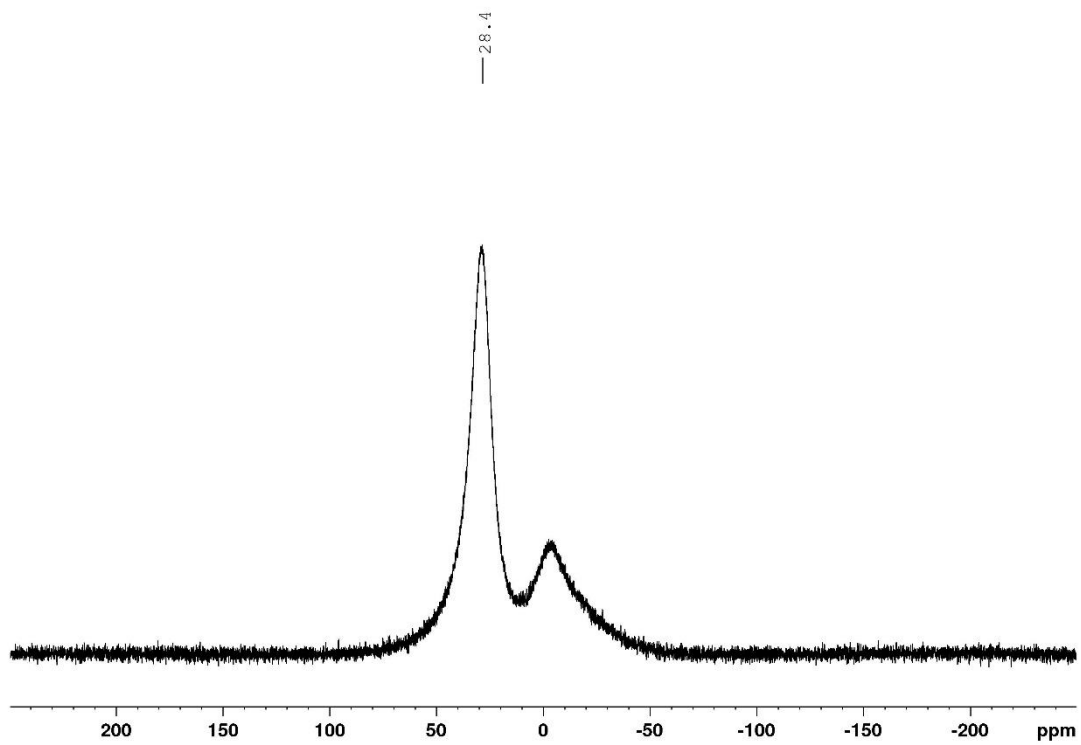
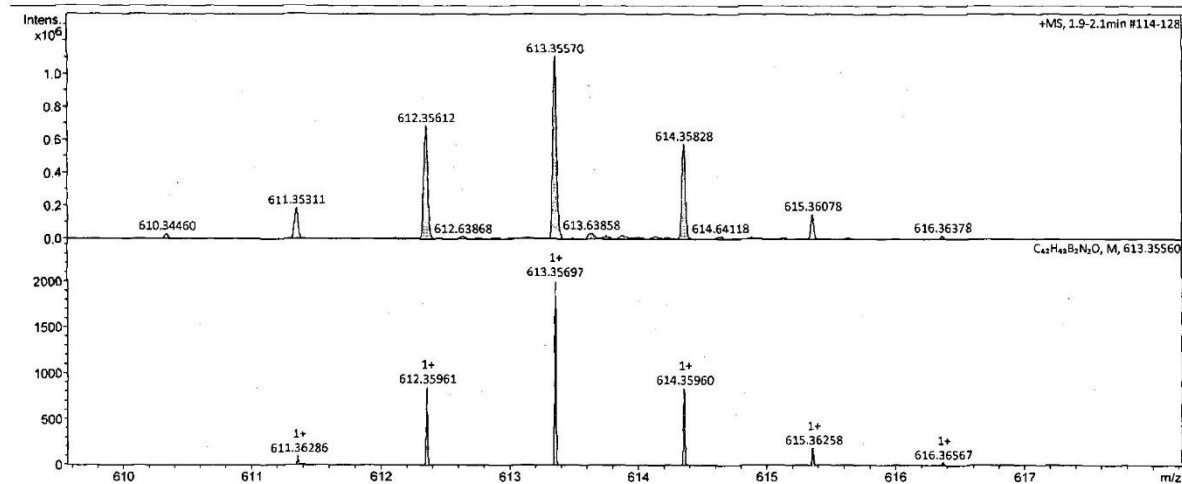


Figure S28: ^{11}B -NMR of **3e** in CD_2Cl_2 .

Display Report

Analysis Info		Acquisition Date	11/26/2020 9:48:19 AM
Analysis Name	D:\Data\01\Fingerle_MF 202000001.d	Operator	BDAL@DE
Method	DIP_ms_100-2200_pos_apci_neu.m	Instrument	maXis
Sample Name	Fingerle MF 202		288882.21253
Comment	DIP / APCI		

Acquisition Parameter					
Source Type	APCI	Ion Polarity	Positive	Set Nebulizer	2.0 Bar
Focus	Not active	Set Capillary	4500 V	Set Dry Heater	220 °C
Scan Begin	100 m/z	Set End Plate Offset	-500 V	Set Dry Gas	3.0 l/min
Scan End	2200 m/z	Set Charging Voltage	0 V	Set Divert Valve	Source
		Set Corona	4000 nA	Set APCI Heater	400 °C



Fingerle_MF 202000001.d
 Bruker Compass DataAnalysis 4.2 printed: 11/26/2020 2:02:23 PM by: BDAL@DE Page 1 of 1

Figure S29: High resolution MS of **3e**.

High Resolution MS DIP-APCI

- FT-ICR-MS.
- ESI- oder APCI-TOF-MS (MS/MS möglich)
- egal (je nach freien Kapazitäten)

Name: Michael Fingerle

AK: Bettinger

Tel. 76250

email:

Datum: 12.11.2020

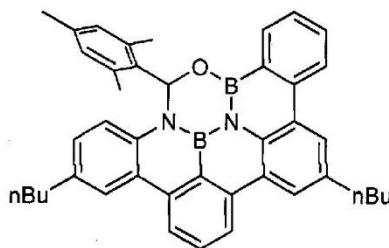
Probenbezeichnung: MF202

nominelle Masse:

Falls Masse nicht bekannt, welcher Massenbereich soll gemessen werden:

Summenformel (falls bekannt):

Strukturformel (falls bekannt):



Chemical Formula: $C_{42}H_{42}B_2N_2O$
Exact Mass: 612,35

Einwaage (zwischen 0,1mg und 2 mg):

Löslich in:

Falls schon gelöst, in welchem Lösemittel und in welcher Konzentration:

Hinweise bezüglich Zersetzlichkeit:

Hinweise bezüglich Toxizität (wenn bekannt):

Hohe Massengenauigkeit erwünscht? ja/nein

Massenanalyse erwünscht?

Wenn ja, welche Elemente sollen berücksichtigt werden?

MS/MS erwünscht?:

Ergebnis:

$[M + H]^+$ (theor.) = 613,35697

Gemessen = 613,35570

Relative Massenabweichung = 2,0 ppm

Figure S30: Data sheet high resolution MS of **3e**.

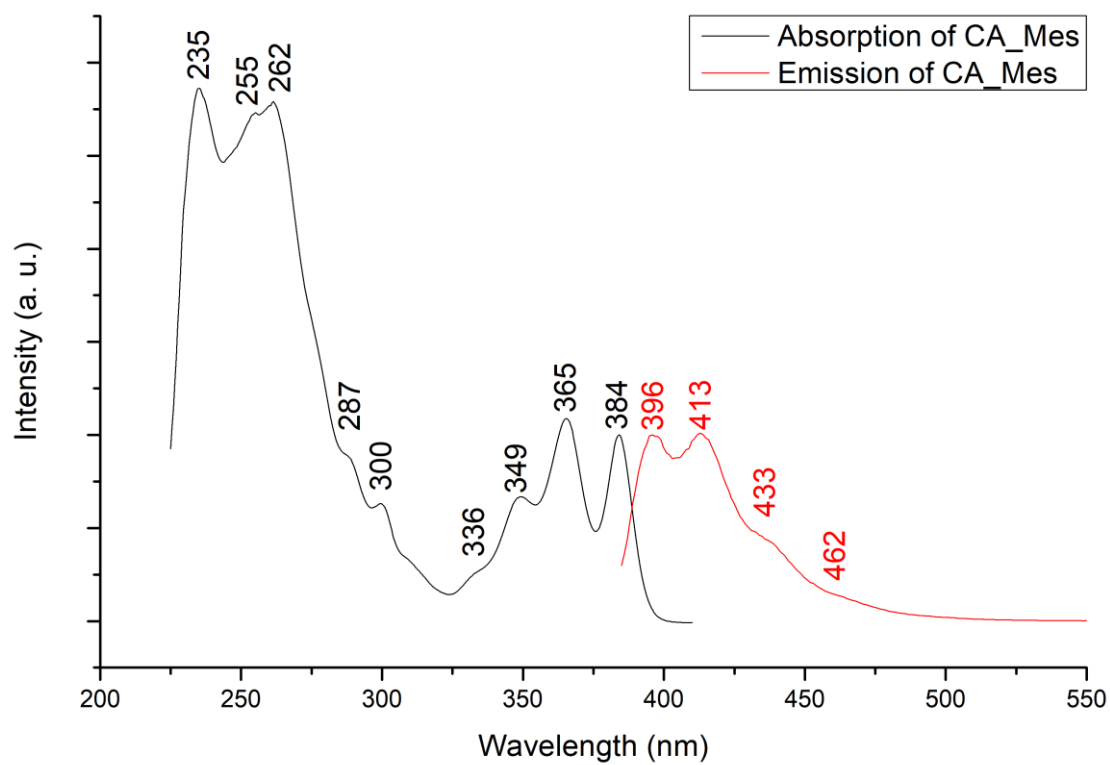


Figure S31: Absorption and emission spectra of **3e** (10^{-5} mol/L) in CD_2Cl_2 .

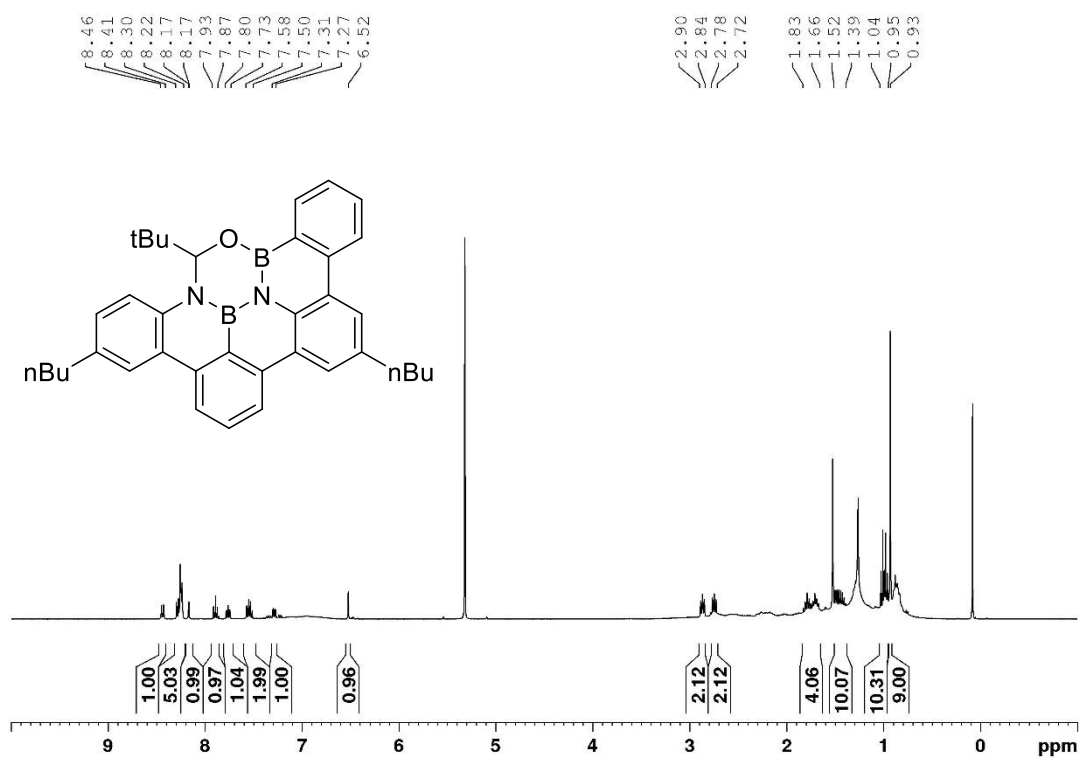


Figure S32: $^1\text{H-NMR}$ of **3f** in CD_2Cl_2 .

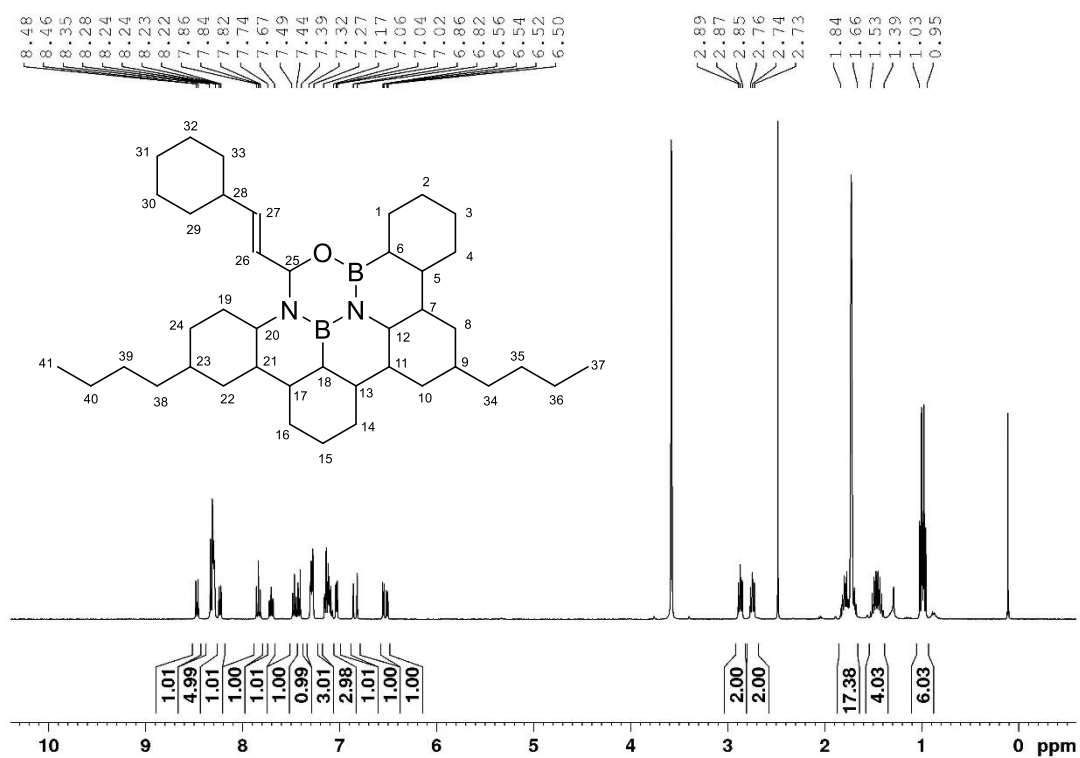


Figure S33: $^1\text{H-NMR}$ of **3g** in CD_2Cl_2 .

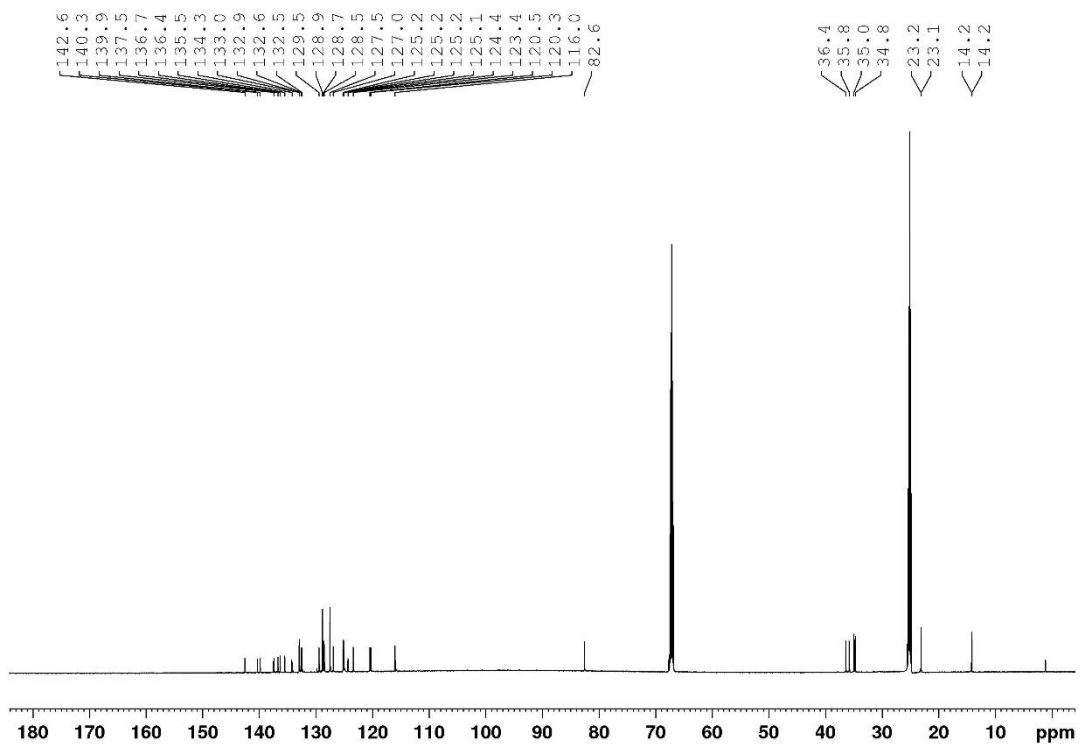


Figure S34: $^{13}\text{C-NMR}$ of **3g** in CD_2Cl_2 .

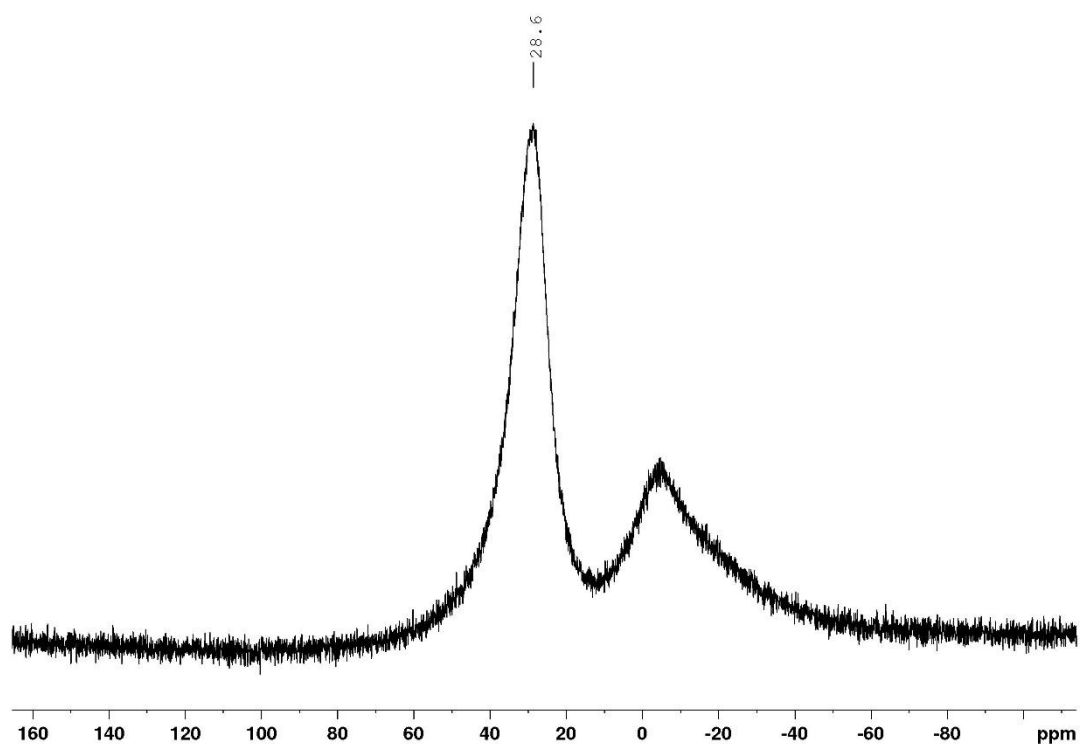


Figure S35: ^{11}B -NMR of **3g** in CD_2Cl_2 .

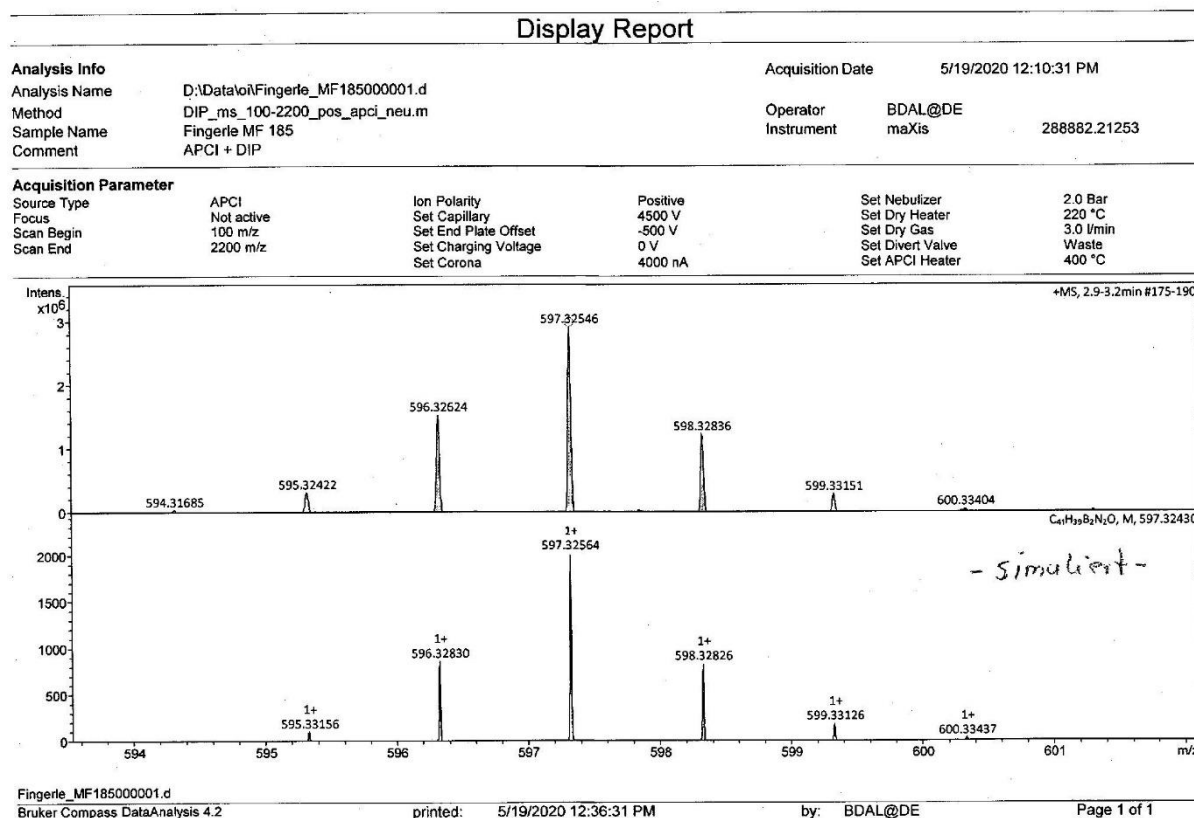


Figure S36: High resolution MS of **3g**.

High Resolution MS DIP-APCI

- FT-ICR-MS
- ESI- oder APCI-TOF-MS (MS/MS möglich)
- egal (je nach freien Kapazitäten)

Name: Michael Fingerle

AK: Bettinger

Tel. 76250

email:

Datum: 11.05.2020

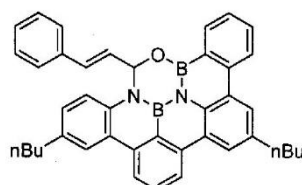
Probenbezeichnung: MF185

nominelle Masse:

Falls Masse nicht bekannt, welcher Massenbereich soll gemessen werden:

Summenformel (falls bekannt):

Strukturformel (falls bekannt):



Chemical Formula: $C_{41}H_{38}B_2N_2O$
Exact Mass: 596,32

Einwaage (zwischen 0,1 mg und 2 mg):

Löslich in:

Falls schon gelöst, in welchem Lösemittel und in welcher Konzentration:

Hinweise bezüglich Zersetzlichkeit:

Hinweise bezüglich Toxizität (wenn bekannt):

Hohe Massengenauigkeit erwünscht? ja/nein

Massenanalyse erwünscht?

Wenn ja, welche Elemente sollen berücksichtigt werden?

MS/MS erwünscht?:

Ergebnis:

$[M + H]^+$ (theor.) = 597,32564

Gemessen = 597,32546

Relative Massenabweichung = 0,30 ppm

Figure S37: Data sheet high resolution MS of **3g**.

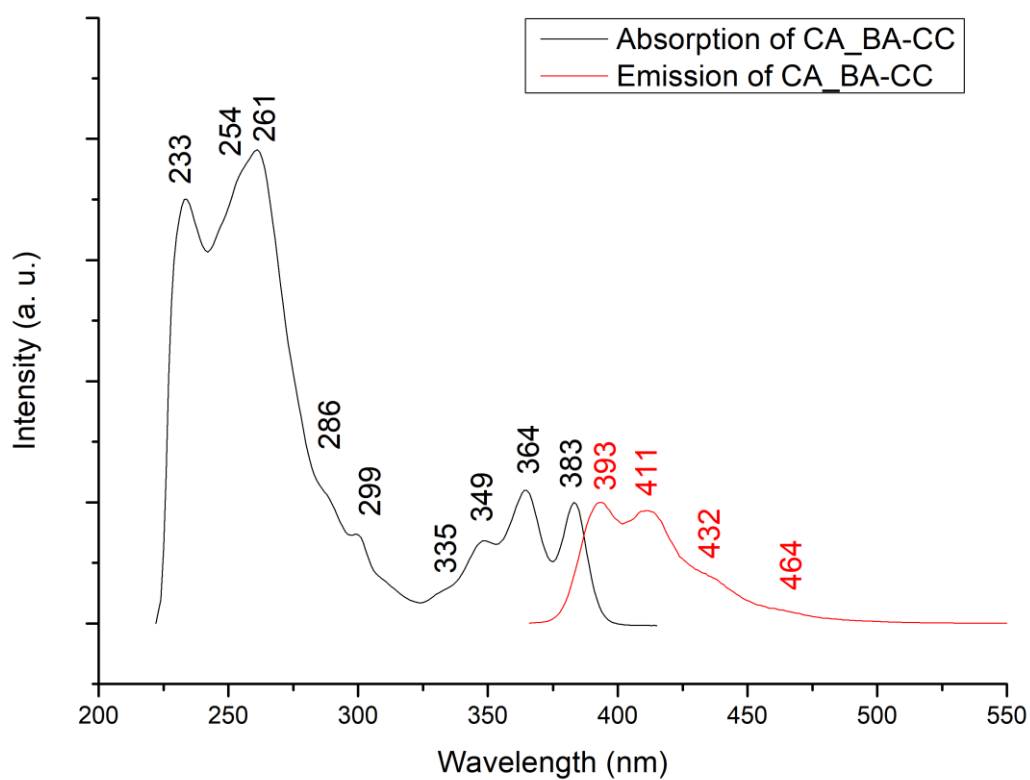


Figure S38: Absorption and emission spectra of **3g** (10^{-5} mol/L) in CD_2Cl_2 .

4. X-Ray Crystallographic Data

Empirical formula	C ₃₉ H ₃₆ B ₂ N ₂ O
Formula weight / [g/mol]	570.32
Temperature / [K]	100(2)
Radiation wavelength / [Å]	0.71073
Crystal system	Triclinic
Space group	P-1
Unit cell dimensions	a = 11.1035(3) Å; α = 107.688(2) ° b = 12.5038(5) Å; β = 108.360(2) ° c = 12.9042(4) Å; γ = 107.158(2) °
Volume / [Å ³]	1460.95(9)
Z	2
Radiation	MoKα
Density / [mg m ⁻³]	1.296
Absorption coefficient	0.076
F(000)	604
Crystal size / [mm]	0.16 x 0.14 x 0.12
Theta range for data collection / [°]	2.162-24.845
Limiting indices	-13 ≤ h ≤ 13 -14 ≤ k ≤ 11 -15 ≤ l ≤ 15
Reflections collected	13539
Independent reflects	4971
R _{int}	0.05
Completeness / [%]	98.2
Absorption correction	Multi-scan
Trans. (max., min.)	0.7451, 0.6696
Goodness-of-fit on F ²	1.014
Parameters / restrain	399/0
R ₁ , wR ₂ / [I > 2σ(I)]	0.0491, 0.1029
R ₁ , wR ₂ / [all data]	0.0944, 0.1214
Δρ _{max,min} / [e·Å ⁻³]	0.252, -0.206

5. Computational Investigations

5.1 Cycloaddition-dehydration with other dienophiles

The computational investigation (M062X/6-311+G**) of the cycloaddition-dehydration sequence with other hetero dienophiles are summarized in Figure S39. The reaction with nitrile, isonitrile, and CO₂ are strongly endergonic, while those with imine and iminium ion are exergonic. Note, however, that the cycloaddition product **B** does not correspond to a stationary point for the reaction with imine, indicating that the sequence **A** → **B** → **C** is not feasible for this reagent. Most exergonic is the reaction with the iminoborane yielding the borazine core.

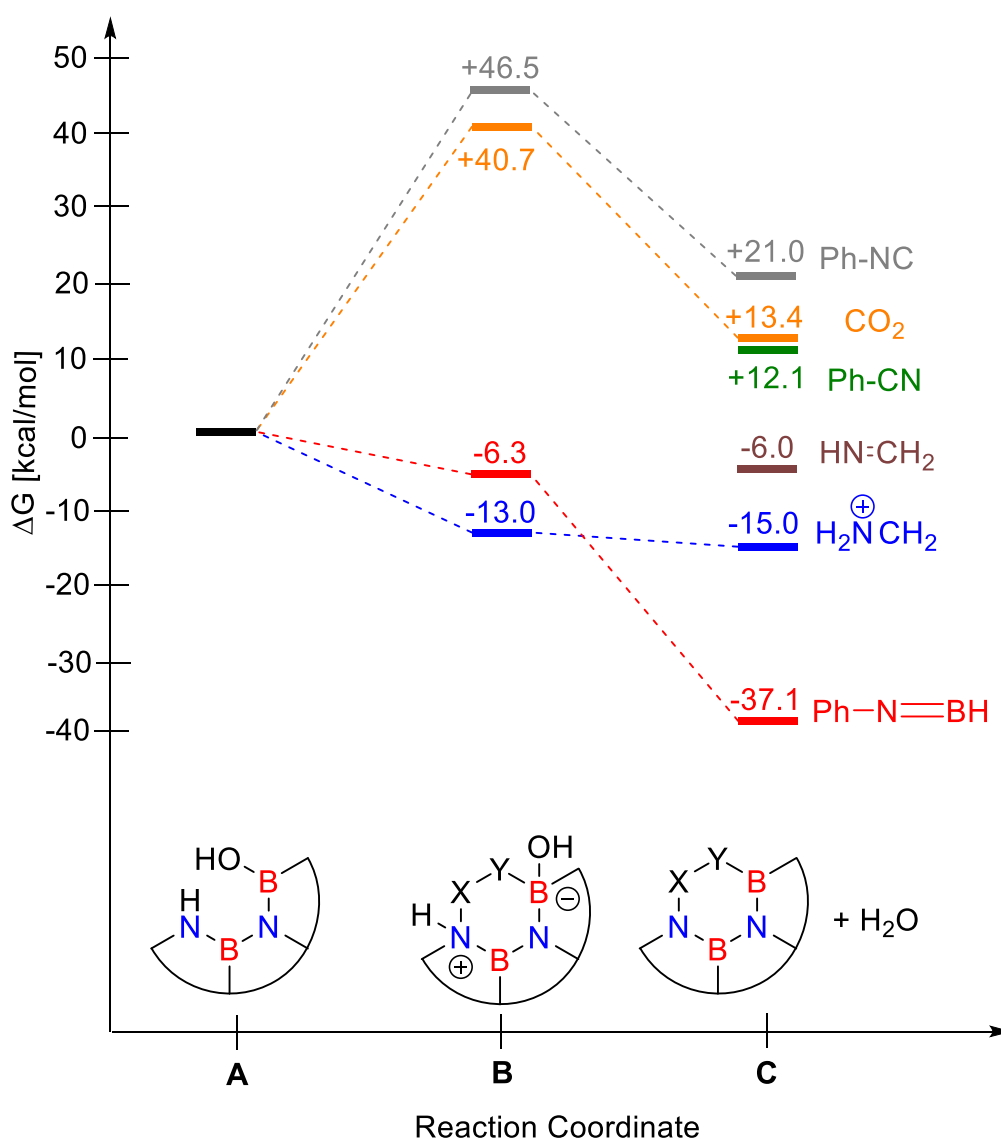


Figure S39: Gibbs free enthalpies for reaction of **A** with other hetero dienophiles.

5.2 NICS computations for 3a

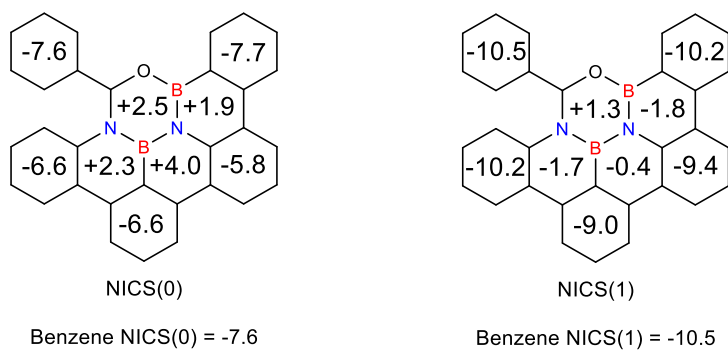


Figure S40. NICS(0) and NICS(1) computed for **A** at the M062X/6-311+G** level of theory. The values for benzene computed at the same level of theory are given for comparison.

6. Cyclic Voltammetry

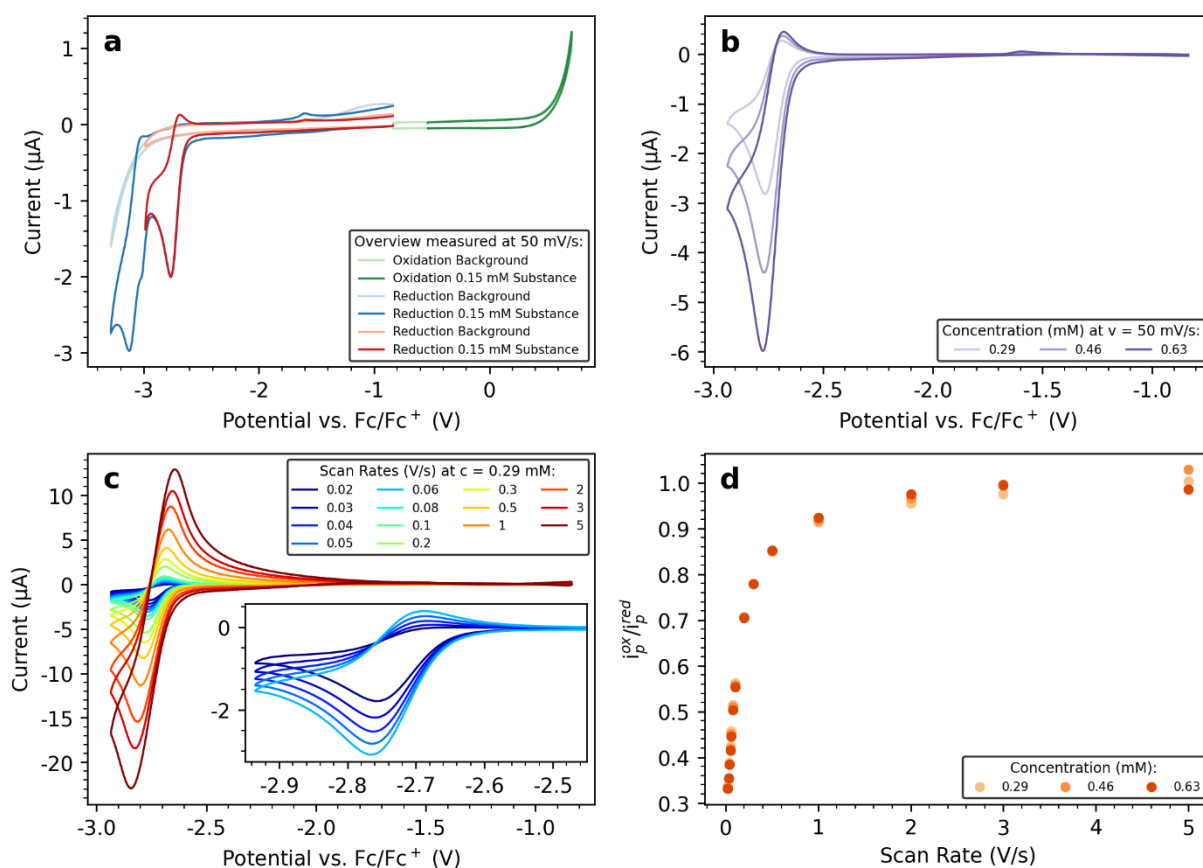


Figure S41. Cyclic voltammetry of the **3a** in 0.1 M TBAHFP/THF. **(a)** Electrolyte background scans (light colours) and measurements of **3a** (dark colours) in oxidative and reductive direction. **(b)** Concentration-dependent CV with 50 mV/s scan rate. **(c)** Scan rate-dependent CV at a fixed concentration of 0.29 mM. The inset shows CV measurements recorded at slower scan rates. **(d)** Scan rate-dependent peak current height ratios for all three substance concentrations.

In Figure S41 (a), an overview of the electrochemical response of a 0.15 mM solution of **3a** (dark colours) in 0.1 TBAHFP/THF is shown. The measurements were carried out with a scan rate of 50 mV/s and are displayed without background correction. The respective background electrolyte scans are depicted in light colours. In the oxidative direction, no electrochemical reaction of the Dibenzoperylene occurs within the electrochemical measurement window. In the reductive direction, three consecutive signals at approx. -2.7, -3.0 and -3.1 V vs. Fc/Fc⁺ (dark blue curve) can be observed in the forward scan. When reversing the potential scan direction at approx. -2.9 V vs. Fc/Fc⁺, a reverse peak of the first reduction can be seen (dark red curve). Only the first reduction wave was analyzed in more detail.

Figure S41 (b) shows concentration-dependent CV measurements of the first reduction of **3a** at a fixed scan rate of 50 mV/s. With increasing concentration, a small shift of the peak potential of the reduction towards more negative potentials can be observed, indicating an incomplete iR -compensation. Additionally, a small oxidative feature at around -1.6 V vs. Fc/Fc⁺ can be observed in the backward scan. Scan rate-dependent CV measurements of the first reduction at a constant concentration of 0.29 mM are displayed in figure S41 (c). The scans at slow scan rates are magnified in the inset for a better overview. With increasing scan rate, the oxidative backward peak becomes more pronounced. This indicates a transition of an EC mechanism to a quasi-reversible electron transfer with E^0 of -2.724 ± 0.007 V vs. Fc/Fc⁺. Simultaneously, the additional oxidative feature at approx. -1.6 V vs. Fc/Fc⁺ disappears with increasing scan rate, suggesting that it is related to a follow-up reaction after the first reduction. However, this was not further investigated.

We calculate the scan rate-dependent peak/current ratios of the redox wave at -2.724 V vs. Fc/Fc⁺ by using the empirical formula found by Nicholson^[8]

$$\frac{i_p^{ox}}{i_p^{red}} = \left| \frac{i_p^{ox}}{i_p^{red}} \right| + 0.485 \cdot \left| \frac{i^{rev}}{i_p^{red}} \right| + 0.086$$

with i_p^{ox} and i_p^{red} as peak currents of the oxidative and reductive wave, and i^{rev} as the current at the potential where the scan direction is reversed. Figure S41 (d) displays the results for measurements made with all three concentrations of Dibenzoperylene **3a** used in Figure S41 (b). We find that a peak/current ratio of approx. one is achieved for scan rates greater than 2 V/s for all three concentrations. No further kinetic studies for the electrochemical reaction mechanisms were made.

7. Cartesian Coordinates of Stationary Points in Å

7.1 Calculations without solvent

(BN)₂ dibenzoperylene (C₁), S₀

45

Scf done: -1158.72276779

6	-3.590187000	-2.791290000	-0.137170000
6	-2.923373000	-1.557607000	-0.070342000
6	-3.662402000	-0.361717000	0.030880000
6	-5.063268000	-0.460483000	0.054090000
6	-5.715052000	-1.677198000	-0.013034000
6	-4.968187000	-2.853993000	-0.108245000
7	-1.537492000	-1.541444000	-0.101030000
5	-0.765721000	-0.355723000	-0.063365000
6	-1.548239000	0.952106000	0.016809000
6	-0.836611000	2.161998000	0.054572000
6	-1.544773000	3.353107000	0.234082000
6	-2.930761000	3.330298000	0.330726000
6	-3.638935000	2.142037000	0.254052000
6	-2.957944000	0.928481000	0.101179000
6	0.636862000	2.128605000	-0.086949000
6	1.324082000	3.332386000	-0.250568000
6	2.701349000	3.383349000	-0.360140000
6	3.420706000	2.209202000	-0.270514000
6	2.793623000	0.969683000	-0.109837000
6	1.372717000	0.910670000	-0.079086000
6	3.626163000	-0.242787000	0.019377000
6	3.011538000	-1.502997000	0.010959000
6	3.798765000	-2.658617000	0.130749000
6	5.172480000	-2.587632000	0.259716000
6	5.780719000	-1.331082000	0.287671000
6	5.023742000	-0.179934000	0.175197000
7	0.703603000	-0.337817000	-0.060303000
5	1.473477000	-1.556284000	-0.084872000
1	4.496655000	2.257621000	-0.353220000
1	3.206680000	4.328741000	-0.511462000
1	0.767910000	4.255995000	-0.320005000
8	0.808966000	-2.760850000	-0.178517000
1	-4.717079000	2.173649000	0.331566000
1	-1.041675000	4.305622000	0.321533000
1	-3.467220000	4.261521000	0.472927000
1	3.337132000	-3.642665000	0.137301000
1	5.767226000	-3.488043000	0.352469000
1	6.854874000	-1.252819000	0.408963000
1	5.536133000	0.769886000	0.231358000
1	-5.660291000	0.439189000	0.122052000
1	-6.796937000	-1.714726000	0.006244000
1	-5.465353000	-3.815175000	-0.161698000
1	-3.000136000	-3.698601000	-0.213552000
1	-1.091657000	-2.446008000	-0.151313000
1	1.402365000	-3.512037000	-0.219530000

Compound tetramethylethylene (TME) (C₂), S₀

18

scf done: -235.788685613

6	0.669805000	0.000034000	-0.000040000
6	-0.669795000	0.000057000	0.000031000
6	1.512002000	1.252679000	0.034065000
1	2.332309000	1.122145000	0.746563000
1	1.972169000	1.437138000	-0.942783000
1	0.960720000	2.143218000	0.327531000
6	1.511796000	-1.252733000	-0.034093000
1	1.971361000	-1.437597000	0.943071000
1	0.960524000	-2.143087000	-0.328148000
1	2.332614000	-1.122151000	-0.745975000
6	-1.511850000	-1.252673000	0.034095000
1	-2.332322000	-1.122229000	0.746404000

1	-1.971879000	-1.437259000	-0.942949000
1	-0.960497000	-2.143153000	0.327652000
6	-1.511936000	1.252711000	-0.034083000
1	-2.331699000	1.122567000	-0.747277000
1	-1.972972000	1.436527000	0.942570000
1	-0.960461000	2.143434000	-0.326503000

Compound tetracyanoethylene (TCNE) (D_{2h}), S_0

10
scf done: -447.474600814

6	0.000000000	0.000000000	0.676823000
6	0.000000000	0.000000000	-0.676823000
6	0.000000000	1.223271000	1.420850000
7	0.000000000	2.200576000	2.024438000
6	0.000000000	-1.223271000	1.420850000
7	0.000000000	-2.200576000	2.024438000
6	0.000000000	1.223271000	-1.420850000
7	0.000000000	2.200576000	-2.024438000
6	0.000000000	-1.223271000	-1.420850000
7	0.000000000	-2.200576000	-2.024438000

Compound methoxyethene (C_1), S_0

10
scf done: -193.080751986

6	0.737628000	-0.566341000	0.000049000
6	1.432581000	0.569956000	0.000043000
1	1.221463000	-1.536134000	0.000101000
1	0.977202000	1.550266000	-0.000097000
1	2.511578000	0.514972000	0.000124000
8	-0.603656000	-0.714765000	-0.000045000
6	-1.364982000	0.475174000	-0.000035000
1	-1.151453000	1.071697000	-0.892500000
1	-2.409376000	0.172914000	-0.000070000
1	-1.151528000	1.071675000	0.892461000

Compound benzaldehyde (C_s), S_0

14
scf done: -345.515805225

6	-1.323799000	-1.324811000	-0.000029000
6	0.044055000	-1.099668000	-0.000031000
6	-2.208294000	-0.245599000	-0.000031000
1	0.754511000	-1.918267000	-0.000027000
1	-3.276953000	-0.425492000	-0.000028000
6	0.529193000	0.209556000	-0.000041000
6	-1.727255000	1.059461000	-0.000037000
1	-2.417715000	1.893947000	-0.000038000
6	-0.355388000	1.286014000	-0.000045000
1	0.033812000	2.299479000	-0.000050000
1	-1.707527000	-2.337857000	-0.000025000
6	1.990039000	0.466280000	-0.000032000
8	2.830717000	-0.394492000	0.000188000
1	2.276829000	1.536723000	0.000145000

Compound H_2O (C_{2v}), S_0

3
scf done: -76.4208334206

8	0.000000000	0.000000000	0.116605000
---	-------------	-------------	-------------

1	0.000000000	0.761605000	-0.466419000
1	0.000000000	-0.761605000	-0.466419000

Compound B with TME (C₁), S₀

63

scf done: -1394.47271134

6	-2.790707000	-1.064292000	-0.598554000
6	-3.534750000	0.115192000	-0.400621000
6	-4.906864000	0.056626000	-0.672639000
6	-5.515638000	-1.096661000	-1.143273000
6	-4.750567000	-2.228591000	-1.397859000
6	-3.389398000	-2.202801000	-1.130244000
6	-2.885668000	1.406308000	-0.054713000
6	-1.488422000	1.488656000	-0.206269000
6	-0.773926000	2.681263000	-0.012504000
6	-1.515090000	3.824862000	0.348103000
6	-2.883589000	3.739251000	0.526297000
6	-3.581983000	2.540805000	0.333619000
6	0.691667000	2.657013000	-0.128401000
6	1.431909000	3.839617000	0.028331000
6	2.808844000	3.824185000	0.042325000
6	3.485870000	2.615161000	-0.102720000
6	2.815565000	1.416522000	-0.312432000
6	1.393285000	1.432769000	-0.335547000
6	3.571425000	0.144088000	-0.468890000
6	2.919761000	-1.093788000	-0.325039000
6	3.683375000	-2.262703000	-0.448212000
6	5.048315000	-2.231822000	-0.698449000
6	5.677770000	-1.002109000	-0.871008000
6	4.943513000	0.168830000	-0.767585000
5	1.324101000	-1.194832000	-0.215009000
8	0.807498000	-2.179238000	-1.215339000
7	0.703172000	0.238202000	-0.500957000
5	-0.674500000	0.245064000	-0.427155000
7	-1.361152000	-1.115105000	-0.310190000
6	0.640325000	-1.602031000	1.250827000
6	-0.918086000	-1.818479000	1.076086000
1	4.565011000	2.618031000	-0.028982000
1	3.364142000	4.742651000	0.186840000
1	0.918805000	4.782978000	0.157533000
1	-4.651668000	2.523510000	0.500041000
1	-1.031942000	4.777092000	0.519822000
1	-3.432061000	4.623802000	0.829205000
1	3.181973000	-3.221742000	-0.359971000
1	5.613597000	-3.153160000	-0.781560000
1	6.735778000	-0.954921000	-1.101827000
1	5.449496000	1.108209000	-0.950226000
1	-5.504971000	0.950493000	-0.552731000
1	-6.579299000	-1.098410000	-1.347682000
1	-5.203050000	-3.120889000	-1.811833000
1	-2.776809000	-3.070076000	-1.344211000
1	-0.864345000	-1.720089000	-0.995220000
1	1.341026000	-2.160424000	-2.012937000
6	-1.299601000	-3.290094000	0.925855000
1	-2.378059000	-3.405719000	0.818315000
1	-0.785986000	-3.751121000	0.079828000
1	-1.011265000	-3.823349000	1.830947000
6	1.311272000	-2.871933000	1.798331000
1	0.879252000	-3.193681000	2.753843000
1	1.266315000	-3.707296000	1.097185000
1	2.365305000	-2.652762000	1.982047000
6	-1.775694000	-1.201380000	2.175866000
1	-2.831388000	-1.441444000	2.028877000
1	-1.464253000	-1.627000000	3.132184000
1	-1.667990000	-0.117968000	2.237861000
6	0.956283000	-0.483219000	2.263569000
1	0.456660000	0.463935000	2.047042000
1	0.696015000	-0.770983000	3.287666000
1	2.032418000	-0.286068000	2.244017000

Compound B with TCNE (C_1), S_0

55

scf done: -1606.16401315

6	-2.804478000	-0.854241000	-0.786853000
6	-3.510160000	0.338272000	-0.546437000
6	-4.887962000	0.301890000	-0.787994000
6	-5.525417000	-0.841744000	-1.244319000
6	-4.794055000	-1.992865000	-1.510360000
6	-3.425480000	-1.993447000	-1.285586000
6	-2.835684000	1.604407000	-0.163678000
6	-1.436849000	1.672568000	-0.305821000
6	-0.698396000	2.837297000	-0.040560000
6	-1.420415000	3.971367000	0.378570000
6	-2.791415000	3.901054000	0.541082000
6	-3.511489000	2.728898000	0.280194000
6	0.767851000	2.796550000	-0.149448000
6	1.522322000	3.962237000	0.049749000
6	2.899027000	3.927194000	0.058699000
6	3.562465000	2.718774000	-0.131118000
6	2.877557000	1.535157000	-0.379248000
6	1.460102000	1.579339000	-0.399082000
6	3.617372000	0.257219000	-0.565763000
6	2.942093000	-0.974778000	-0.516158000
6	3.675363000	-2.161809000	-0.637331000
6	5.051702000	-2.150297000	-0.812188000
6	5.711432000	-0.928425000	-0.901895000
6	5.002504000	0.257503000	-0.787209000
5	1.365024000	-1.017242000	-0.503037000
8	0.778099000	-1.950806000	-1.470384000
7	0.741443000	0.398367000	-0.616936000
5	-0.635744000	0.443821000	-0.581786000
7	-1.352775000	-0.931086000	-0.546356000
6	0.618732000	-1.553587000	1.014058000
6	-0.946270000	-1.669947000	0.769331000
1	4.641046000	2.709928000	-0.059804000
1	3.465806000	4.832580000	0.235817000
1	1.022459000	4.906715000	0.214068000
1	-4.580220000	2.720784000	0.450208000
1	-0.920574000	4.900667000	0.613955000
1	-3.325076000	4.775908000	0.893521000
1	3.156124000	-3.114106000	-0.585981000
1	5.602522000	-3.079833000	-0.891229000
1	6.781840000	-0.897285000	-1.068376000
1	5.544545000	1.187827000	-0.891635000
1	-5.470073000	1.202119000	-0.643406000
1	-6.594329000	-0.824634000	-1.417875000
1	-5.276860000	-2.881467000	-1.895641000
1	-2.840576000	-2.879572000	-1.499113000
1	-0.872450000	-1.504542000	-1.275834000
1	1.408756000	-2.229654000	-2.137383000
6	-1.345880000	-3.078541000	0.625881000
7	-1.673500000	-4.170699000	0.506351000
6	1.194479000	-2.832672000	1.396554000
7	1.685195000	-3.839751000	1.651969000
6	-1.741253000	-1.075447000	1.854877000
7	-2.370111000	-0.603402000	2.689644000
6	0.926321000	-0.537318000	2.011422000
7	1.178485000	0.315208000	2.739568000

Compound B with methoxyethene (C_1), S_0

55

scf done: -1351.76975761

6	-2.704788000	-1.154437000	-0.517468000
6	-3.400539000	0.066947000	-0.445566000
6	-4.790241000	0.002163000	-0.618516000
6	-5.452972000	-1.192908000	-0.851928000
6	-4.736454000	-2.381204000	-0.949529000
6	-3.360491000	-2.352004000	-0.784936000
6	-2.712140000	1.370315000	-0.235878000
6	-1.304954000	1.381511000	-0.222853000

6	-0.549302000	2.556666000	-0.078104000
6	-1.262935000	3.764504000	0.051608000
6	-2.645687000	3.758128000	0.052893000
6	-3.382598000	2.576048000	-0.084948000
6	0.919358000	2.462819000	-0.037821000
6	1.696609000	3.619320000	0.127289000
6	3.068340000	3.547853000	0.227235000
6	3.704585000	2.310901000	0.154230000
6	3.002556000	1.127177000	-0.040683000
6	1.583587000	1.203414000	-0.128575000
6	3.717752000	-0.180079000	-0.132460000
6	3.004373000	-1.391842000	-0.145226000
6	3.718186000	-2.594981000	-0.203464000
6	5.103975000	-2.627428000	-0.251126000
6	5.805441000	-1.424478000	-0.266279000
6	5.120255000	-0.220887000	-0.214695000
5	1.412851000	-1.436382000	-0.191585000
8	0.902095000	-2.217106000	-1.364472000
7	0.847216000	0.037120000	-0.277513000
5	-0.529476000	0.102713000	-0.299561000
7	-1.269099000	-1.234528000	-0.289879000
6	0.655773000	-2.086084000	1.115003000
1	4.779245000	2.287139000	0.267359000
1	3.652546000	4.447954000	0.373307000
1	1.218756000	4.587163000	0.193898000
1	-4.462909000	2.634918000	-0.067674000
1	-0.752849000	4.711527000	0.163211000
1	-3.176918000	4.696189000	0.165990000
1	3.159390000	-3.526443000	-0.225478000
1	5.634260000	-3.572128000	-0.291376000
1	6.887678000	-1.422336000	-0.327331000
1	5.701399000	0.690539000	-0.256762000
1	-5.370217000	0.914417000	-0.582524000
1	-6.528815000	-1.193152000	-0.977563000
1	-5.240061000	-3.316825000	-1.157241000
1	-2.779925000	-3.265175000	-0.864450000
1	-0.787389000	-1.804279000	-1.020277000
6	-0.864426000	-1.989432000	1.045521000
1	1.422152000	-2.039749000	-2.151397000
1	-1.357832000	-2.960542000	0.940744000
1	0.929633000	-3.137960000	1.230408000
8	-1.383581000	-1.284867000	2.113467000
6	-2.680263000	-1.639199000	2.577938000
1	-3.470019000	-1.155476000	1.999429000
1	-2.817877000	-2.724744000	2.542362000
1	-2.735207000	-1.305322000	3.612755000
1	0.965151000	-1.556532000	2.018165000

Compound B with benzaldehyde (C_1), S_0

59

scf done: -1504.22394411

6	-2.518907000	-1.274742000	-1.018431000
6	-3.244690000	-0.073249000	-0.916656000
6	-4.635306000	-0.173891000	-1.056519000
6	-5.271461000	-1.385248000	-1.279506000
6	-4.527290000	-2.554809000	-1.394825000
6	-3.148605000	-2.489978000	-1.265654000
6	-2.586052000	1.246442000	-0.714088000
6	-1.181167000	1.298693000	-0.757280000
6	-0.449533000	2.484671000	-0.581689000
6	-1.186735000	3.666738000	-0.379681000
6	-2.568949000	3.622909000	-0.336562000
6	-3.280392000	2.427737000	-0.492935000
6	1.022493000	2.423892000	-0.555560000
6	1.783246000	3.600344000	-0.495865000
6	3.157934000	3.553075000	-0.405986000
6	3.807729000	2.323214000	-0.329495000
6	3.118153000	1.116575000	-0.382605000
6	1.707956000	1.174386000	-0.560752000
6	3.822034000	-0.189203000	-0.203159000
6	3.113052000	-1.402860000	-0.247639000
6	3.791691000	-2.599633000	0.003726000
6	5.152004000	-2.627649000	0.272420000

6	5.856994000	-1.427108000	0.297700000
6	5.199654000	-0.228196000	0.070986000
5	1.575086000	-1.436420000	-0.629286000
8	1.250703000	-2.088652000	-1.909889000
7	0.992480000	-0.000646000	-0.721426000
5	-0.377600000	0.040562000	-0.851984000
7	-1.076153000	-1.313648000	-0.841752000
8	0.771685000	-2.143499000	0.462452000
1	4.883406000	2.326725000	-0.224888000
1	3.734223000	4.469521000	-0.377491000
1	1.291957000	4.563519000	-0.532746000
1	-4.359857000	2.453884000	-0.422238000
1	-0.694035000	4.617240000	-0.224575000
1	-3.119468000	4.539977000	-0.160721000
1	3.227903000	-3.528815000	0.000508000
1	5.659045000	-3.565979000	0.465652000
1	6.920740000	-1.422163000	0.505762000
1	5.783917000	0.680474000	0.122042000
1	-5.237017000	0.723398000	-1.003050000
1	-6.349534000	-1.413486000	-1.380303000
1	-5.011570000	-3.503587000	-1.588180000
1	-2.546098000	-3.388019000	-1.355598000
1	-0.619669000	-1.901152000	-1.561256000
6	-0.569177000	-2.017240000	0.527113000
1	-1.086172000	-2.983439000	0.499337000
1	1.863123000	-2.798031000	-2.110037000
6	-1.071564000	-1.171367000	1.678936000
6	-2.397753000	-1.266512000	2.100478000
6	-0.211335000	-0.266760000	2.299310000
6	-2.872286000	-0.433368000	3.107792000
6	-0.687901000	0.565748000	3.305023000
6	-2.019489000	0.490634000	3.703208000
1	-3.064025000	-1.989668000	1.640121000
1	0.826813000	-0.228761000	1.990134000
1	-3.904292000	-0.509001000	3.429017000
1	-0.017389000	1.272261000	3.779381000
1	-2.388917000	1.142196000	4.486375000

Compound C with TME (C₁), S₀

60

scf done: -1318.04344173

6	3.463295000	-2.079976000	-0.929595000
6	2.777034000	-0.964492000	-0.413914000
6	3.504856000	0.251476000	-0.309787000
6	4.863270000	0.267436000	-0.655600000
6	5.527773000	-0.855176000	-1.108448000
6	4.805949000	-2.033599000	-1.260282000
7	1.409332000	-1.025385000	-0.053102000
5	0.677327000	0.201220000	-0.019344000
6	1.431795000	1.527039000	0.010278000
6	0.713372000	2.719269000	0.204841000
6	1.419517000	3.882047000	0.522394000
6	2.805653000	3.847420000	0.625796000
6	3.518188000	2.681950000	0.384647000
6	2.833445000	1.507287000	0.054012000
6	-0.755878000	2.692461000	0.055937000
6	-1.479506000	3.882412000	-0.008867000
6	-2.860761000	3.887503000	-0.124161000
6	-3.538666000	2.686160000	-0.211961000
6	-2.860524000	1.462618000	-0.197329000
6	-1.456487000	1.462852000	-0.034829000
6	-3.591570000	0.194946000	-0.366920000
6	-2.966607000	-1.033184000	-0.051188000
6	-3.695878000	-2.219354000	-0.262274000
6	-4.989499000	-2.208859000	-0.751502000
6	-5.594833000	-0.990484000	-1.056828000
6	-4.902347000	0.191432000	-0.874463000
7	-0.774410000	0.240664000	0.085655000
5	-1.465314000	-0.990526000	0.345333000
1	-4.617758000	2.700514000	-0.279845000
1	-3.403234000	4.824317000	-0.147306000
1	-0.956612000	4.828339000	0.030203000
1	4.595906000	2.696662000	0.478918000

1	0.908150000	4.814167000	0.721077000
1	3.339287000	4.750262000	0.900204000
1	-3.236306000	-3.175436000	-0.064134000
1	-5.520768000	-3.139655000	-0.910100000
1	-6.601639000	-0.966576000	-1.457725000
1	-5.378870000	1.117065000	-1.167192000
1	5.403691000	1.203091000	-0.599394000
1	6.576698000	-0.805083000	-1.371769000
1	5.281712000	-2.922938000	-1.656583000
1	2.943894000	-3.005213000	-1.102791000
6	-0.553465000	-2.077005000	1.092821000
6	0.764335000	-2.345062000	0.276903000
6	0.379880000	-3.075937000	-1.028536000
6	-0.242086000	-1.436857000	2.471253000
6	1.718418000	-3.182125000	1.156965000
6	-1.291989000	-3.391071000	1.403246000
1	0.262181000	-4.147715000	-0.855597000
1	1.125159000	-2.936531000	-1.808641000
1	-0.567145000	-2.692735000	-1.421231000
1	2.440140000	-3.762953000	0.590680000
1	2.272559000	-2.535805000	1.839676000
1	1.149228000	-3.894452000	1.750445000
1	0.233337000	-2.163189000	3.135958000
1	0.410465000	-0.565226000	2.397598000
1	-1.169416000	-1.114907000	2.955404000
1	-2.253437000	-3.164702000	1.868802000
1	-1.480174000	-4.003324000	0.521049000
1	-0.741649000	-4.005147000	2.118836000

Compound C with TCNE (C_1), S_0

52

scf done: -1529.74174007

6	3.744839000	-2.028855000	-0.178351000
6	3.003460000	-0.834833000	-0.078021000
6	3.634067000	0.394191000	-0.387157000
6	4.969648000	0.377003000	-0.820347000
6	5.672713000	-0.809530000	-0.912861000
6	5.065125000	-2.021381000	-0.582555000
5	1.509926000	-0.763988000	0.215511000
7	0.797503000	0.454222000	0.044565000
6	1.496772000	1.679951000	-0.064566000
6	0.803397000	2.910559000	0.050380000
6	1.533355000	4.094512000	-0.032037000
6	2.910623000	4.088469000	-0.187611000
6	3.579585000	2.885001000	-0.287025000
6	2.896954000	1.662585000	-0.249335000
6	-0.663244000	2.957297000	0.227728000
6	-1.350208000	4.124898000	0.566785000
6	-2.735809000	4.106755000	0.676368000
6	-3.469384000	2.956577000	0.419147000
6	-2.806687000	1.776221000	0.073993000
6	-1.402750000	1.780810000	0.028113000
6	-3.507822000	0.539350000	-0.309698000
6	-2.808055000	-0.679082000	-0.459004000
6	-3.473097000	-1.791203000	-0.986774000
6	-4.822005000	-1.734094000	-1.297743000
6	-5.532668000	-0.555845000	-1.107448000
6	-4.868649000	0.562622000	-0.637298000
5	-0.656571000	0.463755000	-0.030690000
7	-1.429794000	-0.745249000	-0.103000000
1	-4.546585000	2.988788000	0.512560000
1	-3.254939000	5.012903000	0.966181000
1	-0.825369000	5.046778000	0.776616000
1	4.655993000	2.896761000	-0.380071000
1	1.018778000	5.043934000	0.021213000
1	3.458139000	5.021494000	-0.229170000
1	-2.953999000	-2.717548000	-1.188167000
1	-5.307735000	-2.613046000	-1.702460000
1	-6.585642000	-0.501115000	-1.352544000
1	-5.413191000	1.493322000	-0.550516000
1	5.466225000	1.290879000	-1.114333000
1	6.700914000	-0.794261000	-1.255257000
1	5.616198000	-2.950312000	-0.659032000

1	3.282990000	-2.979412000	0.042766000
6	-0.809250000	-2.051352000	0.034400000
6	0.546064000	-1.937629000	0.842129000
6	1.118086000	-3.283391000	0.941009000
7	1.517098000	-4.356552000	1.015814000
6	0.247252000	-1.465052000	2.203795000
7	0.037820000	-1.047990000	3.252543000
6	-1.663182000	-2.995367000	0.796711000
7	-2.249538000	-3.739263000	1.442890000
6	-0.477120000	-2.630122000	-1.293922000
7	-0.183178000	-3.024082000	-2.330629000

Compound C with methoxyethene (C₁), S₀

52

scf done: -1275.36408994

6	-2.801068000	-1.150527000	-0.371196000
6	-3.478364000	0.094429000	-0.349971000
6	-4.859332000	0.108602000	-0.595762000
6	-5.579703000	-1.043939000	-0.842453000
6	-4.907135000	-2.262331000	-0.874371000
6	-3.542965000	-2.311334000	-0.653043000
6	-2.746790000	1.349064000	-0.104611000
6	-1.340064000	1.322161000	-0.114038000
6	-0.578401000	2.487278000	0.077772000
6	-1.252264000	3.689110000	0.313412000
6	-2.641221000	3.714594000	0.343197000
6	-3.391845000	2.567196000	0.133958000
6	0.898640000	2.394039000	0.035421000
6	1.658442000	3.563431000	0.051168000
6	3.041509000	3.534426000	0.014913000
6	3.689881000	2.316911000	-0.045068000
6	2.988162000	1.106994000	-0.078736000
6	1.568863000	1.142337000	-0.043594000
6	3.727814000	-0.168733000	-0.171381000
6	3.015613000	-1.378873000	-0.256108000
6	3.718625000	-2.590107000	-0.372362000
6	5.099313000	-2.622917000	-0.399905000
6	5.804219000	-1.421274000	-0.298738000
6	5.134430000	-0.217001000	-0.185721000
5	1.480712000	-1.335688000	-0.205067000
7	0.833324000	-0.059241000	-0.095426000
5	-0.622433000	-0.016675000	-0.150893000
7	-1.411204000	-1.211367000	-0.156979000
6	0.574543000	-2.624834000	-0.325567000
1	4.769319000	2.314400000	-0.080071000
1	3.608756000	4.456640000	0.024484000
1	1.163670000	4.523849000	0.075310000
1	-4.470035000	2.633351000	0.186976000
1	-0.719598000	4.610567000	0.501791000
1	-3.148314000	4.651297000	0.544731000
1	3.164746000	-3.519683000	-0.441178000
1	5.629825000	-3.563020000	-0.491278000
1	6.888211000	-1.427486000	-0.307546000
1	5.727572000	0.682861000	-0.106862000
1	-5.380077000	1.056678000	-0.613535000
1	-6.644700000	-0.993750000	-1.030350000
1	-5.441491000	-3.178666000	-1.095371000
1	-3.051814000	-3.269017000	-0.738467000
6	-0.773409000	-2.437922000	0.333635000
1	-1.429988000	-3.288890000	0.152808000
1	0.421845000	-2.849305000	-1.388982000
8	-0.535442000	-2.351318000	1.721911000
6	-1.707494000	-2.215159000	2.498489000
1	-2.193330000	-1.249082000	2.325083000
1	-2.423102000	-3.016258000	2.274503000
1	-1.404760000	-2.282026000	3.541996000
1	1.050574000	-3.499561000	0.121254000

Compound C with benzaldehyde (C₁), S₀

56

scf done: -1427.82426909

6	-2.731716000	-0.113255000	-0.768070000
6	-3.232502000	1.196785000	-0.546169000
6	-4.611364000	1.405533000	-0.687772000
6	-5.489279000	0.387143000	-1.009081000
6	-4.993539000	-0.900479000	-1.184795000
6	-3.637929000	-1.147341000	-1.060787000
6	-2.339016000	2.304742000	-0.154198000
6	-0.962255000	2.047867000	-0.034359000
6	-0.041116000	3.037451000	0.357750000
6	-0.532599000	4.318393000	0.623525000
6	-1.892839000	4.580279000	0.504022000
6	-2.796039000	3.598060000	0.123972000
6	1.398247000	2.691795000	0.457964000
6	2.322766000	3.650627000	0.875883000
6	3.677087000	3.372813000	0.942113000
6	4.137588000	2.121756000	0.571543000
6	3.267332000	1.113591000	0.149354000
6	1.877438000	1.399257000	0.117911000
6	3.793268000	-0.208063000	-0.269643000
6	2.909861000	-1.205753000	-0.719454000
6	3.397479000	-2.453556000	-1.129878000
6	4.751987000	-2.729217000	-1.105419000
6	5.633765000	-1.743089000	-0.657158000
6	5.167403000	-0.506506000	-0.246000000
5	1.409275000	-0.892872000	-0.702058000
7	0.972970000	0.396524000	-0.259995000
5	-0.440900000	0.659323000	-0.333165000
7	-1.354323000	-0.375256000	-0.684868000
8	0.489960000	-1.816305000	-1.125392000
1	5.200952000	1.934346000	0.612789000
1	4.373580000	4.133331000	1.272057000
1	1.985013000	4.638111000	1.157013000
1	-3.843101000	3.858438000	0.054817000
1	0.119996000	5.128045000	0.918518000
1	-2.257013000	5.579532000	0.714098000
1	2.688111000	-3.202499000	-1.464817000
1	5.127616000	-3.694200000	-1.423808000
1	6.698632000	-1.944024000	-0.627996000
1	5.892401000	0.220178000	0.092961000
1	-5.011757000	2.398964000	-0.539001000
1	-6.547842000	0.591192000	-1.108533000
1	-5.662823000	-1.721277000	-1.412841000
1	-3.293615000	-2.165191000	-1.172484000
6	-0.895356000	-1.750163000	-0.864089000
1	-1.372153000	-2.165035000	-1.755798000
6	-1.206303000	-2.638678000	0.334369000
6	-1.095950000	-4.019100000	0.171160000
6	-1.549521000	-2.119084000	1.577844000
6	-1.322426000	-4.873681000	1.242144000
6	-1.774813000	-2.975403000	2.652657000
6	-1.662156000	-4.350657000	2.487448000
1	-0.822462000	-4.420523000	-0.799665000
1	-1.652559000	-1.047580000	1.708365000
1	-1.235222000	-5.945278000	1.107617000
1	-2.043238000	-2.564874000	3.618718000
1	-1.841620000	-5.014747000	3.324546000

Compound **3a** (C_1), S_0

56

scf done: -1428.37106587

6	-2.741927000	-0.038606000	-0.759391000
6	-3.205985000	1.293732000	-0.549170000
6	-4.574415000	1.550609000	-0.746108000
6	-5.476166000	0.564908000	-1.110533000
6	-5.018539000	-0.740085000	-1.280750000
6	-3.675735000	-1.035228000	-1.102944000
6	-2.289276000	2.368765000	-0.129568000
6	-0.913734000	2.074128000	-0.009896000
6	0.032535000	3.045895000	0.388279000
6	-0.433975000	4.337339000	0.670410000

6	-1.790188000	4.631818000	0.559935000
6	-2.715781000	3.672522000	0.167566000
6	1.463207000	2.671998000	0.476350000
6	2.415759000	3.611960000	0.889186000
6	3.766572000	3.305635000	0.941319000
6	4.199871000	2.046122000	0.559022000
6	3.305130000	1.053248000	0.137026000
6	1.914753000	1.366396000	0.125625000
6	3.801511000	-0.272302000	-0.298507000
6	2.888506000	-1.263030000	-0.727229000
6	3.357519000	-2.517321000	-1.153281000
6	4.711623000	-2.808851000	-1.165850000
6	5.619010000	-1.832255000	-0.740975000
6	5.175461000	-0.589577000	-0.315334000
5	1.395499000	-0.924024000	-0.676292000
7	0.984663000	0.379703000	-0.239978000
5	-0.428796000	0.672503000	-0.297785000
7	-1.374604000	-0.350035000	-0.623231000
8	0.448340000	-1.838868000	-1.063933000
1	5.259701000	1.836205000	0.590266000
1	4.481721000	4.050862000	1.269177000
1	2.100379000	4.605713000	1.175268000
1	-3.758287000	3.953896000	0.104931000
1	0.239347000	5.127388000	0.973531000
1	-2.132243000	5.636186000	0.785893000
1	2.635546000	-3.260764000	-1.472248000
1	5.066598000	-3.778401000	-1.496591000
1	6.682797000	-2.044508000	-0.742926000
1	5.916165000	0.131921000	0.001653000
1	-4.943615000	2.558302000	-0.610860000
1	-6.522402000	0.808210000	-1.252376000
1	-5.705970000	-1.534545000	-1.548092000
1	-3.362481000	-2.061789000	-1.218358000
6	-0.946830000	-1.743178000	-0.808452000
1	-1.422765000	-2.135897000	-1.710418000
6	-1.286370000	-2.655182000	0.369552000
6	-1.370081000	-4.031667000	0.141135000
6	-1.458123000	-2.169067000	1.665774000
6	-1.616282000	-4.910812000	1.192208000
6	-1.703128000	-3.047979000	2.720098000
6	-1.782246000	-4.419183000	2.486745000
1	-1.235604000	-4.416982000	-0.864882000
1	-1.411912000	-1.103124000	1.854301000
1	-1.680353000	-5.976370000	1.002122000
1	-1.836766000	-2.659135000	3.723335000
1	-1.976558000	-5.100826000	3.307131000

Compound **3c** (C_1), S_0

58

scf done: -1632.93383773

6	-1.152413000	2.321813000	-1.124785000
6	-0.543452000	3.517313000	-0.641650000
6	-1.221199000	4.730262000	-0.856683000
6	-2.449680000	4.799219000	-1.492455000
6	-3.050551000	3.622140000	-1.932485000
6	-2.412710000	2.404928000	-1.746545000
6	0.748313000	3.489282000	0.068468000
6	1.421330000	2.254810000	0.197847000
6	2.662591000	2.139525000	0.864407000
6	3.223167000	3.303158000	1.409080000
6	2.560980000	4.521834000	1.289934000
6	1.341146000	4.629031000	0.632716000
6	3.320840000	0.815183000	0.948833000
6	4.542917000	0.674118000	1.618149000
6	5.202994000	-0.543085000	1.680159000
6	4.659246000	-1.651972000	1.051981000
6	3.439237000	-1.587678000	0.364808000
6	2.751131000	-0.340422000	0.340283000
6	2.899718000	-2.781399000	-0.325656000
6	1.670598000	-2.701724000	-1.020508000
6	1.163139000	-3.829639000	-1.688108000
6	1.848624000	-5.033051000	-1.682822000

6	3.063870000	-5.117506000	-0.994565000
6	3.580245000	-4.016347000	-0.329152000
5	0.922822000	-1.367378000	-0.984877000
7	1.500330000	-0.251246000	-0.295208000
5	0.793512000	1.005419000	-0.371696000
7	-0.502220000	1.078719000	-0.976639000
8	-0.287363000	-1.216709000	-1.623665000
1	5.201027000	-2.585977000	1.099082000
1	6.145267000	-0.624979000	2.208867000
1	4.992893000	1.530413000	2.100852000
1	0.867282000	5.599607000	0.575875000
1	4.172386000	3.283935000	1.926644000
1	3.009263000	5.410263000	1.721589000
1	0.217179000	-3.743237000	-2.210967000
1	1.451883000	-5.898998000	-2.200432000
1	3.612533000	-6.053023000	-0.978662000
1	4.523734000	-4.132116000	0.186517000
1	-0.768578000	5.651450000	-0.515503000
1	-2.935809000	5.756557000	-1.636854000
1	-4.018961000	3.645947000	-2.418833000
1	-2.918863000	1.512728000	-2.083877000
6	-1.182065000	-0.131355000	-1.445003000
1	-1.597694000	0.060633000	-2.437457000
6	-2.310012000	-0.601825000	-0.521649000
6	-3.266461000	-1.480167000	-1.042401000
6	-2.380208000	-0.229861000	0.821536000
6	-4.278822000	-1.987883000	-0.239038000
6	-3.386332000	-0.730202000	1.642203000
6	-4.320649000	-1.603084000	1.097805000
1	-3.214436000	-1.774874000	-2.084892000
1	-1.654194000	0.460957000	1.231063000
1	-5.026340000	-2.666621000	-0.625546000
1	-3.456455000	-0.452369000	2.684732000
7	-5.396828000	-2.134327000	1.963069000
8	-6.212908000	-2.892585000	1.453830000
8	-5.407974000	-1.785084000	3.136572000

Phenyl isocyanide (C_{2v}), S_0

13
scf done: -324.406124755

6	0.000000000	0.000000000	3.188287000
7	0.000000000	0.000000000	2.018364000
6	0.000000000	0.000000000	0.628139000
6	0.000000000	-1.213512000	-0.055930000
6	0.000000000	1.213512000	-0.055930000
6	0.000000000	-1.205330000	-1.444553000
6	0.000000000	1.205330000	-1.444553000
6	0.000000000	0.000000000	-2.140044000
1	0.000000000	-2.139445000	0.504504000
1	0.000000000	2.139445000	0.504504000
1	0.000000000	-2.144736000	-1.983501000
1	0.000000000	2.144736000	-1.983501000
1	0.000000000	0.000000000	-3.223048000

CO₂ ($D_{\infty h}$), S_0

3
scf done: -188.574879675

6	0.000000000	0.000000000	0.000000000
8	0.000000000	0.000000000	1.154787000
8	0.000000000	0.000000000	-1.154787000

Benzonitrile (C_{2v}), S_0

13
scf done: -324.437625172

6	0.000000000	0.000000000	2.040818000
7	0.000000000	0.000000000	3.191068000
6	0.000000000	0.000000000	0.602978000
6	0.000000000	1.213045000	-0.089553000
6	0.000000000	-1.213045000	-0.089553000
6	0.000000000	1.206868000	-1.477769000
6	0.000000000	-1.206868000	-1.477769000
6	0.000000000	0.000000000	-2.170997000
1	0.000000000	2.144453000	0.462450000
1	0.000000000	-2.144453000	0.462450000
1	0.000000000	2.145166000	-2.018489000
1	0.000000000	-2.145166000	-2.018489000
1	0.000000000	0.000000000	-3.254328000

Imine H₂CNH (C_s), S₀

5
scf done: -94.6103969974

7	-0.665447000	-0.154636000	0.000005000
6	0.584402000	0.028847000	-0.000031000
1	1.068884000	1.010185000	0.000058000
1	1.242915000	-0.839866000	0.000075000
1	-1.160078000	0.739046000	0.000021000

Iminium ion H₂CNH₂⁺ (C_{2v}), S₀

6
scf done: -94.9506168492

6	0.000000000	0.000000000	-0.673213000
7	0.000000000	0.000000000	0.598478000
1	0.000000000	0.943814000	-1.210293000
1	0.000000000	-0.943814000	-1.210293000
1	0.000000000	0.867598000	1.135260000
1	0.000000000	-0.867598000	1.135260000

Phenyl iminoborane (C_{2v}), S₀

14
scf done: -311.818143001

7	0.000000000	0.000000000	3.310134000
5	0.000000000	0.000000000	2.071590000
1	0.000000000	0.000000000	4.303607000
6	0.000000000	0.000000000	0.543339000
6	0.000000000	1.205716000	-0.169980000
6	0.000000000	-1.205716000	-0.169980000
6	0.000000000	1.205216000	-1.559642000
6	0.000000000	-1.205216000	-1.559642000
6	0.000000000	0.000000000	-2.255184000
1	0.000000000	2.147817000	0.366167000
1	0.000000000	-2.147817000	0.366167000
1	0.000000000	2.144446000	-2.099735000
1	0.000000000	-2.144446000	-2.099735000
1	0.000000000	0.000000000	-3.338824000

Compound B with phenyl isocyanide (C₁), S₀

58
scf done: -1483.07993988

6	-2.766840000	-1.766538000	-0.491598000
6	-3.847499000	-0.959391000	-0.095683000
6	-5.103130000	-1.581301000	-0.039603000
6	-5.278707000	-2.919464000	-0.350471000
6	-4.189030000	-3.695089000	-0.732661000

6	-2.934475000	-3.111773000	-0.797571000
6	-3.693093000	0.482388000	0.242816000
6	-2.417450000	1.063230000	0.117723000
6	-2.154286000	2.412908000	0.409445000
6	-3.240465000	3.200908000	0.831700000
6	-4.497432000	2.636340000	0.956996000
6	-4.738759000	1.288339000	0.673588000
6	-0.774822000	2.919867000	0.286854000
6	-0.476191000	4.248762000	0.616528000
6	0.814296000	4.729547000	0.547347000
6	1.848323000	3.884723000	0.156998000
6	1.626729000	2.554869000	-0.188034000
6	0.289688000	2.074125000	-0.140080000
6	2.755142000	1.664142000	-0.588366000
6	2.526857000	0.322711000	-0.942254000
6	3.606651000	-0.473220000	-1.346560000
6	4.902199000	0.014522000	-1.377874000
6	5.131152000	1.337929000	-1.005610000
6	4.075333000	2.148640000	-0.624066000
5	1.064124000	-0.283614000	-0.957113000
8	0.676015000	-0.905708000	-2.229328000
7	0.022469000	0.759554000	-0.496239000
5	-1.253589000	0.245798000	-0.348944000
7	-1.409761000	-1.243207000	-0.603204000
7	0.789396000	-1.534197000	0.081480000
1	2.848680000	4.292143000	0.128544000
1	1.026973000	5.759450000	0.805431000
1	-1.263825000	4.915499000	0.939608000
1	-5.742443000	0.905787000	0.800865000
1	-3.120543000	4.249118000	1.068638000
1	-5.322049000	3.256689000	1.289012000
1	3.414972000	-1.504685000	-1.628292000
1	5.725055000	-0.621064000	-1.683163000
1	6.136722000	1.742491000	-1.018168000
1	4.301197000	3.171176000	-0.355112000
1	-5.968860000	-1.002445000	0.251720000
1	-6.267693000	-3.357484000	-0.293626000
1	-4.313042000	-4.743653000	-0.972166000
1	-2.062512000	-3.695333000	-1.067835000
1	-1.035904000	-1.394268000	-1.558808000
6	-0.366646000	-2.073962000	0.282550000
1	0.990174000	-0.389297000	-2.973827000
6	1.890371000	-2.148789000	0.774971000
6	2.214026000	-3.476156000	0.528096000
6	2.640393000	-1.385491000	1.663779000
6	3.304645000	-4.046347000	1.177506000
6	3.725089000	-1.962317000	2.310538000
6	4.061906000	-3.291433000	2.066021000
1	1.612704000	-4.044104000	-0.170885000
1	2.375766000	-0.348167000	1.833533000
1	3.561501000	-5.081232000	0.985595000
1	4.311027000	-1.370852000	3.003479000
1	4.912731000	-3.736148000	2.567955000

Compound B with CO₂ (C₁), S₀

48

scf done: -1347.25435785

6	-2.814565000	-1.263949000	-0.203676000
6	-3.526289000	-0.058826000	-0.059469000
6	-4.924399000	-0.160868000	-0.062881000
6	-5.576908000	-1.374581000	-0.202375000
6	-4.845510000	-2.547497000	-0.353906000
6	-3.462202000	-2.484366000	-0.352362000
6	-2.861105000	1.269556000	0.051390000
6	-1.458130000	1.320772000	-0.038215000
6	-0.720956000	2.516711000	0.030056000
6	-1.451998000	3.707431000	0.196502000
6	-2.831354000	3.664680000	0.292623000
6	-3.546882000	2.464007000	0.223930000
6	0.749962000	2.463649000	-0.047120000
6	1.509627000	3.642500000	-0.038192000
6	2.886916000	3.602129000	-0.083234000
6	3.547376000	2.376058000	-0.098525000
6	2.859058000	1.167819000	-0.092366000

6	1.439876000	1.220898000	-0.120140000
6	3.580309000	-0.137280000	-0.026516000
6	2.883537000	-1.355055000	-0.124159000
6	3.587475000	-2.560691000	-0.040256000
6	4.961512000	-2.587988000	0.142531000
6	5.651113000	-1.382436000	0.248826000
6	4.970737000	-0.177734000	0.169424000
5	1.324472000	-1.376384000	-0.360215000
7	0.717730000	0.039421000	-0.214446000
5	-0.658858000	0.068478000	-0.183614000
7	-1.353016000	-1.297159000	-0.228012000
8	0.595461000	-2.199017000	0.763861000
6	-0.665427000	-2.207604000	0.897357000
8	-1.387096000	-2.739778000	1.670779000
1	4.628124000	2.381663000	-0.118513000
1	3.458149000	4.521951000	-0.095097000
1	1.015696000	4.604103000	-0.006458000
1	-4.624149000	2.499734000	0.313568000
1	-0.958412000	4.667029000	0.267120000
1	-3.377718000	4.590618000	0.430550000
1	3.033372000	-3.491683000	-0.112441000
1	5.491460000	-3.530747000	0.211078000
1	6.723900000	-1.379848000	0.403529000
1	5.543386000	0.732998000	0.280297000
1	-5.520376000	0.735812000	0.036352000
1	-6.659618000	-1.403467000	-0.198650000
1	-5.344347000	-3.501552000	-0.466117000
1	-2.870965000	-3.387058000	-0.449620000
1	-1.006170000	-1.741888000	-1.097851000
8	0.848058000	-2.022505000	-1.577833000
1	1.484575000	-1.967566000	-2.291324000

Compound **B** with iminium ion (H_2CNH_2^+) (C_1), S_0

51

scf done: -1253.72155028

6	2.856054000	-1.402711000	0.112325000
6	3.580593000	-0.204931000	0.000184000
6	4.976680000	-0.332310000	0.030700000
6	5.606255000	-1.559285000	0.165488000
6	4.857197000	-2.723904000	0.295962000
6	3.474474000	-2.637569000	0.270836000
6	2.930580000	1.130517000	-0.086203000
6	1.530470000	1.203650000	0.057079000
6	0.817155000	2.415991000	0.023094000
6	1.565994000	3.593968000	-0.153327000
6	2.938856000	3.526394000	-0.302766000
6	3.632164000	2.310380000	-0.277063000
6	-0.652912000	2.394757000	0.125494000
6	-1.378928000	3.594186000	0.155082000
6	-2.756632000	3.592448000	0.192388000
6	-3.450921000	2.387971000	0.160743000
6	-2.795206000	1.160874000	0.126296000
6	-1.378040000	1.173239000	0.164629000
6	-3.560827000	-0.114923000	0.031636000
6	-2.900590000	-1.355878000	0.086345000
6	-3.642697000	-2.541420000	0.013253000
6	-5.020755000	-2.526615000	-0.135476000
6	-5.672089000	-1.298141000	-0.209168000
6	-4.955720000	-0.114298000	-0.124991000
5	-1.345024000	-1.413643000	0.255924000
8	-0.791519000	-2.321181000	1.241858000
7	-0.677359000	-0.041219000	0.225431000
5	0.705281000	-0.027853000	0.192093000
7	1.378058000	-1.417453000	0.086586000
7	-0.626062000	-2.128853000	-1.151728000
1	-4.530646000	2.425294000	0.170239000
1	-3.300766000	4.527221000	0.233045000
1	-0.859124000	4.541895000	0.158526000
1	4.704891000	2.325183000	-0.413783000
1	1.091015000	4.564013000	-0.195549000
1	3.497566000	4.442749000	-0.451353000
1	-3.130569000	-3.498194000	0.091228000
1	-5.582465000	-3.450877000	-0.191002000
1	-6.747933000	-1.261058000	-0.330780000

1	-5.508015000	0.812377000	-0.191965000
1	5.589498000	0.556044000	-0.034070000
1	6.687887000	-1.604571000	0.186769000
1	5.340255000	-3.683570000	0.425684000
1	2.872536000	-3.532531000	0.395482000
1	1.010442000	-1.974565000	0.878609000
6	0.854894000	-2.088317000	-1.165640000
1	1.265125000	-3.093815000	-1.210223000
1	-1.378271000	-2.466863000	1.987453000
1	1.221796000	-1.503947000	-2.007778000
1	-0.958967000	-3.091831000	-1.176385000
1	-1.012137000	-1.647800000	-1.962524000

Compound B with phenyl iminoborane (C₁), S₀

59

scf done: -1470.57784969

6	-2.445139000	0.277425000	-1.112429000
6	-2.781876000	1.589784000	-0.738066000
6	-4.104466000	1.988946000	-0.981869000
6	-5.036311000	1.144718000	-1.562920000
6	-4.670689000	-0.144398000	-1.937369000
6	-3.373307000	-0.570118000	-1.707456000
6	-1.793663000	2.532166000	-0.143894000
6	-0.450000000	2.119286000	-0.049357000
6	0.575275000	2.951765000	0.434896000
6	0.205939000	4.242343000	0.859622000
6	-1.115683000	4.643750000	0.792470000
6	-2.121158000	3.808197000	0.294448000
6	1.954294000	2.438424000	0.489407000
6	3.001688000	3.268105000	0.916021000
6	4.295867000	2.801856000	0.989747000
6	4.573208000	1.476666000	0.663965000
6	3.585092000	0.593055000	0.244705000
6	2.258144000	1.095362000	0.117274000
6	3.907925000	-0.835583000	-0.047528000
6	2.925413000	-1.711003000	-0.541812000
6	3.270867000	-3.038952000	-0.819150000
6	4.551423000	-3.524265000	-0.602196000
6	5.518639000	-2.661172000	-0.092723000
6	5.200718000	-1.340049000	0.178780000
5	1.435196000	-1.233575000	-0.816085000
7	1.255919000	0.266558000	-0.358318000
5	-0.043132000	0.730599000	-0.438604000
7	-1.112262000	-0.272524000	-0.885769000
7	0.341693000	-2.021659000	-0.019930000
5	-0.949343000	-1.573317000	0.020309000
1	5.597807000	1.142531000	0.743420000
1	5.095936000	3.459002000	1.306982000
1	2.801750000	4.296366000	1.184746000
1	-3.136253000	4.181089000	0.266184000
1	0.935177000	4.935823000	1.255310000
1	-1.382553000	5.636959000	1.135102000
1	2.507896000	-3.697494000	-1.225853000
1	4.797952000	-4.556429000	-0.823088000
1	6.524941000	-3.017665000	0.094921000
1	5.982449000	-0.710700000	0.581452000
1	-4.410339000	2.993157000	-0.721771000
1	-6.046559000	1.496696000	-1.732140000
1	-5.387456000	-0.812783000	-2.397239000
1	-3.070326000	-1.578130000	-1.969975000
1	-0.713620000	-0.633411000	-1.779517000
8	0.997626000	-1.339346000	-2.229284000
1	1.658147000	-0.973018000	-2.820848000
1	0.621836000	-2.806807000	0.550482000
6	-2.160850000	-2.158598000	0.810294000
6	-2.323135000	-3.547958000	0.882880000
6	-3.071344000	-1.351597000	1.506506000
6	-3.362489000	-4.114216000	1.613835000
6	-4.101331000	-1.912515000	2.251758000
6	-4.252467000	-3.295624000	2.300955000
1	-1.631513000	-4.193621000	0.350865000
1	-2.974393000	-0.270530000	1.475179000
1	-3.476459000	-5.191346000	1.649154000
1	-4.788612000	-1.271870000	2.791650000

1 -5.061382000 -3.733016000 2.874504000

Compound C with phenyl isocyanide (C₁), S₀

55

scf done: -1195.54253095

6	2.818901000	-1.506528000	-0.000036000
6	3.548698000	-0.297517000	0.000042000
6	4.950609000	-0.385580000	0.000093000
6	5.613945000	-1.596498000	0.000049000
6	4.875916000	-2.777628000	-0.000058000
6	3.494544000	-2.732209000	-0.000098000
6	2.886957000	1.028063000	0.000053000
6	1.482557000	1.079157000	0.000016000
6	0.765567000	2.289996000	0.000013000
6	1.498640000	3.481433000	0.000057000
6	2.886391000	3.439026000	0.000091000
6	3.585566000	2.237123000	0.000085000
6	-0.716002000	2.258470000	-0.000033000
6	-1.453171000	3.444331000	-0.000092000
6	-2.837480000	3.433732000	-0.000145000
6	-3.520640000	2.229492000	-0.000115000
6	-2.846773000	1.005591000	-0.000036000
6	-1.429614000	1.033219000	-0.000028000
6	-3.594388000	-0.275169000	0.000023000
6	-2.899071000	-1.500281000	-0.000032000
6	-3.596700000	-2.716142000	0.000002000
6	-4.978726000	-2.736551000	0.000095000
6	-5.673998000	-1.524792000	0.000176000
6	-4.999420000	-0.316148000	0.000144000
5	-1.374743000	-1.440718000	-0.000057000
7	-0.721915000	-0.178318000	-0.000028000
5	0.703845000	-0.210456000	-0.000023000
7	1.380108000	-1.495078000	-0.000052000
8	-0.588861000	-2.588594000	-0.000078000
6	0.744004000	-2.711150000	-0.000063000
1	-4.600910000	2.252333000	-0.000173000
1	-3.386317000	4.367120000	-0.000214000
1	-0.943508000	4.397475000	-0.000111000
1	4.666011000	2.270542000	0.000103000
1	1.014042000	4.447717000	0.000068000
1	3.441215000	4.370276000	0.000120000
1	-3.029795000	-3.640681000	-0.000042000
1	-5.518511000	-3.675640000	0.000119000
1	-6.757955000	-1.525631000	0.000273000
1	-5.585997000	0.591906000	0.000236000
1	5.538905000	0.521391000	0.000176000
1	6.696628000	-1.621219000	0.000094000
1	5.376664000	-3.738257000	-0.000109000
1	2.909693000	-3.639573000	-0.000170000

Compound C with CO₂ (C₁), S₀

45

scf done: -1270.85710948

6	2.819258000	-1.296350000	-0.091740000
6	3.510191000	-0.061253000	-0.057871000
6	4.898334000	-0.076325000	-0.256666000
6	5.599390000	-1.244651000	-0.483014000
6	4.904022000	-2.446988000	-0.541175000
6	3.533011000	-2.472838000	-0.353792000
6	2.809511000	1.229824000	0.105434000
6	1.409205000	1.241795000	0.013216000
6	0.659725000	2.429726000	0.088414000
6	1.350333000	3.628258000	0.292222000
6	2.734090000	3.618283000	0.414544000
6	3.468760000	2.442307000	0.321442000
6	-0.814548000	2.366259000	-0.031778000
6	-1.567546000	3.535295000	-0.152246000
6	-2.948318000	3.496687000	-0.245757000
6	-3.606844000	2.279379000	-0.220094000

6	-2.912325000	1.070781000	-0.118087000
6	-1.498647000	1.125673000	-0.034381000
6	-3.637995000	-0.222205000	-0.097035000
6	-2.925093000	-1.429431000	0.033449000
6	-3.600311000	-2.657162000	0.070801000
6	-4.978190000	-2.707258000	-0.025856000
6	-5.691031000	-1.513529000	-0.161748000
6	-5.038193000	-0.293379000	-0.196323000
5	-1.404814000	-1.337771000	0.119449000
7	-0.765022000	-0.069385000	0.048626000
5	0.666581000	-0.072731000	0.006230000
7	1.394138000	-1.321358000	0.062869000
8	-0.615857000	-2.463207000	0.271449000
6	0.730903000	-2.513465000	0.399530000
1	-4.685349000	2.278218000	-0.286484000
1	-3.512316000	4.416085000	-0.340261000
1	-1.069787000	4.494534000	-0.187319000
1	4.542441000	2.489293000	0.441480000
1	0.829430000	4.570975000	0.388355000
1	3.253852000	4.552144000	0.595531000
1	-3.020749000	-3.567748000	0.176947000
1	-5.500996000	-3.655449000	0.002638000
1	-6.771832000	-1.537624000	-0.240769000
1	-5.637741000	0.599772000	-0.302947000
1	5.438472000	0.860475000	-0.261847000
1	6.671220000	-1.215972000	-0.634394000
1	5.425454000	-3.375002000	-0.741558000
1	3.015846000	-3.415898000	-0.405220000
8	1.248765000	-3.522130000	0.773307000

Compound C with benzonitrile (C_{cov}), S_0

55

scf done: -1406.72651510

6	-2.410493000	0.630403000	-0.678177000
6	-2.519040000	2.027728000	-0.488906000
6	-3.705862000	2.654151000	-0.895482000
6	-4.741661000	1.954491000	-1.486786000
6	-4.590989000	0.591878000	-1.731372000
6	-3.432261000	-0.056744000	-1.343823000
6	-1.380693000	2.829030000	0.009612000
6	-0.114650000	2.221014000	0.029435000
6	1.051890000	2.919822000	0.379154000
6	0.919350000	4.260810000	0.760466000
6	-0.335285000	4.856772000	0.778340000
6	-1.482537000	4.163837000	0.402208000
6	2.351438000	2.212643000	0.330476000
6	3.545617000	2.922543000	0.465468000
6	4.772827000	2.283666000	0.414096000
6	4.829836000	0.915635000	0.207858000
6	3.673835000	0.147777000	0.043225000
6	2.421729000	0.809289000	0.120298000
6	3.759600000	-1.311171000	-0.204478000
6	2.584474000	-2.084549000	-0.265076000
6	2.663603000	-3.470065000	-0.464638000
6	3.885034000	-4.097556000	-0.624946000
6	5.051454000	-3.329594000	-0.585673000
6	4.993773000	-1.962361000	-0.377903000
5	1.228957000	-1.375818000	-0.125500000
7	1.241721000	0.063407000	-0.012301000
5	-0.018064000	0.720596000	-0.128578000
7	-1.229153000	-0.052320000	-0.272901000
7	-0.032507000	-2.062346000	-0.033018000
1	5.800570000	0.441801000	0.175877000
1	5.686899000	2.853104000	0.527507000
1	3.521004000	3.995415000	0.599905000
1	-2.438405000	4.670122000	0.440360000
1	1.774265000	4.845943000	1.071562000
1	-0.423220000	5.889139000	1.097024000
1	1.739703000	-4.037852000	-0.487155000
1	3.942335000	-5.168273000	-0.780670000
1	6.016371000	-3.805666000	-0.718069000
1	5.924358000	-1.411899000	-0.361602000
1	-3.800217000	3.725851000	-0.777728000
1	-5.642181000	2.472349000	-1.792506000

1	-5.367498000	0.035294000	-2.241640000
1	-3.313803000	-1.108313000	-1.565179000
6	-1.146835000	-1.429910000	-0.010248000
6	-2.365041000	-2.157861000	0.454869000
6	-2.538514000	-3.488333000	0.077352000
6	-3.269849000	-1.564455000	1.336738000
6	-3.628492000	-4.210029000	0.548194000
6	-4.345000000	-2.295684000	1.825168000
6	-4.533129000	-3.614970000	1.422727000
1	-1.807118000	-3.942414000	-0.580040000
1	-3.129726000	-0.534354000	1.644666000
1	-3.766858000	-5.239700000	0.240872000
1	-5.037533000	-1.834684000	2.519021000
1	-5.378610000	-4.180160000	1.796681000

Compound C with imine (H₂CNH) (C₁), S₀

47

scf done: -1176.92918138

6	-2.842305000	-1.441313000	0.000011000
6	-3.575979000	-0.226544000	-0.000016000
6	-4.974763000	-0.300611000	-0.000005000
6	-5.658775000	-1.502803000	0.000021000
6	-4.933839000	-2.688447000	0.000041000
6	-3.549728000	-2.657516000	0.000038000
6	-2.888141000	1.077211000	-0.000044000
6	-1.481567000	1.097160000	-0.000009000
6	-0.756310000	2.303573000	-0.000013000
6	-1.473512000	3.503869000	-0.000071000
6	-2.862291000	3.487088000	-0.000119000
6	-3.573541000	2.296786000	-0.000104000
6	0.724304000	2.261495000	0.000038000
6	1.453782000	3.452217000	0.000104000
6	2.836235000	3.458649000	0.000154000
6	3.520083000	2.256118000	0.000118000
6	2.854249000	1.028716000	0.000040000
6	1.433013000	1.030263000	0.000029000
6	3.629482000	-0.235952000	-0.000017000
6	2.960573000	-1.472259000	0.000011000
6	3.703319000	-2.661032000	-0.000012000
6	5.085722000	-2.652526000	-0.000076000
6	5.749970000	-1.425384000	-0.000131000
6	5.036746000	-0.240489000	-0.000104000
5	1.415586000	-1.454876000	0.000025000
7	0.732574000	-0.183549000	0.000015000
5	-0.709785000	-0.211291000	0.000010000
7	-1.440263000	-1.440436000	0.000012000
7	0.639567000	-2.630100000	0.000022000
1	4.599838000	2.285152000	0.000167000
1	3.378920000	4.395501000	0.000221000
1	0.936426000	4.400770000	0.000128000
1	-4.653636000	2.341197000	-0.000146000
1	-0.976227000	4.463222000	-0.000089000
1	-3.402023000	4.427249000	-0.000171000
1	3.191620000	-3.618601000	0.000020000
1	5.645330000	-3.580080000	-0.000091000
1	6.833410000	-1.395090000	-0.000200000
1	5.597980000	0.682914000	-0.000166000
1	-5.551082000	0.614215000	-0.000014000
1	-6.741314000	-1.514426000	0.000029000
1	-5.442743000	-3.644981000	0.000062000
1	-3.024400000	-3.600647000	0.000057000
6	-0.798626000	-2.749837000	0.000042000
1	-1.128812000	-3.307089000	-0.886556000
1	-1.128797000	-3.307038000	0.886678000
1	1.104762000	-3.523425000	-0.000001000

Compound C with iminium ion (H₂CNH₂⁺) (C₁), S₀

48

scf done: -1177.28204005

6	2.847339000	-1.445747000	-0.133627000
6	3.572247000	-0.240210000	0.026434000
6	4.971140000	-0.313876000	-0.020733000
6	5.645655000	-1.501288000	-0.236290000
6	4.918694000	-2.667341000	-0.441565000
6	3.534357000	-2.637182000	-0.396784000
6	2.889602000	1.060646000	0.170344000
6	1.488332000	1.102219000	0.064898000
6	0.764854000	2.308518000	0.097405000
6	1.472176000	3.492299000	0.299283000
6	2.856610000	3.455501000	0.441484000
6	3.568887000	2.267336000	0.369527000
6	-0.706694000	2.272750000	-0.084162000
6	-1.421124000	3.453812000	-0.268989000
6	-2.802610000	3.455841000	-0.399641000
6	-3.501839000	2.268258000	-0.336825000
6	-2.843591000	1.041070000	-0.172999000
6	-1.431937000	1.056022000	-0.073629000
6	-3.614611000	-0.213467000	-0.077804000
6	-2.957306000	-1.434645000	0.206646000
6	-3.699381000	-2.623493000	0.351671000
6	-5.069201000	-2.626834000	0.209414000
6	-5.718375000	-1.424527000	-0.095301000
6	-5.011907000	-0.245649000	-0.236359000
5	-1.458638000	-1.349091000	0.261443000
7	-0.737712000	-0.172731000	0.058579000
5	0.725474000	-0.189714000	0.005334000
7	1.428069000	-1.430097000	-0.044366000
7	-0.565036000	-2.588336000	0.593753000
1	-4.578721000	2.302138000	-0.410922000
1	-3.331573000	4.389593000	-0.540422000
1	-0.894553000	4.396541000	-0.320134000
1	4.643686000	2.302893000	0.478825000
1	0.971983000	4.448199000	0.369960000
1	3.392601000	4.381949000	0.610119000
1	-3.204195000	-3.564035000	0.580175000
1	-5.636798000	-3.541554000	0.322569000
1	-6.794197000	-1.415497000	-0.223501000
1	-5.565031000	0.650356000	-0.477509000
1	5.551207000	0.590682000	0.097126000
1	6.727306000	-1.513663000	-0.268415000
1	5.423803000	-3.602376000	-0.648934000
1	3.009147000	-3.559313000	-0.603595000
6	0.712952000	-2.668550000	-0.192903000
1	1.277027000	-3.506004000	0.209940000
1	0.432253000	-2.876013000	-1.231124000
1	-1.095548000	-3.451397000	0.458311000
1	-0.325431000	-2.549101000	1.590902000

Compound C with phenyl iminoborane (C₁), S₀

56

scf done: -1394.18651355

6	-2.404151000	0.826968000	-0.638288000
6	-2.437765000	2.219722000	-0.406936000
6	-3.608324000	2.921497000	-0.732098000
6	-4.710305000	2.295558000	-1.283580000
6	-4.645418000	0.933154000	-1.566682000
6	-3.502370000	0.217413000	-1.260996000
6	-1.238169000	2.936456000	0.065015000
6	-0.006747000	2.257871000	0.027056000
6	1.197436000	2.901479000	0.351185000
6	1.146592000	4.234645000	0.775241000
6	-0.073602000	4.892093000	0.853754000
6	-1.260755000	4.264070000	0.495957000
6	2.461807000	2.143973000	0.246459000
6	3.680776000	2.819076000	0.330703000
6	4.887370000	2.146147000	0.271413000
6	4.889898000	0.771475000	0.119950000
6	3.705714000	0.039448000	-0.001980000
6	2.469446000	0.736951000	0.052773000
6	3.760109000	-1.430437000	-0.171590000
6	2.568636000	-2.175859000	-0.173065000
6	2.622721000	-3.570525000	-0.312178000
6	3.826587000	-4.235919000	-0.448139000

6	5.008793000	-3.493679000	-0.460179000
6	4.977941000	-2.117191000	-0.328230000
5	1.235095000	-1.409077000	-0.090377000
7	1.255492000	0.033324000	-0.067569000
5	0.002034000	0.748868000	-0.165936000
7	-1.255294000	0.054428000	-0.318243000
7	-0.044249000	-2.044232000	-0.022734000
5	-1.298982000	-1.370072000	-0.034247000
1	5.842071000	0.261675000	0.098994000
1	5.821329000	2.688944000	0.345003000
1	3.688927000	3.895289000	0.434048000
1	-2.190082000	4.811986000	0.579455000
1	2.039143000	4.764263000	1.078951000
1	-0.100754000	5.916743000	1.206628000
1	1.702304000	-4.145696000	-0.327305000
1	3.854619000	-5.313506000	-0.555204000
1	5.961919000	-3.995704000	-0.579917000
1	5.918668000	-1.586010000	-0.360145000
1	-3.639973000	3.992583000	-0.580956000
1	-5.596351000	2.868385000	-1.527633000
1	-5.477514000	0.430574000	-2.044864000
1	-3.451686000	-0.831454000	-1.516978000
1	-0.067521000	-3.035310000	0.171193000
6	-2.585262000	-2.183023000	0.363302000
6	-2.792759000	-3.483798000	-0.109632000
6	-3.512652000	-1.660572000	1.274685000
6	-3.893685000	-4.233397000	0.296214000
6	-4.602065000	-2.410278000	1.699972000
6	-4.798352000	-3.697707000	1.205851000
1	-2.095684000	-3.915471000	-0.822691000
1	-3.381094000	-0.650780000	1.651115000
1	-4.043341000	-5.233202000	-0.094557000
1	-5.302706000	-1.990423000	2.412267000
1	-5.653328000	-4.279771000	1.529472000

7.2 Calculations in thf solution

Compound A - (BN)₂ dibenzoperylene (C₁), S₀

45

scf done: -1158.73325543

6	-3.588456000	-2.795389000	-0.115398000
6	-2.922500000	-1.559510000	-0.059776000
6	-3.662792000	-0.363251000	0.036631000
6	-5.064579000	-0.462308000	0.071028000
6	-5.715245000	-1.681122000	0.015933000
6	-4.967002000	-2.858566000	-0.077703000
7	-1.536895000	-1.542541000	-0.097272000
5	-0.763418000	-0.356140000	-0.063965000
6	-1.547956000	0.952313000	0.012756000
6	-0.837795000	2.164446000	0.040430000
6	-1.550121000	3.358158000	0.193644000
6	-2.937267000	3.334850000	0.281455000
6	-3.643837000	2.143653000	0.221845000
6	-2.959036000	0.928944000	0.091424000
6	0.638037000	2.131237000	-0.082737000
6	1.327968000	3.337958000	-0.222557000
6	2.706691000	3.388510000	-0.315572000
6	3.424690000	2.211628000	-0.233954000
6	2.795211000	0.970360000	-0.094300000
6	1.373058000	0.911854000	-0.075871000
6	3.627848000	-0.244716000	0.026009000
6	3.013079000	-1.505073000	-0.001946000
6	3.799120000	-2.663590000	0.105690000
6	5.172920000	-2.591848000	0.243723000
6	5.781459000	-1.335413000	0.291036000
6	5.024974000	-0.181683000	0.188386000
7	0.703999000	-0.336576000	-0.068178000
5	1.475517000	-1.559438000	-0.105195000
1	4.501568000	2.262265000	-0.302228000
1	3.214799000	4.335449000	-0.446596000

1	0.776495000	4.264984000	-0.281834000
8	0.803962000	-2.753809000	-0.215368000
1	-4.722613000	2.176403000	0.290664000
1	-1.052367000	4.314854000	0.262673000
1	-3.475798000	4.267850000	0.401817000
1	3.337762000	-3.646754000	0.093132000
1	5.767513000	-3.493278000	0.327202000
1	6.855023000	-1.258407000	0.417899000
1	5.539376000	0.766395000	0.255424000
1	-5.663073000	0.436442000	0.139665000
1	-6.797008000	-1.719774000	0.043912000
1	-5.463404000	-3.820680000	-0.122040000
1	-2.998149000	-3.702550000	-0.189222000
1	-1.090970000	-2.447961000	-0.149489000
1	1.378103000	-3.521709000	-0.255152000

H₂O (C_{2v}), S₀

3
scf done: -76.4274369894

8	0.000000000	0.000000000	0.117430000
1	0.000000000	0.760525000	-0.469718000
1	0.000000000	-0.760525000	-0.469718000

Compound 4 (C₁), S₀

42
scf done: -1082.15382441

6	-2.444431000	-2.870788000	0.217995000
6	-2.084606000	-1.536002000	0.406305000
6	-2.984915000	-0.488501000	0.013946000
6	-4.227772000	-0.876314000	-0.502172000
6	-4.579146000	-2.207806000	-0.668980000
6	-3.675560000	-3.209673000	-0.322268000
7	-0.867005000	-1.217140000	1.040941000
5	-0.627202000	0.179017000	1.224820000
6	-1.361267000	1.289346000	0.578003000
6	-0.640651000	2.474079000	0.330884000
6	-1.358711000	3.500251000	-0.287947000
6	-2.673184000	3.256135000	-0.705660000
6	-3.283732000	2.003712000	-0.618283000
6	-2.599489000	0.959389000	0.020982000
6	0.860068000	2.397415000	0.424515000
6	1.686091000	3.359846000	-0.164431000
6	2.998031000	3.057005000	-0.521348000
6	3.470909000	1.749150000	-0.429798000
6	2.694773000	0.758804000	0.177615000
6	1.478528000	1.160503000	0.757399000
6	2.945712000	-0.708392000	0.023141000
6	1.875628000	-1.654219000	0.134424000
6	2.093958000	-2.988102000	-0.218175000
6	3.343558000	-3.424879000	-0.641604000
6	4.395280000	-2.515378000	-0.705094000
6	4.197997000	-1.176787000	-0.382840000
7	0.774765000	0.192961000	1.463685000
5	0.609715000	-1.129540000	0.844406000
1	4.418593000	1.500527000	-0.891939000
1	3.615456000	3.817895000	-0.982303000
1	1.284534000	4.333187000	-0.421391000
1	-4.252850000	1.863682000	-1.080557000
1	-0.909593000	4.460615000	-0.511025000
1	-3.213811000	4.059248000	-1.193865000
1	1.276807000	-3.696701000	-0.133581000
1	3.502194000	-4.463967000	-0.902882000
1	5.379775000	-2.848205000	-1.012889000
1	5.036177000	-0.493790000	-0.450492000
1	-4.938668000	-0.111246000	-0.789924000
1	-5.550999000	-2.462432000	-1.073311000
1	-3.935601000	-4.252675000	-0.457730000
1	-1.741320000	-3.637042000	0.523720000

Benzaldehyde (C_s), S₀

14
scf done: -345.521814275

6	1.327734000	-1.325082000	0.000035000
6	-0.041126000	-1.103602000	0.000004000
6	2.208943000	-0.241875000	0.000054000
1	-0.743702000	-1.928833000	-0.000011000
1	3.278067000	-0.418838000	0.000079000
6	-0.530078000	0.205798000	-0.000008000
6	1.724269000	1.062705000	0.000043000
1	2.412371000	1.899011000	0.000058000
6	0.351396000	1.286516000	0.000011000
1	-0.040019000	2.298783000	0.000002000
1	1.714883000	-2.336729000	0.000045000
6	-1.986892000	0.466661000	-0.000043000
8	-2.834493000	-0.394412000	-0.000087000
1	-2.271119000	1.535175000	-0.000056000

Compound B with benzaldehyde (C₁), S₀

59
scf done: -1504.24080983

6	-2.549287000	-1.242652000	-1.020096000
6	-3.264987000	-0.038204000	-0.893871000
6	-4.658962000	-0.126719000	-1.010370000
6	-5.305708000	-1.332250000	-1.236832000
6	-4.570118000	-2.504716000	-1.377807000
6	-3.188540000	-2.451890000	-1.270618000
6	-2.596141000	1.275943000	-0.687337000
6	-1.190286000	1.321665000	-0.731404000
6	-0.454599000	2.504798000	-0.551425000
6	-1.183704000	3.691125000	-0.345733000
6	-2.566943000	3.653062000	-0.303063000
6	-3.283974000	2.461404000	-0.462726000
6	1.018631000	2.437470000	-0.526429000
6	1.782401000	3.611076000	-0.445134000
6	3.158164000	3.560378000	-0.355018000
6	3.804877000	2.328047000	-0.295825000
6	3.109629000	1.124069000	-0.367698000
6	1.700108000	1.185786000	-0.552257000
6	3.811317000	-0.184984000	-0.202282000
6	3.103668000	-1.397528000	-0.291511000
6	3.784080000	-2.600633000	-0.070850000
6	5.140395000	-2.634477000	0.220799000
6	5.841497000	-1.432661000	0.300876000
6	5.184798000	-0.228206000	0.097988000
5	1.566110000	-1.419392000	-0.692823000
8	1.271146000	-2.010523000	-2.012099000
7	0.981507000	0.014133000	-0.738714000
5	-0.393551000	0.061130000	-0.851470000
7	-1.097882000	-1.290936000	-0.869632000
8	0.765562000	-2.186304000	0.355113000
1	4.880566000	2.327985000	-0.189797000
1	3.735818000	4.475290000	-0.310433000
1	1.293962000	4.576129000	-0.462115000
1	-4.363254000	2.494661000	-0.395910000
1	-0.688480000	4.640298000	-0.191182000
1	-3.113610000	4.572153000	-0.126764000
1	3.229084000	-3.533633000	-0.125198000
1	5.647415000	-3.577901000	0.388001000
1	6.900856000	-1.431647000	0.530484000
1	5.765335000	0.679746000	0.189692000
1	-5.256092000	0.771856000	-0.934293000
1	-6.385409000	-1.353016000	-1.318393000
1	-5.062904000	-3.448640000	-1.572680000
1	-2.598731000	-3.355657000	-1.380890000
1	-0.665309000	-1.851052000	-1.622905000
6	-0.580995000	-2.036322000	0.451676000

1	-1.104451000	-2.996431000	0.415352000
1	1.698556000	-2.865913000	-2.104191000
6	-1.041017000	-1.223545000	1.645982000
6	-2.356811000	-1.327882000	2.099062000
6	-0.160518000	-0.345709000	2.277892000
6	-2.800337000	-0.530509000	3.149491000
6	-0.605080000	0.450364000	3.327968000
6	-1.926932000	0.366407000	3.758144000
1	-3.038191000	-2.031683000	1.631353000
1	0.869702000	-0.295046000	1.944647000
1	-3.824072000	-0.613661000	3.494282000
1	0.081720000	1.134445000	3.812023000
1	-2.272102000	0.989021000	4.575139000

Transition state with benzaldehyde (C1), S₀

59

scf done: -1504.22286991

6	-2.390439000	-0.892724000	-1.292048000
6	-3.064694000	0.315474000	-1.030219000
6	-4.457533000	0.304701000	-1.181367000
6	-5.148503000	-0.829546000	-1.578248000
6	-4.456836000	-2.003470000	-1.862111000
6	-3.079215000	-2.027448000	-1.717077000
6	-2.330153000	1.555739000	-0.667299000
6	-0.921121000	1.525285000	-0.667865000
6	-0.136331000	2.639950000	-0.330972000
6	-0.809790000	3.834302000	-0.015494000
6	-2.193370000	3.871625000	-0.021563000
6	-2.962562000	2.747324000	-0.334193000
6	1.326708000	2.484520000	-0.248248000
6	2.139217000	3.598590000	0.007015000
6	3.495653000	3.462750000	0.208734000
6	4.071695000	2.196065000	0.183512000
6	3.332621000	1.052813000	-0.100321000
6	1.941447000	1.203269000	-0.363362000
6	3.971703000	-0.293040000	-0.063619000
6	3.185872000	-1.455024000	-0.133155000
6	3.800409000	-2.705413000	-0.002293000
6	5.169460000	-2.830115000	0.179584000
6	5.952887000	-1.678375000	0.203910000
6	5.362808000	-0.430614000	0.081384000
5	1.648187000	-1.383740000	-0.501765000
8	1.273240000	-2.232741000	-1.636715000
7	1.184193000	0.091547000	-0.714109000
5	-0.189439000	0.231357000	-0.898939000
7	-0.983400000	-1.018391000	-1.080676000
8	0.721951000	-1.815838000	0.652274000
1	5.125625000	2.113578000	0.408561000
1	4.108266000	4.332415000	0.411426000
1	1.699600000	4.585798000	0.053116000
1	-4.040703000	2.830556000	-0.297360000
1	-0.270518000	4.728584000	0.265941000
1	-2.696733000	4.795545000	0.239667000
1	3.179907000	-3.595591000	-0.050123000
1	5.626948000	-3.806813000	0.287139000
1	7.028413000	-1.751998000	0.317146000
1	6.009316000	0.436542000	0.091625000
1	-5.017696000	1.212052000	-0.999065000
1	-6.225792000	-0.792332000	-1.683829000
1	-4.984174000	-2.889181000	-2.194152000
1	-2.518590000	-2.932550000	-1.929772000
1	-0.523274000	-1.643195000	-1.751609000
6	-0.547022000	-2.024561000	0.423161000
1	-0.820708000	-2.976965000	-0.042279000
1	2.014893000	-2.371605000	-2.226710000
6	-1.489026000	-1.523027000	1.458875000
6	-2.740499000	-2.113618000	1.625544000
6	-1.141114000	-0.396206000	2.205302000
6	-3.649245000	-1.573165000	2.528176000
6	-2.053210000	0.145829000	3.100832000
6	-3.307441000	-0.439616000	3.259306000
1	-3.004782000	-2.991208000	1.045486000
1	-0.158344000	0.042717000	2.070949000

1	-4.621486000	-2.032959000	2.657732000
1	-1.787761000	1.025541000	3.674546000
1	-4.017469000	-0.014110000	3.958817000

Transition state with p-hydroxy benzaldehyde (C₁), S₀

60
scf done: -1579.46671915

6	-2.168000000	-0.811866000	-1.595287000
6	-2.846604000	0.392265000	-1.325309000
6	-4.232531000	0.398980000	-1.536034000
6	-4.911550000	-0.716922000	-2.001504000
6	-4.213653000	-1.885556000	-2.295079000
6	-2.843803000	-1.926554000	-2.089344000
6	-2.120548000	1.615003000	-0.892983000
6	-0.714255000	1.566114000	-0.803825000
6	0.058312000	2.667166000	-0.399623000
6	-0.617635000	3.865982000	-0.107763000
6	-1.998448000	3.920610000	-0.201737000
6	-2.758750000	2.810846000	-0.581645000
6	1.512958000	2.493670000	-0.230045000
6	2.318579000	3.596039000	0.090265000
6	3.661170000	3.445216000	0.368308000
6	4.224663000	2.172562000	0.364178000
6	3.489837000	1.039105000	0.027688000
6	2.120214000	1.206547000	-0.328346000
6	4.109436000	-0.315206000	0.101274000
6	3.321892000	-1.466245000	-0.069114000
6	3.911405000	-2.726906000	0.086313000
6	5.255878000	-2.872999000	0.395636000
6	6.043312000	-1.730201000	0.529656000
6	5.479012000	-0.472405000	0.382238000
5	1.817561000	-1.373011000	-0.563716000
8	1.536615000	-2.184265000	-1.749533000
7	1.378400000	0.111619000	-0.757133000
5	0.016327000	0.268669000	-1.027822000
7	-0.774509000	-0.957723000	-1.316573000
8	0.814015000	-1.847752000	0.502389000
1	5.264079000	2.079796000	0.645802000
1	4.269283000	4.306640000	0.614965000
1	1.885880000	4.586706000	0.126781000
1	-3.835458000	2.909956000	-0.617703000
1	-0.088255000	4.750406000	0.219927000
1	-2.506907000	4.846904000	0.040043000
1	3.293036000	-3.609394000	-0.049797000
1	5.692441000	-3.857545000	0.518365000
1	7.101313000	-1.818356000	0.748649000
1	6.129843000	0.385166000	0.486269000
1	-4.797262000	1.301723000	-1.344963000
1	-5.983220000	-0.669164000	-2.150354000
1	-4.730949000	-2.756664000	-2.677475000
1	-2.283195000	-2.830714000	-2.304194000
1	-0.289569000	-1.565783000	-1.982706000
6	-0.442652000	-2.045978000	0.183549000
1	-0.681226000	-2.968293000	-0.352691000
1	2.285901000	-2.198689000	-2.347985000
6	-1.450069000	-1.598118000	1.168356000
6	-2.708370000	-2.201723000	1.224467000
6	-1.181329000	-0.494646000	1.980684000
6	-3.689698000	-1.710578000	2.070464000
6	-2.157265000	0.008539000	2.826390000
6	-3.415098000	-0.597292000	2.865136000
1	-2.922405000	-3.061503000	0.599093000
1	-0.202350000	-0.029262000	1.939203000
1	-4.668557000	-2.170173000	2.126313000
1	-1.950844000	0.868238000	3.454876000
8	-4.410955000	-0.146645000	3.668492000
1	-4.114113000	0.621073000	4.168638000

Transition state with p-nitro benzaldehyde (C₁), S₀

61
scf done: -1708.72869223

6	-1.635047000	-2.173729000	-1.102781000
6	-2.527007000	-1.140579000	-1.448493000
6	-3.852043000	-1.504704000	-1.723264000
6	-4.280315000	-2.820865000	-1.641416000
6	-3.382099000	-3.827537000	-1.290945000
6	-2.062218000	-3.500142000	-1.025609000
6	-2.071681000	0.268245000	-1.526687000
6	-0.687042000	0.534025000	-1.480586000
6	-0.175183000	1.840080000	-1.501709000
6	-1.090198000	2.904184000	-1.591589000
6	-2.451027000	2.646059000	-1.634109000
6	-2.953284000	1.342635000	-1.597363000
6	1.272607000	2.041511000	-1.310180000
6	1.833772000	3.311624000	-1.503595000
6	3.156036000	3.563021000	-1.200035000
6	3.940279000	2.547913000	-0.661440000
6	3.454891000	1.254993000	-0.481034000
6	2.111546000	0.979263000	-0.863401000
6	4.304236000	0.212313000	0.158812000
6	3.741057000	-1.014258000	0.547502000
6	4.533579000	-1.944638000	1.230828000
6	5.865578000	-1.691489000	1.525903000
6	6.433445000	-0.490858000	1.101782000
6	5.665264000	0.444704000	0.425637000
5	2.278814000	-1.420519000	0.096174000
8	2.193331000	-2.743982000	-0.507001000
7	1.616315000	-0.321770000	-0.775981000
5	0.280709000	-0.569671000	-1.123810000
7	-0.286404000	-1.887221000	-0.763646000
8	1.281019000	-1.480742000	1.314068000
1	4.951849000	2.790224000	-0.367203000
1	3.574950000	4.549903000	-1.352316000
1	1.222673000	4.113240000	-1.897101000
1	-4.026085000	1.196627000	-1.593652000
1	-0.759376000	3.934204000	-1.578185000
1	-3.145707000	3.477276000	-1.671377000
1	4.089152000	-2.890713000	1.525934000
1	6.461690000	-2.420660000	2.062339000
1	7.479455000	-0.283184000	1.295993000
1	6.148985000	1.356769000	0.102595000
1	-4.562461000	-0.744584000	-2.021562000
1	-5.312384000	-3.064248000	-1.861581000
1	-3.706362000	-4.859000000	-1.231928000
1	-1.346477000	-4.270112000	-0.756486000
1	0.357770000	-2.665970000	-0.929685000
6	0.047196000	-1.851045000	1.176912000
1	-0.193114000	-2.913697000	1.264674000
1	2.990763000	-2.962489000	-0.993286000
6	-0.999073000	-0.889796000	1.609515000
6	-2.321742000	-1.309410000	1.761125000
6	-0.667087000	0.464313000	1.721275000
6	-3.327646000	-0.374440000	1.964988000
6	-1.659260000	1.408414000	1.925553000
6	-2.972218000	0.964864000	2.019404000
1	-2.572288000	-2.361840000	1.688789000
1	0.367075000	0.769418000	1.610458000
1	-4.363538000	-0.668932000	2.058171000
1	-1.433768000	2.464089000	1.984895000
7	-4.043711000	1.970316000	2.165839000
8	-5.191677000	1.577118000	2.181748000
8	-3.719636000	3.136022000	2.249336000

Transition state with p-fluoro benzaldehyde (C₁), S₀

59
scf done: -1603.47981099

6	-2.174031000	-0.771321000	-1.593640000
6	-2.845335000	0.432252000	-1.302907000
6	-4.232933000	0.447751000	-1.502885000
6	-4.920229000	-0.658543000	-1.978919000
6	-4.229553000	-1.826003000	-2.294208000

6	-2.858620000	-1.876179000	-2.098609000
6	-2.109367000	1.645441000	-0.861549000
6	-0.702898000	1.586428000	-0.777675000
6	0.077252000	2.678625000	-0.364015000
6	-0.590205000	3.878156000	-0.056899000
6	-1.970903000	3.942774000	-0.146396000
6	-2.739056000	2.842117000	-0.535924000
6	1.531451000	2.495065000	-0.201128000
6	2.343687000	3.589910000	0.127902000
6	3.686170000	3.429562000	0.400929000
6	4.242763000	2.154237000	0.382709000
6	3.501024000	1.028127000	0.036694000
6	2.131406000	1.205912000	-0.314275000
6	4.114553000	-0.329372000	0.095625000
6	3.320685000	-1.474382000	-0.083866000
6	3.903176000	-2.739956000	0.057197000
6	5.247626000	-2.896320000	0.361477000
6	6.041472000	-1.759138000	0.504791000
6	5.483902000	-0.496783000	0.371404000
5	1.816926000	-1.366036000	-0.572460000
8	1.518219000	-2.175661000	-1.752185000
7	1.382455000	0.118991000	-0.753874000
5	0.019657000	0.287507000	-1.021398000
7	-0.781222000	-0.926692000	-1.324885000
8	0.807643000	-1.832967000	0.505015000
1	5.282297000	2.052964000	0.660844000
1	4.299271000	4.285343000	0.654701000
1	1.916246000	4.582338000	0.175629000
1	-3.815175000	2.948540000	-0.567975000
1	-0.054399000	4.755328000	0.279518000
1	-2.472784000	4.869431000	0.107253000
1	3.279793000	-3.617858000	-0.085800000
1	5.679147000	-3.884347000	0.473276000
1	7.099494000	-1.855264000	0.720208000
1	6.139766000	0.356043000	0.482291000
1	-4.792163000	1.350187000	-1.294988000
1	-5.992681000	-0.603958000	-2.119524000
1	-4.753449000	-2.689131000	-2.685627000
1	-2.303509000	-2.779672000	-2.330246000
1	-0.303721000	-1.537496000	-1.993087000
6	-0.437042000	-2.047648000	0.177052000
1	-0.662219000	-2.958639000	-0.383085000
1	2.271454000	-2.222856000	-2.343847000
6	-1.462827000	-1.613718000	1.153285000
6	-2.710984000	-2.235778000	1.188251000
6	-1.207562000	-0.509466000	1.970303000
6	-3.710172000	-1.757869000	2.026830000
6	-2.197120000	-0.016984000	2.808379000
6	-3.428757000	-0.652513000	2.810703000
1	-2.906720000	-3.094775000	0.556770000
1	-0.232154000	-0.036799000	1.937019000
1	-4.687089000	-2.221001000	2.076129000
1	-2.031889000	0.840705000	3.447722000
9	-4.393702000	-0.176647000	3.618551000

p-hydroxy benzaldehyde (C_s), S₀

15

scf done: -420.751938717

6	0.936215000	-1.227679000	0.000018000
6	-0.435100000	-1.070101000	0.000009000
6	1.760841000	-0.095832000	0.000029000
1	-1.089521000	-1.933862000	0.000002000
6	-1.001178000	0.211327000	0.000012000
6	1.210117000	1.185995000	0.000031000
1	1.859138000	2.054527000	0.000040000
6	-0.169718000	1.331156000	0.000021000
1	-0.605202000	2.325131000	0.000023000
1	1.395418000	-2.208393000	0.000017000
6	-2.461714000	0.392630000	0.000009000
8	-3.267466000	-0.510963000	-0.000136000
1	-2.801523000	1.445133000	-0.000123000
8	3.096467000	-0.310816000	0.000038000
1	3.572892000	0.526725000	0.000047000

p-nitro benzaldehyde (C_s), S_0

16
scf done: -550.011721900

6	-0.284324000	-1.159377000	-0.000006000
6	1.096061000	-1.048504000	0.000023000
6	-1.034345000	0.010918000	-0.000024000
1	1.722864000	-1.931637000	0.000038000
6	1.692740000	0.213971000	0.000031000
6	-0.470781000	1.276969000	-0.000016000
1	-1.101154000	2.154934000	-0.000031000
6	0.915077000	1.370185000	0.000012000
1	1.391133000	2.344296000	0.000019000
1	-0.778285000	-2.120892000	-0.000013000
6	3.175917000	0.338340000	0.000062000
8	3.923666000	-0.606505000	0.000063000
1	3.563653000	1.372302000	0.000046000
7	-2.509634000	-0.100130000	-0.000054000
8	-2.991855000	-1.212262000	-0.000039000
8	-3.153418000	0.927130000	-0.000046000

p-fluoro benzaldehyde (C_s), S_0

14
scf done: -444.764217366

6	-0.954252000	-1.224726000	-0.000019000
6	0.421519000	-1.068743000	-0.000044000
6	-1.743101000	-0.082113000	-0.000015000
1	1.075614000	-1.932364000	-0.000050000
6	0.982764000	0.211905000	-0.000067000
6	-1.221529000	1.199755000	-0.000034000
1	-1.886730000	2.053330000	-0.000029000
6	0.160581000	1.338896000	-0.000058000
1	0.602624000	2.329510000	-0.000073000
1	-1.423559000	-2.200087000	-0.000003000
6	2.450441000	0.387408000	-0.000112000
8	3.244445000	-0.523628000	0.000241000
1	2.797712000	1.436687000	0.000243000
9	-3.077750000	-0.230261000	0.000009000

Compound **B** with p-hydroxy benzaldehyde (C_1), S_0

60
scf done: -1579.46965305

6	-2.385638000	-1.476226000	-1.137721000
6	-3.131201000	-0.284226000	-1.184083000
6	-4.515508000	-0.421285000	-1.355563000
6	-5.125496000	-1.661145000	-1.472501000
6	-4.360268000	-2.822713000	-1.442627000
6	-2.987113000	-2.722309000	-1.277037000
6	-2.499654000	1.061248000	-1.096906000
6	-1.094479000	1.137517000	-1.084173000
6	-0.392613000	2.351802000	-1.005857000
6	-1.154230000	3.534691000	-0.964685000
6	-2.537021000	3.466388000	-0.977743000
6	-3.221246000	2.246520000	-1.035514000
6	1.078895000	2.325183000	-0.909130000
6	1.815247000	3.518430000	-0.942262000
6	3.186277000	3.513548000	-0.786874000
6	3.852590000	2.314623000	-0.543969000
6	3.184264000	1.094333000	-0.494218000
6	1.784666000	1.097120000	-0.750664000
6	3.900271000	-0.165264000	-0.128260000
6	3.220655000	-1.396755000	-0.098445000

6	3.908752000	-2.543487000	0.314904000
6	5.246482000	-2.505015000	0.682032000
6	5.920650000	-1.285929000	0.641837000
6	5.255015000	-0.134583000	0.248723000
5	1.709282000	-1.508543000	-0.579172000
8	1.504789000	-2.258410000	-1.833084000
7	1.099530000	-0.106476000	-0.827444000
5	-0.268306000	-0.108471000	-1.016815000
7	-0.944163000	-1.470039000	-0.912690000
8	0.866514000	-2.169395000	0.506633000
1	4.921886000	2.353986000	-0.390945000
1	3.743787000	4.440735000	-0.834338000
1	1.309273000	4.461093000	-1.102750000
1	-4.302917000	2.259204000	-1.018961000
1	-0.685601000	4.507073000	-0.893448000
1	-3.109994000	4.384972000	-0.927035000
1	3.374699000	-3.489238000	0.354230000
1	5.759678000	-3.405725000	0.999000000
1	6.965026000	-1.228622000	0.926389000
1	5.812751000	0.792147000	0.253196000
1	-5.133858000	0.464330000	-1.411542000
1	-6.199142000	-1.718887000	-1.602241000
1	-4.823801000	-3.794999000	-1.550428000
1	-2.373433000	-3.616685000	-1.254638000
1	-0.462569000	-2.104853000	-1.570203000
6	-0.485781000	-2.040319000	0.518760000
1	-0.991190000	-3.009559000	0.566362000
1	1.947129000	-3.110327000	-1.794336000
6	-1.019025000	-1.102998000	1.578549000
6	-2.356462000	-1.167624000	1.975783000
6	-0.191292000	-0.135334000	2.145003000
6	-2.871002000	-0.260024000	2.889760000
6	-0.694308000	0.777593000	3.062296000
6	-2.039330000	0.722127000	3.425452000
1	-3.008041000	-1.933999000	1.567845000
1	0.855792000	-0.101518000	1.866869000
1	-3.907296000	-0.302059000	3.201545000
1	-0.044785000	1.529750000	3.497453000
8	-2.591597000	1.591070000	4.313285000
1	-1.930073000	2.222398000	4.615004000

Compound B with p-nitro benzaldehyde (C₁), S₀

61
scf done: -1708.73436038

6	1.864971000	2.335452000	-0.659772000
6	2.698037000	1.406820000	-1.308888000
6	4.022945000	1.807250000	-1.529497000
6	4.494207000	3.048006000	-1.127176000
6	3.641791000	3.952133000	-0.500943000
6	2.322743000	3.589759000	-0.272443000
6	2.209358000	0.079474000	-1.772233000
6	0.829520000	-0.188738000	-1.690750000
6	0.262023000	-1.411036000	-2.087723000
6	1.131169000	-2.381657000	-2.620970000
6	2.488204000	-2.122085000	-2.706669000
6	3.041854000	-0.908986000	-2.280127000
6	-1.177010000	-1.641281000	-1.861708000
6	-1.787594000	-2.816826000	-2.322955000
6	-3.111377000	-3.087444000	-2.044998000
6	-3.851294000	-2.203203000	-1.263820000
6	-3.312800000	-1.013369000	-0.781353000
6	-1.969368000	-0.705120000	-1.134263000
6	-4.102757000	-0.116618000	0.115223000
6	-3.534037000	1.055939000	0.644688000
6	-4.288170000	1.844309000	1.522283000
6	-5.582584000	1.503161000	1.885734000
6	-6.150194000	0.348296000	1.348984000
6	-5.421672000	-0.447036000	0.478146000
5	-2.088694000	1.554896000	0.213083000
8	-2.066313000	2.885273000	-0.425886000
7	-1.420406000	0.509241000	-0.743247000
5	-0.094505000	0.777960000	-1.019656000
7	0.476493000	2.018905000	-0.335327000
8	-1.159124000	1.693403000	1.395721000

1	-4.872255000	-2.470674000	-1.031398000
1	-3.571443000	-3.995510000	-2.414357000
1	-1.219910000	-3.527354000	-2.908605000
1	4.113738000	-0.777456000	-2.345424000
1	0.770161000	-3.349410000	-2.941866000
1	3.146585000	-2.887634000	-3.100302000
1	-3.838942000	2.749004000	1.920915000
1	-6.148046000	2.125021000	2.570302000
1	-7.163345000	0.064801000	1.610122000
1	-5.903376000	-1.333812000	0.089464000
1	4.702056000	1.138088000	-2.040486000
1	5.526472000	3.314744000	-1.317127000
1	3.995633000	4.929465000	-0.198811000
1	1.640066000	4.283140000	0.207593000
1	-0.149493000	2.810278000	-0.567076000
6	0.182843000	1.799115000	1.214530000
1	0.593172000	2.697801000	1.684485000
1	-2.712922000	2.944547000	-1.133336000
6	0.961163000	0.568507000	1.649607000
6	2.329003000	0.661960000	1.910706000
6	0.312209000	-0.662188000	1.746862000
6	3.063322000	-0.475302000	2.217012000
6	1.030780000	-1.808918000	2.053008000
6	2.396156000	-1.689962000	2.267791000
1	2.829498000	1.623100000	1.870575000
1	-0.756334000	-0.717168000	1.578665000
1	4.125175000	-0.427184000	2.413715000
1	0.550018000	-2.774844000	2.122021000
7	3.170959000	-2.906371000	2.579853000
8	4.368921000	-2.791285000	2.736426000
8	2.570208000	-3.957156000	2.659378000

Compound B with p-fluoro benzaldehyde (C₁), S₀

59

scf done: -1603.48397291

6	-2.331926000	-1.557601000	-1.085930000
6	-3.088068000	-0.378259000	-1.208579000
6	-4.465075000	-0.539216000	-1.414419000
6	-5.057926000	-1.790816000	-1.487949000
6	-4.282033000	-2.940523000	-1.377491000
6	-2.915027000	-2.816304000	-1.179373000
6	-2.472206000	0.975825000	-1.160542000
6	-1.067586000	1.068820000	-1.138735000
6	-0.382090000	2.293513000	-1.082677000
6	-1.158792000	3.467608000	-1.083240000
6	-2.540271000	3.382303000	-1.108268000
6	-3.208894000	2.152723000	-1.137055000
6	1.087049000	2.287849000	-0.953562000
6	1.805649000	3.491911000	-0.984375000
6	3.169583000	3.512512000	-0.778519000
6	3.846532000	2.328141000	-0.497917000
6	3.198877000	1.096090000	-0.462363000
6	1.805670000	1.072720000	-0.751263000
6	3.932231000	-0.150495000	-0.087240000
6	3.261123000	-1.384032000	-0.003505000
6	3.972434000	-2.521357000	0.398621000
6	5.320978000	-2.467729000	0.718744000
6	5.987482000	-1.246719000	0.623617000
6	5.303496000	-0.108224000	0.226468000
5	1.736844000	-1.540453000	-0.428017000
8	1.510106000	-2.489795000	-1.537023000
7	1.139392000	-0.143640000	-0.812190000
5	-0.226907000	-0.163454000	-1.015260000
7	-0.896496000	-1.520874000	-0.826654000
8	0.884138000	-2.063975000	0.699080000
1	4.907091000	2.390143000	-0.299608000
1	3.712366000	4.448925000	-0.813815000
1	1.290728000	4.423895000	-1.175307000
1	-4.290794000	2.151002000	-1.125842000
1	-0.703449000	4.447441000	-1.032284000
1	-3.124615000	4.294832000	-1.087553000
1	3.444774000	-3.468872000	0.453868000
1	5.851896000	-3.359327000	1.032354000

1	7.043155000	-1.179876000	0.860656000
1	5.861985000	0.816124000	0.169843000
1	-5.089752000	0.335723000	-1.534024000
1	-6.126410000	-1.867892000	-1.646954000
1	-4.732282000	-3.922275000	-1.449753000
1	-2.292071000	-3.700545000	-1.096250000
1	-0.392192000	-2.198550000	-1.423868000
6	-0.472793000	-1.982169000	0.646357000
1	-0.947878000	-2.962863000	0.744241000
1	2.091626000	-2.304392000	-2.278286000
6	-1.071332000	-0.993360000	1.624847000
6	-2.411840000	-1.097404000	1.997267000
6	-0.296920000	0.055761000	2.120379000
6	-2.992215000	-0.142913000	2.824773000
6	-0.861126000	1.018149000	2.948248000
6	-2.201651000	0.900624000	3.271600000
1	-3.014362000	-1.925705000	1.639164000
1	0.752359000	0.115317000	1.856049000
1	-4.030692000	-0.201630000	3.124321000
1	-0.281229000	1.843744000	3.340742000
9	-2.757129000	1.833502000	4.069625000

pTSA (C₁), S₀

19
scf done: -895.303141303

6	0.122167000	0.000533000	-0.095948000
6	-0.551414000	1.215451000	-0.090677000
6	-0.553556000	-1.215152000	-0.057674000
1	-0.000941000	2.146998000	-0.138980000
1	-0.003261000	-2.147872000	-0.078107000
6	-1.939877000	1.205203000	-0.042537000
6	-1.939332000	-1.201633000	-0.008908000
1	-2.478955000	2.145589000	-0.047431000
1	-2.480400000	-2.140907000	0.013375000
6	-2.649983000	0.003557000	0.004697000
16	1.888128000	-0.003882000	-0.117491000
8	2.361612000	-1.233672000	-0.703405000
8	2.362181000	1.277984000	-0.593829000
8	2.289900000	-0.130735000	1.440253000
6	-4.152029000	-0.001538000	0.084687000
1	-4.472791000	-0.156382000	1.118371000
1	-4.568787000	0.945190000	-0.258654000
1	-4.572446000	-0.809217000	-0.515861000
1	2.242129000	0.731573000	1.881132000

pTSA anion (C₁), S₀

18
scf done: -894.861777275

6	-0.159317000	0.007497000	-0.045554000
6	0.528777000	-1.200881000	-0.028402000
6	0.534130000	1.210921000	-0.028321000
1	-0.024509000	-2.132708000	-0.046471000
1	-0.016298000	2.143949000	-0.046287000
6	1.918414000	-1.198890000	0.001071000
6	1.925377000	1.200826000	0.000934000
1	2.455038000	-2.141999000	0.012797000
1	2.466849000	2.141156000	0.012917000
6	2.636697000	-0.000239000	0.015004000
16	-1.954616000	0.000289000	0.003389000
8	-2.371527000	1.303736000	-0.550983000
8	-2.365666000	-1.153025000	-0.822626000
8	-2.309288000	-0.160557000	1.430134000
6	4.143367000	-0.005219000	0.010892000
1	4.535227000	-0.884702000	0.523910000
1	4.523686000	-0.022230000	-1.014329000
1	4.541051000	0.886591000	0.497291000

Compound D with benzaldehyde (C₁), S₀

57

scf done: -1428.22462532

6	-2.591424000	-0.807840000	-1.312642000
6	-3.221799000	0.384781000	-0.928199000
6	-4.617251000	0.412114000	-1.058017000
6	-5.333019000	-0.667536000	-1.551554000
6	-4.670694000	-1.818689000	-1.965242000
6	-3.290919000	-1.881841000	-1.847702000
6	-2.470941000	1.582374000	-0.465461000
6	-1.062878000	1.540887000	-0.470371000
6	-0.263395000	2.623281000	-0.058347000
6	-0.920178000	3.791284000	0.356383000
6	-2.305011000	3.837087000	0.361946000
6	-3.088066000	2.750373000	-0.037774000
6	1.207157000	2.478039000	-0.054025000
6	2.032141000	3.582866000	0.185138000
6	3.407576000	3.449557000	0.239723000
6	3.994412000	2.204519000	0.061305000
6	3.229491000	1.066295000	-0.199265000
6	1.825529000	1.221766000	-0.266177000
6	3.868028000	-0.262643000	-0.375208000
6	3.075730000	-1.427214000	-0.453008000
6	3.675197000	-2.690616000	-0.553906000
6	5.052108000	-2.816287000	-0.601088000
6	5.839456000	-1.663779000	-0.551745000
6	5.262394000	-0.408391000	-0.439201000
5	1.564124000	-1.247216000	-0.480648000
7	1.023792000	0.094798000	-0.544106000
5	-0.353372000	0.264450000	-0.755675000
7	-1.129999000	-0.986731000	-1.184216000
8	0.677195000	-2.306409000	-0.444308000
1	5.069977000	2.128856000	0.136112000
1	4.028429000	4.315744000	0.429447000
1	1.596285000	4.562051000	0.327500000
1	-4.163928000	2.846892000	0.007340000
1	-0.372041000	4.657407000	0.700372000
1	-2.799490000	4.740719000	0.697941000
1	3.043623000	-3.570852000	-0.603407000
1	5.516009000	-3.791390000	-0.682805000
1	6.918798000	-1.746525000	-0.601843000
1	5.916151000	0.452224000	-0.411392000
1	-5.160096000	1.305012000	-0.781285000
1	-6.410595000	-0.600786000	-1.632391000
1	-5.217359000	-2.656385000	-2.378019000
1	-2.759696000	-2.769425000	-2.174009000
1	-0.784820000	-1.277738000	-2.108058000
6	-0.686115000	-2.134506000	-0.231988000
1	-1.199379000	-3.025067000	-0.588098000
6	-1.079037000	-1.817882000	1.194915000
6	-2.412020000	-1.997630000	1.574744000
6	-0.151643000	-1.365563000	2.133457000
6	-2.818280000	-1.687945000	2.866895000
6	-0.561314000	-1.062062000	3.427385000
6	-1.894741000	-1.212078000	3.792591000
1	-3.133952000	-2.391095000	0.868039000
1	0.898059000	-1.266538000	1.884390000
1	-3.853270000	-1.830245000	3.151731000
1	0.166817000	-0.715595000	4.150103000
1	-2.210375000	-0.974962000	4.801275000

Compound D with 4-hydroxy benzaldehyde (C₁), S₀

58

scf done: -1503.45378808

6	-2.440338000	-0.626374000	-1.671675000
6	-3.078437000	0.540342000	-1.223890000
6	-4.465975000	0.595512000	-1.415086000

6	-5.167273000	-0.431318000	-2.027536000
6	-4.496144000	-1.553419000	-2.501972000
6	-3.124365000	-1.644775000	-2.323833000
6	-2.340516000	1.688670000	-0.632545000
6	-0.935192000	1.624643000	-0.562487000
6	-0.146459000	2.660616000	-0.028719000
6	-0.810825000	3.804987000	0.436242000
6	-2.193040000	3.873862000	0.367347000
6	-2.965893000	2.833310000	-0.155921000
6	1.320034000	2.492072000	0.042464000
6	2.144166000	3.563167000	0.405494000
6	3.513215000	3.404646000	0.521150000
6	4.093816000	2.166936000	0.281883000
6	3.330306000	1.062782000	-0.101035000
6	1.933838000	1.245110000	-0.230030000
6	3.961408000	-0.259680000	-0.342196000
6	3.160662000	-1.401152000	-0.556279000
6	3.749336000	-2.662468000	-0.724563000
6	5.125023000	-2.807360000	-0.704471000
6	5.922337000	-1.676087000	-0.517170000
6	5.355273000	-0.424009000	-0.337050000
5	1.654718000	-1.195692000	-0.650200000
7	1.134831000	0.155401000	-0.634747000
5	-0.226926000	0.362079000	-0.906488000
7	-0.990802000	-0.837122000	-1.478525000
8	0.755993000	-2.241047000	-0.744326000
1	5.163256000	2.070012000	0.404434000
1	4.133424000	4.244980000	0.805643000
1	1.713421000	4.536490000	0.596147000
1	-4.040943000	2.946979000	-0.167501000
1	-0.272146000	4.633622000	0.874471000
1	-2.694197000	4.758740000	0.741197000
1	3.110682000	-3.525091000	-0.880008000
1	5.580645000	-3.780550000	-0.838823000
1	7.001654000	-1.773020000	-0.511493000
1	6.017298000	0.419746000	-0.200717000
1	-5.013884000	1.468664000	-1.089784000
1	-6.239325000	-0.345065000	-2.151866000
1	-5.029945000	-2.348201000	-3.006325000
1	-2.589160000	-2.512616000	-2.693392000
1	-0.593076000	-1.059045000	-2.400219000
6	-0.615699000	-2.066087000	-0.592588000
1	-1.119140000	-2.915113000	-1.050221000
6	-1.079058000	-1.852937000	0.827323000
6	-2.436353000	-2.014650000	1.129582000
6	-0.199970000	-1.502155000	1.850927000
6	-2.910850000	-1.782923000	2.408566000
6	-0.664596000	-1.275594000	3.139051000
6	-2.025119000	-1.398472000	3.415952000
1	-3.133331000	-2.333581000	0.362879000
1	0.865956000	-1.422608000	1.673884000
1	-3.959887000	-1.905174000	2.646431000
1	0.031162000	-1.011020000	3.927400000
8	-2.544202000	-1.178344000	4.645411000
1	-1.853836000	-0.916070000	5.263916000

Compound D with 4-nitro benzaldehyde (C₁), S₀

59

scf done: -1632.71284199

6	2.034779000	-0.814190000	-2.145537000
6	2.677943000	-1.622023000	-1.195721000
6	4.020632000	-1.927909000	-1.457773000
6	4.672064000	-1.474333000	-2.594051000
6	3.990436000	-0.711722000	-3.536733000
6	2.662249000	-0.386472000	-3.308941000
6	1.983091000	-2.182958000	-0.006254000
6	0.602403000	-1.946287000	0.143930000
6	-0.146439000	-2.440474000	1.228578000
6	0.531613000	-3.212893000	2.183038000
6	1.889475000	-3.448010000	2.039561000
6	2.624400000	-2.941681000	0.963419000
6	-1.582671000	-2.108882000	1.329305000
6	-2.390226000	-2.722467000	2.293458000

6	-3.724736000	-2.385371000	2.427312000
6	-4.285801000	-1.419740000	1.603289000
6	-3.539746000	-0.782823000	0.610108000
6	-2.180982000	-1.150248000	0.475870000
6	-4.147494000	0.258777000	-0.256275000
6	-3.341498000	1.012231000	-1.135546000
6	-3.898854000	2.040483000	-1.909247000
6	-5.251700000	2.320268000	-1.840188000
6	-6.057890000	1.559758000	-0.990230000
6	-5.519853000	0.548191000	-0.209905000
5	-1.873192000	0.630179000	-1.239763000
7	-1.402050000	-0.539946000	-0.530596000
5	-0.098709000	-1.003792000	-0.767262000
7	0.631171000	-0.380624000	-1.966949000
8	-0.952820000	1.363268000	-1.969523000
1	-5.324890000	-1.161327000	1.750406000
1	-4.332275000	-2.869542000	3.181044000
1	-1.974386000	-3.477605000	2.945985000
1	3.684563000	-3.148892000	0.921010000
1	0.025879000	-3.612888000	3.050864000
1	2.403271000	-4.034337000	2.791927000
1	-3.255561000	2.610278000	-2.570752000
1	-5.684010000	3.111760000	-2.439578000
1	-7.121490000	1.759859000	-0.935575000
1	-6.188309000	-0.013642000	0.427356000
1	4.569271000	-2.550322000	-0.764941000
1	5.710754000	-1.734875000	-2.753196000
1	4.481580000	-0.376204000	-4.440661000
1	2.117750000	0.200492000	-4.040729000
1	0.124442000	-0.652741000	-2.819438000
6	0.415492000	1.151961000	-1.879109000
1	0.883548000	1.573086000	-2.766849000
6	1.064048000	1.697174000	-0.619508000
6	2.453947000	1.843351000	-0.594998000
6	0.307220000	2.054354000	0.496045000
6	3.091836000	2.293949000	0.551191000
6	0.932028000	2.510873000	1.648897000
6	2.313058000	2.605582000	1.653677000
1	3.047997000	1.618165000	-1.472201000
1	-0.773973000	2.005874000	0.484509000
1	4.165820000	2.409873000	0.589399000
1	0.361437000	2.789427000	2.523728000
7	2.985528000	3.078573000	2.883444000
8	4.194002000	3.166758000	2.864483000
8	2.289144000	3.345571000	3.838233000

Compound D with 4-fluoro benzaldehyde (C₁), S₀

57

scf done: -1527.46578150

6	-2.443305000	-0.587012000	-1.672565000
6	-3.075662000	0.576637000	-1.208917000
6	-4.462544000	0.641912000	-1.402021000
6	-5.168173000	-0.372448000	-2.030037000
6	-4.502271000	-1.491200000	-2.519530000
6	-3.131229000	-1.592158000	-2.340880000
6	-2.332836000	1.712827000	-0.600678000
6	-0.927413000	1.643435000	-0.536039000
6	-0.134056000	2.668256000	0.012512000
6	-0.793724000	3.806468000	0.498724000
6	-2.175921000	3.880055000	0.436054000
6	-2.953449000	2.850567000	-0.102230000
6	1.331917000	2.494547000	0.076929000
6	2.160528000	3.558800000	0.449648000
6	3.529342000	3.394295000	0.559064000
6	4.105013000	2.157303000	0.304588000
6	3.336705000	1.059823000	-0.087839000
6	1.940849000	1.249017000	-0.211684000
6	3.962118000	-0.262546000	-0.343784000
6	3.156546000	-1.398096000	-0.571605000
6	3.739626000	-2.660070000	-0.754603000
6	5.114579000	-2.811151000	-0.735559000
6	5.916664000	-1.685716000	-0.533794000
6	5.355150000	-0.433308000	-0.339124000

5	1.652209000	-1.184932000	-0.662460000
7	1.136515000	0.167034000	-0.627845000
5	-0.223825000	0.383725000	-0.897664000
7	-0.993721000	-0.807070000	-1.482460000
8	0.748292000	-2.226039000	-0.767952000
1	5.174495000	2.055736000	0.422603000
1	4.153349000	4.229304000	0.850784000
1	1.733469000	4.531322000	0.652229000
1	-4.028276000	2.966720000	-0.106919000
1	-0.251167000	4.625678000	0.949696000
1	-2.673412000	4.759412000	0.827377000
1	3.097321000	-3.517999000	-0.920677000
1	5.566038000	-3.784621000	-0.881311000
1	6.995511000	-1.787587000	-0.528013000
1	6.020959000	0.405484000	-0.191294000
1	-5.006091000	1.513986000	-1.066629000
1	-6.239457000	-0.278486000	-2.155339000
1	-5.039254000	-2.275592000	-3.036588000
1	-2.599898000	-2.456755000	-2.723366000
1	-0.597606000	-1.017370000	-2.407941000
6	-0.622279000	-2.048338000	-0.620125000
1	-1.126451000	-2.890972000	-1.088827000
6	-1.090833000	-1.860529000	0.805696000
6	-2.447142000	-2.037943000	1.095025000
6	-0.208664000	-1.526314000	1.833471000
6	-2.927330000	-1.840540000	2.381731000
6	-0.674204000	-1.331475000	3.127321000
6	-2.027526000	-1.480738000	3.369768000
1	-3.138668000	-2.343906000	0.318691000
1	0.855683000	-1.436375000	1.655222000
1	-3.973531000	-1.973412000	2.624226000
1	-0.003905000	-1.076301000	3.937615000
9	-2.483308000	-1.288870000	4.616413000

protonated compound A (C₁), S₀

46

scf done: -1159.10105732

6	5.019979000	-0.491674000	0.053586000
6	3.621628000	-0.373309000	-0.011577000
6	2.886807000	-1.541735000	-0.292792000
6	3.539562000	-2.755332000	-0.530181000
6	4.918527000	-2.834578000	-0.473862000
6	5.664451000	-1.694807000	-0.169566000
6	2.938565000	0.925606000	0.151965000
6	1.533577000	0.974897000	0.055339000
6	0.822337000	2.186004000	0.120960000
6	1.536788000	3.361252000	0.358673000
6	2.921818000	3.314190000	0.487980000
6	3.626543000	2.123571000	0.373588000
6	-0.646523000	2.167970000	-0.079645000
6	-1.339694000	3.366789000	-0.249716000
6	-2.719032000	3.396771000	-0.381990000
6	-3.436807000	2.217424000	-0.332556000
6	-2.798750000	0.979034000	-0.190158000
6	-1.386441000	0.959860000	-0.094826000
6	-3.599257000	-0.259431000	-0.099740000
6	-4.984597000	-0.276163000	-0.334087000
6	-5.713608000	-1.442840000	-0.186854000
6	-5.095100000	-2.638780000	0.191709000
6	-3.731579000	-2.649162000	0.404635000
6	-2.975975000	-1.472162000	0.262367000
5	-1.473757000	-1.412891000	0.347014000
7	-0.705762000	-0.285790000	0.020207000
5	0.753850000	-0.307393000	-0.114757000
7	1.475493000	-1.520069000	-0.326988000
1	-4.514394000	2.266167000	-0.392825000
1	-3.232625000	4.341315000	-0.506985000
1	-0.795310000	4.300239000	-0.281667000
1	4.704223000	2.149309000	0.458727000
1	1.041342000	4.316974000	0.459298000
1	3.464623000	4.233148000	0.675446000
1	-3.252523000	-3.587845000	0.665007000
1	-5.677006000	-3.545010000	0.300360000

1	-6.780521000	-1.427154000	-0.374701000
1	-5.508392000	0.616584000	-0.644647000
1	5.619928000	0.380425000	0.275845000
1	6.744364000	-1.747007000	-0.113972000
1	5.411731000	-3.780730000	-0.659466000
1	2.948999000	-3.638245000	-0.751352000
1	1.084860000	-2.288387000	-0.862287000
8	-0.721434000	-2.604313000	0.781944000
1	0.248099000	-2.503346000	0.934215000
1	-1.143827000	-3.269852000	1.350134000

8. References

- [1] a) L. Farrugia, *J. Appl. Crystallogr.* **1999**, *32*, 837-838; b) C. B. Hubschle, G. M. Sheldrick, B. Dittrich, *J. Appl. Crystallogr.* **2011**, *44*, 1281-1284; c) G. Sheldrick, *Acta Crystallogr. Sect. A* **2008**, *64*, 112-122; d) G. Sheldrick, *Bruker AXS Inc. Madison, Wisconsin, USA* **2007**; e) G. M. Sheldrick, *University of Göttingen, Germany* **1996**.
- [2] a) B. Gollas, B. Krauß, B. Speiser, H. Stahl, *Curr. Sep.* **1994**, *13*, 42-44; b) A. W. Bott, *Curr. Sep.* **1995**, *14*, 64-68.
- [3] Y. Zhao, D. G. Truhlar, *Theor. Chem. Acc.* **2008**, *120*, 215-241.
- [4] M. J. Frisch, G. W. Trucks, H. B. Schlegel, G. E. Scuseria, M. A. Robb, J. R. Cheeseman, G. Scalmani, V. Barone, G. A. Petersson, H. Nakatsuji, X. Li, M. Caricato, A. V. Marenich, J. Bloino, B. G. Janesko, R. Gomperts, B. Mennucci, H. P. Hratchian, J. V. Ortiz, A. F. Izmaylov, J. L. Sonnenberg, Williams, F. Ding, F. Lipparini, F. Egidi, J. Goings, B. Peng, A. Petrone, T. Henderson, D. Ranasinghe, V. G. Zakrzewski, J. Gao, N. Rega, G. Zheng, W. Liang, M. Hada, M. Ehara, K. Toyota, R. Fukuda, J. Hasegawa, M. Ishida, T. Nakajima, Y. Honda, O. Kitao, H. Nakai, T. Vreven, K. Throssell, J. A. Montgomery Jr., J. E. Peralta, F. Ogliaro, M. J. Bearpark, J. J. Heyd, E. N. Brothers, K. N. Kudin, V. N. Staroverov, T. A. Keith, R. Kobayashi, J. Normand, K. Raghavachari, A. P. Rendell, J. C. Burant, S. S. Iyengar, J. Tomasi, M. Cossi, J. M. Millam, M. Klene, C. Adamo, R. Cammi, J. W. Ochterski, R. L. Martin, K. Morokuma, O. Farkas, J. B. Foresman, D. J. Fox, *Gaussian 16 Rev. C.01*, Wallingford, CT, **2016**.
- [5] R. Krishnan, J. S. Binkley, R. Seeger, J. A. Pople, *J. Chem. Phys.* **1980**, *72*, 650-654.
- [6] J. Tomasi, B. Mennucci, R. Cammi, *Chem. Rev.* **2005**, *105*, 2999-3094.
- [7] K. Wolinski, J. F. Hinton, P. Pulay, *J. Am. Chem. Soc.* **1990**, *112*, 8251-8260.
- [8] R. S. Nicholson, *Anal. Chem.* **1966**, *38*, 1406-1406.